Developing a novel test method to determine the efficacy of antimicrobial materials

A J Cunliffe

PhD 2023

Developing a novel test method to determine the efficacy of antimicrobial materials

Alexander James Cunliffe

A thesis submitted in partial fulfilment of the requirements of Manchester Metropolitan University for the degree of Doctor of Philosophy

Department of Natural Sciences

Manchester Metropolitan University in collaboration with the International Biodeterioration Research Group

2023

Summary abstract

Antimicrobial materials are becoming increasingly popular as a method of controlling microbial growth due to the raised awareness of infection control and hygiene. Standardised test methods help to demonstrate the efficacy of these materials before they are implemented in end-use scenarios. However, some methods do not reflect the in-use conditions of the materials, such as the use of high relative humidity that prevents an inoculum from evaporating on a surface. This in turn allows an antimicrobial material to remain active if it requires moisture, which is often the case. It is of utmost importance to ensure that these standardised test methods accurately simulate the end-use environment to provide confidence that their efficacy will remain once applied to the point-of-use. To achieve this, a series of experimental decisions were tested including environmental conditions (e.g., temperature, relative humidity, and airflow) as well as other factors (e.g., inoculum volume and concentration, incubation period). To reproducibly assess these parameters, an environmental control chamber was designed, and 3D printed. Additionally, the impact of droplet evaporation on bacterial deposition and the prolonged efficacy of antimicrobial materials was assessed. The environmental conditions significantly ($p < 0.05$) affected the survival of bacteria on an inert (stainless steel) surface by causing the evaporation of the inoculum on the surface, promoting cell death via desiccation. Furthermore, a prototype environmental control chamber was developed that was capable of maintaining temperature (room temperature to 37 ^{o}C), relative humidity (15 to 100 %) and airflow in a stable manner. The environmental conditions (temperature, relative humidity) as well as methodological decisions (surface composition, droplet volume, droplet contamination with microorganisms) significantly affected the evaporation rate of droplets on a surface in some instances. All of the factors described affect the ability of an antimicrobial material to exhibit or retain its efficacy, and novel standardised test methods need to accommodate these factors if they are to accurately simulate a variety of end-use scenarios. Future work should aim to continue to develop both the novel chamber and realistic conditions in standardised test methods to determine antimicrobial material efficacy more accurately when in use.

Acknowledgements

I would like to start by thanking the Manchester Metropolitan University and the International Biodeterioration Research Group for funding this research. Specifically, I would like to thank my supervisory team of Dr. James Redfern and Professor Joanna Verran, as well as Dr. Ina Stephan, Peter Askew and Gillian Iredale for their guidance and mentoring throughout the years. I would like to acknowledge the T3.02 team of Dr. Ryan Marsh, Dr. Lauren Hatfield, Dr. Helen Gavillet and Dr. Michelle Hardman along with all of the other researchers and technical staff, especially Dr. Paul Benson-White who's been a consistent lifeline of support. Also, Dr. Nicole Britten has been one of my closest friends throughout my time at MMU and has been an amazing support throughout.

A special thanks goes to my family, particularly my mum Shirley and dad Paul, who have unconditionally supported me through this endeavour and believed in me from start to finish.

Finally, my partner Chloe has been there for me throughout this project, from reading my first published paper to helping prepare for interviews and presentations. I truly would not have been able to do this without her and I can't thank her enough for everything she's done.

COVID-19 impact statement

The progress of this PhD has been significantly impacted through the COVID-19 pandemic, whereby the second lockdown impeded access to the laboratories and caused subsequent difficulties that slowed progress. Additionally, university restrictions have been implemented following construction work to the building that caused laboratories to be inaccessible for some time. Despite this, the projects progression has occurred on schedule and considerable strides have been made to further the field of standardised testing for non-porous antimicrobial materials.

Contents

Table of tables

Table of figures

Glossary of terms

AMM – Antimicrobial material – A material that has been functionalised to reduce or eliminate microbial growth or survival.

Bioaccumulation – The increasing concentration of a compound in living things as it moves up the food chain.

Bioburden – The number of microorganisms present on a surface that has not been antimicrobially treated.

Biocide – A substance that destroys living things.

Biofouling – The contamination of a surface by microorganisms and small animals, usually in a marine context.

Desiccation – The removal of moisture from the environment.

Experimental decisions – In the context of this thesis, it relates only to the variables of a standardised test method that can be altered. For example, the inoculum volume applied to the surface. A subsection of this term is the environmental conditions that can be altered in a standardised test method, such as temperature and relative humidity.

Fomite – An object or material that is likely to transfer disease.

Hydrophobicity – The ability to repel or fail to mix with water.

Leaching – The disassociation of antimicrobial (or other) compounds from a material into the environment.

Nanoparticle – A discrete nano-object with all dimensions lower than 100 nm.

Photocatalytic – The excitation of a particle or chemical reaction by light.

Potentiated surface – A surface that has been functionalised with antimicrobials.

Reactive oxygen species – Molecules that contain at least one oxygen atom and at least one unpaired electron.

Relative humidity – The ratio of water vapour in the air as a function of the maximum possible at a specified temperature.

Saturated salts -A slushy mixture of distilled water and a chemically pure salt.

Soiling – The addition of proteins or other compounds on to a material.

STM – Standardised test method – Methods used for a variety of purposes (including assessing antimicrobial material efficacy) with the intention of providing reproducible results. In the context of this thesis, any use of the term STM refers only to non-porous antimicrobial material testing unless otherwise stated.

Surface tension – The attractive force exerted on the surface molecules of a liquid by the molecules beneath.

Surface topography – Surface orientation and roughness, characterised by peaks and valleys.

Treated article – Any substance or article that intentionally incorporates one or more biocidal products.

Vapour pressure – A measure of the tendency of a material to change into its gaseous / vapour states.

1. Introduction: Antimicrobial materials and standardised test methods

1.1. Preface

Some of the contents of this chapter have been previously published in the journal Antibiotics (Cunliffe et al., 2021), which focused solely on antibacterial materials and STMs, with the work presented here not only representing additional STMs relating to antiviral and antifungal properties but also offering a more up to date analysis using the most recent literature available and integrating that into the wider context of the field. The complete work is shown in Appendix A. This author was the primary individual responsible for reviewing the literature, drafting the manuscript, and subsequently editing reviewers' comments to allow for publication.

1.2. Why is it important to test antimicrobial materials

The movement of microorganisms throughout an environment is a prominent method of transfer between hosts. This typically occurs via aerosols(Mirhoseini et al., 2015; M. Wu et al., 2020), direct contact (I. Y. Jung et al., 2019; Szczesny et al., 2022), or indirect contact via fomites (Stephens et al., 2019). A fomite is any surface on which pathogens are commonly found. Some microorganisms can retain their pathogenic potential whilst outside their host for extended periods of time (Pommepuy et al., 1996), with studies suggesting survival for days and even weeks on inanimate surfaces such as plastics and metals which are often considered to be 'hygienic surfaces' (Neely, 2000; Heller and Edelblute, 2018). Many of these materials are used to construct FTS such as door handles, lift buttons, light switches, and digital locks (Xiao et al., 2019; Jaradat et al., 2020). Viability of microorganisms on FTS has been demonstrated, and more critically, the evidence of transfer of potentially harmful microorganisms from the FTS to a biological surface (e.g., human skin) via touch has also been reported numerous times in the literature (Suwantarat et al., 2017; Kraay et al., 2018; Weber et al., 2020). In the clinical setting, studies highlight bedsteads, supply carts, over-bed tables, lockers, patient bodies, bed-linen, curtains and intravenous pumps as frequently touched when specifically considering interactions between hospital staff and patients (Huslage et al., 2010; V. C. C. Cheng et al., 2015). These patient-care items can serve as a potential reservoir for pathogenic microorganisms and may be the cause of infection, and cross-infection, between hospital patients. Furthermore, non-clinical environmental reservoirs of pathogens can cause further problems where compounding factors also occur, such as on cruise ships where advanced medical treatments are not available (Xiaofei Liu and Chang, 2020).The transmission of pathogens

via fomites is of growing concern, particularly with the increase in prevalence of antimicrobial resistance. This means infection will be harder to treat (Laxminarayan et al., 2016). One approach to controlling microorganisms in these environments is to use materials that are antimicrobial, i.e. can kill or prevent the growth of a microorganism should it come into contact (Michael et al., 2014). Antimicrobial materials provide the benefit of reducing human error and do not impact on the availability of facilities. Such materials may be innately antimicrobial, produced with a biocide embedded within, or there may be some coating or treatment that confers antimicrobial properties onto the surface—many of which have gained popularity over recent years (Page et al., 2009). For example, in some hospitals and other end-use environments, Cu has been exploited as an AMM (Dunne et al., 2018), whilst brass has also been used extensively for FTS, demonstrating an oligodynamic (present even at low concentrations) effect (Dauvergne and Mullié, 2021). Other materials and additives are now gaining focus in the literature, for example, materials with photocatalytic properties such as certain forms of titanium dioxide, various metal salts and oxides as well as certain dyes (Salazar et al., 2020), other metal ions (Lemire et al., 2013) and some organic agents (Oosterhof et al., 2006) and materials used in their nano form, such as Ag, Cu and Zn (Khadka et al., 2018).

1.2.1. Droplet transmission

Droplet transmission of microbes is one of the most common ways to spread airborne disease in any environment (S. K. Das et al., 2020), both through person-to-person transmission (Y.-H. Cheng et al., 2016) and with fomites as a proxy (Van Doremalen et al., 2020). There are several methods for droplets to facilitate transmission, with the most common resulting from coughing (Al Maghlouth et al., 2004; Wainwright et al., 2009; Jayaweera et al., 2020) but could also include other bodily fluids such as blood spatter (Gallagher et al., 2020) (particularly prevalent in healthcare settings) or waste fluids (i.e. urine (Arena et al., 2021; Cao et al., 2022)) when proper sanitisation procedures are not maintained. Many antimicrobial materials (AMMs) require a level of moisture to be active (James Redfern et al., 2018), for example silver (Ag) (Michels et al., 2009). Droplets containing microorganisms can provide this required moisture, however this means that antimicrobial efficacy is directly proportional to the evaporation time of the droplet (i.e. once it has evaporated, the material will no longer be antimicrobial). The process of decreasing antimicrobial efficacy post-evaporation heavily favours the use of materials that

exhibit their antimicrobial effect rapidly. However, this may also cause a depletion of the active ingredient over time, especially if the material employs an antibiotic-release mechanism (Bhattacharjee et al., 2022). Interestingly, although copper (Cu) has been extensively reported as an effective AMM, a recent study demonstrates reduced antimicrobial efficacy of Cu when bacteria are deposited in a dry manner and incubated at 40 % relative humidity (McDonald et al., 2020), although these findings are disputed. Droplets originating from humans can also travel a great distance, modelled to be up to two meters with no wind present and up to six meters when wind was applied (Dbouk and Drikakis, 2020), implying that the spread of microorganisms in an indoor environment (such as a hospital) may be relatively vast with continuous recontamination. Therefore, intermittent cleaning regimes may not act fast enough to stop the rapid spread of disease between patients and staff.

1.2.2. End-use applications of antimicrobial materials

Care must be taken when considering the end-use environment of the AMMs implementation, as applications and end-use environments will be diverse. For example, one study found that the relative humidity of teaching hospitals in Boston, USA to be between 20-30 % (Quraishi et al., 2020). Thus, materials that require extended periods of moisture on the surface will likely not be as efficacious as current standardised test methods (STMs) are predicting them to be. On the other hand, Tokyo, Japan has an outdoor mean relative humidity of between ~60-70 % in the previous ten years (J. M. Agency), and so materials implemented there can have a greater reliance on moisture, such as materials with Ag, as their prolonged efficacy can be assured with longer evaporation times. Due to the varying environmental factors in end-use scenarios, some generalisation is required. As an example, simply moving from one room to another in a hospital building will likely present different airflow, light exposure and relative humidity values, and different times of the day and year will present varying environmental conditions (Ramos et al., 2015). This is further compounded when comparing different areas of a country, between countries or even intercontinental, and creates issues for demonstrating reliable efficacy claims across a wide range of end-use scenarios. This makes it difficult to accurately compare efficacy results of materials intended for different end-use scenarios if realistic testing were implemented. Therefore, a more generalised and balanced approach that uses ranges of environmental conditions for efficacy testing would likely provide a greater

confidence in the antimicrobial efficacy of the material when implementing it into multiple use cases. For example, a material would be tested multiple times based on the conditions present in its intended end-use case (i.e., ~22 °C and 50 % relative humidity in indoor acclimatised buildings) and approved appropriately.

Four common generalised settings where AMMs are used are healthcare, food and industrial, the built environment, and marine. Each with a unique set of challenges to determine what AMM to utilise and how to determine its efficacy.

1.2.2.1. Healthcare

Healthcare settings are the most clinically relevant use of AMMs, as a reduction in the spread of pathogenic microorganisms can noticeably impact on patient clinical outcome and safety of staff and visitors (Schreiber et al., 2018), but also the direct cost to the economy (Serra-Burriel et al., 2020). This is because secondary healthcare associated infections (HCAIs) increase the average time of a patient visit in hospital by up to 2.5 times (De Angelis et al., 2010), as well as the potential time required to remove and refit bioburden-laden indwelling devices such as catheters and implants (Scott, 2009). Meanwhile the direct cost of HCAIs in the United States of America alone is $33 billion each year (Zimlichman et al., 2013). AMMs must be used alongside other already effective systems of cleaning in order to minimise the impact of human error (Carpenter et al., 2015), and complacency in sanitation practices should be prevented. The two areas within the healthcare setting where AMMs would provide the most noticeable impact are frequently touched surfaces (FTS) and medical equipment and devices.

1.2.2.1.1. Frequently touched surfaces

Antimicrobial materials are often utilised for FTS. As the cost of these materials is often much higher than their non-antimicrobial counterpart (Basnett et al., 2020), usage might be restricted to where they will be most effective. The common FTS in a healthcare setting can include bed steads, bed rails, bedside equipment, bedside tables, door handles etc (Grass et al., 2011). Antimicrobially enhanced textiles have also been developed and implemented in hospitals over recent years to further reduce the transmission of microorganisms (Laird and Riley, 2016), particularly via staff members who will interact with many patients per day (Mitchell et al., 2015). Other areas such as curtains and seat covers are also considered (Schweizer et al., 2012).

1.2.2.1.2. Medical equipment and devices

The implementation of AMMs into medical devices and equipment, both internal (i.e., catheters and implants) and external (i.e., wound dressings) increases patient wellbeing and reduces the burden on additional healthcare required by secondary infections that often arise from devices interacting with patients. For example, dental prosthesis (Karimzadeh et al., 2021), catheters (Atkins et al., 2020) and wound dressings (Church et al., 2006), among other applications, all continue to benefit from advances in AMMs.

1.2.2.2. Food and industrial

Antimicrobial materials are also used in the food industry (e.g. as packaging (S. Ahmed et al., 2022)) in order to increase the shelf life of a product (Moustafa et al., 2019). This in turn generates a lower degree of food waste and allows for greater efficiency of supply chains if products can be held for a longer time before reaching the customer (Azeredo et al., 2019). Approximately one third of global food is wasted each year with an equally large impact on the global economy (Seberini, 2020). In South Africa alone overall food waste has been estimated at 177 kg / capita / annum (Oelofse and Nahman, 2013). Materials used in food packaging must abide by strict regulation regarding the toxicity of the material being used and avoid leaching where possible, although this heavily depends on the country in which the material will be used. For example, the food and drug administration (FDA) in the US (J. H. Han, 2003). Also, the microorganisms that need to be considered differ from those in other sectors (Malhotra et al., 2015). One of the most common causes of foodborne infections is *Salmonella spp. (Popa and Papa, 2021)*, with one study assessing gold nanoparticles supported on zeolites that were effective at reducing the bioburden of both *Escherichia coli* and *Salmonella typhi* by 90-95 % (Lima et al., 2013). The prevention of drinking water contamination is also of great concern, particularly to the developing world (H. A. Hasan and Muhammad, 2020) where mortality rates due to contaminated water are much higher (Gadgil, 1998), although this has been improving in recent years (Bijekar et al., 2022). One study used a polypropylene pipe with Ag nanoparticles embedded in order to achieve an antimicrobial effect to treat drinking water (Damian and Patachia, 2016). The environmental conditions present in water treatment offer an advantage to Ag-based (among others e.g., titanium dioxide) materials that can consistently leach into the water. However, as in other applications, toxicity of the material being used is of the utmost concern, particularly for nanoparticles that can move through filters in water systems. This

application is both able to reduce the blockage of filters and pipes in developed countries (Xiong et al., 2021; Zhenchao Zhou et al., 2021) and reduce the risk of infection through contaminated water in countries without access to clean potable water (Li and Wu, 2019). The use of AMMs in water treatment is particularly important when considering the prevalence of cholera, which is estimated to cause 1.3-4 million cases and between 21,000-143,000 deaths globally each year (W. h. organisation, 2022).

The construction industry can also benefit greatly from the use of AMMs. Microbiologically-induced concrete corrosion (MICC) is a serious issue that reduces the effective lifespan of structures by more than half (M. Wu et al., 2020). There are several environmental factors to consider concerning biofouling (the accumulation of microorganisms, plants, algae, and small animals on structures with a mechanical function that results in damage and degradation) in the construction industry, mainly relating to which type of organism will grow. For example, phototrophic eukaryotes dominate building structure degradation when given access to high light levels and a tropical environment (high temperature and relative humidity) (Kirthika et al., 2022). On the other hand, sulphur-reducing bacteria will prevail in sewage networks due to the high volume of sulphur in the environment, this leads to the production of hydrogen sulphide which compromises the structural integrity of the sewage pipes (Grengg et al., 2015). Promising candidates for reducing MICC in the literature include Cu (Jędrzejczak et al., 2022), Ag (Mu et al., 2021) and zinc (Zn) (Aldosari et al., 2019).

1.2.2.3. The built environment

The built environment considers mostly how the public interact with AMMs, with public transport (Danko et al., 2021) and restaurants (e.g., menus) (Patel, 2020) as common examples. Public transport contains a variety of FTS that are considered for AMM use (Kalb et al., 2022), such as call (stop) buttons, poles (on buses and trams where the call buttons and hand rails / supports are placed), tables and armrests (on trains and aeroplanes) (B. Zhao et al., 2019) and seating. As the environmental conditions in each of the public transport systems is so varied, it is difficult to determine a set of environmental conditions to encompass them all, but it should be noted that in all these cases it is likely that the same microbial species will be present due to them all sharing frequent human interaction, common examples include *proteobacteria, Enterobacteriaceae and Salmonella (Guevarra*

et al., 2022). Also, the increased movement of people through these environments likely increases the bioburden generated and the risk of transmission (Xia Yang et al., 2020). Soiling is also a significant issue in this environment due to insufficient cleaning practices and high frequency touching in many cases (Ren et al., 2020). Aircraft interiors are a well-known area of surface contamination with equally high transmission rates and are especially prominent perpetuators of intercountry transmission during pandemics (Murphy et al., 2020). Commonly contaminated surfaces may include armrests, tray tables, all relevant lavatory surfaces, window shades and seat covers / pockets (McManus and Kelley, 2005; McKernan et al., 2008; Vaglenov, 2014). Additionally, fungi and viruses are found in aircraft interior-based textiles such as seating (Fu et al., 2013; Sze-To et al., 2014) as well as in those areas previously mentioned (McKERNAN et al., 2007; Thornley et al., 2011; W. Yang et al., 2011; Lei et al., 2017).

1.2.2.4. Marine

The marine application of AMMs offers a unique set of challenges. These mainly relate to the widely ranging contaminating species (where bacteria (Iswadi et al., 2022), fungi (Dobretsov et al., 2021) and animals such as barnacles (Holm, 2012) all cause biofouling) as well as the strategic placement of the materials, often requiring resistance to high-salt conditions. Whilst ship hulls are a common target for AMMs, there are also underwater pipelines, jetties, offshore oil rigs etc. As any AMMs in these applications are submerged in water at almost all times, it is likely that they will remain active for the duration of their lifespan. Therefore, it is more important to address their potency to microorganisms and low toxicity because environmental impact mitigation is paramount at the present time (Qiu et al., 2022), both in terms of bioaccumulation of biocides and metal nanoparticles in the food chain (e.g. Ag nanoparticles (Kakakhel et al., 2021)) as well as the increased risk of developing antimicrobial resistance through long-term low dose exposure conditions (Lu et al., 2020; Ahmad et al., 2021). Sea-dwelling creatures such as barnacles cause a major issue in that they create a barrier between the microorganisms and the AMM, therefore materials often used in marine environments aim to be anti-adhesive to also prevent this problem (Callow, 1986). Current shipping practices endorse the use of anti-adhesive properties combined with those that release biocidal compounds (Bieser et al., 2011) which mainly focus on the release of copper ions from the surface in combination with a highly hydrophobic material (Terlizzi et al., 2000), and in some cases the use of additional biocides

if deemed necessary. Biofouling is a great concern to the shipping industry as it creates increased costs to the process of transportation with estimates of up to a 40 % increase in fuel usage (Yebra et al., 2004). This also translates to the wider marine built environment such as static structures, where antifouling paints have been utilised in many areas to reduce the effects of microbially induced corrosion and therefore reduce potential damage and repair costs, with an estimated $5.7 billion worldwide being saved annually (Yebra et al., 2005; Hellio and Yebra, 2009; Dafforn et al., 2011).

1.2.3. Different microorganisms in standardised test methods

The choice of microorganisms for a given STM should depend entirely on the intended end-use of the product. However, as this is in many cases too specific and varied, model organisms are often specified in STMs. For example, many bacterial test methods use either *E. coli* or *S. aureus* as a gram-negative and gram-positive organism respectively. Similarly, *C. albicans* is often used for fungal test methods. While these species are highly clinically relevant and cause many infections per year (Bonten et al., 2021; Talapko et al., 2021; Bai et al., 2022), it does not represent the range of species that would be present in most end-use scenarios. Furthermore, the use of a single species in many STMs (e.g. ISO2296) does not adequately account for the complexity involved in the use of AMMs in end-use scenarios. Testing against a consortium of relevant microorganisms would provide increased confidence in the ability of the AMM to reduce the survival and / or growth of microorganisms on the surface when in use. Ideally, the decision of microorganism choice should be at the discretion of the AMM manufacturers and testers based on previous research into the most relevant species for the intended use of the product, which could then be verified, and approval granted by the regulators via a report of the AMM. Nevertheless, basic minimum requirements for organism choice may still be beneficial. For example, due to the physiological differences in gram-positive and gram-negative organisms, testing against at least one organism from each would provide a more complete assessment of AMM efficacy. Graphene oxide presents different mechanisms of action depending on the gram status of the bacteria tested, whereby gram-positive organisms are subjected to cell entrapment whereas gram-negative organisms experience more traditional membrane disruption due to the contact with the material (Pulingam et al., 2019). Additionally, when considering copper oxide nanoparticles, the increased sensitivity

of gram-positive organisms (as opposed to gram-negative organisms) was associated a greater proportion of amines and carboxyl groups on the cell surface (Beveridge and Murray, 1980). Differences in organism characteristics and how it impacts on AMM efficacy can also be extended to enveloped and non-enveloped viruses. One study found that inactivation of both enveloped and non-enveloped viruses occurred due to surface spike dispersal, irreversible RNA damage and structural damage when exposed to copper alloy surfaces. However, due to additional envelope disintegration, enveloped viruses were inactivated faster than non-enveloped viruses (Govind et al., 2021). The differences in microbial physiology, inter-species interactions and the effects of environmental conditions are all important factors even before applying an antimicrobial component to a surface. Desiccation is the removal of moisture from an organism and will kill / inactivate microorganisms even when no other antimicrobial effects are taking effect. The process and speed of desiccation differs between organisms. Gram-positive bacteria are generally capable of surviving for months at a time on inanimate surfaces, whereas gram-negative bacteria are much more strain dependent on whether they can survive for a comparable amount of time or for only a few hours (Kramer and Assadian, 2014). Interestingly, *E. coli* has been shown to be particularly sensitive to desiccation (Hübner et al., 2011), and so care must be taken when applying more realistic conditions to STMs to remove this factor where possible to allow differentiation between candidate materials and negative controls. Fungi present strong survival on inanimate surfaces (up to four months) but in a relative humidity dependent manner (high relative humidity improves fungal persistence) (Baudisch et al., 2009). The persistence of viruses are also dependent on the relative humidity depending on whether they are enveloped, non-enveloped viruses survive longer in higher relative humidity environments while the reverse is true for enveloped viruses (Julian W Tang, 2009). This phenomenon has been attributed to cross-linking of the surface proteins (Cox, 1989). The development of resistance to desiccation can occur via several methods, such as via the presentation of intrinsically disordered proteins (Hincha and Thalhammer, 2012), this is often naturally occurring in eukaryotic cells (fungi) but can also develop in bacterial cells where these proteins inhibit the aggregation of surrounding denatured proteins, limiting desiccation stress (Chakrabortee et al., 2007). An additional mechanism of desiccation resistance that is particularly prevalent in *E. coli* is the use of trehalose, a non-reducing disaccharide (Jiang et al., 2018) that stabilises and promotes the refolding of

denatured proteins (Tapia and Koshland, 2014), as well as preventing carbon stress via protein acetylation and aggregation induced carbon overflow (Moruno Algara et al., 2019).

1.3. Antimicrobial materials

1.3.1. Current non-material practices for controlling microbial growth

There are various methods that can be utilised to control microorganisms on surfaces in these settings. In clinical environments, methods to chemically disinfect surfaces are often used, but may be performed inadequately (through poor adherence to cleaning protocols), allowing pathogens to be spread more rapidly throughout wards, following recontamination of disinfected surfaces via contact with fomites (Meinke et al., 2012). Additionally, disinfectants may themselves drive the evolution of resistance. For example, quaternary ammonium compounds (QAC) have long been considered an effective class of disinfectants and were once thought to be impervious to bacterial resistance. However, an approximate 30 % increase of QAC resistance genes has been observed in methicillin-resistant *Staphylococcus aureus* (MRSA) isolates in the years 1990–2010 (Jennings et al., 2015). To compound this issue further, QAC resistance can undergo horizontal gene transfer to spread resistance and can also propagate the transfer of other antibiotic resistance genes (Y. Han et al., 2019). Disinfecting rooms through exposure to high intensity UV light can be effective at killing the majority of microorganisms it illuminates, but requires all staff and patients to leave the room during the process as a safety requirement (Hosein et al., 2016).

1.3.2. Classifications of antimicrobial materials

The mechanism of action of AMMs can be divided into three major subgroups: biocide release, contact active, and anti-adhesive properties (Adlhart et al., 2018). Each of these approaches has their own advantages and limitations in situ (Sjollema et al., 2018). Contact active-based claims are the most abundant in the literature, being delivered by both active substance release systems and those with potentiated surfaces. Arguably, systems that release less active substance may mitigate any increase in prevalence of antimicrobial resistance associated with AMMs (Kaur and Liu, 2016).

Active substance release systems discharge a biocide or antimicrobial agent and this is often triggered through hydration which is then intended to kill microorganisms on the surface and can be highly effective (Shukla et al., 2010). They can be applied to and

incorporated into a wide range of materials (e.g., synthetic polymers) and deployed in a wide range of environments. This can range from FTS in hospital wards to internal devices in patients such as orthopaedic and cardiovascular implants (P. Wu and Grainger, 2006), as well as in non-clinical environments such as call buttons and in coatings on hand rails on public transport (Buhat et al., 2020).

Potentiated surface-based AMMs can be fabricated by the inclusion of a biocide, metal, peptides, or amines on the surface of the material to add an antimicrobial function to that surface (Tiller et al., 2001; Campoccia et al., 2013; Hans et al., 2013). Common materials used include Ag nanoparticles (AgNPs) (Sondi and Salopek-Sondi, 2004; Khadka et al., 2018; Yan et al., 2018), Cu (S. L. Warnes and Keevil, 2011; Chandraleka et al., 2014; Giannousi et al., 2014; Vincent et al., 2018), tin disulphide (SnS_2) (Fakhri and Behrouz, 2015), ruthenium (Ru) (Bolhuis et al., 2011; Vaishampayan et al., 2018) and titanium dioxide (TiO_2) (F. Chen et al., 2009). Within this subcategory of AMMs are photocatalytic materials, that present their antimicrobial effect when exposed to irradiation (e.g., TiO_2). However, a longer working time can be required for photocatalytic materials to significantly reduce the microbial bioburden (Sichel et al., 2007). However, doping (e.g., nitrogen (Lee et al., 2013)) does add further potential for increased efficacy (Burda et al., 2003).

In addition to the mechanisms described above, which focus on a molecule entering or interacting with a cell in some detrimental way, other mechanisms for modifying and potentiating surfaces also exist. For example, carbon nanomaterials (e.g., graphene oxide) have also been shown to be effective at reducing the microbial bioburden on a surface by piercing / damaging cells using jagged, sharp, and sturdy surface features (Omid Akhavan and Ghaderi, 2010). Graphene oxide can also ‘generate’ reactive oxygen species (ROS) (Azizi-Lalabadi et al., 2020), and therefore uses multiple features to achieve the desired antimicrobial effect (Zheng et al., 2019).

Non-adhesive AMMs have been designed to combat the transfer of microorganisms, as they prevent a microorganism from being able to adhere to the surface, which is therefore also easily cleaned (e.g., by presenting hydrophilic properties (Holmes et al., 2009)). However, it is important to note that an AMM only incorporating this method would likely not reduce the rate of infection in patients, as studies have shown that, particularly

bacteria, are able to overcome this 'line of defence' when no other antimicrobial properties are being exhibited (Salwiczek et al., 2014).

There exists a range of applications for which an antimicrobial surface may be a desired option in some settings, with numerous options for manufacturers including different materials / additives and manufacturing processes. However, the variation in approach means that not all AMMs are equal and are likely to all exhibit individual levels of efficacy specific to their product design and intended end-use. As the market for these materials increases, manufacturers of AMMs are required to demonstrate their materials work as intended—meaning efficacy testing is a critical component in AMM development, sale, purchase, and end-use decision-making.

1.3.3. Examples of common antimicrobial materials

Antimicrobial materials can be separated into distinct categories based on the primary mechanism of action. A popular approach to developing AMMs is incorporating a metal ion or nanoparticle into the material to confer antimicrobial properties (Beyth et al., 2015), whilst other methods utilise anti-adhesive (Teixeira-Santos et al., 2021) and photocatalytic (Shenfu Chen et al., 2010) properties. Common AMMs include:

1.3.3.1. Silver

Silver has high effectiveness and low toxicity (Mei et al., 2017), making it an ideal candidate in appropriate applications. For example, the agricultural sector (Sharma et al., 2012; Abd-Elsalam, 2021), biomedical sector (Z. Huang et al., 2011) and water-treatment sector (S. A. Khan et al., 2022) among others have all benefited from the implementation of Ag-based nanomaterials. There are numerous mechanisms of action of Ag, which hinders the development of antimicrobial-resistance that is becoming increasingly relevant to the modern world. The exact mechanisms of the antimicrobial action of nanoparticles incorporating Ag are not fully understood. However, it is likely a combination of cell wall and membrane damage due to positive ion interaction with the negatively charged bacterial cell wall (Hamouda et al., 2019) as well as deactivating respiratory enzymes and producing reactive oxygen species (ROS) that disrupts adenosine triphosphate (ATP) production (Arif and Uddin, 2021). Furthermore, the size of the nanoparticle influences the antimicrobial efficacy, whereby smaller nanoparticles allow for greater antibacterial action via increased penetration into the bacterial cell (Shaikh et al., 2019). On the other hand,

several studies dispute the antimicrobial efficacy of Ag nanoparticles under low relative humidity environments (Trond Møretrø et al., 2012; Dominguez-Wong et al., 2014), likely owing to the lack of mobilisation of Ag^+ ions without the presence of moisture. Therefore, the applications of Ag are best restricted to those with high moisture levels, such as indwelling devices (S. Zhang et al., 2019; Coman et al., 2021) and water treatment (Lalley et al., 2014; Parandhaman et al., 2015). Leaching is also of significant concern with the use of several antimicrobial materials such as Ag due to the release of a significant number of ions into the environment, although leaching concerns have been mitigated with recent advances (Lalley et al., 2014). Although this does allow for an antimicrobial effect, it is important to consider the environmental impact of any material as well to create a more rounded approach.

1.3.3.2. Copper

Copper (Cu) provides excellent antimicrobial properties and is used in many applications, such as for antibiofouling in marine environments (Delauney et al., 2009), healthcare applications (e.g., catheter and implant coatings (Burghardt et al., 2015; Gu et al., 2022)), and the built environment (Khan and Horner, 2007; Schmidt et al., 2016), among others. The antimicrobial properties of Cu (and Ag) have also been exploited across history to the earliest civilisations and was prescribed for septic processes approximately 2,500 years ago in ancient Rome (Lewis, 2009). Its mechanism of action is similar to that of Ag, with membrane depolarisation and ROS generation (depending on the oxidation state of the Cu ions) being responsible (Mitra et al., 2019). However Cu used in sheet form can cause physical damage to bacterial cells due to its sharpness and rigidity at the microscale (when used as CuO) (S. Das et al., 2014). Meanwhile ROS generation (Bezza et al., 2020) also damages the cells through secondary effects such as DNA damage, preventing the cell from replicating properly or producing proteins (Dryden et al., 2017). Cu does not appear to exhibit the same issues presented with Ag regarding low relative humidity environments, and still shows high efficacy in typical indoor environments (Michels et al., 2009), although this is disputed (Mayr et al., 2023).

1.3.3.3. Titanium dioxide

Titanium dioxide (TiO_2) is a commonly used additive in food packaging materials that exhibits an antimicrobial effect when exposed to ultraviolet light. Additional uses of TiO_2 include paints to retard spoilage and increase shelf life (Ganguli and Chaudhuri, 2021; M.

C. Chen et al., 2022) and water treatment (C. Han et al., 2016; Kusiak-Nejman and Morawski, 2019), among others. However, this is heavily influenced by the size, shape, and structure of the TiO_2 nanoparticles because a greater surface area will allow for more light activation. Titanium dioxide exhibits its antimicrobial effect through ROS generation in the same manner as Ag and Cu (Venkatasubbu et al., 2016), and therefore requires moisture to be able to move inside the cell. The combination of TiO_2 with other antimicrobial agents (by chemical binding) has also been investigated. Combination with Ag nanoparticles, Cu, and iron (Fe) all show enhanced antimicrobial efficacy (Werapun and Pechwang, 2019; Alotaibi et al., 2020; Younis et al., 2022). However, the antimicrobial effects of TiO_2 in low relative humidity conditions have not been studied, limiting their known use cases to where moisture is often present. Interestingly, TiO_2 nanoparticles have shown high efficacy when incorporated into face masks (O. B. Ahmed and Alamro, 2022) and in FTS in hospital wards (Reid et al., 2018), highlighting use in high relative humidity.

1.3.3.4. Graphene

Graphene is a carbon-based material that is arranged as a layer of honeycomb like lattices (Meyer et al., 2007). Its antimicrobial activity has been extensively studied and shows a range of mechanisms of action (Gomes et al., 2018; Pandit et al., 2021), and has also been shown to possess significant antiviral efficacy (O Akhavan et al., 2012; Ziem et al., 2017). The antimicrobial activity of graphene can depend on several characteristics of the specific product. For example, the number of sheet-layers present may alter the antimicrobial efficacy although this is somewhat disputed in the literature (Yaragalla et al., 2021). One study found that increasing the number of layers reduces the "nanoknife" effect, whereby the material will physically pierce the membranes of microorganisms, and that three sheets with corner sites to pierce cells is optimal (Jiuling Wang et al., 2013). However, it is also noted that an increased sheet number has been reportedly linked to a greater antimicrobial effect against microorganisms that come into direct contact with the surface of the material (Romero-Vargas Castrillón et al., 2015), although it should be noted that graphene oxide was used in this case. As the mechanism of action of graphene does not require moisture to be active, very few studies focus on the effects that relative humidity plays on the antimicrobial efficacy of graphene. However, one study found high efficacy of a graphene / zinc oxide PVA hydrogel in low relative humidity conditions (Shuang Chen et al., 2023).

1.4. Global regulations to antimicrobial materials to address regulation issues

Regulation is a mechanism by which governments and decision-making bodies can control the actions of a particular industry. For antimicrobial materials, this comes in the guise of controlling the use of biocides and other antimicrobial additives. Approval of a biocidal product incorporated in the treated article (the term used in many regulatory processes to describe an antimicrobial surface) must occur before any product is commercialised in the UK, or indeed many global markets including the EU, US and across Asia.

The European Union uses the same system as Great Britain (GB), whereby the competent authorities of every member country are involved in regulation change and approval of products. The agency responsible for biocide approval is known as the European Chemicals Agency (ECHA). ECHA specifies all approved biocidal products in an article 95 list, which is updated as biocides are approved or removed. Initially, the GB list was transferred directly from ECHA as the UK separated from EU rule during Brexit, but each product was required to be re-approved.

A key feature of regulation of antimicrobial surfaces is the antimicrobial 'claim' – the label with which the manufacturer can publicly claim efficacy. These claims are regulated for new products, and when combining an already approved treated article into a more complex article (UK, 2022b). Labelling treated articles involves providing any instructions and precautions (if required to prevent harm to humans, animals and / or the environment). Additionally, labelling must identify and include all active substances (the components that are involved directly in the antimicrobial effect) and nanomaterials.

When a new biocidal product is brought to market in the UK, it must be added to the GB Article 95 list before use (UK, 2022a), which includes all available to sell and distribute biocides in Great Britain. To add a biocidal product or active substance to the list, an application to the Health Security Agency (HSA) should be completed that includes a variety of information about the product, including data on efficacy and safety in all capacities that is then thoroughly verified before approval. Technical equivalence also needs to be evaluated, whereby if there is a change in the manufacturing process of the product or if the source of the product has changed, then re-approval (although not as extensive a process) is required to determine if there is a significant increase in the hazardous properties of the product (Executive, 2022).

The United States of America (USA) uses the Environmental Protection Agency (EPA) and the Food and Drug Administration (FDA) to set and uphold the regulation of biocidal products with the use of the Federal Insecticide, Fungicide, and Rodenticide Act (FIFRA) (U. S. E. P. Agency, 2022). In this case, biocides that are used in non-medical devices are incorporated as antimicrobial pesticides. As with many laws in the US, products generally must be approved in each desired State (i.e., New York State) before having the ability to market within that State. FIFRA does prevent states from requiring additional labelling and packaging requirements but does allow states to require additional data. Many aspects of United States regulation are like that in the UK and EU with regards to approval of products, including testing for efficacy and safety of the product.

Japan has a much more general approach to the regulation of biocides, with the chemical substances control law (CSCL) (ChemSafetyPro, 2015), which regulates the production and import of any chemical that could pose a risk to human health or the environment. The industrial safety and health law (ISHL) is also in place to protect the health of workers and involves approval by the ministry of labour and welfare before production or import is allowed, and whether a safety data sheet (SDS) is required. In a similar manner to other governing bodies, Japan also has a list (such as article 95) of existing and new chemical substances (ENCS) that are pre-approved to use and requires a similar application process through the laws above to add an additional chemical / biocide. Additionally, the Society of Industrial Technology for Antimicrobial Articles (SIAA) (Articles) provides a logo to any product deemed to be antimicrobial via testing in a Japan National Laboratory Accreditation (JNLA) approved laboratory (Evaluation).

1.5. Standardised methods as an answer for regulators

A significant part of applying for registration to a list of approved biocides is demonstrating the efficacy of the biocide to the regulators. STMs allow users to follow a method that has been designed and tested reproducibly, promoting a level of confidence that the material will be antimicrobial when implemented. This also allows for a simple transition to other markets if required as efficacy has already been demonstrated in a reproducible manner. As STMs are often created and tested through international collaborations and committees such as the International Biodeterioration Research Group (IBRG), the American Society of Testing and Materials (ASTM), and the International Standards Organisation (ISO), they

allow for additional assurance that the product has been approved in a manner that many regulators can support. Additionally, STMs are designed in a way where they are relatively easy to perform, understand and communicate, which can help when considering the complicated process of biocide product approval in many countries. As the methods are standardised, the results of similar products are often comparable; therefore, it is easier to judge the relative efficacy improvement of one product over another and whether any increase in human, animal, and environmental hazards is justified.

Standardised test methods are a necessary and important step in the development of a novel AMM. To define a material as antimicrobial, efficacy should be assessed under reproducible conditions that mimic later in-use environments. If the predetermined threshold (usually a 2 or 3-log reduction in viable cells although often individually agreed upon by all parties involved) is not met, then the surface cannot be considered as antimicrobial. This process should enable those interested in AMM's to ascertain a level of confidence in their material, providing some preliminary positive data that encourages further exploration for testing the material either under conditions more appropriate to the intended point of use or even in practice. For example, bacterial inocula used in standardised testing (~10^5–10^8 CFU / mL) are significantly higher than those found in most potential end-use settings (e.g., ~10^2–10^4) (Sinclair and Gerba, 2011).

Additionally, in order to validate the reproducibility of an AMM, ideally several different labs should perform the relevant STM and achieve results that are all within the natural error range (Bloomfield and Looney, 1992). Whilst the validity of individual STM data should be acknowledged, a growing need exists for precise and reproducible methods, as many different AMM´s fall short when being tested by independent reviewers (Ioannidis, 2005).

In several cases, the STM used to determine the efficacy of an AMM are inadequate due to a variety of factors including the incubation time / environmental conditions. In some cases, this can artificially favour the increased and / or prolonged efficacy of the material, particularly by raising the relative humidity to >90 %, a condition which is almost never seen in end-use environments (Noyce et al., 2006; Michels et al., 2009). Many of the materials used in AMM's require moisture to be antimicrobial, metallic Ag for example, which is ionised in the presence of moisture to form Ag^+ ions which have numerous

antimicrobial properties. Therefore, knowledge of the length of time a surface remains moist for (the evaporation time of the deposit carrying the contaminating microorganism on the surface) is vital for an accurate judgement on the efficacy of the surface (Rai et al., 2009). This reliance on moisture must be considered when testing surfaces for effectiveness at point of use. Indeed, knowing the time it takes for an inoculum (a suspension of microbial cells of any manner) applied as a liquid to evaporate in each environment is key to assessing the activity of many AMMs.

1.6. Review of current standardised test methods available for non-porous antimicrobial materials

There are five general categories of test for an AMM in vitro (Sjollema et al., 2018):

(1) high surface area to volume ratio tests,

(2) agar zone of inhibition tests,

(3) suspension tests,

(4) adhesion tests,

(5) biofilm tests.

These tests differ depending on the method of action they are evaluating but also come with unique advantages and disadvantages. Many STMs are constructed and defined by several different method development organisations such as ISO (International Standards Organisation), BS (British Standards), IBRG (International Biodeterioration Research Group), and ASTM (American Society for Testing and Materials). There have been many iterations and modifications of these methods described in the literature that deviate based on the individual preferences or limitations of the testing laboratory, which then makes a comparison of the data generated for similar materials in different laboratories problematic. There has also been a significant shift to more realistic STMs in recent times to focus on how the materials would be exhibiting their antimicrobial effects while in use. However, the ease of use of the STM as well as the ability to perform any new methods with as little additional expense as possible should also be considered.

1.6.1. High surface area to volume ratio

1.6.1.1. Bacteria

These methods focus on maximising the contact between the surface and the microorganism, so the cells and the surface are essentially always touching and interacting. This is usually done by placing the bacteria between the test sample and another sterilised

non-antimicrobial material such as glass or plastic. However, this creates unrealistic conditions as it prevents the inoculum from evaporating on the surface, promoting an extended antimicrobial effect for the material that is to be tested. The most used STM for AMMs in this category is ISO 22196:2011 (ISO, 2011) (and similar methods such as JIS Z 2801 (Standards, 2012)). Here, a surface is inoculated with a bacterial suspension of known concentration and volume. A polyethylene film is placed on top of the inoculum, and the material is incubated at 35 °C in upwards of 90 % relative humidity for 24 h. Bacteria are removed from the surface by mechanical detachment and re-suspension in a neutralising diluent, before the number of colony forming units (CFUs) is determined by plate count. This method is relatively straight-forward and low-cost, and so has been widely adopted. However, many of the experimental conditions do not relate to end-use environments. Indeed, in most cases, the opposite is true, ISO 22196:2011 keeps a microbial inoculum wet for the duration of the 24 h test, allowing the AMM to provide a sustained antimicrobial action by dissolving into the water and this way ensuring contact between the cell wall of a microorganism and the biocidal active substance—which will not mirror the conditions when an AMM is implemented. To overcome such shortcomings, recent developments include an STM where bacteria are aerosolised, so they are deposited onto a dry surface, in an attempt to reduce artificial antimicrobial action resulting from the deposition of a wet microbial inoculum (ISO, 2011). However, dry deposition is not without its own challenges, for example ensuring reproducible inoculum quantity and ensuring a safe working environment from the release of pathogens into the air. Thus far, the development of a simulated splash test has been of increasing priority to address some of these shortcomings from both methods. In this case, an inoculum of either 1µl or 25µl would be applied many times to a test material and a covering film would not be applied, this is in line with allowing the inoculum to evaporate when placed in more realistic conditions (ambient conditions of 24 ^{o}C and ~50 % relative humidity) and provides the method with a direct end-use condition of either droplets from coughing etc. coming into contact with the material or larger droplets from more substantial bodily secretions or spilt drinks etc.

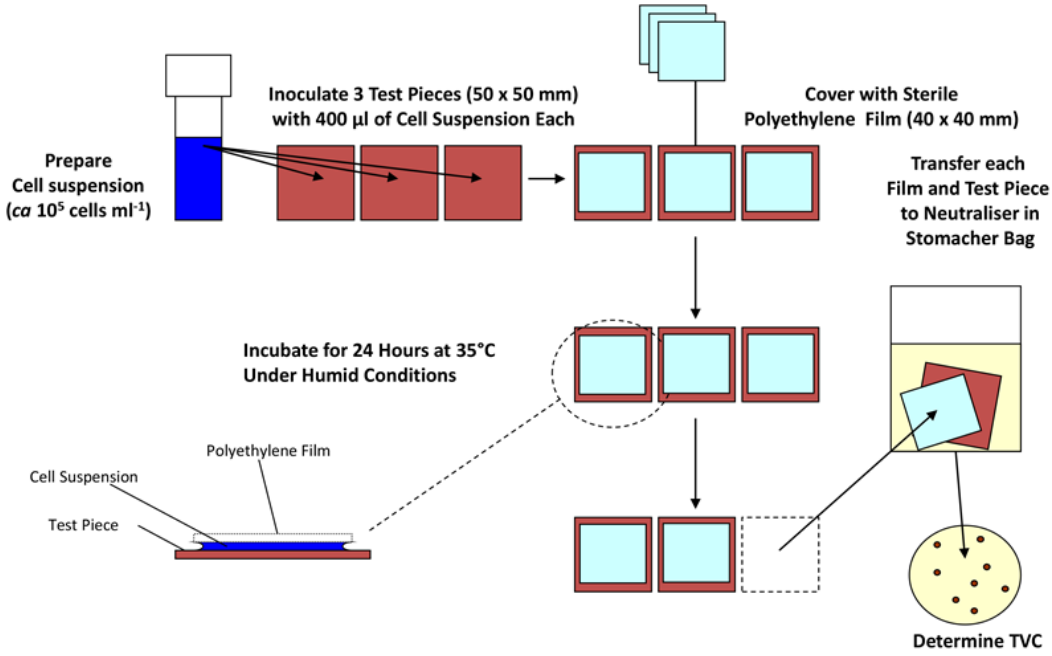

Figure 1 Diagram describing important steps in the ISO 22196 antimicrobial materials efficacy test (Cunliffe et al., 2021).

Other methods using a high surface area to volume ratio have been reported in the literature. One method (a modification of ISO 22196:2011) involves inoculation of the AMM with a bacterial suspension within a film of agar (commonly made into a slurry) to ensure that contact is maintained between the AMM and the test organism. When recovering the bacteria from the material, a neutraliser is used to resuspend the inoculum (neutralising diluent is a key step in many antimicrobial STMs to prevent superfluous interactions between the material and microorganism) and bacterial viability is determined. However, it is possible that the slurry (when required) has a soiling effect on the material preventing it from performing its antimicrobial effect as efficiently as possible due to different diffusion rates and characteristics into an agar slurry (Elsmore, 2013; Sjollema et al., 2017). Another modification of ISO 22196:2011 uses a filter that has been inoculated with bacteria as the top layer rather than a polyethylene film to reduce loss of microorganisms through fewer manipulations (omitting droplet inoculation) (van de Lagemaat et al., 2017). Alternatively, a liquid bacterial suspension can be sprayed (to simulate the typical deposition of airborne bacteria on to a surface by coughing, etc.) on to the AMM from 15cm, followed by live-dead staining after being air-dried for two minutes. Spraying of microbes rather than deposition has the advantage of being more representative of a patient in a hospital in most cases but is more complicated to run (and standardise) than simply placing a droplet of inoculum on to the surface, as it requires specialist equipment.

Another pitfall of this STM (and many others) is that a consortium of microorganisms is not used, this therefore does not represent the end-use conditions that the material would encounter, whereby a range of different species would be present that may even be a mix of fungi, viruses, and bacteria. It is understandable to not further complicate the method by adding in more variables that could be changed between laboratories, making any comparison more difficult (the current ISO 22916 method allows for up to two different bacterial strains to be used). However, this would allow a more representative example of how an AMM would perform when implemented into an end-use scenario and provide purchasers of the AMM additional confidence in the materials efficacy.

In conclusion, several authors have developed methods that are related to ISO 22196, presumably due to their ease of use and relatively low cost. However, there are many limitations in the translation of the results obtained, with most relating to the dissimilarity of the conditions standardised in ISO 22196 compared to end-use environments (both clinical and non-clinical) and others arising from difficulties in comparing results from methods that slightly differ between laboratories.

1.6.1.2. Virus

Although there is an STM for demonstrating the antiviral activity of a non-porous material (ASTM E2721-16 (ASTM, 2016)), there are few papers that employ it. Of those that do, only specific areas of the STM are employed, such as for the production of artificial saliva (Thomas Wu, 2022) and to inform on a soiling agent to use (J. Alt et al., 2022). The STM assesses the virucidal properties of surfaces when inoculated with aerosolised droplets of human respiratory viruses and is in some ways more realistic than its bacterial counterpart, as the viral load is sprayed on to the surface that aims to represent the deposition of the virus from human respiratory origin. Also, the STM uses a comprehensive soiling agent (as opposed to often no soiling agent in other STMs) that aims to mimic human saliva, that would be seen in end-use conditions.

The methods more often used in the literature are paper specific and have many differences between them, making any comparison of the methods and materials that were tested unreliable. The environmental conditions employed in these methods are often highly different or not recorded. For example, one paper assessing a Cu surface used no soiling but tested at 22 ^{o}C and between 50-60 % relative humidity, which could be

considered realistic environmental conditions (Noyce et al., 2007). Whereas another paper testing sol gel coatings did not use a soiling agent and also did not record either temperature or relative humidity during the test, this does not allow a direct comparison between the materials in any way (Hodek et al., 2016). One other consideration is the contact time, which ranges from one minute (Campos et al., 2012) to 24 hours in the literature but is most often around two hours (Park et al., 2014; Sarah L. Warnes et al., 2015), this allows for an incredible range of results due to longer exposure to the material and the fact that viruses do not often survive on inanimate objects for long periods of time whether antimicrobial or not. It is important to note that even the standard E2721 does not specify temperature and relative humidity requirements and therefore no guidance has been provided on the topic despite the importance of environmental conditions on AMM efficacy.

1.6.1.3. Fungi

The STM for the antifungal efficacy of a material is ASTM G21 (ASTM, 2021c), this method is much more extensively used in the literature than the viral equivalent and allows for the evaluation of resistance to fungal growth on plastics and synthetic polymeric materials. The STM does still use some unrealistic environmental conditions, such as a temperature of 28-30 ^{o}C and >85 % relative humidity but does show a long incubation period of 28 days allowing for a more detailed analysis of the material's fungal resistance. Also, this test does use a consortium of five relevant fungal species (inoculated in spore form), which allows for a more representative analysis of end-use conditions. Interestingly, staining is used in this STM as opposed to bacterial viability assessment (likely due to the larger size of most fungi making accurate counting difficult), with a general allowance of no more than 10 % of the coupon covered by fungi post-incubation.

Despite a somewhat acceptable STM being present, some of the literature still deviates, this may allow for better extrapolation to a specific end-use scenario but does hinder the comparison of materials that are tested. For example, one paper describes using ASTM G21 in the expected manner but adds a submersion in water for the first four hours of the test (H.-L. Huang et al., 2015). This would allow increased antifungal efficacy from the material if an active material is present but may map well on to some cases such as intermittently used water pipes.

1.6.2. Agar zone of inhibition

Methods that utilise zones of inhibition, for which there are two existing STMs, are relatively quick and simple but may provide only an indicator of whether any antimicrobial effect might be present under permanently wet conditions. The first, ISO 20645:2004 (ISO, 2004a) is based on a disk diffusion method, where the AMM is placed on top of an inoculated nutrient agar plate, incubated at the required temperature for a set time depending on the requirements for the bacteria being tested (such as at 37 °C for 24 h for *E. coli*) (ISO, 2004b). The second, AATCC 30 (which evaluates fungi rather than bacteria), places a spore suspension on to a solid agar medium and covers that with the AMM. Inoculation with spores also occurs on top of the AMM after placement, the petri dish is then sealed to maintain the relative humidity and efficacy evaluation is based on macroscopic or microscopic visibility of fungi (AATCC, 2017). These methods have limitations such as (i) the incubation temperature is not relevant to end-use scenarios (often it is the optimal growth temperature for the test organism), (ii) incubation time is not reflective of expected cleaning protocols (FTS's are likely to be touched more than once per day), and (iii) the nutrients present from the agar would likely not be present so abundantly on surfaces, all of which reduce the similarity to end-use environments. In addition, if the active substance is not emitted from the AMM, activity is unlikely to be measured, limiting applicability to a subset of AMMs. Furthermore, the viability of the test microorganisms may be compromised by the material being placed directly on top, even when exhibiting no antimicrobial effect. Nonetheless, the results provided from these STMs can allow a quick and simple approach to determining whether a material has at least some antimicrobial activity, which may be all that is required at the first stages of product development. Additionally, these methods can be used as a reliable quality control step during the production of an AMM once approved (Åhman et al., 2019).

It should be noted that both STMs assess the efficacy of textiles as opposed to non-porous surfaces, but both of which are used extensively in the literature. Methods conforming to ISO 20645 often did so according to the STM, allowing for a more representative comparison between materials (Dhanapriya and Ratna; Gaidau et al., 2019; Özkan et al., 2019; Habibi Mohraz et al., 2021; Akyildiz et al., 2022).

1.6.3. Suspension

Suspension methods focus on inoculating and incubating bacteria in a liquid medium containing an AMM, and then determining bacterial viability by taking an aliquot of this liquid and performing a dilution plate count. This allows assessment of AMMs that exhibit antimicrobial-release properties. However, due to the inoculum not being placed directly on the material, only surfaces that release antimicrobials can be tested. There are two current STMs. The first, ASTM E2149-13a (ASTM, 2013), requires that the material is immersed in the medium (that is most appropriate for the bacteria used) following bacterial inoculation, then after incubation while shaking to enable increased contact of the AMM to the bacteria, then the bacterial viability is determined via CFU quantification. This method was developed with the intention of determining the effectiveness of silane QACs by agitating the suspension with sufficient vigour to cause cells to come into contact with the QAC 'tails' (Caschera et al., 2019), although this method is somewhat disputed. A modification to this method has also been developed whereby the entire suspension container is treated with the antimicrobial to prevent biofilms forming and to avoid complications arising from the extensive agitation that is required for the STM. The second, JIS L 1902 (and also the absorption method within ISO 20743), describes the incubation of a porous material absorbing a specified volume of the appropriate medium, bacteria are then detached from the porous material using a stomacher in 20 mL neutralising diluent, and bacterial viability is determined in the resultant suspension (ISO, 2021). For methods where an antimicrobial substance has leached into a liquid medium (which will then be diluted and plated onto agar), in which both suspension methods utilise, a neutralising solution is essential—to ensure continued antimicrobial action does not occur during the dilution and bacterial viability determining incubation stages (24 h at the most appropriate temperature for the bacterial strain used). As these methods do not assess contact-killing materials, it is not possible to assess efficacy for using such materials in some end-use conditions, for example, as a touch surface. These methods are actively used in the literature with no major changes allowing for comparison of materials. Additionally due to the requirements of the methods, relative humidity is not a factor, but temperature is kept artificially high at 37 ^{o}C throughout the test which would likely not represent the end-use conditions for the AMMs.

1.6.4. Adhesion

These tests focus on quantifying the number of bacteria that can adhere to an AMM. There are two approaches to this form of testing. The first requires that the test surface is inoculated with the bacteria and incubated for 1 to 4 h. Non-adhering bacteria are removed and either the surface with attached cells is added to a liquid medium or an agar slab is placed on top of the surface and incubated (for determination of bacterial viability), or the microorganisms can be stained (e.g., live-dead staining) to determine cells per unit area (Héquet et al., 2011). The second method specifies a flow of bacterial suspension through a chamber containing the AMM, then live-dead staining is performed on the cells attached to the surface to determine the survival status of adhered cells. Alternatively, the cells are detached from the surface of the AMM and re-suspended so that the bacterial viability of the resultant suspension can be calculated (Albright et al., 2017). Finally, a proliferation assay can be used, which involves inoculating an AMM for a given time, followed by rinsing and placing in a soy medium. The efficacy of the AMM is determined by the number of clonal counterparts produced by the surviving bacteria that are attached to the AMM; real-time spectrophotometer readings are essential to creating a growth curve to compare a control to the AMM (V. Alt et al., 2004). In both methods, there are issues that arise from how effectively the detachment of bacteria occurs, even by sonication (which can cause the diluent to heat up), as this may also reduce the viability of the organisms and their growth on media.

These methods have many advantages in being able to test for non-adhering materials, but also come with drawbacks. Firstly, the temperature used is again at 37 ^{o}C, an unlikely scenario for any AMM. Secondly, if an agar slab is placed on top of the coupons with the aim of growth for assessment of bacterial viability, this may reduce the available air to the microorganisms and reduce their viability (assuming aerobic requirements).

1.6.5. Biofilm

A biofilm is an assemblage of microorganisms that are associated with a surface and often become encased in a matrix of polysaccharide (Donlan, 2002; Schachter, 2003; Kim et al., 2019). They are one of the most common forms that microorganisms take on Earth and can cause significant problems when they form in certain artificial environments. Due to their impact on health, industry and the environment, the ability to either destroy a biofilm or to stop it from initially forming using AMMs is a focus of increasing importance. However,

biofilm development and testing are complex, and whilst recent efforts to advance standardised biofilm growth (e.g., ASTM E2647—20 (ASTM, 2020) and ASTM E3161—21 (ASTM, 2021a)) and efficacy testing of disinfectants against biofilm exist (Goeres et al., 2019; ASTM, 2021b), methods for efficacy testing of anti-biofilm materials are limited and suffer from problems regarding quantification of the bacteria, as staining will offer little insight and sonication may cause a reduction in viability, although some use of bioreactors for biofilm testing is taking place (Dumitrache et al., 2015). As biofilm STMs are outside the scope of this work and would add significant complexity, further analysis of biofilm test methods will not be focused upon.

1.6.6. Incubation / environmental factors affecting the efficacy of antimicrobial materials in standardised test methods

If an STM should inform on the efficacy of an AMM under end-use conditions, the environmental conditions of that STM need to be considered carefully. For example, if moisture is essential for activity of an AMM, an STM that includes a high relative humidity, no airflow and warm temperature will result in the bacterial inoculum remaining wet for the duration of the test and will provide optimal results for that AMM. However, if that putative AMM would be used in a more realistic setting (such as a hospital ward), relative humidity is likely to be considerably lower (30 % to 65 %) as will the temperature (18 °C to 28 °C), and there will be air circulating (e.g., via movement of doors, people, and air conditioning) (England and Improvement). Contaminating droplets of liquid are likely to evaporate quickly, reducing the time for which the AMM is active and essentially allowing efficacy to become a function of evaporation time. Most existing STMs for AMM testing vary in their environmental condition stipulations, but only to a relatively small degree. Environmental conditions such as these can alter the efficacy of an AMM, and therefore careful consideration should be given when designing or interpreting data from an STM.

Table 1 Examples of methodological test conditions used in several standardized efficacy test methods.

Name of Standard	Material Type	Organisms Used	Time	Relative humidity	Temperature (°C)	Criteria for Being AM	Other Conditions
EN ISO 846:1997	Plastics	*Aspergillus niger; Penicillium funiculosum; Paecilomyces variotii; Gliocladium virens; Chaetomium globosum; Pseudomonas aeruginosa*	4 weeks	97 %	29	No visible growth to the naked eye	None
EN ISO 20743:2013	Textiles	*Staphylococcus aureus; Klebsiella pneumoniae*	18–24 h	70 %	37 ± 2	CFUs < 1 × 10^5 reduction of life of 50 %	None
EN ISO 22196:2011	Plastics / non-porous	*S. aureus; Escherichia coli*	24 ± 1 h	>90 %	35 ± 2	Agreed upon by case	None
ISO 27447:2019	Ceramics / photocatalytic	*S. aureus; K. pneumoniae; E. coli*	18–24 h	No mention	37 ± 1	Log reduction of 0.8	None
EN 16615:2015	Non-porous surfaces	*S. aureus; Enterococcus hirae; P. aeruginosa; Candida albicans*	60 min	No mention	4–30 ± 2	5 log reduction	None
ISO 18184:2019	Textiles	Influenza A; Feline Calcivirus	3–5 days	No mention	34	Antiviral efficiency of >2	5 % CO_2
ISO 21702:2019	Plastics / non-porous	Influenza A; Feline Calcivirus	2–3 days	No mention	34	Agreed upon by case	5 % CO_2
ISO 18061:2014	Ceramics / photocatalytic	Bacteriophage Q beta; *E. coli*	24 h	No mention	37 ± 1	Log reduction of 0.8	None

1.6.6.1. Relative humidity

Relative humidity is an important determinant for the evaporation time of liquid droplets (James Redfern et al., 2018), and therefore is most likely linked to AMM efficacy. In most cases, a reduction in the relative humidity of the environment results in a lower antimicrobial efficacy of an AMM because of the reduction in moisture at the surface through evaporation. For example, when assessing the activity of a Cu alloy surface (with varying Cu quantities in the alloy), incubating at 37 °C and 100 % relative humidity can provide a 4-log reduction in around 30 min for all alloys higher than 70 % Cu content (Hassan et al., 2014). However, when the environmental conditions are more analogous to that of an indoor room, at approximately 20 °C and 40–50 % relative humidity, the time taken to achieve the same 4-log reduction of viable bacterial load is doubled to 60 min (Ojeil et al., 2013). Despite this, Cu exhibits a greater affinity to retain its antimicrobial activity under varying environmental conditions than most. For example, Ag^+ ions released from zeolites have demonstrated significant antimicrobial effect at >90 % relative humidity, but the same composition showed no significant antimicrobial effects at 24 % relative humidity and a temperature of 20 °C. Although neither relative humidity used in this study can be considered typical, it highlights the importance of the role that relative humidity plays in either increasing or reducing the antimicrobial efficacy of an AMM (Michels et al., 2009). Noyce, Michels and Keevil (Noyce et al., 2006) suggests that Ag^+ ions exhibit significantly decreased antimicrobial efficacy when the relative humidity is reduced to around 20 %, again emphasizing the requirement for relative humidity to be considered when performing AMM STMs. Furthermore, Ronan et al. (Ronan et al., 2013) have shown that desiccation resistance is also significantly affected by the relative humidity, and this has downstream effects on the microbial survival on a surface, whereby survival of microorganisms can be greater at lower (~25 %) relative humidity's compared to higher (~95 %), this work also highlights that interactions between bacterial species allow for greater survival on materials compared to pure cultures. Finally, this work uses aerosolisation to deposit bacteria on to the surfaces, alleviating the disadvantages that droplets at high relative humidity possess on the antimicrobial efficacy of an AMM. It should be noted that different mechanisms of action will affect whether relative humidity plays a role in the antimicrobial efficacy of the material. For instance, AMMs that are designed to puncture cells through nano-spike based methods will not be reliant on

moisture in any way in order present high efficacy, but metal ion releasing materials, such as those discussed above will have a low tolerance to reductions in the relative humidity in the surrounding environment.

1.6.6.2. Temperature

Temperature has been shown to affect the survival of microorganisms on a surface (J. Redfern and Verran, 2017), and has also been shown to significantly affect the release of antimicrobial compounds from an AMM (Kashiri et al., 2016). Additionally, temperature does significantly affect the evaporation time of water on non-porous surfaces (James Redfern et al., 2018) and therefore potentially affects antimicrobial efficacy due to the resulting change in relative humidity that occurs. For STMs to become more realistic, changing temperature is required. Most STMs use ~37 ^{o}C as it is the optimal temperature for growth in many human commensal and pathogenic organisms, but this is not what is found in many end-use scenarios, and a reduction to between 18-24 ^{o}C would more closely reflect the conditions seen in indoor acclimatised areas (Ormandy and Ezratty, 2012). Although an artificially high temperature benefits the microorganism rather than the material (assuming the microorganism favours the temperatures used currently), it still disassociates any results gathered from end-use scenarios.

1.6.6.3. Airflow

There is limited published research into the effect of airflow on the evaporation time and / or antimicrobial efficacy of a material. However, the evaporation time of a liquid droplet on a non-porous material has been shown to be slower in the absence of airflow (James Redfern et al., 2018). In addition, the transfer of infectious aerosols in hospitals is well understood and the ventilation system has been associated with much of this concern (J. W. Tang et al., 2006). Thus, airflow is perhaps an important environmental factor that has been significantly overlooked in the design of testing AMMs—even more so than relative humidity and temperature as it has never been considered in a relevant STM. When considering the inclusion of airflow, it is important to consider that a new STM with realistic conditions will allow the evaporation of inocula on the test material and thus airflow will promote a difference in the antimicrobial efficacy of the material by increasing the evaporation rate. How the flow dynamics of the airflow will affect the evaporation time of the droplet and how the microorganisms within the droplet will act is yet to be well researched.

1.6.6.4. Hydrophobicity, hydrophilicity, and surface topography

In addition to the environmental conditions described above, the surface features such as hydrophobicity and surface roughness can have a significant impact on how long moisture takes to evaporate on the surface (Richard et al., 2020). While a hydrophilic surface allows water to spread out evenly over the whole surface and to evaporate more uniformly, a hydrophobic surface results in the formation of droplets that cover the surface only in parts and that will evaporate slower compared to the same volume when placed on a hydrophilic material. Hydrophobicity and surface roughness will dictate the contact angle created with a droplet; when the contact angle is larger from an increased hydrophobicity, the droplet will possess a lower surface area to volume ratio, also therefore decreasing the evaporation time (Kulinich and Farzaneh, 2009). The surface topography is the underlying mechanism behind many anti-adhesive materials, but the evaporation mechanism of other materials which is caused by the surface tension (which is in part due to the surface topography) also plays a role in the efficacy of an AMM via the deposition of bacteria in the droplet as it dries.

1.6.6.5. Spreading of the inoculum

Spreading plays an important part of some antimicrobial tests. Spreading generally occurs by adding a sterile plastic (non-antimicrobial) film on to the inoculum immediately after inoculation onto the material (e.g., ISO22196) but other methods such as manual spreading via a pipette tip is also used (Gross et al., 2019). However, increased care should be taken when considering the spreading of the inoculum, as inconsistencies in the spreading process are almost inevitable between laboratories and even individual persons, leading to differences in the evaporation time of the droplets / inoculums and the repeatability of the results. Spreading must also be considered alongside hydrophobicity data of the AMM, as hydrophobicity will partially dictate how easily, if at all, the inoculum spreads across the surface, further increasing the possibility of unreliable results (Nakajima, 2011). If hydrophobicity / hydrophilicity is part of the function of the AMM, comparing results from materials on which the inoculum exhibits dissimilar spreading rates may be problematic and will need to be taken into consideration. In some STMs (such as ISO 22196), particularly hydrophilic surfaces may cause the inoculum to spill beyond the edge of the coupon, in the case of this thickening agents such as agar may be added to encourage hydrophobicity, but

this will likely have major consequences to the survival of the microorganisms on the surface, although these are currently yet to be thoroughly researched.

1.6.6.6. Exposure time

A longer exposure time will allow more interactions between the microorganism and the AMM, potentially causing an increase in observed antimicrobial effect. Current STMs take this into account and specify an exact incubation period within which the STM should occur. However, relating this period to the intended end-use is essential, particularly where an AMM is anticipated to be touched with high frequency. For example, current hospital cleaning requirements mandate that every material that is to come into contact with patients should be thoroughly cleaned at least daily and in most cases after every interaction (Healthcare, 2018).

1.6.6.7. Threshold to achieve antimicrobial claim

Often a 2-3 log reduction in microbial viability is required although it is at the discretion of all involved parties to agree to a value that is appropriate to the end-use. The scale and speed of an effect must be appropriate to the benefit that is intended / required. Absolute numbers may also be a valid method of assessing antimicrobial activity, as a reduction of 1-log from a higher original inoculum concentration may be enough in some circumstances to stop the risk of infection and / or damage to infrastructure caused by the growth of microorganisms on the surface.

In addition to those described above, there are other factors that can influence efficacy in end-use situations and are often not considered. For example, the aging of materials through repeated contamination and cleaning procedures can reduce the efficacy of an AMM but are rarely considered in STMs.

1.6.7. Overview of current standardised test methods

As described above, a variety of STMs exist that can determine the antimicrobial activity of a material. With this comes variations and alterations to each method based on the specific conditions of the testing laboratory at the time and date of testing, among other factors. This will likely affect the accuracy and reproducibility of the resulting antimicrobial efficacy of the material. It is worth noting that some modifications may allow the method to be more appropriate to the question being asked. Whilst the methodological variation from a STM is with good intention, for example, using a temperature the investigator considers closer to room temperature, the effect on reproducibility can be profound. For example, if

two different labs were to consider the antimicrobial efficacy of a given material, following an STM, but one used a test chamber / container that was bigger than the other lab, there would be an impact on the time it takes to reach the intended relative humidity. This would affect the ability of the inoculum to remain wet on the surface, and therefore alter the time the AMM is likely to be active for. The same can be true for other experimental factors such as the method of achieving the desired relative humidity (using concentrations of saturated salts), controlling temperature (placing a chamber in an incubator compared to using a heat mat), the speed at which samples are removed from a chamber for different time points and so on. Often, these seemingly small changes to methodology alter the reproducibility between laboratories. For example, one study asked different labs to assess the antimicrobial efficacy of the same materials (polyamide 6 and an antibacterial zinc additive at multiple concentrations) using ISO 22196:2011. Following analysis of the data, several factors were found to be inconsistent between labs, such as extraction medium and method of cell enumeration, which led to a large disparity in the final results obtained, where the microbial reduction ranged from 1.73-log to 6.30-log for the same antimicrobial compound (Wiegand et al., 2018). Care should also be taken to ensure the method of cell enumeration is not only consistent across all laboratories using an STM but also that it is appropriate for the specific STM that is being used, live-dead staining for instance is not always effective, particularly when assessing biofilms (Netuschil et al., 2014).

Whilst many STMs have been designed to be useable and achievable in a range of laboratories, issues remain in terms of the validity of the methods. Most critically, how can efficacy in realistic uses be inferred using the data that the STMs generate—because the current STMs are not reflective of realistic in-use conditions. Additionally, the current methods of microbial viability determination focus mainly upon assessing the colony forming units before and after an incubation period in contact with the prospective AMM. There are two main issues with this method, the first is that contact with an antimicrobial material may induce stress on the microorganisms present so that they are viable but non-culturable (and are still capable of causing infection (Ramamurthy et al., 2014)), reducing the accuracy of the STM. Also, the limit of detection for colony forming unit counts is generally very high, causing difficulties in assessing significance in the data between the active materials and the negative controls. Despite this, it is an extremely common method

of indicating viability of microorganisms on a surface due to simplicity, no requirement for specialised equipment and speed. It is abundantly clear that a considerable improvement is required in test methodology of AMMs if subsequent results are used to support efficacy claims for different environmental conditions while in use. This clash of intention and inference would be best addressed by an interdisciplinary approach to new antimicrobial efficacy STM development. However, the process of making any changes to current STMs should be taken with due diligence, as unexpected consequences are possible. For example, temperature and evaporation time of a droplet have been found to affect the rate of detachment of *Bacillus* spores from a surface once the droplet has dried, which will be more likely to occur if relative humidity is lowered to 40–50 % to keep in-line with a majority of indoor acclimatised settings (Faille et al., 2016).

Additionally, extensive work has been completed on the addition of microorganisms (bacteria and viruses) on the evaporation of droplets on a surface which will be discussed in detail in future chapters. In brief, the addition of microorganisms into a droplet promotes that droplet to evaporate in a constant wetted area mode, whereby the contact line of the droplet on the surface is pinned and the microorganisms congregate at the outer edges of the droplet (Morawska, 2005). This in turn causes the droplet to evaporate at a faster rate due to an increased surface area to volume ratio but also causes the microorganisms to stack on top of each other in many cases, this can create a conditioning film on the material that allows the microorganisms to survive simply by not touching the surface. These concepts will be explored further in this thesis.

Finally, there have been improvements in recent years that show promise in creating more realistic and higher reliability STMs. One potentially useful addition would be the implementation of video protocols to work alongside traditional paper protocols, allowing users to get an exact understanding of the nuances related to the STM. Another answer may lie in the recent advances in both computer simulations of heat / mass transfer and in the decreasing cost of improved microfluidic devices that provide the potential for both cheap and reliable STMs (H. Sun et al., 2019), which when integrated into an environmental control chamber could provide realistic and reliable antimicrobial efficacy assessment.

1.7. Project aims and objectives

Project aim

Develop a method to assess efficacy of non-porous antimicrobial materials using a purpose built and reproducible novel test chamber able to simulate intended end-use environmental conditions.

Project objectives

- Understand and critically appraise existing STMs that assess antimicrobial non-porous surfaces (e.g. plastic or metal), identifying the need for a novel and improved set of test methods.
- Assess the reproducibility of existing quantitative antimicrobial STMs.
- Measure the effect of different conditions (temperature, relative humidity, airflow, optical density, droplet size, material used) on the survival and infectivity of bacteria and viruses in inocula (liquid droplets) and the evaporation time of the droplet placed on a non-porous material.
- Develop a prototype environmental control test chamber to match the intended end-use of the test material, utilising key concepts in design engineering, heat transfer and modelling.

2. Building a reproducible novel test chamber to perform realistic standardised test methods

2.1. Introduction

One major issue with making significant changes to STMs is that some labs may not be equipped to work with them, facing limitations such as space, equipment, and expertise. Chambers with which existing STMs are undertaken are often boxes with water placed in the bottom (to provide relative humidity) and a grid to hold the coupons above in petri dishes. There is often no standard requirement for chamber size, permeability to the outside environment etc, leading to variation between different laboratories due to equipment choice. For example, when trying to raise the relative humidity to >90 % as per ISO22196 and many other STMs, the size of the chamber can make a difference to how quickly an equilibrium can be achieved, which may affect how the microorganisms in an inoculant interact with an AMM (e.g. by altering drying mechanics / time). Therefore, a chamber that can control temperature, relative humidity, and airflow while providing minimal relative humidity changes when opening the chamber to add or retrieve coupons (removing the need to re-equilibrate) is highly advantageous. This may also help with space requirements as an incubator is no longer required, and the chamber would be able to be placed almost anywhere with access to electricity. The comparability and stability of the environmental conditions in the chamber should be verified and thoroughly tested before the chamber can be considered for inclusion in STMs.

Designing and building such a chamber should use materials that are easily accessible, easy to use and that can be reproduced (manufactured) anywhere in the world. 3D printing provides one approach as 3D printers are now accessible consumer products around the globe (Shahrubudin et al., 2019). Electronics required to control environmental conditions would also need to be easy to use and understand, and accessible globally. There are many printed circuit boards (PCBs) that allow for the appropriate level of control an environmental chamber would require, for example, Arduino (Arduino, 2023a).

2.1.1. What parameters should a chamber achieve?

There are a variety of parameters that are important when designing a chamber to be used in AMM efficacy assessment that aim to utilise realistic environmental conditions, including:

- A temperature range of room temperature (~20 ^{o}C) to the maximum currently accepted temperature in a common STM (37 ^{o}C),
- A relative humidity range as wide as possible to simulate a variety of end-use scenarios, with the ideal range between 15-90 %,
- Airflow as even as possible across the testing platform where surfaces would be incubated,
- Maximise space to ensure as many materials as possible can fit in the chamber at any given time,
- Reusability and robustness of the chamber for an extended period (preferably >1 year of continuous use),
- Sustainably built using as many biodegradable materials as possible,
- Built with parts that are as easy to assemble with limited experience,
- The ability to remove samples without impacting the environmental conditions (within an acceptable range),
- Lightweight and easy to move (e.g., between laboratories)

The parameters described above were generated through meetings with industry partners (IBRG) as well as through assessment of the shortcomings of current STMs. For example, a cause for concern for industry partners was that the environmental conditions within a chamber are impacted heavily when opening the chamber to retrieve samples. As the size of the chamber, time of opening the chamber to retrieve samples and density of relative humidity controlling agents lacks standardisation, variation of results from STMs can occur. On the other hand, although not explicitly required by academia or industry to perform STMs, environmental impact is an important consideration in any modern process, therefore using biodegradable materials to construct the chamber reduces environmental burden.

2.1.2. 3D printing

3D printing has gained popularity in a variety of disciplines in recent years as a low-cost and rapid alternative to classic manufacturing techniques by creating a structure from a digital model. Fused filament fabrication is a technique used by many 3D printers involving the addition of successive layers of material until the desired structure has been completed (Singh et al., 2020). Polylactic acid (PLA) is a low cost, easy to print and biodegradable material that is used in a wide variety of applications for 3D printing (Tümer and Erbil, 2021). Polyethylene terephthalate glycol (PET-G) has a greater difficulty to print but an increased thermal tolerance than PLA without the requirement of an extractor fan that is required for other high-temperature tolerant materials (such as acrylonitrile butadiene (ABS)) (Menderes and Ipekci, 2021).

2.1.3. Airflow simulations

To develop an environmental control chamber with the capability to regulate temperature, relative humidity, and airflow, it is important to understand what key criteria need to be met. Evenly distributed airflow is vital for the reproducibility of realistic STMs due to the impact it can have on relative humidity and drying of liquids. Airflow simulations can be used to understand airflow accurately and extensively in a space. Computational fluid dynamics (CFD) involves modelling and simulating the flow of fluids (including gases) through an environment via computer algorithms (Bhatti et al., 2020). These simulations allow for the rapid testing of designs without the requirement for building each design individually, reducing the cost and time used. The use of fans to control the airflow throughout the chamber not only helps to simulate the use of air conditioning in many indoor acclimatised end-use scenarios but also allows the specification of input airflow speeds into the simulation software that is known to have low variability.

2.1.4. Temperature control

There are several methods capable of controlling temperature, including fan induced convection heating (X.-J. Li et al., 2022), typically used in ovens. This system uses a heating element and air currents to direct hot air throughout a chamber. However, the use of this system for the purpose of AMM testing includes several disadvantages, such as the temperature in a specified location being linked to the flow of air over said location, and the safety concerns of high temperature elements, both in terms of risk to the user and risk

of damage to the chamber. Silicone heat pads provide a similar process of heating (a heating element placed between silicone pads to distribute the heat) but is not directly linked to the airflow throughout the chamber and provides a better distribution of heating across the testing platform.

2.1.5. Arduino

The circuitry required for the chamber to operate electronics such as heat pads, fans and sensors are operated with an Arduino. Arduino is a widely recognised open-source platform that consists of a microcontroller (a small computer on a single PCB) to relay instructions (inputs and outputs) from accompanying software (Arduino, 2023b). The Arduino also offers a wide selection of widely available and cheap modules that would allow easy implementation of further capabilities of the chamber and its own integrated development environment (IDE) that allow changes to the code if a setup requires updating. Although other PCBs are available, the Arduino provides an accessible, usable, and simple solution that allows users to correct an issue without having to resort to specialist equipment or personnel.

2.1.6. Chapter specific aims and objectives

Design and build a prototype chamber capable of regulating temperature, relative humidity, and airflow using:

- Computational fluid dynamics to assess airflow and inform on airflow orientation,
- Computer aided design and 3D printing to build the chamber,
- Post-printing construction and testing to ensure the chamber is sealed,
- Arduino-based circuitry to control the various functions of the chamber,
- Programming of the Arduino to control the chamber's functions and log any data.

2.2. Methods

2.2.1. Airflow simulations

Before printing or construction, airflow simulations were carried out to understand the most efficient placement of inlet (fans) and outlet features. Seven air inlet / outlet designs were assessed to understand overall airflow. In each case the design was generated in AutoCAD to a standard size of 274x174x70mm, with input / output holes of size either 25mm or 50mm diameter and an assumption that either one or two fans would be used to generate airflow. The designs were then imported into SimScale (SimScale, 2023) for

simulation, which was used due to the availability and speed of running the simulations. An incompressible fluid simulation (a simulation of a fluid such as air at speeds of less than 0.3 Mach / ~100 m/s, where the density variation is assumed to be negligible) using air was used with input velocity of 3 m/s for all inlets (fans), and a mesh generated (breaking down the 3D model in to many sub-models) with a standard algorithm and fineness of 4 (equivalent to the amount of detail the simulation produces). Once the simulation had concluded, a cutting plane (a visual cross section through the modelled chamber) was generated on the Z-axis, placed at the centre of the inlet / outlet holes. And colouring (visualisation of the airflow) set to velocity magnitude. Also, a particle trace (simulation of an individual air molecule moving through the system) was added with 10 seeds (particles) horizontally and vertically with a spacing of 1.8mm and size $4.4e^{-1}$, placed directly next to the inlet in each case (Figure 2). If more than one inlet was present, multiple particle traces were implemented.

In order build a prototype chamber capable of regulating temperature, relative humidity, and airflow, three prototypes were created, with learnings from each one informing the following version. Each prototype version below describes the methods used to design, print, construct and evaluate the corresponding chamber.

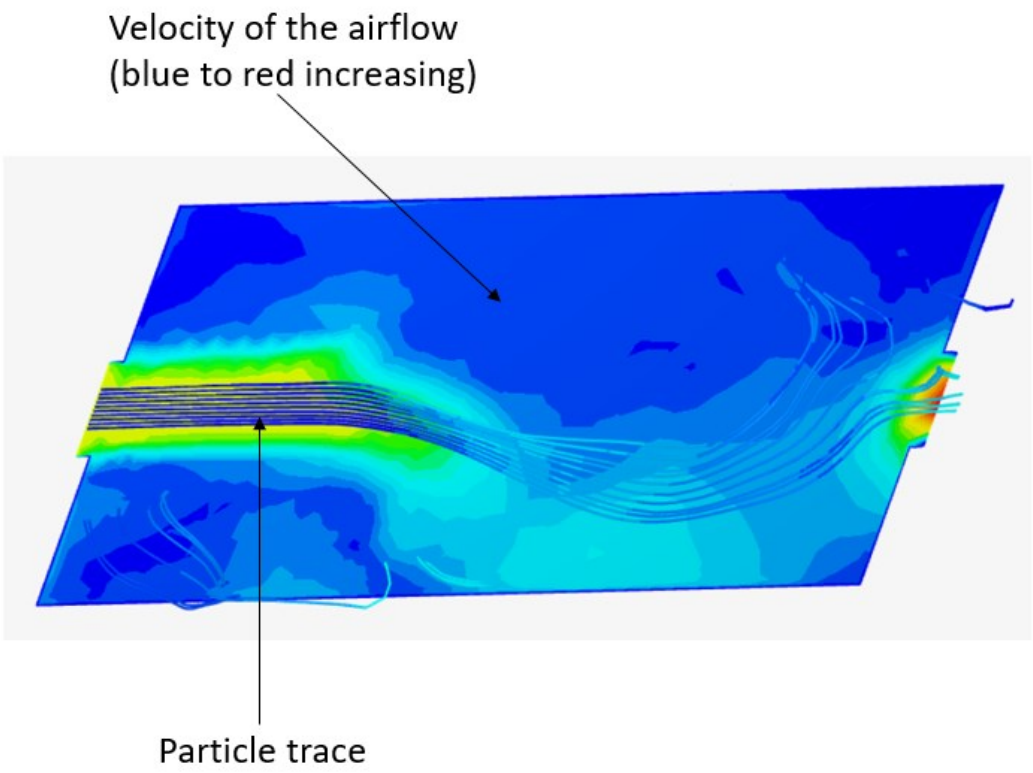

Figure 2 An example of a post processing SimScale simulation, presenting the velocity magnitude of the airflow by the varying colours (darker blue colours represent low airflow, red represents high airflow) and a tracer of individual air particles (particle trace).

2.2.2. Prototype version 1

2.2.2.1. Construction

2.2.2.1.1. AutoCAD designs

Using the preferential airflow intake / outtake placements (Figure 5, page 70), the initial chamber included two compartments, one that would be used to alter relative humidity (HC (humidity control) compartment) using saturated salts and airflow using fans, and the other to regulate temperature and for the test coupons to be placed (MT (material testing) compartment). AutoCAD was used to design each of the individual pieces required to build the chamber and each piece was then exported to .stl file type for compatibility with the printer-specific software(BCN3D Cura).

2.2.2.1.2. BCN3D Cura software, slicing and printing

Once imported into BCN3D Cura, each piece was loaded separately, sliced (process of converting a file from a 3D drawing to 3D printer instructions) and a .gcode file generated for each piece. All the files were loaded on to the SD (memory) card and transferred to the

3D printer and printed using PLA filament according to the standard operating procedure (SOP – Appendix B).

2.2.2.1.3. Post printing construction

To air seal the chamber for relative humidity retention, silicone (RS components) was applied to each of the pieces where they contact the adjacent piece (except for parts G, H and J – see Figure 4, page 69). Finally, the gap (which would subsequently be filled in future versions) at the end of the MT compartment was duct taped during testing to ensure no air (and therefore relative humidity) could leak into the outer environment. Once sealed, a heat pad (or two heat pads) of size 150x100mm and electrical allowance of 12 volts and 15 watts (RS components) was duct taped to the centre of the roof of the MT compartment (Figure 8, page 73 / Figure 9, page 73). A fan (RS components) of size 50x50x10mm was duct taped to the opening in the HC compartment to blow air directly into the MT compartment (fan B, Figure 7, page 72), described as the inlet in the airflow simulations. The wires for the fan were moved through the hole in the roof of the HC compartment and into an Arduino Uno R3's (RS components) 5V and ground inputs. The heat pad was wired out of the gap between parts B and C (Figure 6, page 71) and directly connected to a power pack set to 12 volts and one Ampere, once wired, silicone was applied to the holes thus that they were completely sealed.

2.2.2.2. Testing

Table 2 An overview of each test performed using prototype version one of the environmental control chamber and the parameters used in each.

Test ID	Figure ID	Target temperature	Target relative humidity	Location of sensors	Fans operating	Heat pads
1	Figure 10 – A	Maximum possible	N/A	MT compartment	No fan	One
2	Figure 10 – B	Maximum possible	N/A	MT compartment	One fan	Two
3	Figure 10 – C / D	Maximum possible	75 %	MT compartment	One fan	Two
4	Figure 10 – E / F	Maximum possible	100 %	MT compartment	One fan	Two
5	Figure 10 – G / H	Maximum possible	100 %	MT compartment	Two fans	Two

2.2.2.2.1. Temperature

To also test the effects of airflow on the temperature in the MT compartment, two scenarios were investigated, one without the fan operating (Test ID – 1) and the other with the fan operating (Test ID – 2). In both cases the power supply was set to 12 volts at one Ampere with an RHT10 temperature and relative humidity datalogger (Amazon) placed directly in the centre of the MT compartment. The sensor was set to read data values every 30 seconds for 2,500 time points (~20 hours). In the case of the test involving the fan, the Arduino was powered by an external 9V power supply (RS components) and the fan taped in fan position B (Figure 7).

2.2.2.2.2. Relative humidity

Two heat pads (both as described in 2.2.2.1.3) were implemented into the MT compartment of the chamber (to provide more distributed heating capacity) as shown in Figure 9 and were supplied power in series (power supply and heat pads were connected one after the other in a loop, as shown in Appendix B), but the voltage and current settings on the power supply remained the same. Also, the fan was set up in the same manner as previously described in 2.2.2.1.3. The relative humidity control in the chamber was provided by either saturated salt solutions or distilled water added to the pot in the HC compartment of the chamber. Additionally, in each relative humidity test, a second RHT10 sensor was placed directly on to the pot in the HC compartment. In the first relative

humidity test (Test ID – 3), 160g of potassium chloride salt (Fischer Scientific) was added to 80mL distilled water in the pot (split evenly between the four quadrants) to achieve a RH of 75 %. In the second (Test ID – 4) and third (Test ID – 5) tests, 80mL of distilled water (no salts) was added to the pot (washed thoroughly with water between tests and dried) to achieve a RH of 100 %, with a second fan added to the chamber in the third test. The fan was attached in the same manner as the first but in fan position A (Figure 7).

2.2.3. Prototype version two

Table 3 An overview of each test performed using prototype version two of the environmental control chamber and the parameters used in each.

Test ID	Figure ID	Target temperature	Target relative humidity	Location of sensors	Fans operating
6	Figure 13 – A	Maximum possible	N/A	MT / HC compartment	Two fans
7	Figure 13 – B	Maximum possible	N/A	MT compartment x6	Two fans
8	Figure 13 – C / D	Maximum possible	100 %	MT / HC compartment	Two fans
9	Figure 13 – E / F	Maximum possible	<15 %	MT / HC compartment	Two fans
10	Figure 13 – G / H	Maximum possible	<15 %	MT / HC compartment	Two fans
11	Figure 13 – I / J	Maximum possible	~40 %	MT / HC compartment	Two fans

2.2.3.1. Construction (developed from version one)

There were several changes made to this version of the chamber to improve temperature and relative humidity control features. The first was an increase in power supply so that each heat pad was supplied with 12 volts at one Ampere, as well as slots for the heat pads to be placed into the roof of the MT compartment. The walls and roof of the MT compartment were separated to allow ease of access to the chamber (two walls were connected to the roof in the previous prototype). A seal was designed and printed to reduce the leaking of air to the outer environment from the opening where the tray (that would contain samples) slides into the MT compartment of the chamber, Vaseline was used when gaps were still present to reduce leaking.

2.2.3.2. Testing

To assess the ability of the second version of the chamber to control temperature, two tests were performed. The first (Test ID – 6) involved powering the heat pads to the operational maximum (12 volts at one Ampere). The airflow was still supplied by two fans at the same placements in the chamber during these tests and no relative humidity control was employed (equal to ambient conditions). In the second test (Test ID – 7), a map of the temperature across the MT compartment was generated by placing sensors in the areas

shown in Figure 3. To assess the impact of the slots for the heat pads and the effect on temperature, the first test adhered the pads to the roof of the chamber without placing them in the slots.

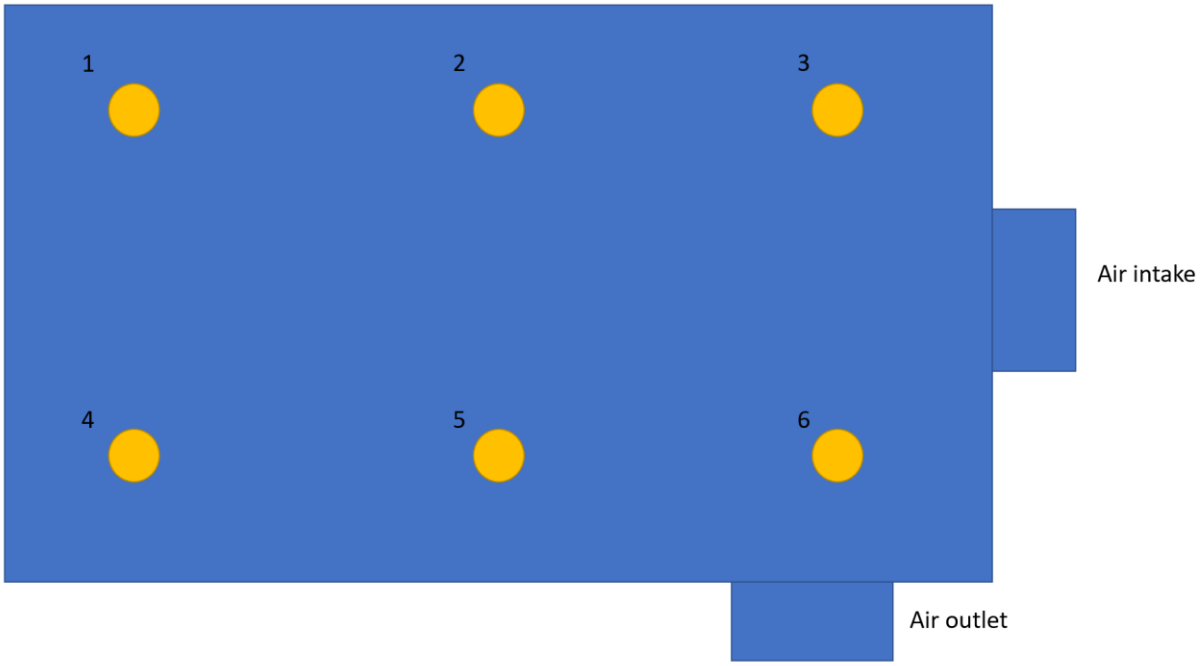

Figure 3 A representation of the RHT10 sensor placement within the MT compartment of the chamber to create a map of temperature and relative humidity.

The relative humidity of the chamber was assessed using water (Test ID – 8), lithium chloride (Test ID – 9 / 10), and potassium carbonate (Test ID – 11). The volume of water and weight of salt added to the pot in the HC compartment was equally divided between the four quadrants and is shown in Table 4. Expected values of relative humidity for potassium carbonate was 43 % (Eggert, 2022) and lithium chloride was 12 % (Wexler and Hasegawa, 1954). These targets were chosen to have a low range value (0-20 % RH) and a mid-range value (40-60 % RH). In each case, the temperature and airflow control were the same as the tests described above (2.2.3.2) and the sensors were placed in the same positions as in 2.2.2.2.2. Between each test (set of variables), the pot was thoroughly washed with water before salt was re-added.

Table 4 Quantities of salts and distilled water added during each of the relative humidity tests for the second version of the environmental control chamber.

Solution	Water volume (mL)	Salt amount (g)
Water	160	0
LiCl	40	80
LiCl	60	160
K_2CO_3	60	120

2.2.4. Prototype version three

Table 5 An overview of each test performed using prototype version three of the environmental control chamber and the parameters used in each.

Test ID	Figure ID	Target temperature	Target relative humidity	Location of sensors	Fans operating
12	Figure 16	Maximum possible	N/A	MT / HC compartment and lab bench	Two fans
13	Figure 17 – A / B	Room temperature (ambient conditions)	100 %	MT / HC compartment and lab bench	Two fans
14	Figure 17 – C / D	26 °C	100 %	MT / HC compartment and lab bench	Two fans
15	Figure 17 – E / F	28 °C	100 %	MT / HC compartment and lab bench	Two fans
16	Figure 17 – G / H	30 °C	100 %	MT / HC compartment and lab bench	Two fans
17	Figure 17 – I / J	30 °C	<15 %	MT / HC compartment and lab bench	Two fans

2.2.4.1. Construction (developed from version two)

The MT compartment of the chamber was altered so that the floor and walls were printed as a single piece to reduce air leakage. A protruding section was added next to the floor of the MT compartment at the opposite side to the HC compartment to allow easy access to the coupon tray and a more easily designed seal to reduce air leakage. The pot to hold water and salts was also double stacked with a gap of 15mm to allow double the quantity of relative humidity controlling agents. Additionally, a new power supply measuring a maximum of 12 volts at three Amperes was implemented and the heat pads were connected in series. The heat pads were replaced with 200x50mm counterparts with 12 volts at 80 watts power allowance. Additionally, as the new heat pads were of a different size, the shape of the holders was changed to accommodate.

2.2.4.2. Testing

Each test relating to the third prototype of the chamber was repeated in duplicate. One temperature-only test (Test ID – 12) was performed, where the voltage and current were set to 12 volts and ~3 amps. The test ran for 2.5 hours, instead of 24 hours as expected, due to the high temperatures generated. No relative humidity control or airflow was employed during this test. Several tests were performed to assess the temperature and relative humidity within the chamber when distilled water was added to the chamber (20mL per quadrant, 160mL total between two pots). Four different temperatures were assessed for this relative humidity set-up (room temperature (Test ID – 13), 26 ^{o}C (Test ID – 14), 28 ^{o}C (Test ID – 15), and 30 ^{o}C (Test ID – 16)) with all other variables as previously described for the second version of the chamber (2.2.3.2). An additional test (Test ID – 17) was performed whereby the distilled water was switched for lithium chloride (OXOID, UK) at 15g salt and 10mL water per quadrant (120g salt and 80mL water total) to determine low relative humidity capabilities. The final version of the code used to control the Arduino is shown in Appendix E. Throughout tests 14 – 17, the target temperature was above ambient but below the maximum achievable for this version of the chamber, therefore a relay module was added into the system whereby the heat pads would be switched off when the temperature sensor read above the target temperature and would be switched on when below the target temperature.

2.3. Results

2.3.1. Airflow simulations

The designs generated by the airflow simulations are shown in Figure 4, with varying inlet / outlet valve locations in each. The results of the Z-cutting plane are shown in Figure 5, with velocity magnitude scales represented by the colours. From these simulations, design F was chosen due to having the greatest overall consistent airflow across the MT (volume of green colouration). Designs B, E, and G were discarded for low airflow overall, while the other designs were discarded due to presenting a higher level of uneven airflow across the platform.

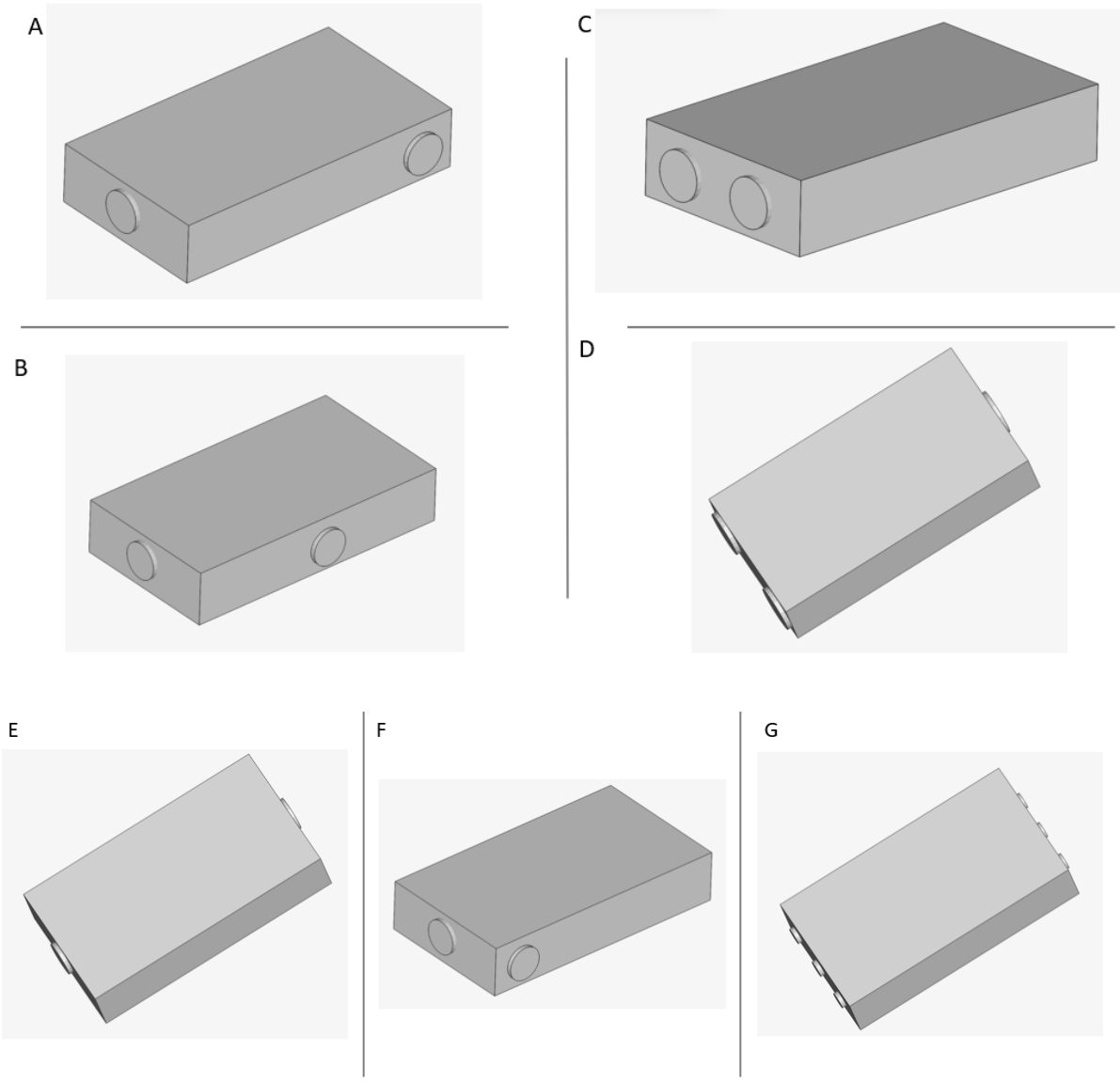

Figure 4 Potential AutoCAD designs for the environmental control chamber. In each case, the chamber was set to a standard size of 274x170x70 mm and protrusions of diameter 50 mm (or 25 mm in design G) for air inflow and outflow.

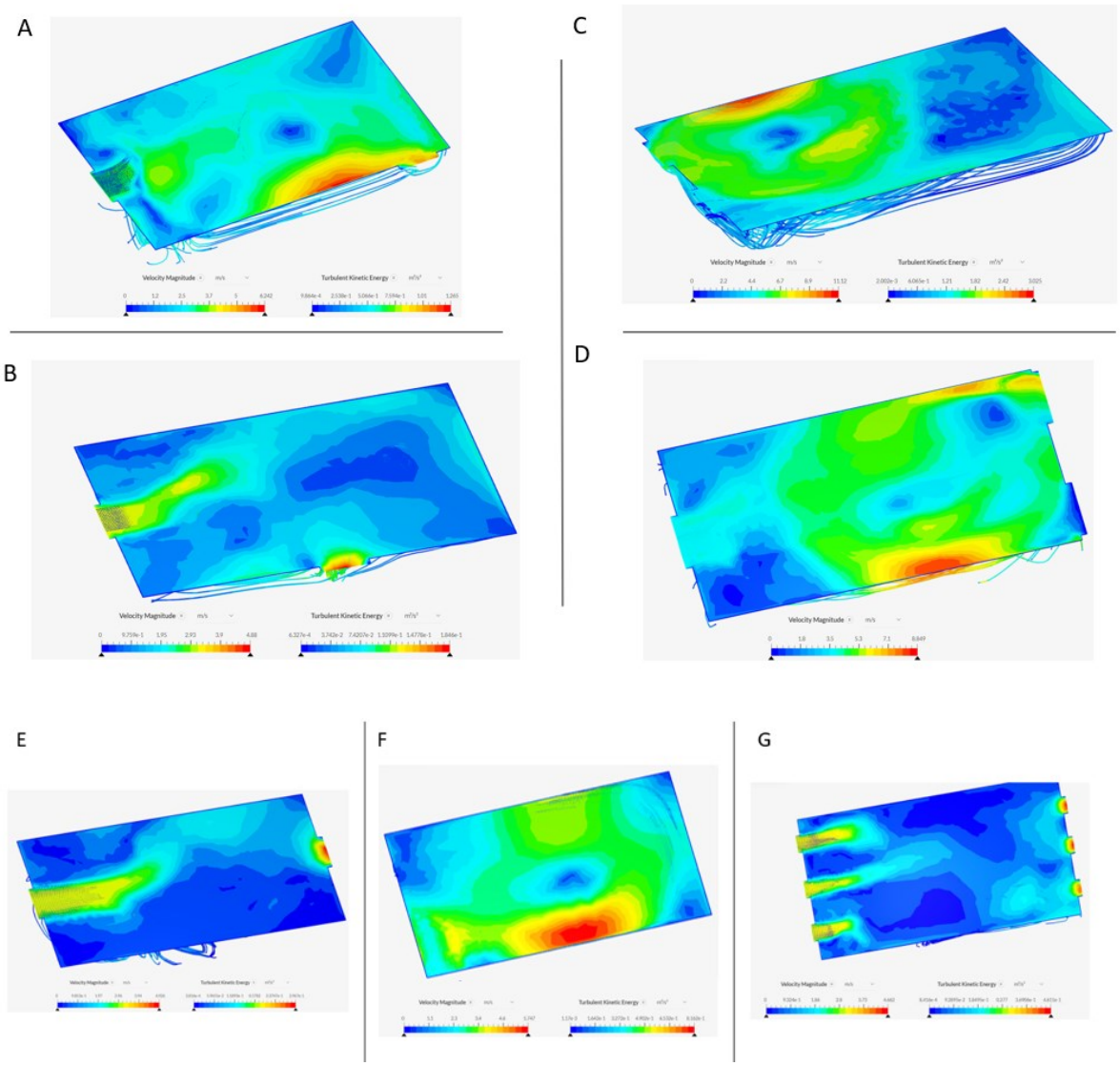

Figure 5 Airflow simulations of the designs for the environmental control chamber in SimScale. In each case the inflow of air originates from the left of each design at a speed of 3 m / s. A Z-cutting plane was used to observe the airflow for each design.

2.3.2. Prototype version one

2.3.2.1. Construction

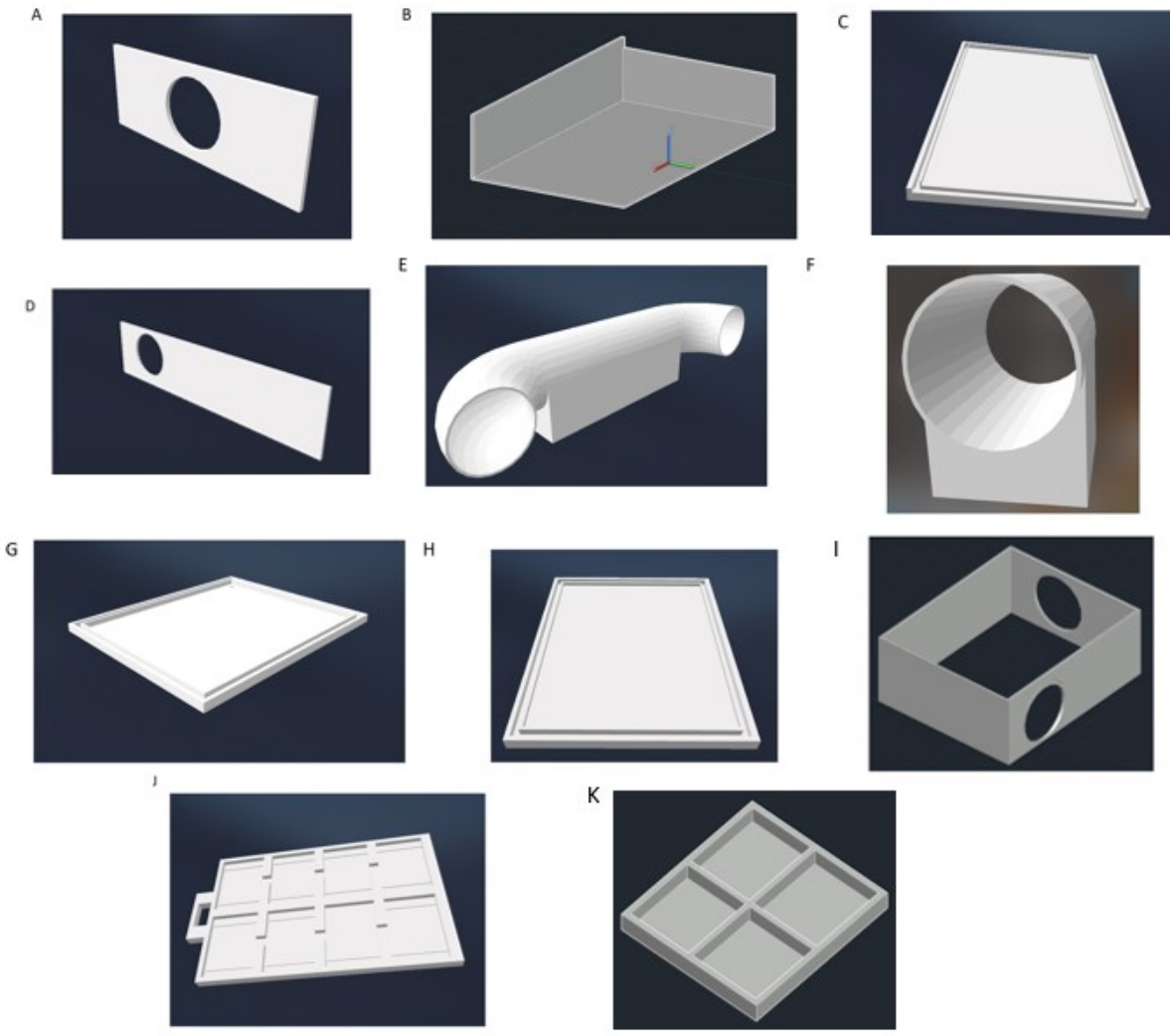

Figure 6 AutoCAD files of each of the pieces used to build the first version of the environmental control chamber. Files are labelled as follows: (A) MT compartment wall one (174x74x2 mm), (B) MT compartment walls two / three and roof (276x172x74 mm), (C) MT compartment base (278x174x10 mm), (D) MT compartment wall four (276x72x2), © Piping to connect compartments (300x81x70 mm), air movement in the direction of MT to HC compartment, (F) Piping to connect compartments (75x50x70 mm), air movement in the direction of HC to MT compartment, (G) HC compartment roof (170x140x4 mm), (H) HC compartment base (170x140x4 mm), (I) HC compartment walls (166x136x72 mm), (J) coupon placement tray (272x170x5), (K) HC compartment salt / water pot (121x109x17 mm).

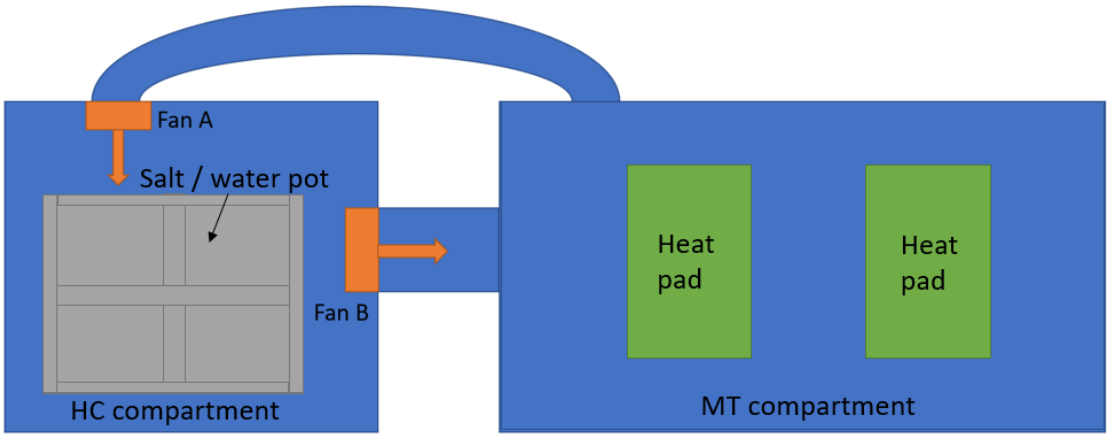

Figure 7 A representation of how prototype version one of the environmental control chamber was constructed. With fans represented in orange and direction of airflow represented by the arrows, when one fan is specified only fan B was operating. The grey represents the salt / water pot used to contain the relative humidity controlling agents and the green colour represents the heat pad locations (this placement was not used for Test ID – 1, where the configuration seen in Figure 8 was used).

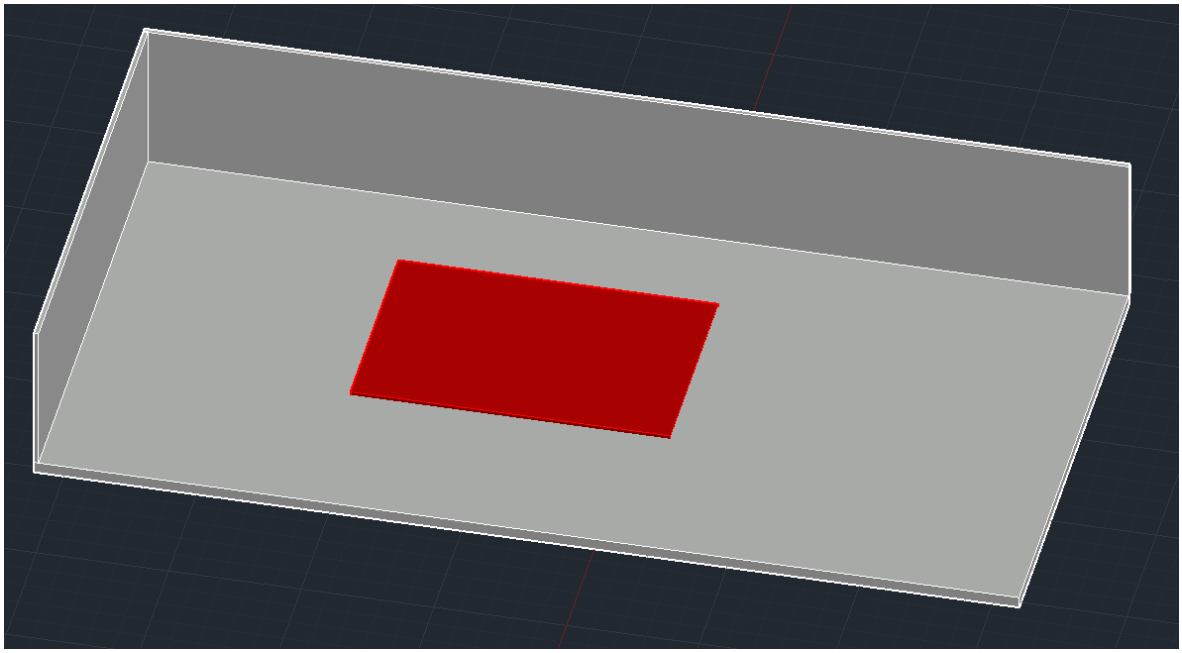

Figure 8 A representation of the MT compartment of the chamber prototype 1 (grey) and where the heat pad was duct taped to the roof of the compartment (red) in AutoCAD. This configuration was initially assessed but found unsuitable.

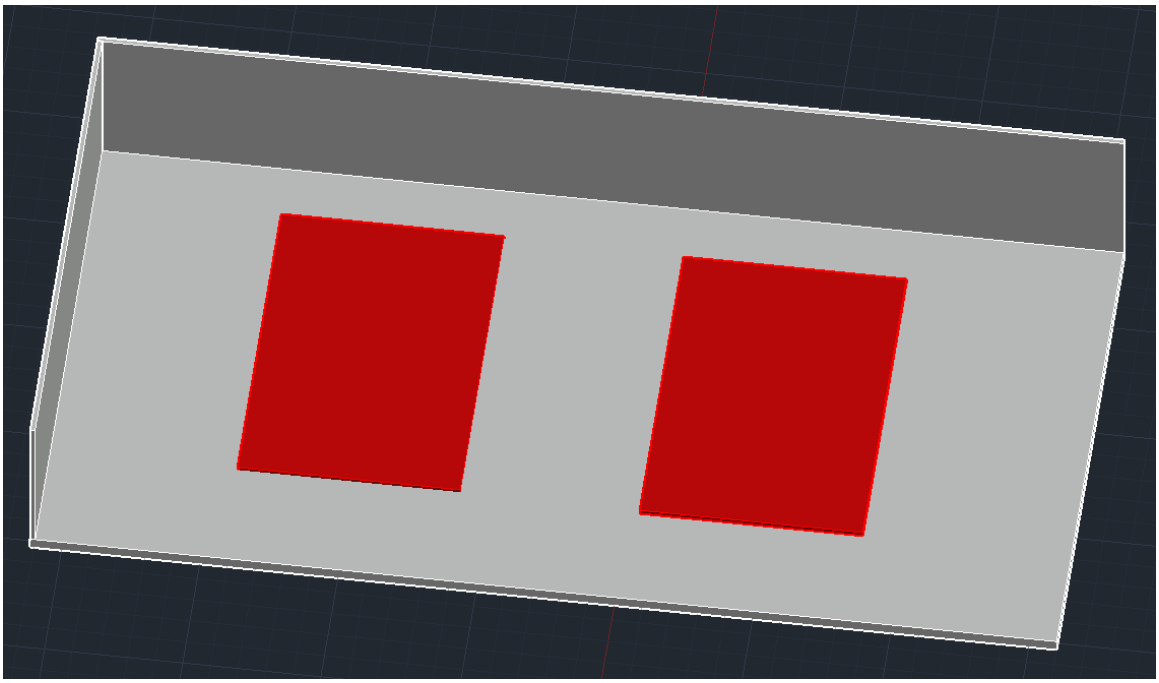

Figure 9 A representation of the MT compartment of the chamber prototype 1 (grey) and where the heat pads were duct taped to the roof of the compartment (red) in AutoCAD.

2.3.2.2. Testing

The first temperature-only test (Test ID–1 - Table 2) generated a consistent temperature across the duration of the experiment, with a variation of 1.7 ^{o}C post stabilisation (the point at which a peak in temperature is achieved for the first time). It took 130 minutes for the temperature to reach the first peak and a maximum and minimum temperature of 24.7 ^{o}C and 23.0 ^{o}C was achieved respectively.

The second temperature-only test (Test ID–2 - Table 2) also generated a consistent temperature across the duration of the experiment, with a variation of 1.5 ^{o}C post stabilisation. It took 190 minutes for the temperature to reach the first peak and a maximum and minimum temperature of 26.9 ^{o}C and 25.4 ^{o}C was achieved respectively.

The first relative humidity test (Test ID–3 - Table 2) generated consistent temperature and relative humidity values in both the MT and HC compartments, with a temperature variation of 2.1 ^{o}C (MT) and 2.2 ^{o}C (HC) and a relative humidity variation of 6 % (MT) and 2.4 % (HC) post stabilisation (relative humidity variation determined between temperature stabilisation and the first temperature trough henceforth). It took 160 (MT) and 260 (HC) minutes for the temperature to reach the first peak and a maximum and minimum temperature of 27.6 ^{o}C (MT) / 24.6 ^{o}C (HC) and 25.5 ^{o}C (MT) / 22.4 ^{o}C (HC) as well as a maximum and minimum relative humidity of 46.0 % (MT) / 50.2 % (HC) and 40.0 % (MT) / 47.8 % (HC) achieved respectively.

The second relative humidity test (Test ID–4 - Table 2) generated consistent temperature and relative humidity values in both the MT and HC compartments, with a temperature variation of 1.6 ^{o}C (MT) and 2.1 ^{o}C (HC) and a relative humidity variation of 2.3 % (MT) and 5.4 % (HC) post stabilisation. It took 160 (MT) and 130 (HC) minutes for the temperature to reach the first peak and a maximum and minimum temperature of 28.9 ^{o}C (MT) / 24.5 ^{o}C (HC) and 27.1 ^{o}C (MT) / 22.4 ^{o}C (HC) as well as a maximum and minimum relative humidity of 56.7 % (MT) / 81.0 % (HC) and 54.4 % (MT) / 75.6 % (HC) achieved respectively.

The third relative humidity test (Test ID 5 - Table 2) generated consistent temperature and relative humidity values in both the MT and HC compartments, with a temperature variation of 3.3 ^{o}C (MT) and 2.4 ^{o}C (HC) and a relative humidity variation of 5.2 % (MT) and 1.8 % (HC) post stabilisation. It took 90 (MT) and 130 (HC) minutes for the temperature to

reach the first peak and a maximum and minimum temperature of 29.1 °C (MT) / 25.0 °C (HC) and 25.8 °C (MT) / 22.6 °C (HC) as well as a maximum and minimum relative humidity of 62.2 % (MT) / 82.0 % (HC) and 57.0 % (MT) / 80.2 % (HC) was achieved respectively.

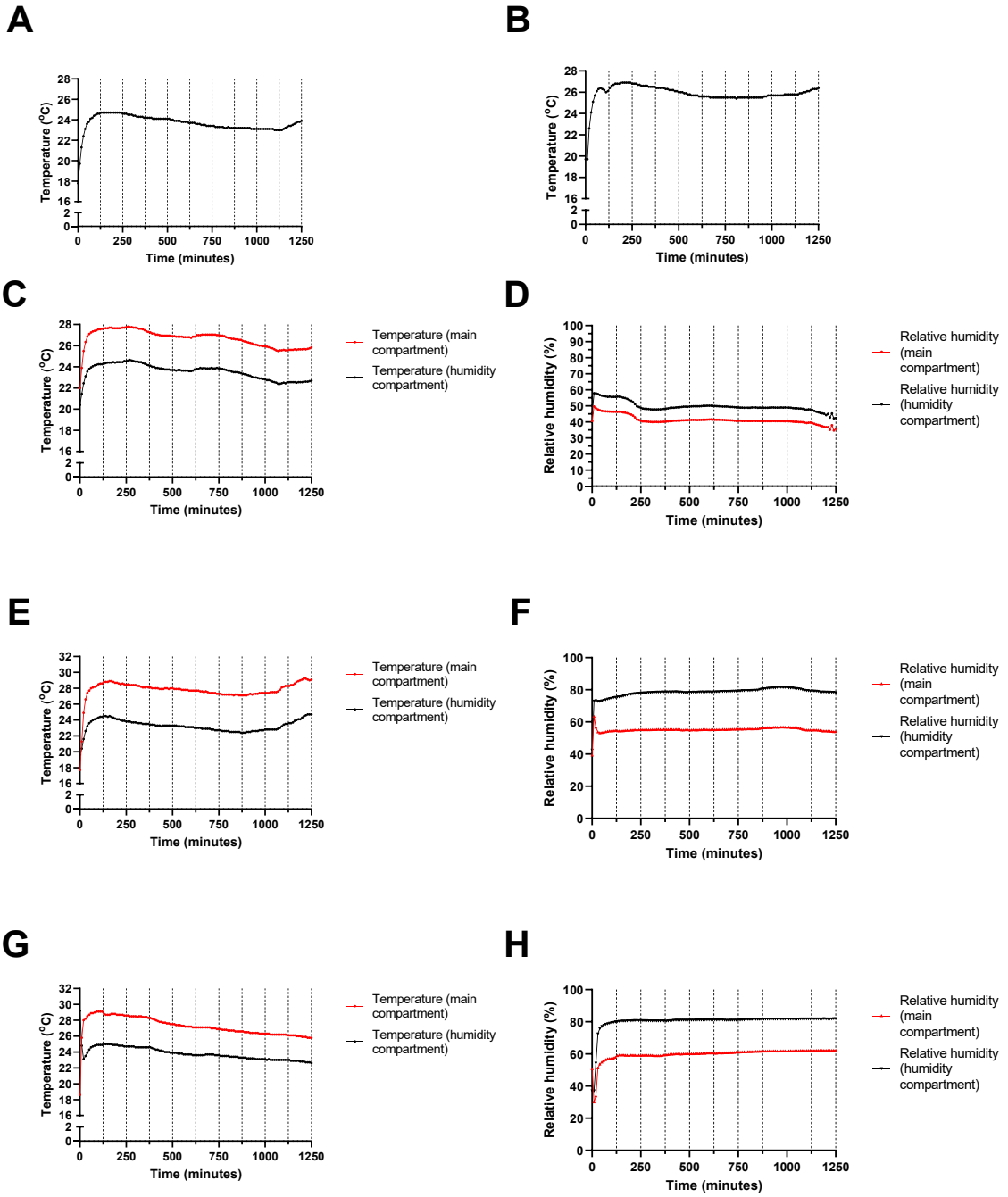

Figure 10 Temperature and / or relative humidity values in the chamber under various conditions of heater-based power, airflow and relative humidity controlling solutions. (A) and (B) represent no relative humidity control, one heat pad present and either (A) one fan operating or (B) two fans operating. (C) and (D) show temperature and relative humidity values respectively across the chamber with two heat pads at half power, two fans operating, and saturated potassium chloride added to the HC compartment. (E-H) show temperature and relative humidity values as described for (C / D) with water replacing potassium chloride and either (E / F) one fan operating or (G / H) two fans operating.

2.3.3. Prototype version two

2.3.3.1. Construction (developed from version one)

The design of the 3D-printed sections that constitute version two of the chamber was shown in Figure 11. Each section was printed separately, and support material (additional material added to allow higher layers with otherwise no material directly underneath to be printed without collapsing) removed where necessary (sections B and E, Figure 11). This prototype of the chamber had changed from prototype version one in the following ways:

- The walls of the MT compartment of the chamber were combined and the roof separated,
- Built in holders for the heat pads were added to the roof of the MT compartment,
- The tray seal for the MT compartment was added,
- The salt / water pots were double stacked,
- Dedicated fan holders were added.

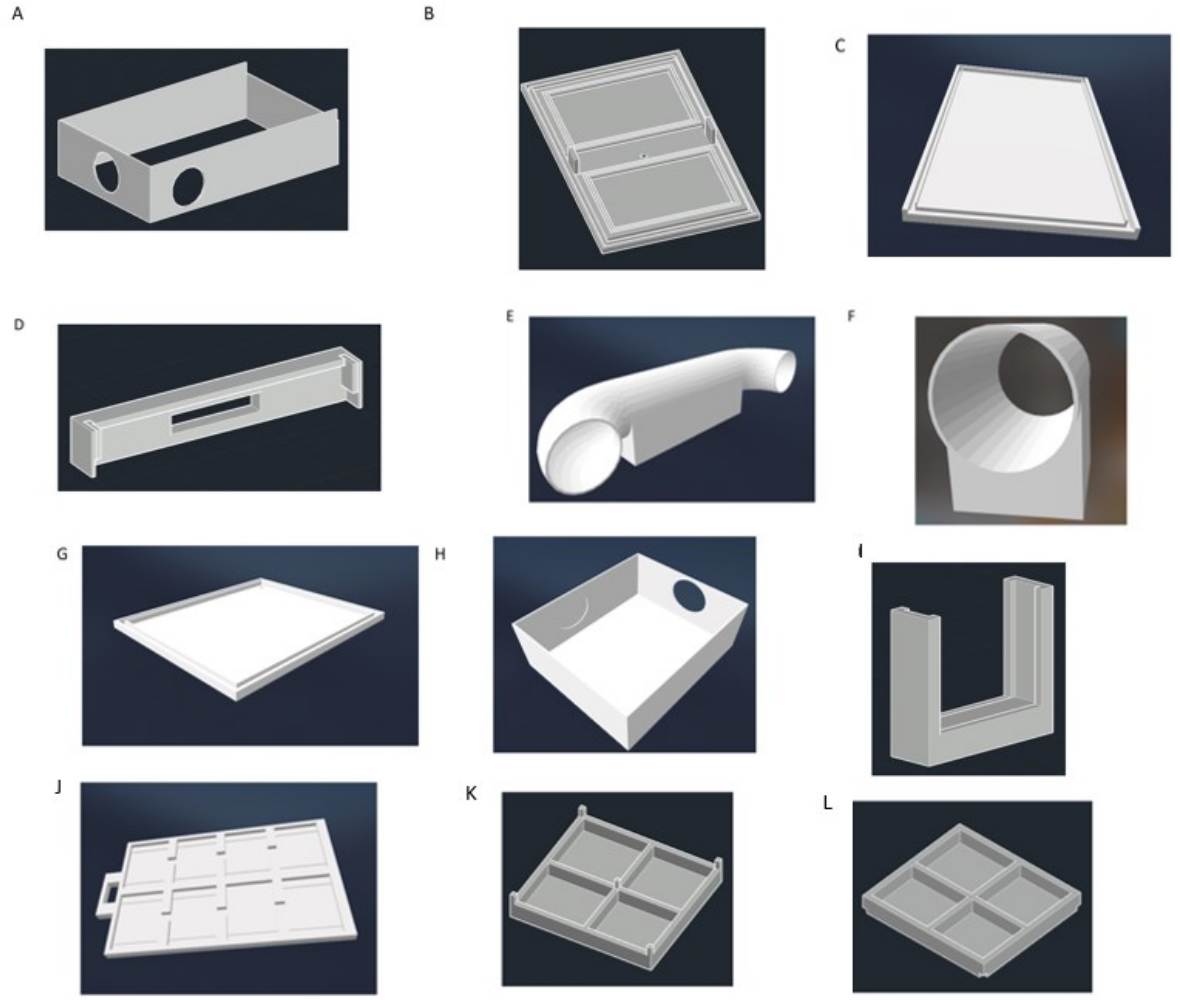

Figure 11 AutoCAD files of each of the pieces used to build the second version of the environmental control chamber. Files are labelled as follows: (A) MT compartment walls (276x174x72 mm, changed from previous prototype), (B) MT compartment roof (280x178x10 mm, changed from previous prototype), (C) MT compartment base (unchanged), (D) MT compartment tray seal (180x19x24 mm), (E) Piping to connect compartments, air movement in the direction of MT to HC compartment (unchanged), (F) Piping to connect compartments, air movement in the direction of HC to MT compartment (unchanged), (G) HC compartment roof (unchanged), (H) HC compartment walls and base (166x136x74 mm, changed from previous prototype), (I) HC compartment fan holder (57x17x50 mm), (J) Coupon placement tray (unchanged), (K) HC compartment salt / water pot layer 1 (121x109x27 mm), (L) HC compartment salt / water pot layer 2 (121x109x17 mm).

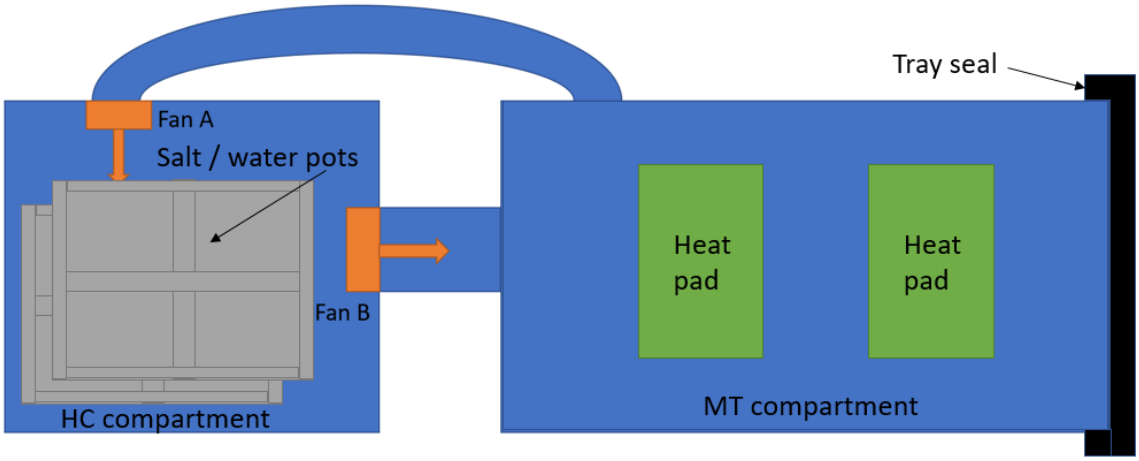

Figure 12 A representation of how prototype version two of the environmental control chamber was constructed. With fans represented in orange and direction of airflow represented by the arrows. The grey represents the salt / water pot used to contain the relative humidity controlling agents. The green colour represents the heat pad locations and black represents the tray seal used to reduce air leakage to the outer environment.

2.3.3.2. Testing

The first temperature-only test (Test ID 6 - Table 3) generated a consistent temperature across the duration of the experiment, with a variation of 1.6 °C post stabilisation in both compartments. It took 100 (MT) / 90 (HC) minutes for the temperature to reach the first peak and a maximum and minimum temperature of 38.0 °C (MT) / 29.8 °C (HC) and 36.4 °C (MT) / 28.2 °C (HC) achieved respectively.

The second temperature-only test (Test ID 7 - Table 3) generated a consistent temperature across the duration of the experiment in all locations, with temperature variations in each position as follows: (1) 3.4 °C, (2) 3.4 °C, (3) 3.7 °C, (4) 3.0 °C, (5) 3.2 °C, and (6) 3.2 °C. It took (1) 110, (2) 90, (3) 120, (4) 120, (5) 120, and (6) 100 minutes for the temperature to reach the first peak and a maximum and minimum temperature of (1) 31.0 °C, (2) 31.8 °C, (3) 30.2 °C, (4) 30.4 °C, (5) 31.1 °C, and (6) 29.5 °C and (1) 27.6 °C, (2) 28.4 °C, (3) 26.5 °C, (4) 27.4 °C, (5) 27.9 °C, and (6) 26.3 °C achieved respectively.

The first relative humidity test (Test ID 8 - Table 3) generated consistent temperature and relative humidity values in both the MT and HC compartments, with a temperature variation of 3.2 °C (MT) and 2.9 °C (HC) and a relative humidity variation of 3.1 % (MT) and 2.5 % (HC) post stabilisation. It took 140 (MT) and 130 (HC) minutes for the temperature to reach the first peak and a maximum and minimum temperature of 32.7 °C (MT) / 28.4 °C (HC) and 29.5 °C (MT) / 25.5 °C (HC) as well as a maximum and minimum relative humidity of 73.4 % (MT) / 88.2 % (HC) and 70.3 % (MT) / 85.7 % (HC) achieved respectively.

The second relative humidity test (Test ID 9 - Table 3) generated consistent temperature and relative humidity values in both the MT and HC compartments, with a temperature variation of 2.7 °C (MT) and 3.1 °C (HC) and a relative humidity variation of 4.4 % (MT) and 1.7 % (HC) post stabilisation. It took 120 (MT) and 90 (HC) minutes for the temperature to reach the first peak and a maximum and minimum temperature of 33.3 °C (MT) / 30.5 °C (HC) and 30.6 °C (MT) / 27.4 °C (HC) as well as a maximum and minimum relative humidity of 17.3 % (MT) / 22.4 % (HC) and 12.9 % (MT) / 20.7 % (HC) achieved respectively.

The third relative humidity test (Test ID 10 - Table 3) generated consistent temperature and relative humidity values in both the MT and HC compartments, with a temperature variation of 3.0 °C (MT) and 2.9 °C (HC) and a relative humidity variation of 1.1 % (MT) and

0.6 % (HC) post stabilisation. It took 200 (MT) and 190 (HC) minutes for the temperature to reach the first peak and a maximum and minimum temperature of 33.3 ^{o}C (MT) / 30.2 ^{o}C (HC) and 30.3 ^{o}C (MT) / 27.3 ^{o}C (HC) as well as a maximum and minimum relative humidity of 12.1 % (MT) / 19.9 % (HC) and 11.0 % (MT) / 19.3 % (HC) achieved respectively.

The fourth relative humidity test (Test ID 11 - Table 3) generated consistent temperature and relative humidity values in both the MT and HC compartments, with a temperature variation of 2.7 ^{o}C (MT) and 2.4 ^{o}C (HC) and a relative humidity variation of 17.0 % (MT) and 21.7 % (HC) post stabilisation. It took 130 (MT) and 200 (HC) minutes for the temperature to reach the first peak and a maximum and minimum temperature of 33.4 ^{o}C (MT) / 30.1 ^{o}C (HC) and 30.7 ^{o}C (MT) / 27.7 ^{o}C (HC) as well as a maximum and minimum relative humidity of 32.2 % (MT) / 15.2 % (HC) and 41.5 % (MT) / 19.8 % (HC) achieved respectively.

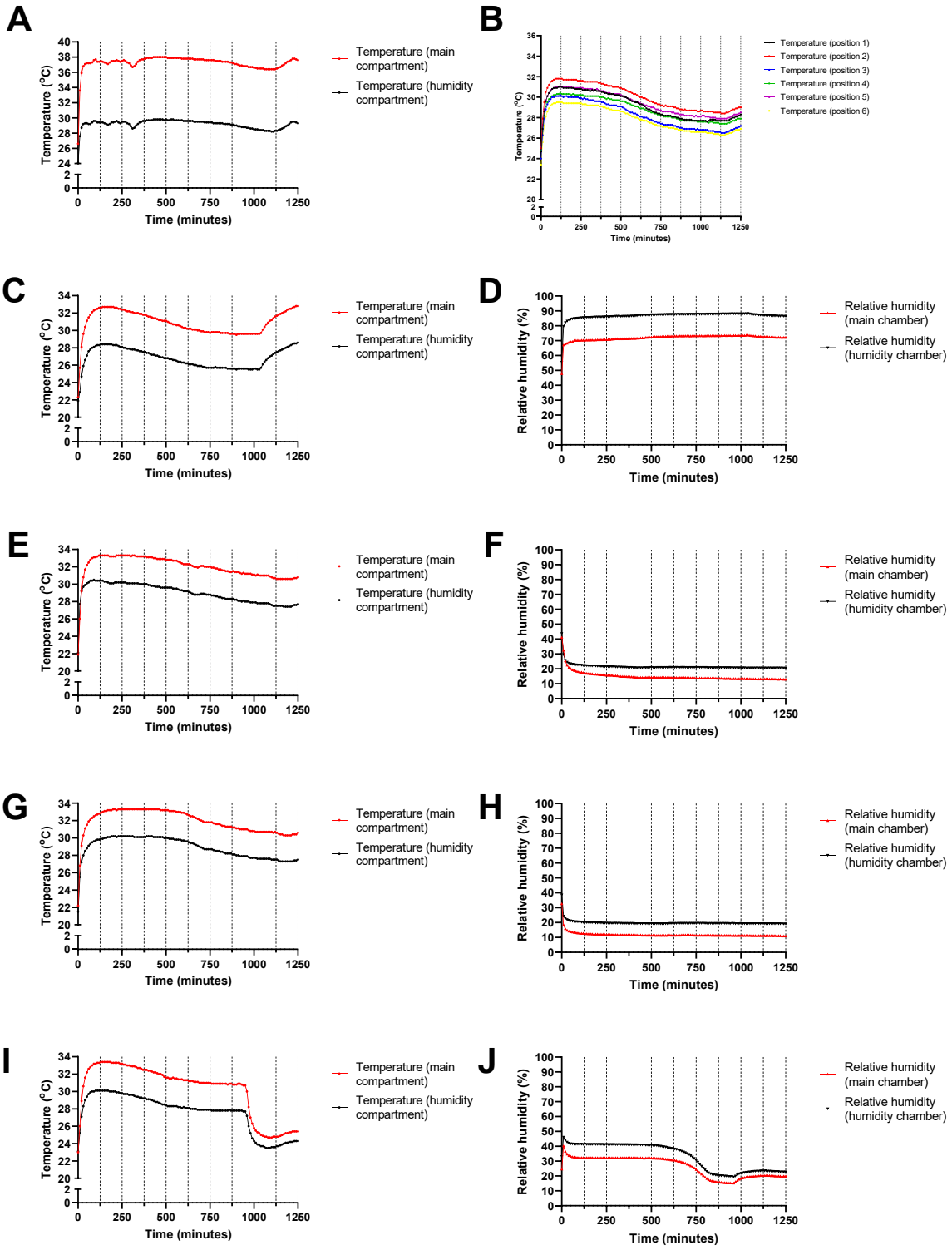

Figure 13 Temperature and / or relative humidity values in the second version of the chamber under various environmental conditions of heater-based power, airflow and relative humidity controlling solutions. (A) the maximum achievable temperature of the chamber when two fans are operating, and (B) shows the temperature values across varying points in the MT compartment of the chamber with two fans. (C / D) shows the temperature and relative humidity values when water was added to the HC compartment of the chamber, two fans were operating, and the heat pads were set to maximum placed in built in holders. (E-J) show the temperature and relative humidity values in the chamber in the same regard as (C / D) but with lithium chloride (E-H) and potassium carbonate (I / J) placed in the HC compartment.

2.3.4. Prototype version three

2.3.4.1. Construction (developed from version two)

The design of the 3D-printed sections that constitute prototype version three of the chamber is shown in Figure 14. Each section was printed separately, and support material was removed if necessary (sections A and G) due to overhanging designs. This prototype of the chamber had changed from prototype version two in the following ways:

- The floor and walls of the MT compartment were combined,
- The fan holders were built into the HC compartment,
- The HC compartment size was increased,
- The pots for the HC compartment were increased in size,
- A redesigned tray seal was added,
- The MT compartment roof was redesigned,
- A 2x2cm coupon tray was designed.

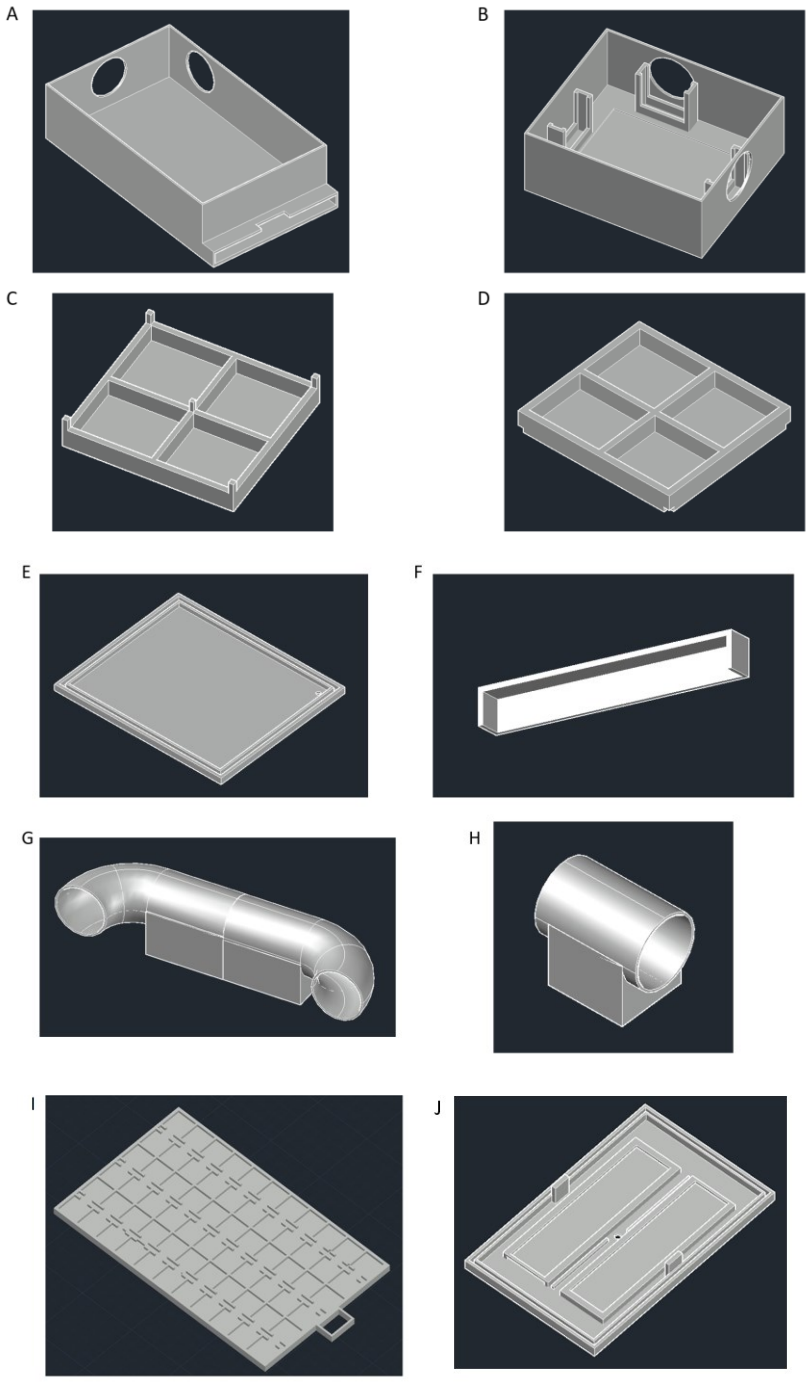

Figure 14 AutoCAD files of each of the pieces used to build the third version of the environmental control chamber. Files are labelled as follows: (A) MT compartment walls and base (298x174x74 mm, changed from previous prototype), (B) HC compartment walls and base (190x160x4 mm, changed from previous prototype), (C) HC compartment salt / water pot layer 1 (141x129x27 mm, changed from previous prototype), (D) HC compartment salt / water pot layer 2 (141x129x17 mm, changed from previous prototype), (E) HC compartment roof (unchanged), (F) MT compartment tray seal (180x19x24 mm, changed from previous prototype) (G) Piping to connect compartments, air movement in the direction of MT to HC compartment (unchanged), (H) Piping to connect compartments, air movement in the direction of HC to MT compartment (unchanged), (I) MT compartment coupon tray (282x170x5 mm, changed from previous prototype), (J) MT compartment roof (280x178x10 mmchanged from previous prototype).

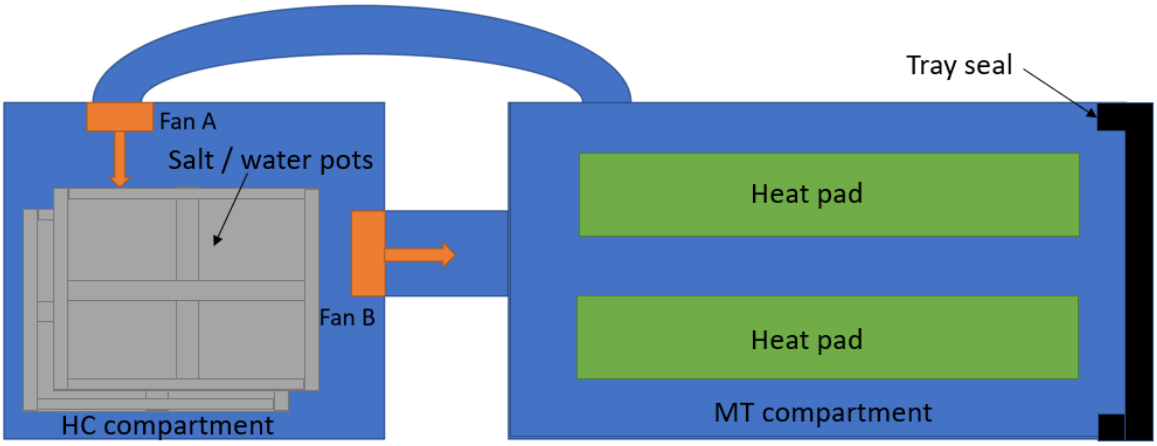

Figure 15 A representation of how prototype version three of the environmental control chamber was constructed. With fans represented in orange and direction of airflow represented by the arrows. The grey represents the salt/water pot used to contain the relative humidity controlling agents (double-layered in the prototype version). The green colour represents the heat pad locations and black represents the tray seal used to reduce air leakage to the outer environment.

2.3.4.2. Testing

The temperature-only test (Test ID 12 - Table 5) generated a consistent and high temperature across the duration of the experiment, with a variation of 1.9 °C (MT) / 0.7 °C (HC) / 1.5 °C (ambient) post stabilisation in both compartments. It took 80 (MT) / 80 (HC) minutes for the temperature to reach the first peak and a maximum and minimum temperature of 53.3 °C (MT) / 27.2 °C (HC) / 27.8 °C (ambient) and 51.4 °C (MT) / 26.5 °C (HC) / 26.3 °C (ambient) achieved respectively. Statistical significance was observed between the temperature values at the MT and HC locations (t-test, $p < 0.0001$).

The first relative humidity test (Test ID 13 - Table 5) generated consistent temperature and relative humidity values in both the MT and HC compartments, with a temperature variation of 1.4 °C (MT) / 1.2 °C (HC) / 1.5 °C (ambient) and a relative humidity variation of 4.7 % (MT) / 3.0 % (HC) / 6.0 % (ambient) post stabilisation. A maximum and minimum temperature of 23.2 °C (MT) / 23.2 °C (HC) / 23 °C (ambient) and 21.8 °C (MT) / 22.0 °C (HC) / 21.5 °C (ambient) as well as a maximum and minimum relative humidity of 95.2 % (MT) / 96.8 % (HC) / 39.0 % (ambient) and 90.5 % (MT) / 93.8 % (HC) / 33.0 % (ambient) achieved respectively. No statistical significance was observed for temperature and relative humidity between the MT and HC compartments.

The second relative humidity test (Test ID 14 - Table 5) generated consistent temperature and relative humidity values in both the MT and HC compartments, with a temperature

variation of 0.4 °C (MT) / 0.5 °C (HC) / 2.4 °C (ambient) and a relative humidity variation of 5.1 % (MT) / 2.8 % (HC) / 4.8 % (ambient) post stabilisation. It took 80 (MT) and 140 (HC) minutes for the temperature to reach the first peak and a maximum and minimum temperature of 25.7 °C (MT) / 25.0 °C (HC) / 24.6 °C (ambient) and 25.3 °C (MT) / 24.5 °C (HC) / 22.2 °C (ambient) as well as a maximum and minimum relative humidity of 92.3 % (MT) / 95.9 % (HC) / 39.8 % (ambient) and 87.2 % (MT) / 93.1 % (HC) / 35.0 % (ambient) achieved respectively. Statistical significance was observed between each of the sensor locations for temperature (one-way ANOVA, $p < 0.0001$) and relative humidity (one-way ANOVA, $p < 0.0001$).

The third relative humidity test (Test ID 15 - Table 5) generated consistent temperature and relative humidity values in both the MT and HC compartments, with a temperature variation of 0.2 °C (MT) / 0.4 °C (HC) / 1.5 °C (ambient) and a relative humidity variation of 1.9 % (MT) / 0.9 % (HC) / 6.0 % (ambient) post stabilisation. It took 80 (MT) and 80 (HC) minutes for the temperature to reach the first peak and a maximum and minimum temperature of 27.6 °C (MT) / 26.5 °C (HC) / 24.2 °C (ambient) and 27.4 °C (MT) / 26.1 °C (HC) / 22.7 °C (ambient) as well as a maximum and minimum relative humidity of 90.5 % (MT) / 97.7 % (HC) / 42.3 % (ambient) and 88.6 % (MT) / 96.8 % (HC) / 36.3 % (ambient) achieved respectively. Statistical significance was observed between each of the sensor locations for temperature (one-way ANOVA, $p < 0.0001$) and relative humidity (one-way ANOVA, $p < 0.0001$).

The fourth relative humidity test (Test ID 16 - Table 5) generated consistent temperature and relative humidity values in both the MT and HC compartments, with a temperature variation of 0.6 °C (MT) / 0.6 °C (HC) / 1.0 °C (ambient) and a relative humidity variation of 3.6 % (MT) / 3.2 % (HC) / 5.4 % (ambient) post stabilisation. It took 120 (MT) and 90 (HC) minutes for the temperature to reach the first peak and a maximum and minimum temperature of 29.8 °C (MT) / 27.3 °C (HC) / 23.8 °C (ambient) and 29.2 °C (MT) / 26.7 °C (HC) / 22.8 °C (ambient) as well as a maximum and minimum relative humidity of 86.9 % (MT) / 98.0 % (HC) / 28.0 % (ambient) and 83.3 % (MT) / 94.8 % (HC) / 22.6 % (ambient) achieved respectively. Statistical significance was observed between each of the sensor locations for temperature (one-way ANOVA, $p < 0.0001$) and relative humidity (one-way ANOVA, $p < 0.0001$).

The fifth relative humidity test (Test ID 17 - Table 5) generated consistent temperature and relative humidity values in both the MT and HC compartments, with a temperature variation of 0.9 °C (MT) / 4.4 °C (HC) / 3.7 °C (ambient) and a relative humidity variation of 5.9 % (MT) / 5.6 % (HC) / 9.2 % (ambient) post stabilisation. It took 20 (MT) and 20 (HC) minutes for the temperature to reach the first peak and a maximum and minimum temperature of 29.9 °C (MT) / 32.8 °C (HC) / 27.3 °C (ambient) and 29.0 °C (MT) / 28.4 °C (HC) / 23.6 °C (ambient) as well as a maximum and minimum relative humidity of 18.2 % (MT) / 19.6 % (HC) / 42.0 % (ambient) and 12.3 % (MT) / 14.0 % (HC) / 32.8 % (ambient) achieved respectively. Statistical significance was observed between each of the sensor locations for temperature (one-way ANOVA, $p < 0.0001$) and relative humidity (one-way ANOVA, $p < 0.0001$).

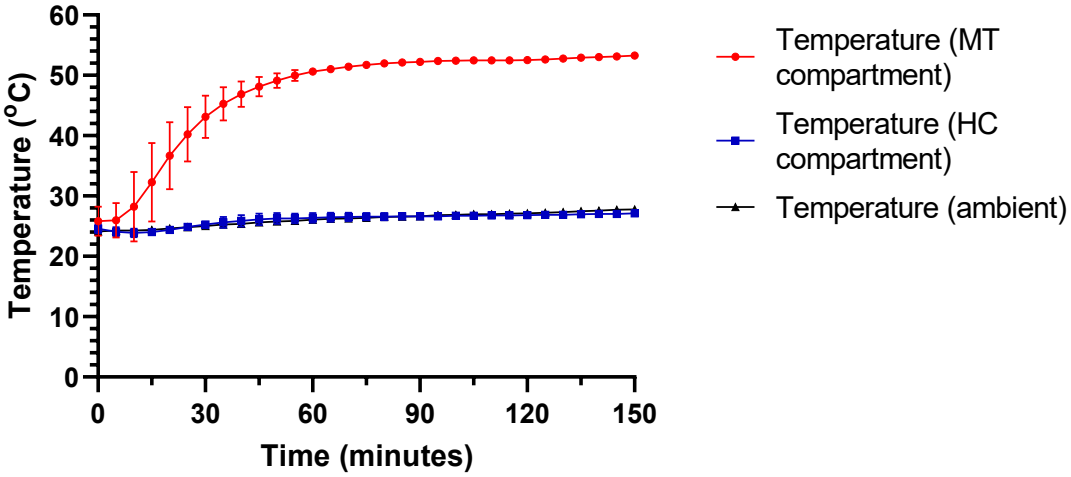

Figure 16 Temperature values in the third version of the chamber when applying maximum power to the heat pads (12 volts at ~3 amperes) with no relative humidity control.

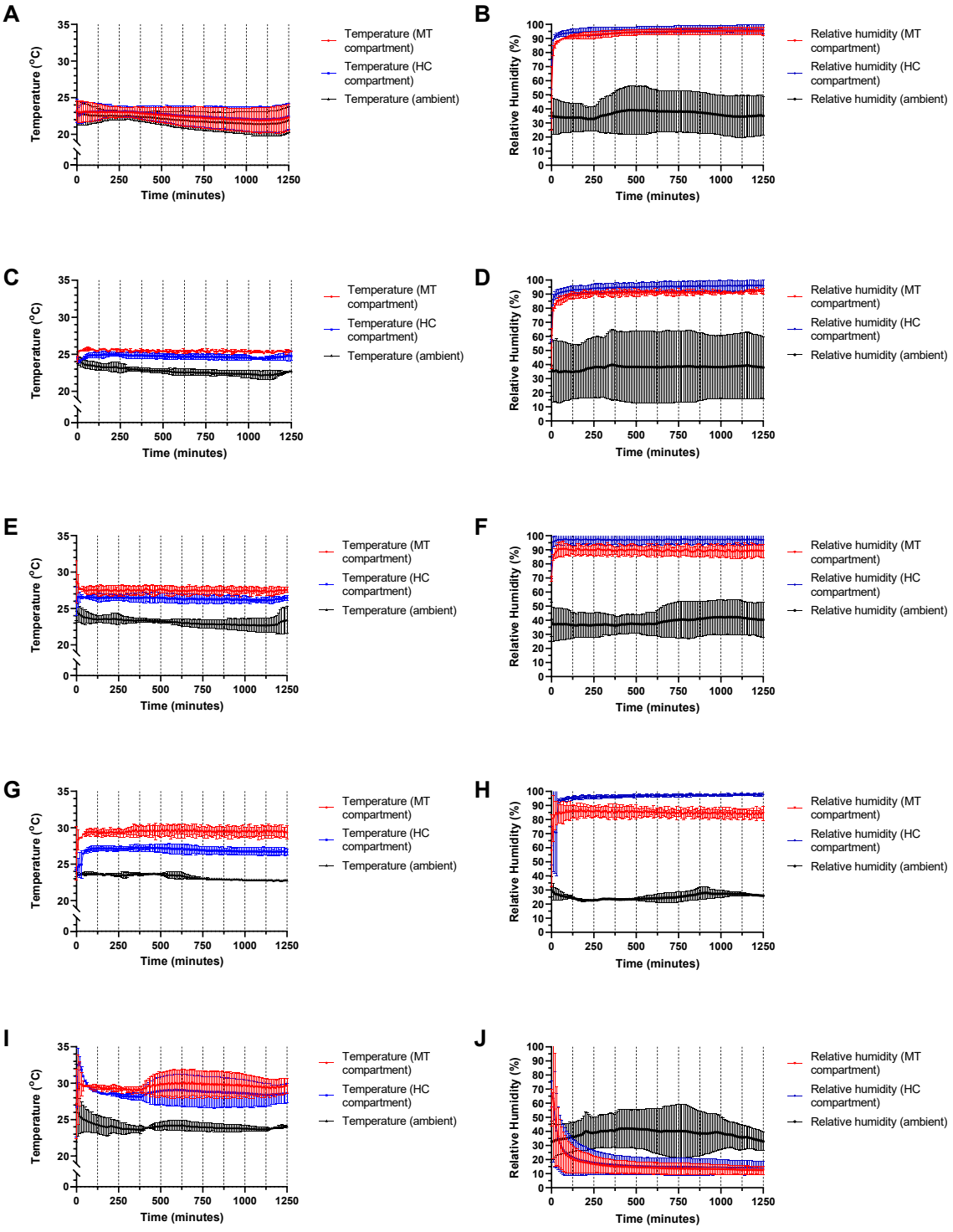

Figure 17 Temperature and / or relative humidity values in the third version of the chamber under various environmental conditions of heater-based power, airflow and relative humidity controlling solutions. (A) shows the maximum achievable temperature when no airflow or relative humidity control was present, and the power supply was set to nine volts and approximately 2.2 amps. (B) the temperature achieved in the chamber when heat pads are set to switch off above 37 °C. (C / D) shows the relative humidity achieved when there was no temperature control in the chamber. (E-J) shows the temperature and relative humidity values in the chamber when the heat pads are switched off at (E / F) 26 °C, (G / H) 28 °C and (I / J) 32 °C and water is added to the HC compartment. (K / L) temperature and relative humidity values when the temperature is set to maximum in the chamber and lithium chloride is added to the HC compartment.

2.4. Discussion

2.4.1. Prototype version one

As this was the first prototype, only general trends were sought and so no experimental repeats were carried out, with more statistically rigorous data generated in future versions of the chamber. Additionally, any variable value choice regarding the airflow simulations in SimScale (e.g., a fineness of 4) was either the default value or was set as a balance between processing speed / computer processing limitations and high detail.

The temperature during the first test (Test ID - 1) highlighted a requirement for a greater heat source to be fitted into the chamber, as the maximum operatable temperature during this test was only 24.7 ^{o}C. This was achieved by increasing both the number of heat pads and the amount of power across the prototype changes. Adding a second heat pad and then undertaking the relative humidity tests improved the maximum achievable temperature of the chamber despite the same output from the power supply. The rise and fall cycles during the tests were also most likely caused by the natural deviation in ambient temperature via by the day-night cycle (ambient temperature dropping during hours with no sunlight), even when in an indoor acclimatised environment. This must be considered when performing any microbiological tests within the chamber in case of reductions to the ambient temperature affecting the internal temperature of the chamber.

The temperature during the potassium chloride test (Test ID - 3) and the two-fan water test (Test ID - 5) did not follow this typical rise and fall pattern but as the variation remained low (less than ±2 ^{o}C) it is likely not of concern. However, temperature variations within the chamber due to changes in ambient temperature became a challenge when designing further prototypes. The temperature during the potassium chloride test (Test ID - 3) was also very similar to that of the second temperature test (Test ID - 2). The relative humidity within the chamber was lower than the expected value despite using saturated potassium chloride (with an expected relative humidity of 75 %). There are two possible explanations for this occurrence, there was not enough saturated salt to modify the relative humidity throughout the entire chamber or air was leaking to the outside environment. This is further evidenced as the saturated salts were visibly dry after the test concluded – but should have remained saturated. As the relative humidity was around 10 % higher in the HC compartment than the MT compartment, it is also likely that the airflow within the

chamber was not sufficient to push the humidified air throughout the entire chamber. Adding a second fan (as shown in Test ID - 5) only marginally lowered the disparity between the compartments.

The water-based relative humidity tests (Test ID – 4 / 5) showed an increase in the relative humidity achieved in both compartments of the chamber but was still greatly below the target relative humidity of 100 %, and below the 90 % target required for performing current STMs. There was general stability of the relative humidity in both tests despite changes in temperature with a gradual increase in relative humidity observed in both compartments (although greater in the MT compartment) as the temperature gradually decreased. This shows this system may be suitable if the target relative humidity can be achieved, and so future versions of the chamber should aim to maximise the surface area of relative humidity controlling agents, reduce air leakage from the chamber and increase airflow.

This first prototype version of the chamber requires improvement in temperature and relative humidity control to achieve the aim of performing AMM efficacy evaluation in a robust and reproducible way. Temperature control could be improved through an increase in the power supply to the heat pads, although this would require changing the heat pads to those with a higher power tolerance. Relative humidity control could be improved both by reducing the amount of air leaking from the chamber (e.g. by fusing as many parts together as possible) and increasing the volume of water and / or saturated salts that the chamber can hold. Additionally, increased airflow may be able to assist in transferring the humidified air to the MT compartment.

2.4.2. Prototype version two

The high temperature and lower variation achieved and maintained during the first temperature test (Test ID - 6) indicates that STMs to assess AMMs could be performed within this chamber and shows improvement in reproducible methodology. However, the map (Test ID - 7) of the chamber highlights how variable the temperature can be across the MT compartment, which may not necessarily pose a problem if it is well mapped and understood but should still be a potential point of improvement in further prototypes. Sample positions two and five within the MT compartment had the highest temperature, which was expected, as these positions were between the two heat pads and so were

receiving heating more efficiently. The lower temperatures in the MT compartment overall were to be somewhat expected as the heat pads were partially covered by the holders, the placement of which should be reconsidered in future prototypes of the chamber. Interestingly, the maximum temperature values in the relative humidity tests (Test ID – 8 / 9 / 10 / 11) were higher than that of the map (Test ID – 7), likely due to the sensor being placed directly in the centre of the MT compartment between the heat pads and so was receiving a combined heating effect.

The temperature during the water-based relative humidity test (Test ID - 8) was as expected and like that of similar tests (Test ID – 7 / 9 / 10 / 11) but had a sharper increase at the end of the test (at ~1,000 minutes). This is most likely the result of the outer environment warming more quickly as opposed to any change in the chambers functionality. The relative humidity control was more reliable in this version of the chamber, despite not achieving the target of >90 % relative humidity. This increase in relative humidity was also combined with a higher temperature alluding to the issue of air-leaking from prototype version 1 being resolved, but also suggests that high temperature and high relative humidity may be difficult to achieve, and lowering the temperature may allow the relative humidity to reach >90 % (Wexler and Hasegawa, 1954).

The temperature variation during the lithium chloride tests (Test ID – 9 / 10) was in line with all other tests for prototype version two. Interestingly, the relative humidity in the MT compartment was lower than that in the HC compartment (consistent with previous tests), despite the relative humidity-controlling saturated salts being placed in the HC compartment. Also, the target relative humidity of ~15 % for lithium chloride was surpassed in both tests (80g and 160g), demonstrating that using less salts can still achieve the desired relative humidity. However, the time taken to achieve equilibrium decreased by around four times when doubling the salt. This is a decision for the user to make on whether the volume of salt or time to stable relative humidity is the most important factor to consider.

Overall, the temperature and relative humidity throughout the chamber in the potassium carbonate relative humidity test (Test ID – 11) was as expected (except a slight difference between the target and achieved relative humidity, possibly due to the higher temperature) until the sharp drop in both. This could have been caused by numerous issues

but was most likely a combination of the air leaking due to user error (not sealing the chamber properly) and / or one of the heat pads not functioning properly, although the temperature does not equalise with the external environment, so some heat was being produced.

The modifications made to the chamber improved the capabilities to control both temperature and relative humidity, and further improvements should aim to allow control within the box to perform current AMM STMs by achieving 35 ^{o}C and >90 % relative humidity.

2.4.3. Prototype version three

As described in the results above 2.3.4.2, there was a clear improvement to the functionality of this version of the chamber. The temperature tests (Test ID – 12 / 13) highlighted that performing antimicrobial efficacy STMs within the chamber may be possible as the desired environmental conditions (37 °C, 100 % relative humidity) were achievable individually. Additionally, as the chamber was now capable of achieving higher temperatures, a system was added to the Arduino whereby the relay module would allow the heat pads to be switched on when under a specified temperature and would switch off when above the specified temperature to act as a temperature regulator in the chamber. One issue that was discovered while operating at these higher temperatures repeatedly is that the roof of the MT compartment (where the heat pads are fitted) began to warp due to the relatively low thermal tolerance of PLA. As a result, the material used to print the MT compartment roof was switched to PET-G, which provides an extra 20 ^{o}C of temperature allowance yet remains mostly simple to print and is widely available (Basurto-Vázquez et al., 2021). Following this switch, no further warping was observed. Also, when increasing the power supply, the wires connecting it to the heat pads were no longer suitable as they only had a maximum current allowance of one Ampere and were changed to allow supply of up to five Amperes of current.

The relative humidity tests (Test ID – 14 / 15 / 16 / 17) also highlighted the ability of the chamber to stay within ±1 ^{o}C of the target temperature for most of the tests and within ±2 ^{o}C for all tests. However, tests of temperature 30 ^{o}C and higher demonstrated the largest variation. Interestingly, the temperature generally stayed around 0.5 ^{o}C lower than the target, this is likely due to the chamber taking a longer period to heat compared to cooling

and should be accounted for when writing the code to control the temperature regulation system (switch heat pads off 0.5 ^{o}C higher or delay switching on or off the heat pads). The relative humidity tests (Test ID – 13 / 14 / 15 / 16 / 17) also showed improvement in the capabilities of the chamber, with the maximum relative humidity heavily depending on the temperature, with >90 % being achievable at temperatures of 24 ^{o}C and lower. This shows the chamber has fulfilled the initial aims in terms of temperature and relative humidity individually.

2.4.4. Overall

The initial aims of the chamber with regards to temperature (room temperature to 37 ^{o}C), relative humidity (15 % to >90 %) and airflow (even airflow as possible) have been fulfilled, with this chamber, following three iterative prototype designs and testing, capable of achieving a temperature range from room temperature to 37 ^{o}C, a relative humidity range of 15 - 100 % depending on the temperature (maximum 75 % at 37 ^{o}C) and modelled airflow throughout the testing area of the chamber. This provides a large range of possible end-use scenarios to simulate with the chamber and allows for increased reproducibility between laboratories by providing a methodology that is capable of utilising 3D printing anywhere with access to a 3D printer, and with easy-to-access electronics. Additionally, as the chamber can be placed in various locations it omits the requirement for large incubation cabinets or rooms and would also be transferrable to other laboratories if required. The chamber could be further adapted to be able to accommodate different sample types and sizes, as the removable sample tray is purpose-designed and printed. It may also be possible to adapt the sample tray to allow for submerging samples in media, enabling submerged biofilm tests within the chamber.

It is important to note that other improvements and modifications could still be made that would allow additional uses of the chamber and further improve the control of the environmental conditions within. However, as the initial aims have been fulfilled it is now beyond the scope of this thesis. Nevertheless, the following changes would allow the chamber to be further improved to control environmental conditions and perform STMs. Firstly, although the airflow within the chamber is sufficient throughout the chamber to drive the humidified air to the MT compartment of the chamber, generating a more even airflow over the testing area would be beneficial, which could include adding additional

piping to enter the MT compartment at other areas, or being able to control the speed of the airflow with an Arduino module controlling the exact power to and therefore speed of the fans. Additional relative humidity control could also enhance the chamber to allow both an increased range of relative humidity values at higher temperatures as well as a faster transition period to the required relative humidity at the start of use. Finally, there are several printed pieces for the chamber that require additional attention once printed before they are ready to use due to added support material such as the main chamber walls (specifically where they meet the tray seal). Small increases in usability could also be achieved by reducing the size (but not diameter) of the piping for airflow by moving it closer to the chamber or reducing the length of the piping, enabling laboratories to use the chamber in smaller workspaces.

2.5. Conclusion

The chamber can maintain a variety of temperature (room temperature, 26 ^{o}C, 28 ^{o}C, 30 ^{o}C, 37 ^{o}C), relative humidity (15 % to >90 % at 24 ^{o}C), and airflow values to test AMMs in a wide variety of end-use environmental conditions. Additionally, this novel chamber design offers an easy-to-use and affordable method of developing reproducible methodologies that use realistic environmental conditions in efficacy testing of antimicrobial activity which could be used to inform new STMs. Before developing novel methods for antimicrobial STMs, it is important now to determine whether existing STMs can be performed in the chamber and to assess the effects. Additionally, as more realistic environmental conditions become implemented into antimicrobial efficacy testing of AMMs, the likelihood of the inoculum evaporating on the surface during the incubation period is high (due to airflow and non-saturated relative humidity) and thus knowledge of evaporation time and the mechanics are crucial to understanding how to interpret data generated by such methods.

3. Proof of concept: Using the novel chamber to undertake an existing standardised test method

3.1. Introduction

The importance of realistic environmental conditions in STMs which aim to generate data on antimicrobial surface efficacy is evident as discussed previously. However, many laboratories do not readily have the capability of reproducibly performing these STMs with conditions more analogous to many end-use scenarios. While the novel environmental control chamber described in the subsequent chapters could provide a platform to enable this, thorough testing must occur to ensure reproducibility (different chambers produce comparable data), repeatability (a single chamber produces comparable data on multiple uses) and robustness (data is comparable to those generated using other methods e.g. the CDC biofilm reactor method ASTM E2562 (ASTM, 2022b)). Additionally, understanding how realistic environmental conditions are implemented into a pre-existing STM and what considerations and impacts changing these conditions may have on usability and potential uptake of a method are important for considering future development of other STMs.

For example, in ISO 22196, airflow is absent. However, in the chamber described previously, airflow has been included as an important environmental variable that would almost certainly be present in any real-world setting that an antimicrobial coating may be installed within. Whilst the airflow is generally consistent across the MT compartment, if coupons were placed in all possible locations, some variation in airflow would be expected. This can be ultimately justified when considering that real-world scenarios, such as hospital wards or other indoor settings will have a similar level of variability in airflow between locations, even within the same room, for example by movement of people and air conditioning (Wong et al., 2019). As each location within the MT compartment of the chamber will have a unique set of environmental conditions present, within a defined range, it is unknown what impact these small variations in airflow would have on the final data providing efficacy of an antimicrobial material (CFU data).

If a transition to realistic STMs for antimicrobial efficacy assessment is to move forward, other considerations such as choice of organism, and how this may impact on the results of any STM must be considered. The frequently used ISO22196 states that either *S. aureus* ATCC 6538P or *E. coli* ATCC 8739 should be used. However, the inclusion of airflow is likely to decrease the evaporation time of droplets (explored in chapter 5), and so differences between a microorganism's likelihood of survival in desiccated conditions is important, as

not to draw conclusions that an antimicrobial effect of a surface has killed an organism, when in reality it may have died due to it drying onto the surface. With reference to ISO 22196, this consideration is important as *S. aureus* is more capable of surviving desiccation than *E. coli* (García de Castro et al., 2000). As such, it's important to understand the relationship between organism choice, use of environmental conditions such as temperature and airflow, and its relation to existing standards such as ISO 22196.

3.1.1. Chapter specific aims and objectives

- Assess the survival of bacteria on inert and antimicrobial surfaces using ISO 22196 when placed in the novel chamber (self-sustained environmental controls) or using standard ISO22196 approach (in a sealed plastic container within an incubator).
- Determine the effects of temperature, relative humidity, and airflow on the survival rates of bacteria placed on inert surfaces within the novel chamber.

3.2. Methods

To compare the ability for bacteria to survive and be recovered from surfaces following incubation described in ISO 22196 (temperature of 35 ± 2°C and relative humidity above 90 %), stainless steel 316L coupons were inoculated with either *S. aureus* ATCC 6538 or *E. coli* NCIMB 8545 as described in 3.2.1 and 3.2.2. Initial experiments described below used the desiccant-resistant *S. aureus* ATCC 6538, which allowed for minimal impact of the environmental conditions on the survival of the bacteria and allowed for a greater focus on whether the chamber is suitable to perform such a method.

3.2.1. Comparison using ISO22196: *Staphylococcus aureus*

3.2.1.1. Coupons placed in petri dishes with lids on

A modified version of ISO22196 was performed to assess the survival of *S. aureus* on stainless steel coupons. In brief, a culture of *S. aureus ATCC 6538* was formed by adding one colony of bacteria from a TSA agar (Fischer Scientific, UK) streak plate to 10mL sterile TSB (Fischer Scientific, UK) and incubating at 37 °C for 24 ± 1 hours shaking at 150 rpm (Sciquip, UK). The culture was then centrifuged (Sigma, UK) at 3500 rpm for 10 minutes, the supernatant discarded and 10mL sterile saline (Fischer Scientific, UK, 0.85 % NaCl solution) added, repeated once, followed by adjusting the suspension to 0.5 OD at 600nm (Jenway 6305, UK). Twelve coupons of 2x2cm stainless steel were sterilised by autoclaving at 121 °C for 20 minutes and left to evaporate overnight in sterile conditions. Six coupons

were inoculated with 100µl sterile saline (negative control) and the other six with 100µl bacterial suspension, and each covered with a polypropylene film (Fischer Scientific, UK) which had previously been prepared by cutting to 18x18 mm and sterilised by submerging in 70 % ethanol for 30 ± 2 seconds and left to evaporate overnight. The six saline coupons were split into pairs and placed in separate petri dishes (three total) and covered with the lid. The same process was used to split the coupons inoculated with *S. aureus* ATCC 6538.

The novel 3D printed chamber was set to 37 ^{o}C, and water added to the HC compartment to achieve >90 % relative humidity with both fans switched on. The plastic box (296x200x200 mm) used to follow the standard ISO 22196 was filled with water to a depth of 20 mm and a porous tray placed so it sat above the water line. One petri dish with saline coupons and one with suspension was placed in each chamber by opening the top / lid, with the Petri dish lid remaining in place. For the 3D printed chamber, the dishes were placed in the centre of the MT compartment. Temperature / relative humidity sensors (RHT10, RS components, UK) were placed in the plastic box (on the porous tray), as well as in both the HC and MT compartments of the 3D printed chamber and a final one on the lab bench to measure ambient conditions. The plastic box was then placed in a 37 ^{o}C incubator. To quantify the number of bacteria recoverable at time zero, the remaining coupons (two saline, two suspension) were placed into 50mL falcon tubes (Fischer Scientific, UK) with 10mL sterile saline and vortexed for 60 ± 2 seconds, then serially diluted 1:10 in saline to 10^{-4}, and the suspension serially diluted to 10^{-6}, followed by using a standard spread plate technique in duplicate on to TSA. This was followed by incubation at 37 ^{o}C for 24 hours and bacterial viability determined. To ensure any reduction in cell numbers after 24 hours was not due to the death of the cell suspension, an inoculum control consisting of the standardised overnight culture was also placed in the plastic box (that was incubated alongside the coupons) for the duration of the experiment. After 24 hours, the inoculum control and all coupons across both the plastic box and the novel chamber were recovered into 10 mL saline, vortexed 60 ± 2 seconds and serially diluted, spread plated and counted as described above. The experiment was repeated once. All statistical analysis and graphing for all tests were performed using GraphPad Prism 9.5.1. In each case of assessing bacterial viability, a one-way ANOVA test was performed alongside a multiple comparisons test of the mean of each column (inoculum at time 0, coupon placement B10 etc) against the mean

of every other column. Temperature and relative humidity values were compared using an ANOVA test in the same manner for each sensor location.

3.2.1.2. Coupons placed in petri dishes with the lids off

The method performed is the exact same as what is described above but the lids of the petri dishes were removed. Experiment was repeated once.

3.2.1.3. Coupons placed in a custom 3D printed tray

To assess whether the survival of microorganisms was impacted by placing stainless steel coupons in the purpose-designed 3D printed tray (that was to be placed in the MT compartment of the chamber), the following method was used. Instead of the lid of the MT compartment being removed for the petri dishes to be placed inside, the tray seal was removed, the tray slid in, and seal replaced to minimize equilibration to the ambient conditions. Additionally, the tray was sterilised by being submerged in 70 % ethanol for two minutes before excess was drained and the tray then dried in a laminar flow cabinet until visibly dry (minimum one hour). The coupons were placed in coupon holders B1, B4, B7, B10, E1, E4, E7, E10, as demonstrated in Figure 18 to spread coupons across the MT compartment. As there had been no contamination of the saline coupons in 4.2.1.1 and 4.2.1.2, the saline coupons were removed, leaving only coupons with bacterial inoculum. All statistical analysis and graphing for all tests were performed using GraphPad Prism 9.5.1. Experiment was repeated once.

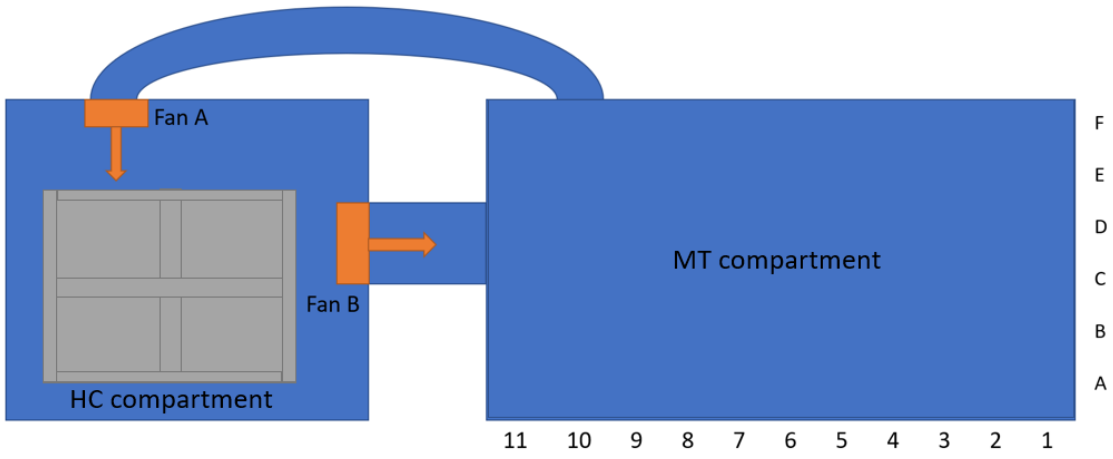

Figure 18 A layout of how the coupon tray is labelled when placed in the MT compartment of the chamber. Fan placements are shown in orange with the arrows representing the flow of air.

3.2.2. Further trial use of the novel chamber to undertake ISO22196: *Escherichia coli*

A modified version of ISO 22196 was performed to assess the survival of *E. coli* NCIMB 8545 on stainless steel 316L. Survival was assessed at 24 ^{o}C and 30 ^{o}C with both fans (RS components, UK) switched on, as well as 30 ^{o}C with fan B (Figure 18) switched off. In each case, a streak plate on tryptone soya agar was performed directly from bacterial stocks kept at -80 ^{o}C in glycerol, and incubated at 37 ^{o}C for 18-24 hours, followed by a second passage streak plate incubated under the same conditions and stored at 4 ^{o}C until required. One colony from the streak plate was then inoculated into 10mL sterile tryptone soya broth and incubated at 37 ^{o}C for 18-24 hours shaking at 150 rpm to create an overnight culture. This culture was then centrifuged at 3500rpm for 10 minutes, the supernatant removed and replaced with 10mL 1/500 nutrient broth (Fischer Scientific, UK), followed by vortex mixing (Clifton, UK) for 30 ± 2 seconds. Centrifugation to vortex was then repeated once more to ensure minimal nutrient carryover. The suspension was then adjusted to 0.5 ± 0.005 OD at 600nm using a spectrophotometer and adding 1/500 nutrient broth as required. The suspension was then diluted 1:10 in 1/500 nutrient broth to achieve a working suspension of 2-7x10^{5} CFU/mL (three dilutions required). Stainless steel 316L coupons (n=12) cut to 20x20x1mm were sterilised by autoclaving at 121 ^{o}C and inoculated with 100µl of the working suspension per coupon. A polypropylene cover slip measuring a maximum of 18x18 mm was then placed on to each coupon which had been previously sterilised by submerging in 70 % ethanol for 30 ± 2 seconds and drying in a laminar flow cabinet for one hour, followed by leaving to dry overnight in a sterile petri dish. Eight coupons were then placed on to the tray in positions B1, B4, B7, B10, E1, E4, E7, E10 (Figure 18) to ensure wide distribution across the MT compartment. The tray had been sterilised by submerging in 70 % ethanol for 30 ± 2 seconds and drying in a laminar flow cabinet for one hour. The tray containing inoculated coupons was placed into the MT compartment of the novel chamber and distilled water added to both layers of the pot in the HC chamber, and the heat pads set to the appropriate temperature. A separate plastic box (as described above in 4.2.1) was also used as a comparison between the new 3D printed chamber and the standard approach to ISO 22196, with 2cm of water covering the base, and a porous polypropylene tray placed within to provide a platform to place samples above the waterline. Two inoculated coupons were placed in the plastic box in a petri dish but with lid removed once in the box and incubated in an incubator at the same temperature as the

novel chamber. A further two coupons were immediately recovered to determine the zero-hour recovery rate. The coupons were recovered into a stomacher bag with 10mL sterile saline and manually agitated for 30 ± 2 seconds, followed by serially diluting to 10^{-2} and spread plating in duplicate on to tryptone soya agar. The inoculum was also serially diluted to 10^{-3} and spread plated in the same manner, followed by incubation of all agar plates at 37 ^{o}C for 18-24 hours and counting colonies to determine CFU/mL. After 24 hours, the remaining 10 coupons (eight in the novel chamber and two in the plastic box) were recovered and bacterial viability was determined in the same manner as described in 3.2.1.1.

Additionally, the 30 ^{o}C experiment (with both fans on) was performed again but the coupons were replaced with Cu (CuSn5, eight coupons at one time in the 3D printed chamber, two coupons placed in the plastic box, two coupons recovered immediately), alongside two stainless steel 316L coupons remaining in the plastic box as a control and recovered after 24 hours for comparison.

Finally, a further test was performed whereby potassium carbonate was added to the HC compartment instead of water (target relative humidity was ~40 %) in a ratio of 20g salt to 10mL distilled water in each quadrant and both layers of the pot (160g salt, 80mL water total). The temperature was set to 24 ^{o}C within the MT compartment with an incubation period of four hours. At hourly intervals (time points: 0, 1, 2, 3, 4 hours), coupons were recovered from the MT compartment (except time 0 where coupons were immediately recovered before going into the chamber) and bacterial viability was determined as described above. Cover slips were not used during this test and the inocula was deposited on to the surface so that the droplets on the surface were as spherical as possible. The positions of, and the order with which coupons were removed at the different time points were randomised using a random number generator (A-F and 1-11). All statistical analysis and graphing were performed using GraphPad Prism 9.5.1. All experiments were repeated once. In each case of assessing bacterial viability, a one-way ANOVA test was performed alongside a multiple comparisons test of the mean of each column (inoculum at time 0, coupon placement B10 etc) against the mean of every other column. Temperature and relative humidity values were compared using an ANOVA test in the same manner for each sensor location.

3.3. Results

3.3.1. Comparison using ISO22196: *Staphylococcus aureus*

3.3.1.1. Coupons placed in petri dishes with lids on

The bacterial viability results (Figure 19) demonstrate the inoculum control had no significant reduction after 24 hours (log reduction = 0.02, p value = 0.6302). Neither the new chamber nor the plastic box CFU/mL data were significantly different from the inoculum at 24 hours (new chamber – p = 0.7457, traditional chamber – p = 0.3253). However, both were significantly different than the CFU/mL count when comparing recovery from coupons at 0 hours and 24 hours (new chamber – log reduction = 0.613 / p = 0.0128, plastic box – log reduction = 1.885 / p = 0.0014). The temperature (Figure 20) remained predominantly stable throughout the test for all locations, with the novel chamber achieving 34.6 ± 1.0 ^{o}C and 31.2 ± 1.2 ^{o}C in the MT and HC compartments respectively whilst the ambient temperature was 22.6 ± 0.9 ^{o}C. The traditional plastic box was approximately 35.4 ± 3.4 ^{o}C with a slight deviation in the first few hours. The average temperature across the duration of the experiment of the MT compartment of the novel chamber and the plastic box was not significantly different (p-value < 0.1122). The relative humidity (Figure 21) was maintained at ~97.3 ± 1.8 % in the plastic box, as well as ~87.0 ± 0.7 % and ~74.5 ± 1.6 % in the HC and MT compartments of the novel chamber respectively, against an ambient outside relative humidity of 50.0-71.6 % (mean value = 64.2 %). The average relative humidity values across the duration of the experiment in the novel chamber compared to the plastic box are significantly different (p-values < 0.0001).

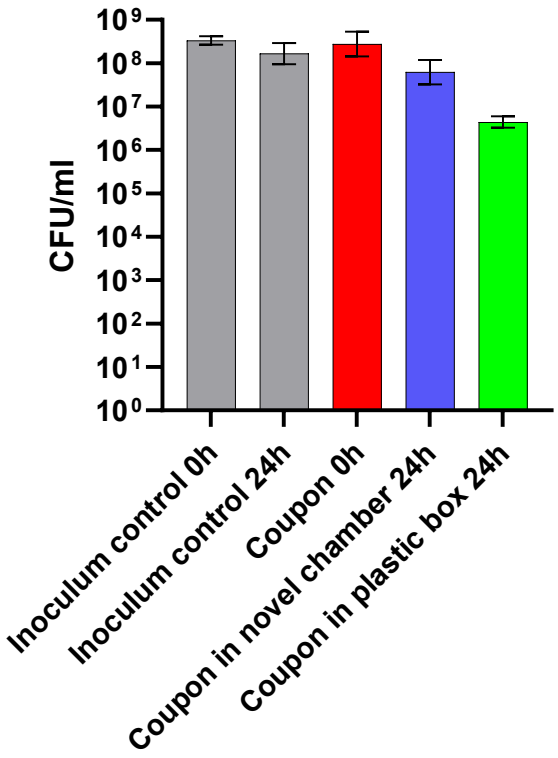

Figure 19 The CFU/mL counts from a liquid inoculum of S. aureus ATCC6538 *and from stainless steel 316L coupons (coupon) inoculated with S. aureus ATCC6538 and recovered after 0 and 24 hours. The inoculum control in each case refers to the remaining bacterial culture that was not applied to the coupons. Novel chamber and plastic box refers to the coupons placed in the novel environmental control chamber and the traditional method of performing ISO22196 respectively.*

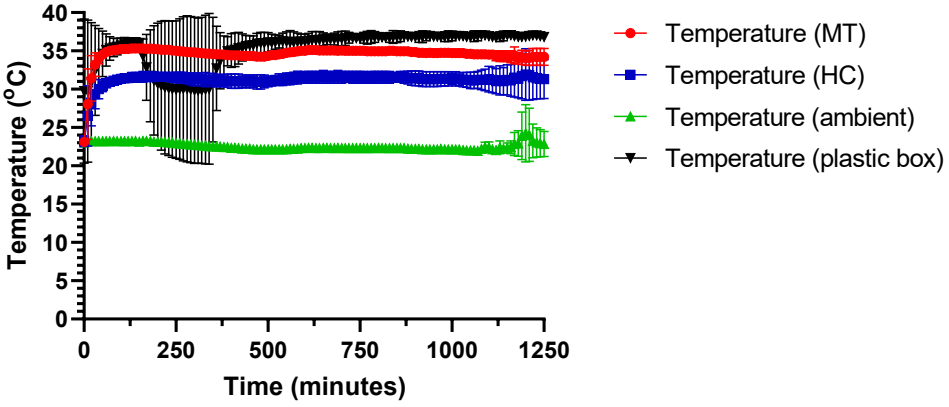

Figure 20 The temperature in each of the compartments of the novel chamber (MT and HC) and the surrounding environment (ambient), as well as inside the plastic box over a 24 hour period. Data collected during experiment to assess the recovery of S. aureus ATCC6538 from stainless steel 316L when placed in a petri dish with the lids on inside the novel environmental control chamber (MT and HC referring to the material placement and humidity control compartments respectively) or a plastic box appropriate for the current method of ISO22196. N= 2.

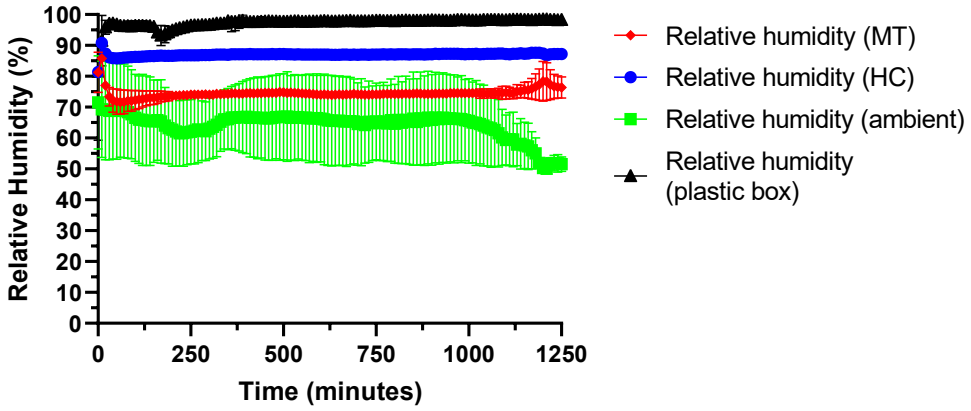

Figure 21 The relative humidity in each of the compartments of the novel chamber (MT and HC) and the surrounding environment (ambient), as well as inside the plastic box over a 24 hour period. Data collected during experiment to assess the recovery of S. aureus ATCC6538 from stainless steel 316L when placed in a petri dish with the lids on inside the novel environmental control chamber (MT and HC referring to the material placement and humidity control compartments respectively) or a plastic box appropriate for the current method of ISO22196. N= 2.

3.3.1.2. Coupons placed in a petri dish with the lids off

The bacterial viability data (Figure 22) show a 0.544-log reduction from the inoculum control compared to the CFU/mL recovered from stainless steel coupons at time 0, followed by a further drop in the CFU/mL recovered from stainless steel coupons from both the novel chamber and the plastic box at 24 hours (plastic box – further log reduction = 1.382, novel chamber – further log reduction = 1.28). The inoculum control at time zero (2.87×10^8) was significantly different from the inoculum control at 24 hours (4.62×10^7, log difference = 0.825, $p < 0.0001$). However, the CFU/mL recovered from stainless steel coupons from both the novel chamber (4.63×10^6) and the plastic box (3.61×10^6) at 24 hours were not significantly different from the inoculum control at 24 hours (p-values - new chamber = 0.5595, traditional chamber 0.5366). The temperature values (Figure 23) maintained minimal variability in all cases and were 35.9 ± 1.5 °C in the plastic box, 33.7 ± 0.4 °C and 29.1 ± 0.3 °C in the MT and HC compartments of the novel chamber and 22.3 ± 0.5 °C in the surrounding environment. The temperature between all locations is significantly different (p-values < 0.0001). The relative humidity values (Figure 24) achieved 99.3 ± 2.2 % in the plastic box, as well as 89.7 ± 1.0 % and 71.6 ± 1.3 % in the HC and MT compartments of the novel chamber respectively, and between 38.5-56.6 % in the ambient conditions. The relative humidity values were significantly different between all locations when considering the entire test period ($p < 0.0001$).

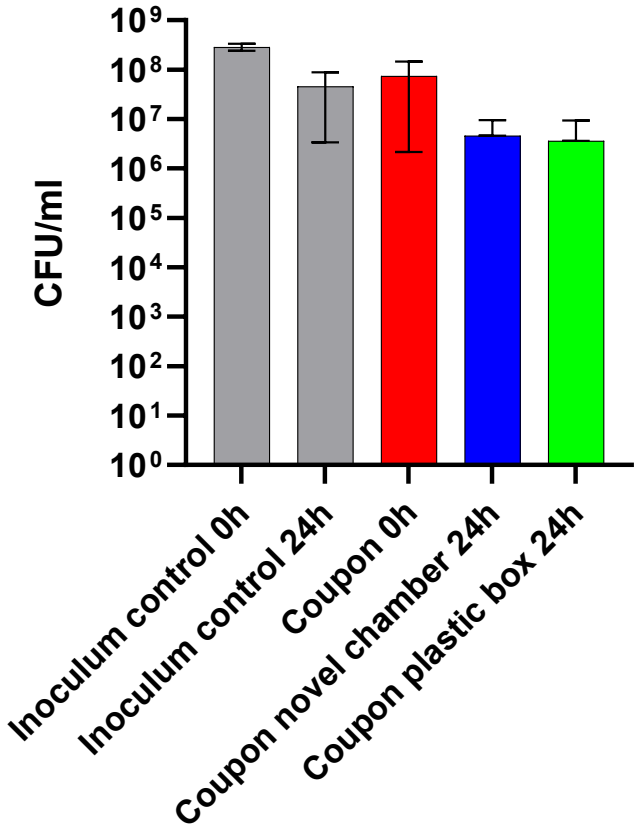

Figure 22 The CFU/mL counts from a liquid inoculum of S. aureus ATCC6538 *and from stainless steel 316L coupons (coupon) inoculated with S. aureus ATCC6538 and recovered after 0 and 24 hours. The inoculum control in each case refers to the remaining bacterial culture that was not applied to the coupons. Novel chamber and plastic box refers to the coupons placed in the novel environmental control chamber and the traditional method of performing ISO22196 respectively.*

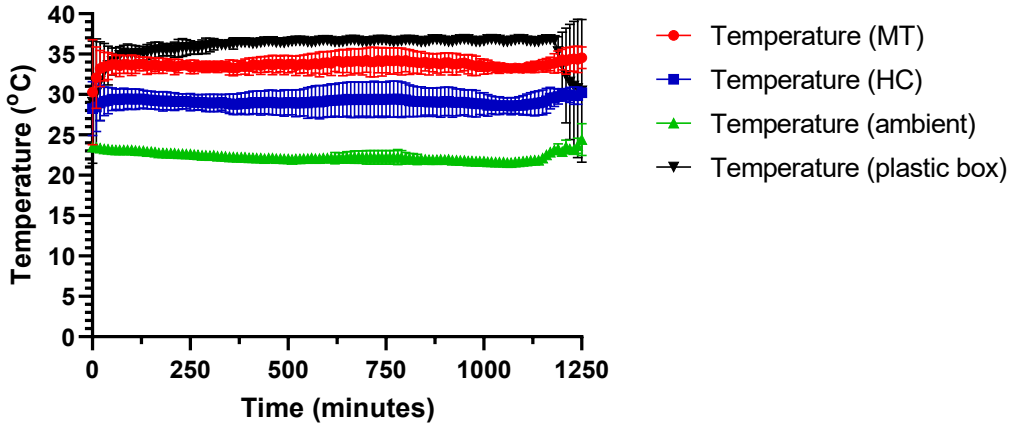

Figure 23 The temperature in each of the compartments of the novel chamber (MT and HC) and the surrounding environment (ambient), as well as inside the plastic box over a 24 hour period. Data collected during experiment to assess the recovery of S. aureus ATCC6538 from stainless steel 316L when placed in a petri dish with the lids off inside the novel environmental control chamber (MT and HC referring to the material placement and humidity control compartments respectively) or a plastic box appropriate for the current method of ISO22196. N= 2.

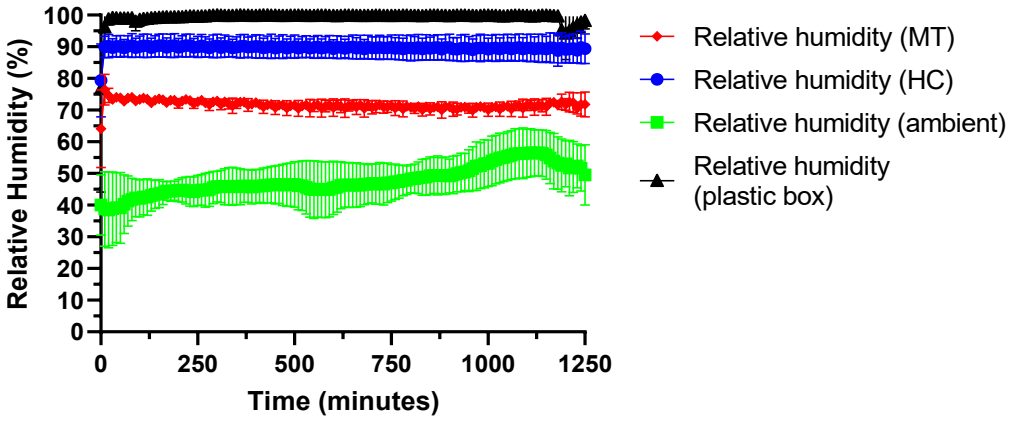

Figure 24 The relative humidity in each of the compartments of the novel chamber (MT and HC) and the surrounding environment (ambient), as well as inside the plastic box (traditional) over a 24 hour period. Data collected during experiment to assess the recovery of S. aureus ATCC6538 from stainless steel 316L when placed in a petri dish with the lids off inside the novel environmental control chamber (MT and HC referring to the material placement and humidity control compartments respectively) or a plastic box appropriate for the current method of ISO22196. N= 2.

3.3.1.3. Coupons placed a custom 3D printed tray

The bacterial viability data (Figure 25) show very little difference between the inoculum ($7.75x10^7$) and the material ($8.69x10^7$) at time 0 ($p = 0.9971$), but a significant drop of 2.39-log in the inoculum is observed after 24 hours ($3.65x10^5$, $p < 0.0001$). The location of the coupon in the MT compartment affected the survival of bacteria on the coupon, with positions B10 ($1.30x10^7$) and E10 ($1.60x10^7$) showing the highest survival, whereas the positions E1 ($9.40x10^5$), E4 ($1.07x10^6$) and E7 ($7.73x10^5$) showed lower survival. Additionally

positions B1 ($1.76x10^5$) and B4 ($2.76x10^5$) were like that of the inoculum at 24 hours ($p > 0.9999$) and position B7 ($8.84x10^3$) showed the greatest reduction from the inoculum at time 0 (log difference = 3.891). The Inoculum and material at time 0 were not significantly different from each other but were from all other inoculum and material points. No coupon position in the novel chamber at 24 hours was significantly different to the inoculum at 24 hours ($p > 0.9$). The temperature (Figure 26) in the plastic box was 35.0 ± 1.9 ^oC throughout the experiment, whereas the MT and HC compartments of the novel chamber had a less variable temperature of 32.0 ± 1.4 ^oC and 28.4 ± 0.9 ^oC respectively. The ambient environment maintained a temperature of 22.7 ± 0.3 ^oC for the duration of the experiment. The temperatures in the plastic box, novel chamber and ambient external temperatures were statistically different from each other (p-values < 0.0001). The relative humidity (Figure 27) in the traditional chamber achieved 99.0 ± 3.2 %, whereas a relative humidity of 90.0 ± 1.3 % and 71.6 ± 1.9 % was achieved in the HC and MT compartments of the novel chamber respectively and an ambient relative humidity range of 49.1-58.2 %. The relative humidity values at each location were also statistically different from all other locations (p-values <0.0001).

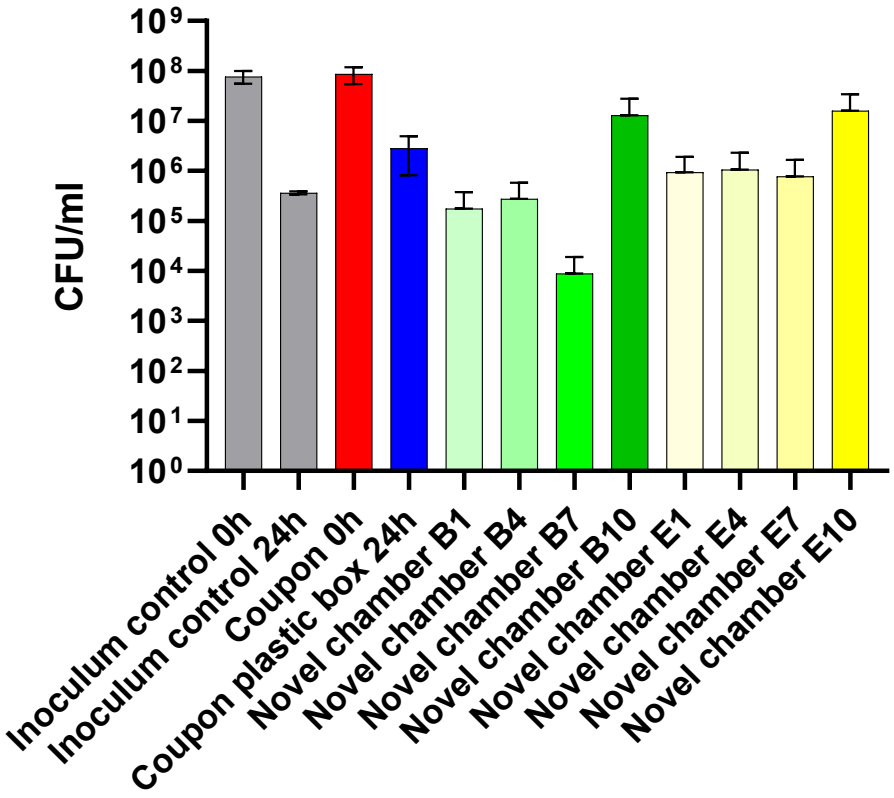

Figure 25 The CFU/mL counts from a liquid inoculum of S. aureus ATCC6538 *and from stainless steel 316L coupons (coupon) inoculated with S. aureus ATCC6538 and recovered after 0 and 24 hours. The inoculum control in each case refers to the remaining bacterial culture that was not applied to the coupons. Novel chamber (positions B1, B4, B7, B10, E1, E4, E7, E10: Figure 18) and plastic box refers to the coupons placed in the novel environmental control chamber and the traditional method of performing ISO22196 respectively.*

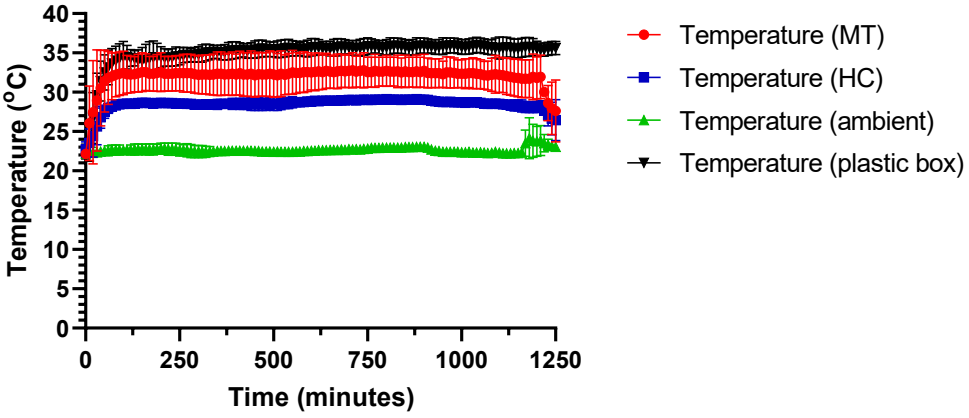

Figure 26 The temperature in each of the compartments of the novel chamber (MT and HC) and the surrounding environment (ambient), as well as inside the plastic box over a 24 hour period. Data collected during experiment to assess the recovery of S. aureus ATCC6538 from stainless steel 316L when placed in a custom designed and 3D printed tray inside the novel environmental control chamber (MT and HC referring to the material placement and humidity control compartments respectively) or in a petri dish (lid removed) placed in a plastic box appropriate for the current method of ISO22196. N= 2.

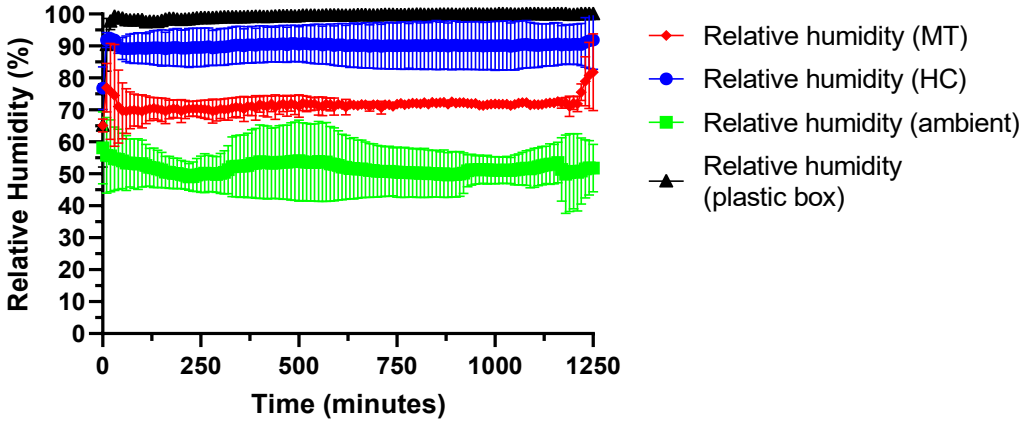

Figure 27 The relative humidity in each of the compartments of the novel chamber (MT and HC) and the surrounding environment (ambient), as well as inside the plastic box over a 24 hour period. Data collected during experiment to assess the recovery of S. aureus ATCC6538 from stainless steel 316L when placed in a custom designed and 3D printed tray inside the novel environmental control chamber (MT and HC referring to the material placement and humidity control compartments respectively) or in a petri dish (lid removed) placed in a plastic box appropriate for the current method of ISO22196. N= 2.

3.3.2. Further trial use of the novel chamber to undertake ISO22196: *Escherichia coli*

3.3.2.1. Survival on steel – 24 °C / >90 % relative humidity

The temperature during this experiment displayed large variation in the MT (22.7 ± 0.8 °C) and HC (22.7 ± 0.6 °C) compartment that follows the trend of the ambient temperature closely (22.0 ± 0.6 °C). The plastic box maintained 23.9 ± 0.4 °C throughout the test. The relative humidity of the plastic box and in both compartments of the novel chamber demonstrate a sharp increase up to >80 %, with a relative humidity of 96.2 ± 5.2 % (MT), 97.3 ± 4.4 % (HC), and 98.0 ± 4.7 % (plastic box) achieved overall. The ambient relative humidity had a range of 34.8-41.7 %. The bacterial viability data show an initial inoculum of 4.41×10^5 CFU/mL, with lower (log reduction – 0.107, $p > 0.9999$) counts recovered from the coupons at the 0h time point (3.34×10^5). After 24 hours, the inoculum (1.09×10^6) was higher (but not statistically significantly) than the 0h recovery from stainless steel coupons ($p > 0.9999$). The coupons recovered from the plastic box at 24 hours (1.11×10^7) was significantly different to both the inoculum control at 24 hours (1.09×10^6, $p = 0.0433$) and the coupons recovered at 0h (3.34×10^5, $p = 0.0018$). All coupons in the novel chamber (5.32×10^5-2.38×10^6) were approximately equal to that in the inoculum after 24 hours (1.09×10^6) and there was no statistically significant difference between the coupon placements in the novel chamber (p values > 0.9999). The bacterial viability data from the coupons in the plastic box was significantly higher than those in the novel chamber except for position E1 ($p < 0.05$, E1 = 0.1271).

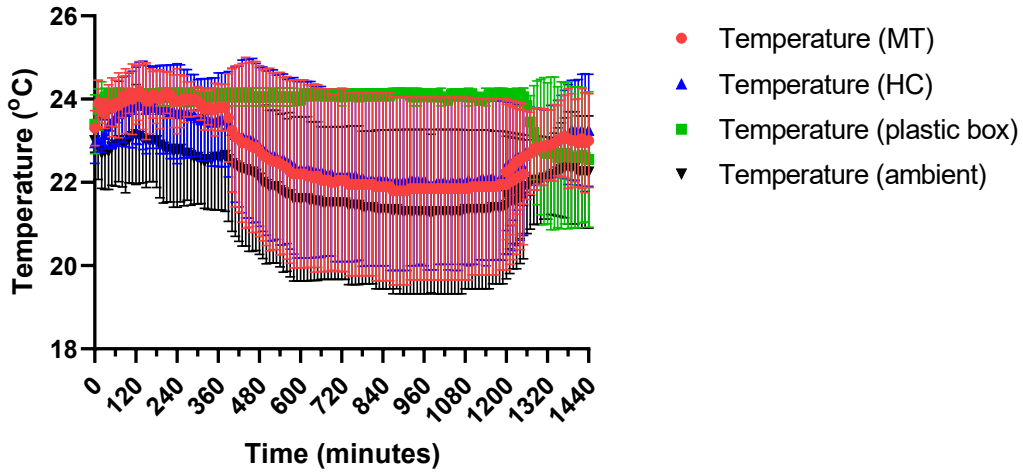

Figure 28 The temperature in each of the compartments of the novel chamber (MT and HC) and the surrounding environment (ambient), as well as inside the plastic box over a 24 hour period. Data collected during experiment to assess the recovery of E. coli NCIMB 8545 from stainless steel 316L when placed in a custom designed and 3D printed tray inside the novel environmental control chamber (MT and HC referring to the material placement and humidity control compartments respectively) or a plastic box appropriate for the current method of ISO22196. N= 2.

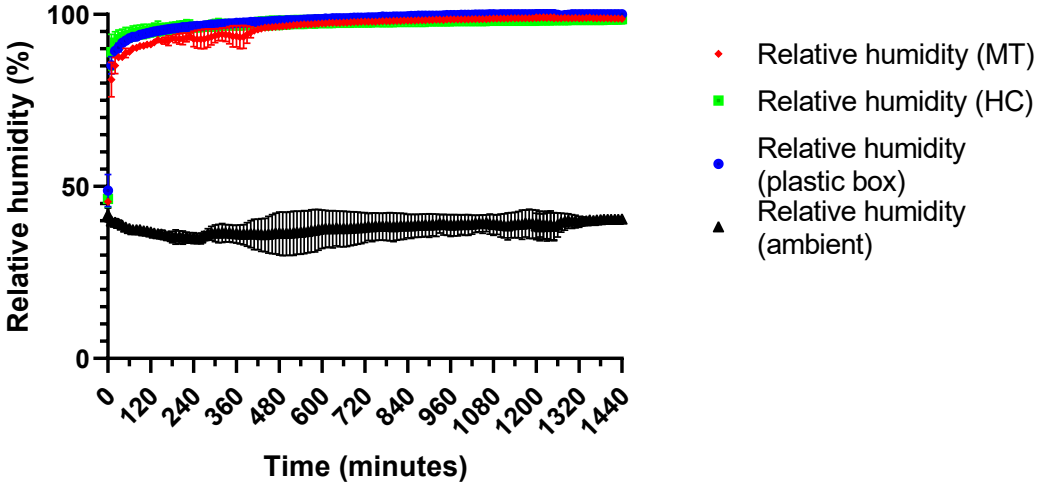

Figure 29 The relative humidity in each of the compartments of the novel chamber (MT and HC) and the surrounding environment (ambient), as well as inside the plastic box over a 24 hour period. Data collected during experiment to assess the recovery of E. coli NCIMB 8545 from stainless steel 316L when placed in a custom designed and 3D printed tray inside the novel environmental control chamber (MT and HC referring to the material placement and humidity control compartments respectively) or a plastic box appropriate for the current method of ISO22196. N= 2.

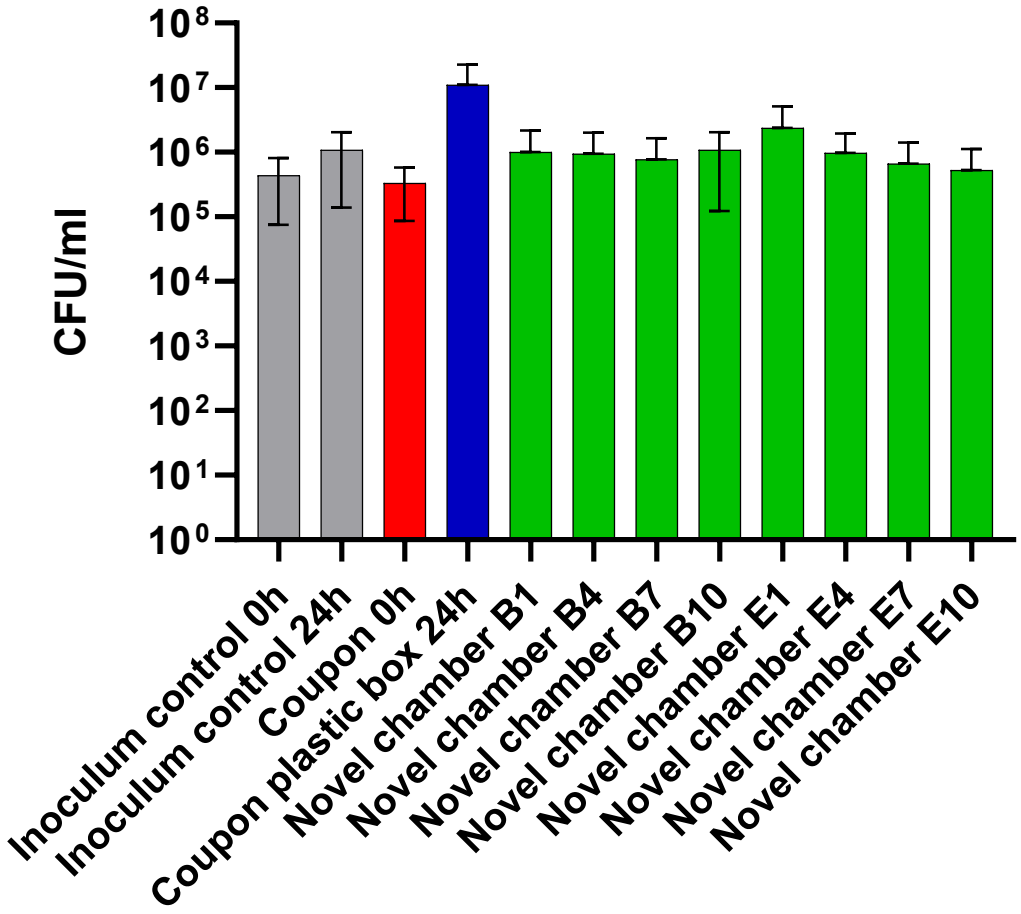

Figure 30 The CFU/mL counts from a liquid inoculum of E. coli NCIMB 8545 and from stainless steel 316L coupons (coupon) inoculated with E. coli NCIMB 8545 and recovered after 0 and 24 hours. The inoculum control in each case refers to the remaining bacterial culture that was not applied to the coupons. Novel chamber (positions B1, B4, B7, B10, E1, E4, E7, E10: Figure 18) and plastic box refers to the coupons placed in the novel environmental control chamber and the traditional method of performing ISO22196 respectively.

3.3.2.2. Survival on copper – 24 °C / >90 % relative humidity

The temperature during this experiment in the plastic box achieved 23.2 ± 0.6 °C. The novel chamber maintained 23.4 ± 0.2 °C and 22.9 ± 0.1 °C for the duration of the test in the MT and HC compartments respectively, while the ambient temperature had a range of 21.0-23.2 °C. The relative humidity in the chambers is like that of the previous experiment (3.3.2.1) with a sharp incline to >80 % within the first hour. The plastic box achieved 97.0 ± 8.3 %, while the MT and HC compartments of the novel chamber achieved 93.6 ± 2.4 % and 96.1 ± 3.1 %. The ambient relative humidity ranged between 39.4-50.7 %. The CFU recovered shows an initial inoculum of 4.78×10^5 CFU/mL as expected with slightly, but not statistically significantly lower counts recovered from the Cu coupons at the 0h time point (2.29×10^5). The inoculum concentration increased slightly after 24 hours (1.16×10^6) as well

as in the steel coupons in the plastic box ($5.13x10^6$). All Cu coupons in both the plastic box and novel chamber recovered no CFU after 24 hours.

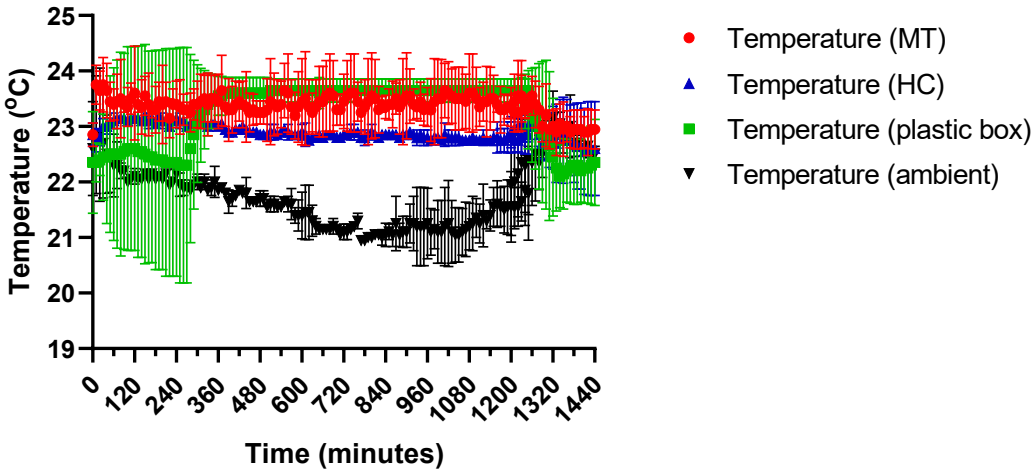

Figure 31 The temperature in each of the compartments of the novel chamber (MT and HC) and the surrounding environment (ambient), as well as inside the plastic box over a 24 hour period. Data collected during experiment to assess the recovery of E. coli NCIMB 8545 from stainless steel 316L and copper (CuSn5) when placed in a custom designed and 3D printed tray inside the novel environmental control chamber (MT and HC referring to the material placement and humidity control compartments respectively) or a plastic box appropriate for the current method of ISO22196. N= 2.

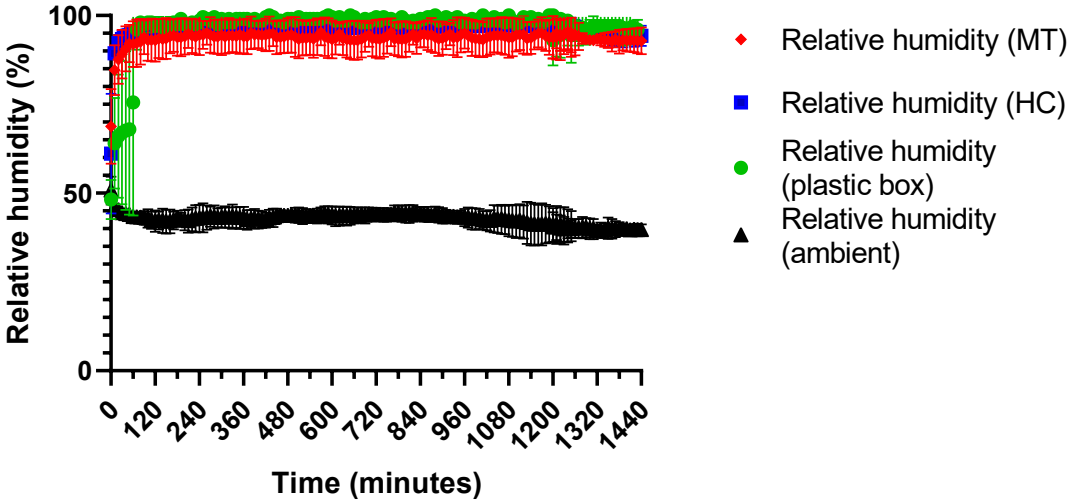

Figure 32 The relative humidity in each of the compartments of the novel chamber (MT and HC) and the surrounding environment (ambient), as well as inside the plastic box over a 24 hour period. Data collected during experiment to assess the recovery of E. coli NCIMB 8545 from stainless steel 316L and copper (CuSn5) when placed in a custom designed and 3D printed tray inside the novel environmental control chamber (MT and HC referring to the material placement and humidity control compartments respectively) or a plastic box appropriate for the current method of ISO22196. N= 2.

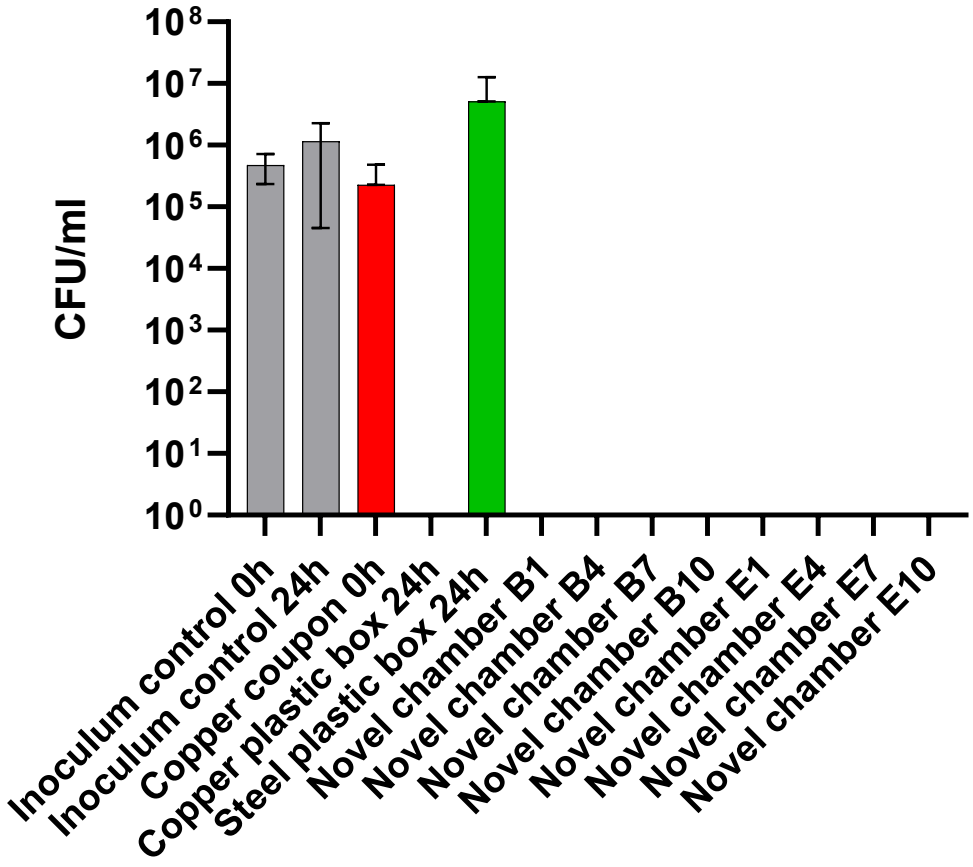

Figure 33 The CFU/mL counts from a liquid inoculum of E. coli NCIMB 8545 and from stainless steel 316L and copper (CuSn5) coupons (coupon) inoculated with E. coli NCIMB 8545 and recovered after 0 and 24 hours. The inoculum control in each case refers to the remaining bacterial culture that was not applied to the coupons. Novel chamber (positions B1, B4, B7, B10, E1, E4, E7, E10: Figure 18) and plastic box refers to the coupons placed in the novel environmental control chamber and the traditional method of performing ISO22196 respectively.

3.3.2.3. Survival on steel – 30 °C / ~75 % relative humidity

The temperature (Figure 34) maintained 29.0 ± 1.1 °C and 28.5 ± 1.9 °C in the MT compartment of the novel chamber and plastic box respectively, and 26.8 ± 0.4 °C in the HC compartment of the novel chamber, with an ambient temperature of 23.9 ± 0.6 °C. The relative humidity (Figure 35) maintained the same trends as the previous tests (e.g. 3.3.2.2) for the HC compartment of the novel chamber (97.7 ± 2.3 %) and the plastic box (97.1 ± 3.8 %). The relative humidity of the MT compartment of the novel chamber was 82.4 ± 2.8 % with an ambient relative humidity range of 25.0-34.7 %. The bacterial viability data (Figure 36) demonstrated an initial inoculum concentration of 3.26×10^5 CFU/mL, with a slightly but not statistically significantly higher recovery from the steel coupons at the 0h time point (8.71×10^5, p = 0.9836). The CFU/mL recovered from the inoculum control (1.39×10^6) and coupons in the plastic box (9.20×10^5) after 24 hours were not statistically different (p =

0.9850). Recovery of *E. coli* on stainless steel that had been incubated after 24 hours in the novel chamber were variable based on coupon placement. Coupons in position B1 recovered no CFU, whilst coupons placed in B10 ($4.80x10^5$) and E10 ($8.99x10^5$) had the highest CFU/mL recovery, with no significant difference from time zero (p values > 0.99). Coupons in positions B4 ($1.89x10^5$), E4 ($1.74x10^5$) and E7 ($1.01x10^5$) decreased slightly (around 1-log from initial coupon recovery). Coupons in placement E1 ($3.79x10^4$) showed slightly reduced recovery again and finally placement B7 ($5.05x10^3$) showed an even greater reduction. Due to variation between the repeats of the experiments, there were no significant differences between each different time point and location but there was a significant difference between the overall means (p-value = 0.0258).

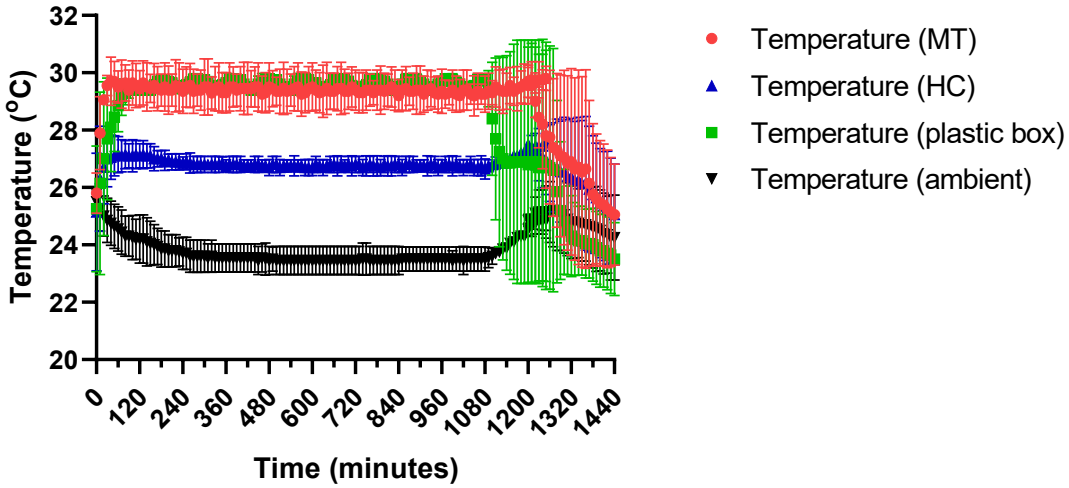

Figure 34 The temperature in each of the compartments of the novel chamber (MT and HC) and the surrounding environment (ambient), as well as inside the plastic box over a 24 hour period. Data collected during experiment to assess the recovery of E. coli NCIMB 8545 from stainless steel 316L when placed in a custom designed and 3D printed tray inside the novel environmental control chamber (MT and HC referring to the material placement and humidity control compartments respectively) or a plastic box appropriate for the current method of ISO22196. N= 2.

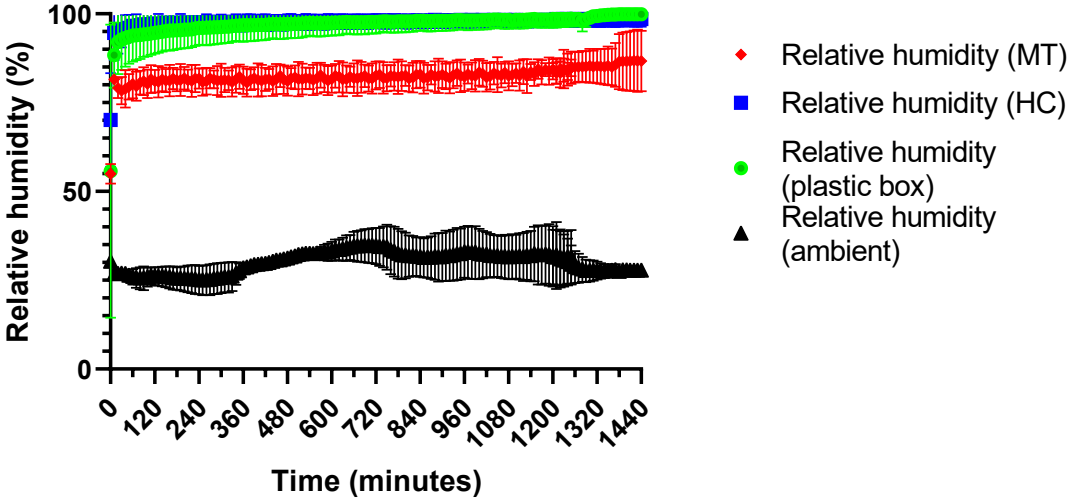

Figure 35 The relative humidity in each of the compartments of the novel chamber (MT and HC) and the surrounding environment (ambient), as well as inside the plastic box over a 24 hour period. Data collected during experiment to assess the recovery of E. coli NCIMB 8545 from stainless steel 316L when placed in a custom designed and 3D printed tray inside the novel environmental control chamber (MT and HC referring to the material placement and humidity control compartments respectively) or a plastic box appropriate for the current method of ISO22196. N= 2.

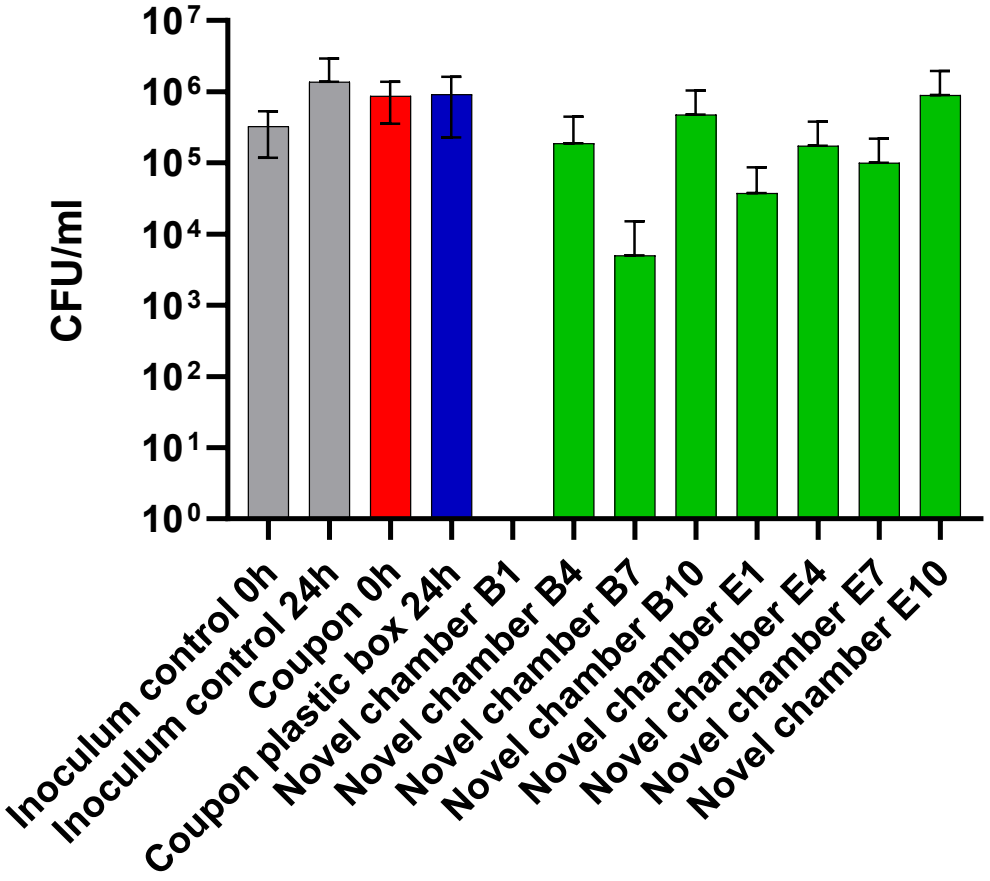

Figure 36 The CFU/mL counts from a liquid inoculum of E. coli NCIMB 8545 and from stainless steel 316L coupons (coupon) inoculated with E. coli NCIMB 8545 and recovered after 0 and 24 hours. The inoculum control in each case refers to the remaining bacterial culture that was not applied to the coupons. Novel chamber (positions B1, B4, B7, B10, E1, E4, E7, E10: Figure 18) and plastic box refers to the coupons placed in the novel environmental control chamber and the traditional method of performing ISO22196 respectively.

3.3.2.4. Survival on steel – 30 °C / ~65 % relative humidity / one fan operating

The temperature (Figure *37*) during this test in both chambers was stable, with 29.8 ± 0.5 °C and 29.6 ± 1.0 °C being maintained in the MT compartment of the novel chamber and plastic box respectively, as well as 26.2 ± 0.3 °C in the HC compartment while the ambient air temperature was 23.3 ± 0.5 °C. The relative humidity (Figure 38) in the plastic box (95.3 ± 4.9 %) followed the trends of previous tests but was lower in the novel chamber at 86.8 ± 2.5 % in the HC compartment and 65.0 ± 2.7 % in the MT compartment. The ambient relative humidity ranged between 24.0-28.9 % during this test. The CFU (Figure 39) recovered initially from the inoculum was 2.38×10^5 CFU/mL, with no statistical difference from the steel coupons when recovered immediately ($p = 0.9998$). There was no significant difference ($p > 0.9999$) in the inoculum after 24 hours (2.89×10^5) and a slight (0.878-log)

increase in the recovery from the coupons recovered from the plastic box ($1.67x10^6$). There was no recovery from any coupons within the novel chamber.

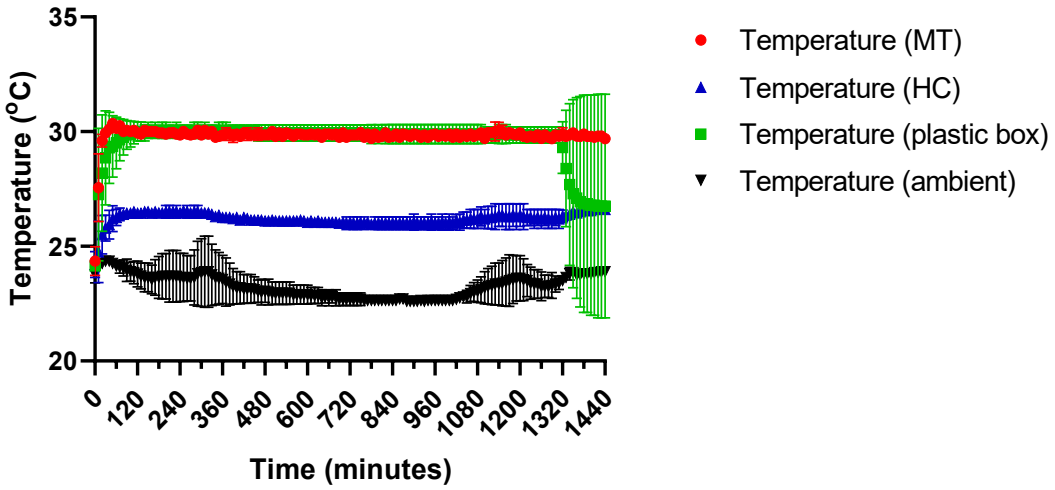

Figure 37 The temperature in each of the compartments of the novel chamber (MT and HC) and the surrounding environment (ambient), as well as inside the plastic box over a 24 hour period. Data collected during experiment to assess the recovery of E. coli NCIMB 8545 from stainless steel 316L when placed in a custom designed and 3D printed tray inside the novel environmental control chamber (MT and HC referring to the material placement and humidity control compartments respectively) or a plastic box appropriate for the current method of ISO22196. N= 2.

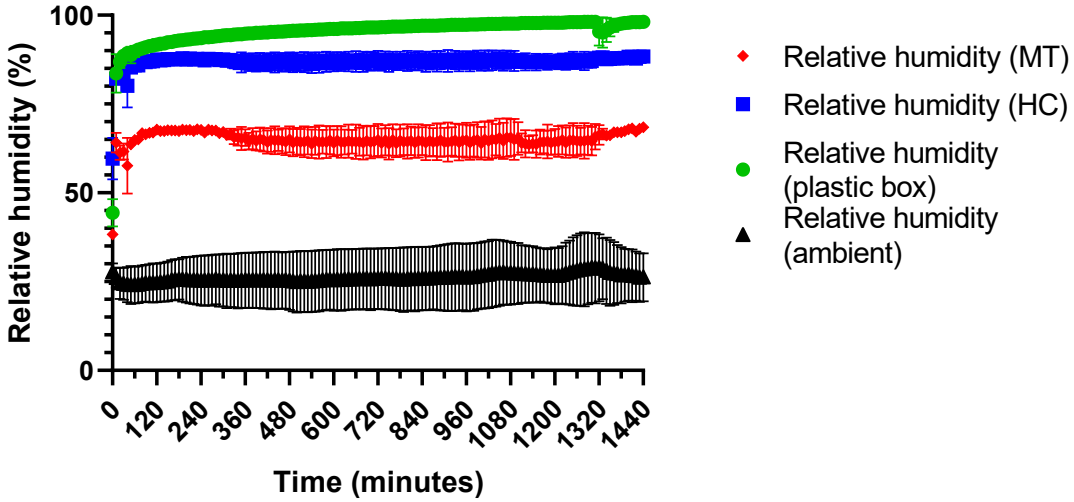

Figure 38 The relative humidity in each of the compartments of the novel chamber (MT and HC) and the surrounding environment (ambient), as well as inside the plastic box over a 24 hour period. Data collected during experiment to assess the recovery of E. coli NCIMB 8545 from stainless steel 316L when placed in a custom designed and 3D printed tray inside the novel environmental control chamber (MT and HC referring to the material placement and humidity control compartments respectively) or a plastic box appropriate for the current method of ISO22196. N= 2.

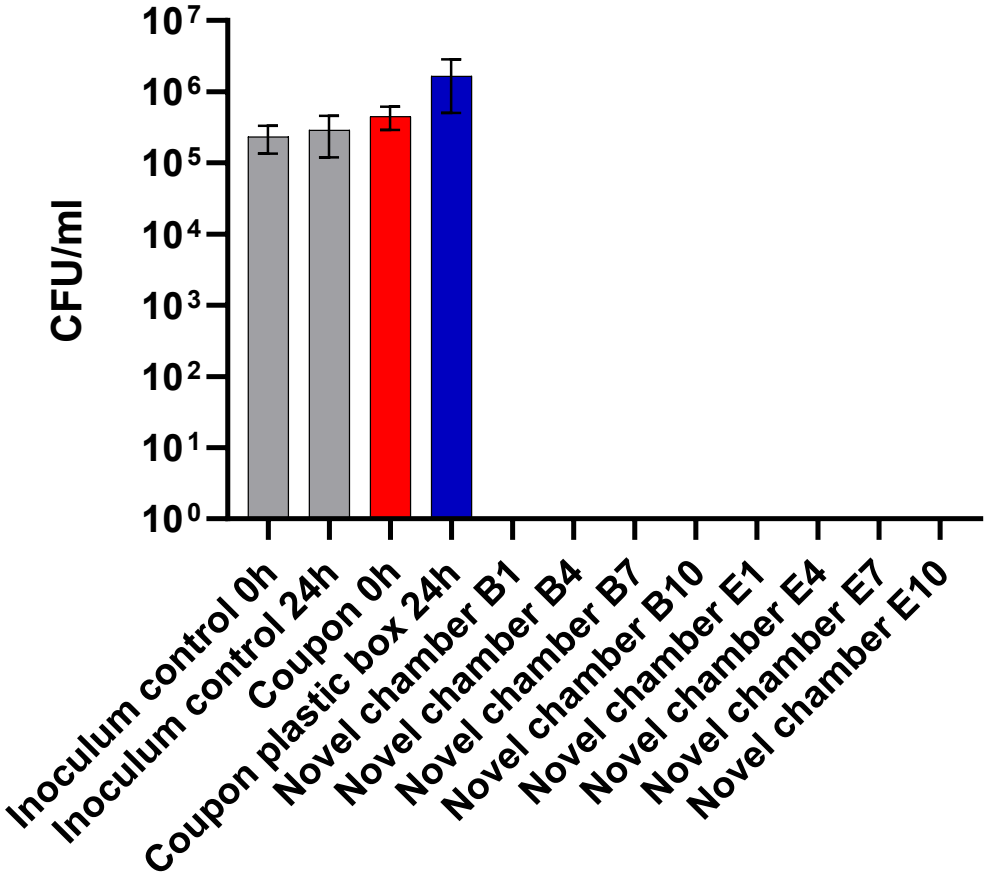

Figure 39 The CFU/mL counts from a liquid inoculum of E. coli NCIMB 8545 and from stainless steel 316L coupons (coupon) inoculated with E. coli NCIMB 8545 and recovered after 0 and 24 hours. The inoculum control in each case refers to the remaining bacterial culture that was not applied to the coupons. Novel chamber (positions B1, B4, B7, B10, E1, E4, E7, E10: Figure 18) and plastic box refers to the coupons placed in the novel environmental control chamber and the traditional method of performing ISO22196 respectively.

3.3.2.5. Survival on steel – 24 °C / ~40 % relative humidity / four hours

A temperature (Figure 40) of 25.3 ± 0.4 °C and 25.6 ± 0.3 °C was seen across the test period within the MT and HC compartments of the novel chamber respectively with a slightly lower ambient temperature range of around 24.6 ± 0.4 °C. The relative humidity (Figure 41) was 46.0 ± 0.1 % and 45 ± 0.2 % in the MT and HC compartments of the novel chamber respectively and a range of 27.1-29.1 % ambient relative humidity. The CFU/mL counts (Figure 42) show the inoculum concentration only minimally reducing across the four hours ($2.73x10^5$-$2.38x10^5$), and a linear reduction in CFU/mL for the first three hours on the material ($2.30x10^5$-$2.63x10^4$) with high variability at two hours and beyond, followed by a steep reduction to zero CFU/mL at four hours. The inoculum and material were statistically significant at 1-hour (p-value < 0.001) and beyond (p-values < 0.0001).

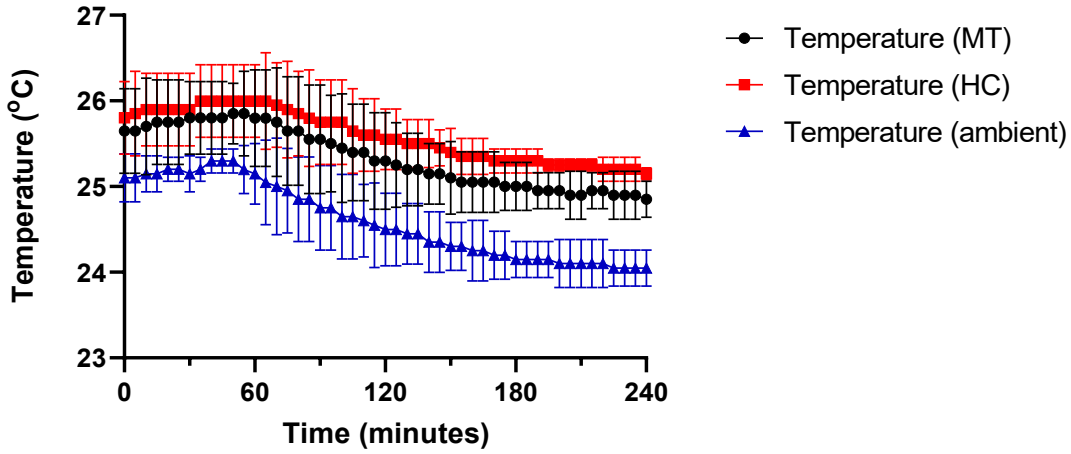

Figure 40 The temperature in each of the compartments of the novel chamber (MT and HC) and the surrounding environment (ambient). Data collected during experiment to assess the recovery of E. coli NCIMB 8545 from stainless steel 316L when placed in a custom designed and 3D printed tray inside the novel environmental control chamber (MT and HC referring to the material placement and humidity control compartments respectively). N= 2.

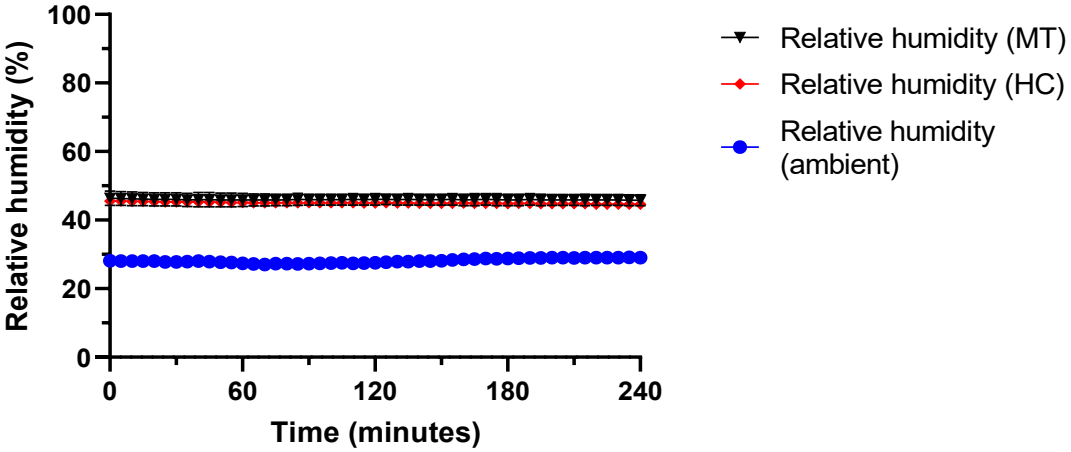

Figure 41 The relative humidity in each of the compartments of the novel chamber (MT and HC) and the surrounding environment (ambient). Data collected during experiment to assess the recovery of E. coli NCIMB 8545 from stainless steel 316L when placed in a custom designed and 3D printed tray inside the novel environmental control chamber (MT and HC referring to the material placement and humidity control compartments respectively). N= 2.

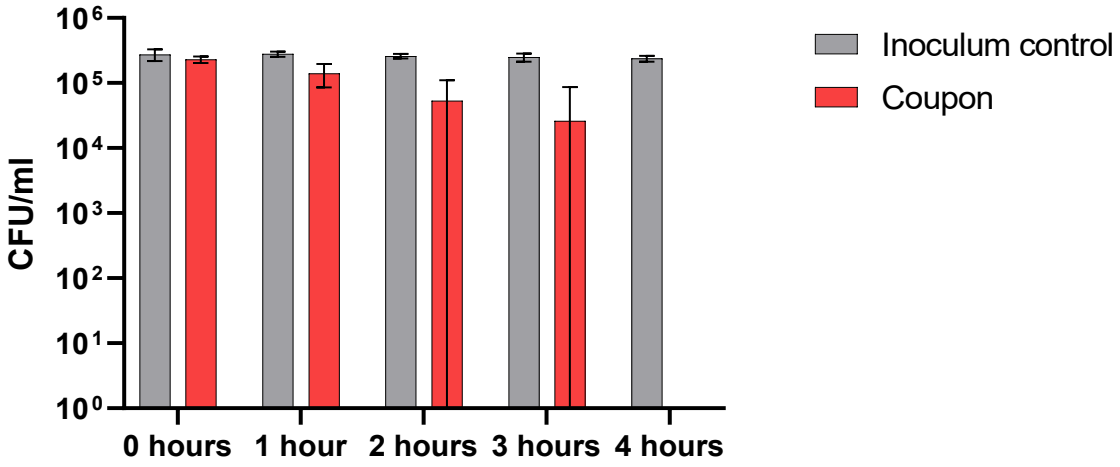

Figure 42 The CFU/mL counts from a liquid inoculum of E. coli NCIMB 8545 and from stainless steel 316L coupons (coupon) inoculated with E. coli NCIMB 8545 and recovered after 0, 1, 2, 3, and 4 hours. The inoculum control in each case refers to the remaining bacterial culture that was not applied to the coupons.

3.4. Discussion

3.4.1. Comparison using ISO22196: *Staphylococcus aureus*

The impact of coupon position on the survival of bacteria on a surface within the chamber highlights the natural variability that will occur even when considering small differences in environmental conditions and using a desiccant-resistant organism (Chaibenjawong and Foster, 2011) (among many other gram-positive organisms (Janning and In't Veld, 1994)). However, it is also important to understand how other factors affect this process. For example, although the addition of the petri dish lid does not change the environmental conditions in a large way (e.g. by creating a microenvironment that can raise the relative humidity slightly further (Oswin et al., 2022)), other factors such as the low nutrient conditions present in the inoculum may affect bacterial survival and viability (Winfield and Groisman, 2003). Furthermore, the process of removing the supernatant (which is used in many STMs such as ISO22196) and replacing it with a low nutrient medium often results in some media remaining in the inoculum. Although this is then diluted, variation is still introduced that should be factored in and considered when assessing the results of an STM.

When specifically considering the test where the petri dish lids were removed (3.3.1.2), the possibility of even intra-laboratory error is potentially observed by the statistically significant difference between the inoculum and material at time 0. This would likely be

further exacerbated when testing materials in multiple different laboratories when considering differences in available equipment and personnel.

The test conducted using the custom 3D printed coupon tray (3.3.1.3) highlighted not only that methodological variation is produced (e.g. a reduction of the bacterial inoculum after 24 hours compared to other tests) but also that the environmental conditions play a large role in the survival and / or viability of bacteria on a surface (Zoz et al., 2016). This is demonstrated by the enhanced survival of *S. aureus* in the coupon locations closer to the HC compartment, as these positions will have a greater supply of humidified air. This phenomenon provides insights into how AMMs may react in an end-use scenario, as these small variations in the environmental conditions (depending on distance from the HC compartment and airflow more generally) would likely be mimicked on a larger scale by air conditioning and movement of people etc in an indoor acclimatised setting (M. F. Hasan et al., 2017). Nevertheless, the differences generated by the different coupon placements throughout the novel chamber were not statistically significant, highlighting both the variability and complexity of incorporating additional variables into STMs. It is also important to consider that these trends would likely be reversed if the relative humidity was targeted to be lower than the ambient conditions. The importance of random placements of the coupons would also be vital in this chamber to ensure the validity of the results. It may also be possible to be able to create zones of placements within the tray that would allow fewer samples to be tested while ensuring each variation of environmental conditions within the chamber is tested.

3.4.2. Further modifications to ISO22196: *Escherichia coli*

Survival on steel – 24 °C / >90 % relative humidity

The larger temperature variations during this test (whereby the MT and HC compartments followed the same pattern as the ambient conditions) highlights the difficulty of maintaining lower temperatures accurately within the chamber, particularly if the surrounding environment maintains a high temperature, and provides potential for further upgrades to the chamber to allow cooling as well as heating. Cooling systems such as a liquid-cooling piping system (often used to cool computer components (Khalaj and Halgamuge, 2017)) would allow a greater range of end-use scenarios to be simulated by the novel chamber. However, it should be noted that the temperature variability in this

test is still within the recommended ±2 °C specified in many current STMs and so is likely not a source of error when regarding the bacterial viability data.

The relative humidity values achieved in the novel chamber highlight a large improvement, by achieving >90 % RH in less than two hours. Such a high relative humidity was also able to allow all coupons to retain their inoculum for the duration of the test, allowing for a somewhat realistic version of ISO22196 to be performed. The CFU recovered from the coupons and inoculum shows that recovering bacteria from steel coupons using this method (stomacher bags) yields an almost exact recovery rate and should be considered when creating more realistic STMs in the future, although there has already been use of this method with current STMs as well (El Jaouhari et al., 2017). Additionally, the increase in CFU in the inoculum and coupons after 24 hours is likely attributed to the nutrients present in the 1/500 nutrient broth or error incurred from suboptimal removal of the nutrient medium when removing the supernatant after centrifugation. The difference between the traditional and novel chamber coupons could possibly be explained by the slightly higher relative humidity resulting in less evaporation of the inoculum of the droplet on the surface but given that both chambers are above 90 % relative humidity, it is unlikely that this is the cause. It could also be that the process of recovery to remove the coupons from the novel chamber is more prone to error and / or less efficient than that in the traditional chamber.

Survival on copper – 24 °C / >90 % relative humidity

The recovery from the inoculum at zero hours and 24 hours as well as the steel coupons in the traditional chamber show a similarity to the other tests with a slightly increased recovery, but interestingly despite the antimicrobial effect of Cu it has caused no significant changes in the recovery rate of bacteria when immediately recovering, this can be expected due to the low contact time (several minutes) which is supported by the literature (lowest time to kill observed at 30 minutes (Chyderiotis et al., 2018)) but highlights the effectiveness of the neutraliser and recovery method. As expected, all Cu coupons recovered zero CFU after 24 hours due to the antimicrobial nature of the material.

Survival on steel – 30 °C / ~75 % relative humidity

The temperature during this test shows that the novel chamber can effectively replicate a standard incubator at 30 °C. Additionally, the relative humidity data demonstrates the large

effect that temperature has on the relative humidity, a six-degree increase causing an approximate 15 % drop in the maximum achievable relative humidity in the chamber. This may not be an issue however as very few end-use scenarios will maintain at or above this temperature and relative humidity simultaneously but could be a potential improvement for the chamber (e.g. by adding more efficient methods of humidifying the air (Byber et al., 2021)). Interestingly, the CFU recovered from the coupons in the novel chamber vary greatly, with a general trend towards higher numbered coupons (closer to the HC compartment) recovering a higher CFU, although this trend does not match exactly as B7 recovered significantly lower CFU than almost all other coupons. In general, this could be expected as coupons in the path of the airflow are receiving a constant supply of humidified air, rendering the inoculum effectively unable to evaporate on the surface and promoting survival. However, other factors such as the desiccation resistance of the bacteria still needs to be considered. Interestingly, none of the CFU values in any case were statistically significant from one another, showing the large variation in these STMs even when simply repeating work when other factors are considered. Even small variations in relative humidity, brought on by differences in equilibration time or otherwise, will impact on how quickly the inoculum will evaporate on the surface and therefore impact the survival of the bacteria.

Survival on steel – 30 °C / ~65 % relative humidity / one fan operating

This test not only highlights the importance of airflow on the evaporation of water (Carrier et al., 2016), which has implications for further developing the novel chamber with enhanced relative humidity control, but also the impact of seemingly minor changes in relative humidity and how it may impact on bacterial survival (Grinberg et al., 2019). Nevertheless, the temperature was not affected by the reduced airflow within the chamber and so the current system often heating can be assumed to have a greater reproducibility. The reduction in relative humidity under lower airflow conditions raises the possibility that adding more fans in to the HC compartment may provide a more efficient humidifying effect to the chamber.

The CFU recovery from the inoculum and coupons that were not in the novel chamber show the same pattern as the previous test (3.3.2.3) but with slightly higher survival in the coupons recovered from the plastic box, showing once again that there is some variability

to the results. Interestingly however, all coupons recovered no CFU whatsoever in the novel chamber, this is likely attributed to the evaporation of the inoculum on the surface but implies that this strain of *E. coli* at the very least cannot survive for 24 hours on an inert material even under what can be reasonably believed to be a high relative humidity for an indoor environment (Asif et al., 2018). This indicates that future STMs that use more realistic environmental conditions will have to consider the incubation time carefully to ensure bacterial survival on an inert surface is guaranteed thus that the AMM can be compared for efficacy, while also considering the speed of antimicrobial action of the AMM being tested, as some AMMs exhibit their antimicrobial effect much faster than others (Bogdanovic et al., 2015).

Survival on steel – 24 °C / ~40 % relative humidity / four hours

The temperature of the chamber during this test was higher than that of the ambient conditions, likely due to the exothermic nature of adding water to potassium carbonate (Gaeini et al., 2019). To alleviate this issue in the future, it should be recommended to prepare the salts several hours and possibly overnight in advance. The stability of the relative humidity during this test shows the advantage of using saturated salts as a method of controlling relative humidity despite the drawbacks (Bui et al., 2017). The CFU recovery from this test shows how the evaporation of the inoculum on the surface is pivotal for the survival of some strains, particularly the desiccant-sensitive *E. coli* NCIMB 8545 that was used during this test. Although this result can be expected based on the characteristics of the strain used, it is vital to consider how these factors may affect novel future STMs with more realistic test conditions, and how current STMs can be adapted to accommodate realistic conditions. Furthermore, while there was no discernible drop in the CFU counts of the inoculum, there is still a decline on the materials during the first three hours of the test before the sharp decline which becomes statistically significant after just one hour of evaporation. This highlights the speed of viability decline of desiccant-sensitive bacteria in droplets. Further tests assessing how non-desiccating bacteria that are common environmental pathogens (e.g., *Acinetobacter baumanii*) would provide useful information on the direction of development for current STMs when implementing more realistic conditions.

3.4.3. Overall discussion

When testing efficacy of an AMM, the impact of inoculum evaporation and environmental conditions can be a significant factor in determining the data that are produced. Considerations such as temperature, relative humidity, airflow, organism choice and inoculum density, and even placement of a coupon within a chamber can all impact the results of efficacy testing, and how an antimicrobial claim may be interpreted. Each of these factors cannot be thought of as individual parameters that can be changed without further and interconnected change, but a web of impacts on the antimicrobial efficacy of the AMM. These may be related to the evaporation of the inoculum on the surface, the biological mechanisms of survival during desiccation or how the active ingredient of the material works. Changing just one of these factors (all of which are required in current STMs, with the exception of airflow) will impact on the evaporation of the inoculum on the surface, this often reduces the antimicrobial ability of the active substance (Wei et al., 2019) but will also cause the death of the organism as well (Esbelin et al., 2018). The mechanism of this death not only potentially lies in the desiccation of organisms in an evaporating droplet but the droplet contents. For example, a droplet of saline will have increasing concentrations of sodium chloride as the water in the droplet evaporates, the osmotic pressure may then be sufficient to kill many organisms even before desiccation (K. Lin and Marr, 2019). This may explain the enhanced survival of *S. aureus* (high-salinity resistant organism (Feng et al., 2022)) compared to *E. coli* (high-salinity sensitive organism (Hrenovic and Ivankovic, 2009)) in this work and provides an even greater complexity to modifying the environmental conditions of an STM.

Therefore, a higher inoculum concentration could be warranted. However, increasing this may impact on the mode of evaporation of the droplet and promote contact line pinning, increasing the rate of evaporation of the droplet again which will cause the increased desiccation of the organisms on the surface. Any novel STM should consider all these factors during initial development and testing, and how it may impact on the testing laboratory's ability to perform these novel STMs. The novel chamber can alleviate some of these concerns by allowing reproducible environmental control. However, it is important to consider the limitations of the novel chamber with regards to performing STMs, whereby the chamber cannot maintain both a high temperature (30 ^{o}C) and a high relative humidity (>90 %) simultaneously. This is likely not of major concern as future STMs that employ more

realistic environmental conditions (the fundamental purpose for the chamber) will likely not require these conditions. Having a standardised chamber to perform these STMs within will allow a greater reproducibility between laboratories as well as provide a cheap and effective way to test materials in precise, reproducible, and realistic conditions, a common problem with some laboratories, as many do not have the equipment available to reliably alter these conditions to match the method. It is also of the utmost importance that any laboratory can manufacture the novel environmental control chamber with minimal difficulty and cost, as well as with parts that are easily replaceable to ease the transition to realistic conditions as best as possible.

Although the original purpose of the chamber was to perform non-porous antimicrobial material STMs, such as ISO22196 and ISO20743, very little adaptation would be required to modify either the testing platform or the chamber more generally to perform a wider variety of STMs including for measuring droplet evaporation rates at controlled temperature, relative humidity and airflow values as well as other microbiological tests, such as adapting the coupon tray to be able to perform static biofilm growth (e.g. ASTM E2799-22 (ASTM, 2022a)). Furthermore, photocatalytic materials are of increasing interest for the reduction of bioburden on surfaces and therefore the transmission of infection, particularly on FTS due to their efficiency, low-cost and non-toxic nature (B. Li et al., 2022). With relatively minimal modifications to the novel chamber, a typical “day-night” cycle could be implemented with light controllers to test these materials accurately and reliably in realistic conditions without the need for large and specialised equipment like that used in current STMs such as ISO22551 (I. S. Organisation, 2020).

3.5. Conclusion

The initial aims of the chamber with regards to performing current STM variations utilising realistic conditions and assessing the impact of these conditions on the survival and viability of bacteria has been fulfilled. Further work to greater understand the impact of these factors would allow for an enhanced set of STMs that can more accurately and reproducibly assess the antimicrobial efficacy of an AMM by using the chamber as a method of reducing inter-laboratory variability. Additionally, a deeper understanding of the effects of evaporation on the survival of microorganisms and the antimicrobial efficacy of an AMM

would allow provide assurances that the decisions made to ensure a realistic manner of performing STMs will not have unintended consequences.

4. Investigating the impact of environmental conditions and experimental decisions on antimicrobial material efficacy assessment

4.1. Introduction

The environmental conditions (e.g., temperature, relative humidity, airflow) as well as other experimental choices (incubation period, inoculum concentration and volume etc) all impact on the results generated using an STM. For the data generated in an STM to be reflective of end-use conditions, each should be carefully considered and assessed for their individual impact on AMM efficacy and overall reproducibility of the STM. Some of the work presented in this chapter has been published previously (Cunliffe et al., 2023), which focused mainly on the mathematical and physical factors of droplet evaporation. This thesis has incorporated the work into the wider field of STM development to allow for better informed decisions and to understand the role of droplets and microorganisms in AMM efficacy. The full journal article is shown in Appendix C. This author was the individual primarily responsible for the laboratory work relating to the sections utilised in this thesis, as well as primarily co-writing and editing the manuscript alongside the supervisory team (when specifically relating to the sections used in this thesis). Co-writing and editing the manuscript occurred between all authors in the wider context of the entire published work (when also including work not used in the thesis).

4.1.1. Recovery methods

The survival of microorganisms on a surface may be affected by the environmental conditions (e.g., via desiccation) just as much as how it affects the material itself. When developing such methods, these conditions and choices should allow for the generation of data that mirrors efficacy in the intended end-use application. The determination of the effects of environmental conditions on the evaporation of a droplet and the mechanics of microorganisms within the droplet during evaporation provides vital information on how to inform on novel STMs that incorporate realistic environmental conditions. Each aspect of the STM should be assessed to determine the interactions between each and demonstrate how a novel STM would incorporate all the parameters at once while remaining as realistic to end-use conditions as possible. Parameters such as relative humidity, inoculum size, and inoculum concentration can be easily altered and may be influential on the recovery of microorganisms from a surface or the overall reproducibility of an STM and so are assessed below.

4.1.2. Droplet evaporation

There are several factors that affect the evaporation of a droplet on a surface, which in turn influences the antimicrobial efficacy of the material if it requires moisture to be active. The major factors include: the environmental conditions, the contact angle of the droplet on the surface and the mode of evaporation of the droplet (Nguyen et al., 2012; Zang et al., 2019).

4.1.2.1. Environmental conditions

The environmental conditions have a clear relationship with the evaporation rate of a droplet, particularly when assessing the effects of temperature, relative humidity, droplet size, material composition and droplet composition. The effects of each individual environmental condition and method decision have been explored thoroughly below.

4.1.2.2. Contact angle

The contact angle of a droplet can be measured using several mathematical formulae, the most common of which is the tangent method (T. Zhao and Jiang, 2018), that simply uses the material as a base line and draws a tangent in the direction the droplet first appears, as shown in Figure 44.

A goniometer is a device used to accurately measure the contact angles of a droplet by using a high-resolution camera and backlight to observe the precise shape of the droplet. Software often accompanying the device is then able to determine the contact angle generated using the provided method (e.g., tangent) and given the densities of the liquid and the material, is able to perform surface tension measurements (Kwok et al., 1997; Dionísio and Sotomayor, 2000). The exact setup of a goniometer is shown in Figure 43 below.

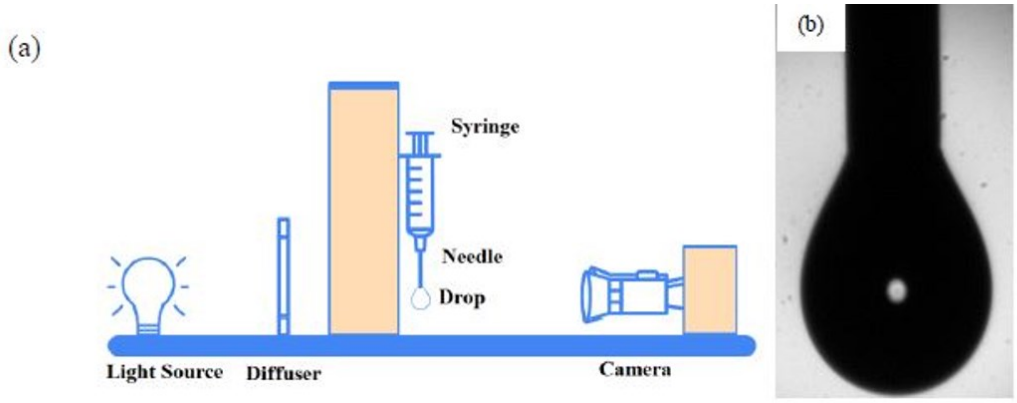

Figure 43 (a) schematic of experimental setup. (b) Image of a Milli-Q water drop dispensed in air using a blunt needle of OD 1.6mm.

The contact angle is to a large degree responsible for the evaporation time of a droplet, as a larger contact angle, shown in the left picture of Figure 44, will also have a lower surface area to volume (SA:V) ratio as it is more spherical and so will evaporate at a slower rate. In contrast, a low contact angle will spread more over the surface, presenting a higher surface area to volume ratio and so will evaporate at a faster rate (W. Zhang et al., 1989). The contact angle is affected by many different factors, most notably the hydrophobicity of the material, but other variables could also be contributing (Mozes and Rouxhet, 1987; Zhu et al., 2016).

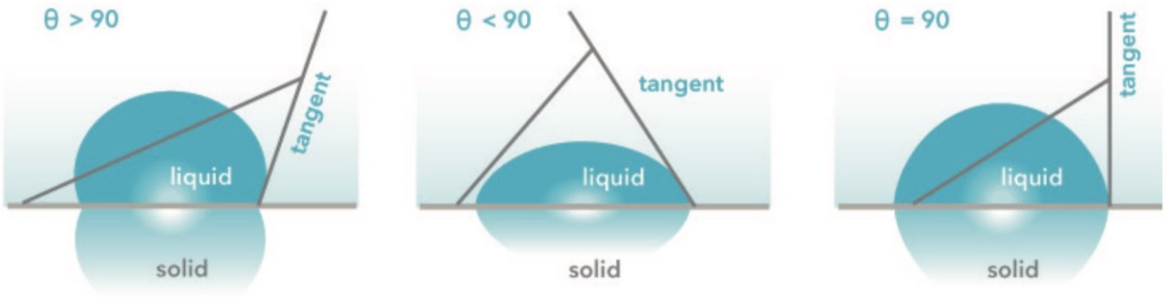

Figure 44 An example of how the tangent method is performed and approximately how a droplet would look in each case. Figure obtained from (Instruments, 2023).

4.1.2.3. Mode of evaporation

There are two potential modes of evaporation of a droplet, being constant wetted area (CWA) (Soboleva and Summ, 2003) and constant contact angle (CCA) (Erbil et al., 2002), or evaporating downwards and evaporating inwards respectively, shown in Figure 45. Which

mode of evaporation is employed is based on the surface tension and vapour pressure within the droplet (Munekata et al., 2013).

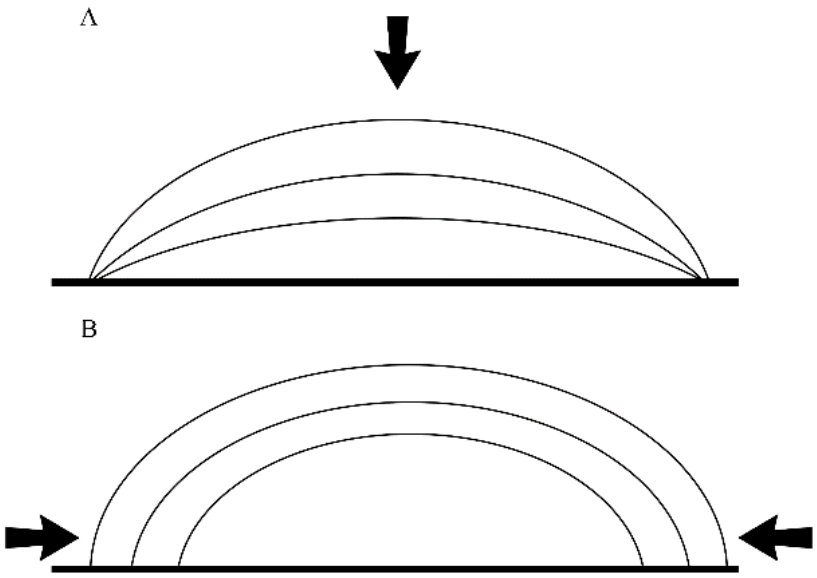

Figure 45 The potential modes of evaporation of a droplet on a material, shown as (A) – Constant wetted area (CWA- evaporating downwards) and (B) – Constant contact angle (CCA- evaporating inwards)

4.1.2.3.1. The consequences of the evaporation method

The evaporation method will influence the evaporation rate and therefore antimicrobial activity of the material. If a droplet evaporated using the constant wetted area mode, it will be at an increased rate compared to constant contact angle due to an average higher surface area to volume ratio, and so the material will be wet for less time. The reasons why a droplet on a material dries in one mode or the other are key to understanding how to improve AMMs because of the reliance on moisture in many cases.

4.1.2.3.2. The coffee ring effect

The coffee ring effect is a phenomenon that underpins advancing and retreating contact angles. Contact line pinning occurs in part due to the addition of suspensions to a droplet that enables the coffee ring effect to occur (Deegan et al., 2000). The coffee ring is a visible ring of solution and suspension that generates at the edge of evaporating droplets. This phenomenon has been well studied as it relates heavily to inkjet printers whereby ink particles would deposit at the initial contact line (Larson, 2014; Soulié et al., 2015; Eales

and Routh, 2016). This process also translates to microorganism-laden (bacterial and viral) suspensions (albeit more dilute), and thus had the same effect on the evaporation of a droplet. The effect of hydrophobic and hydrophilic bacterial spores on the generation of coffee rings on non-porous surfaces has been observed and its implications for current cleaning procedures and possible pitfalls discussed (Deleplace et al., 2022). Briefly, the spores present in the coffee ring itself were easier to remove with cleaning procedures than those dispersed throughout the rest of the evaporated droplet, but general resistance to cleaning procedures was observed for all areas. The effect of bacterial and viral presence in a droplet on evaporation was investigated below (Cunliffe et al., 2023).

4.1.3. Chapter specific aims and objectives

This chapter aims to assess the survival, deposition, and recoverability of bacteria on coupons (stainless steel, Cu, PVC, nitrile, and polypropylene) in a variety of environmental conditions and method parameter choices, by modifying relative humidity, droplet size, and optical density of the inoculum. Additionally, assessing the impact of contact angles as well as environmental and physical conditions on the evaporation time of a droplet on a variety of surfaces.

4.2. Methods

4.2.1. Recovery methods

4.2.1.1. Relative humidity

A working culture of *E. coli* NCIMB 8545 was created by adding one colony from a tryptone soya agar (TSA, Fisher Scientific, UK) plate to 10 mL tryptone soya broth (TSB, Fisher Scientific), incubated at 37 ^{o}C for 24 hours shaking at 150 rpm in an orbital incubator (Sciquip, UK). This was then centrifuged (Sigma, UK) at 3500rpm for 10 minutes, the supernatant removed and 10 mL sterile saline (Fischer Scientific, UK) added and vortexed (Clifton, UK) until mixed well. This process was repeated once. The inoculum was adjusted to 0.5 ± 0.005 OD at 600 nm (a bacterial inoculum of *E. coli* or *S. aureus* at this OD value equates to 1-4x10^{8} CFU/mL) using a spectrophotometer (Jenway 6305, UK). Stainless steel 316L coupons of 20x20x1 mm were sterilised by autoclaving (VITTA, UK) at 121 ^{o}C for 20 minutes. Then the coupons were inoculated in triplicate with 5 µL droplets of inoculum or sterile saline as a control in triplicate and placed in a chamber of size 296x171x51cm with relative humidity controlled by saturated salts. In each case, four petri dishes were filled with 20 g salt and 15 mL distilled water each to achieve the desired relative humidity and

three relative humidity values were tested, 15 % (with lithium chloride (Fisher Scientific)), 40 % (with potassium carbonate (Fisher Scientific)) and 75 % (with potassium chloride (Fisher Scientific)).

The coupons were placed in 90 mm petri dishes (Sarstedt, UK) with the lids removed, placed in the chamber, and left for 60 minutes. Then the coupons were dropped into a 50 mL falcon tube (Sarstedt, UK) with 10 mL sterile saline and vortexed for 60 seconds, followed by 1:10 serial dilution to 10^{-7} in sterile saline and 0.1 mL spread plated on to TSA plates. Plates were then incubated at 37 ^{o}C for 24 hours and colonies counted. The coupons were assessed in triplicate and three technical repeats of the experiment were performed. All statistical analysis and graphing were performed in GraphPad Prism 9.5.1.

4.2.1.2. Inoculum volume and concentration

To assess the impact of inoculum volume and concentration on the ability to recover microorganisms from an inert surface, an inoculum of *E. coli* NCIMB 8545 was prepared in the same manner as 4.2.1.1 but adjusted to the optical densities of 0.5 ± 0.005 and 1.0 ± 0.005 OD at 600nm. The coupons were then inoculated in triplicate with either 5 µL, 10 µL or 20 µL of suspension before being incubated at 75 % relative humidity for 60 minutes before being 1:10 serially diluted, spread plated and counted. The coupons were assessed in triplicate and three technical repeats of the experiment were performed. All statistical analysis and graphing were performed in GraphPad Prism 9.5.1. Statistical significance values between droplet sizes and the inoculum within inoculum concentrations (optical density) were generated via a two-way ANOVA.

4.2.2. Droplet evaporation

4.2.2.1. The impact of environmental conditions on droplet evaporation, contact angles and deposition of microorganisms

4.2.2.1.1. Preparation of materials and a chamber for environmental control

Square coupons measuring 10 mm × 10 mm were cut from copper (CuSn5 (Amazon, UK)), polyvinyl chloride (PVC (Cardiff University, UK)), polypropylene (Fisher Scientific) and nitrile sheet (Fisher Scientific). Prior to use, all coupons were wiped thoroughly with cloth soaked in 70 % ethanol and left to evaporate in aseptic conditions (parafilm-wrapped sterile petri dish) for 60 minutes. Coupons were secured to a polystyrene base plate (127.7 × 85.4 mm, Sarstedt, UK) using double-sided tape and placed inside an environmental control chamber. The environmental control chamber (internal dimensions 296 mm × 171 mm × 51 mm)

allowed temperature and relative humidity to be controlled independently. To maintain the desired relative humidity, saturated solutions of lithium chloride (180 g and 60 mL of water, producing a relative humidity of 15 %) or potassium carbonate (200 g and 60 mL of water, producing a relative humidity of 40 %) were distributed evenly across four Petri dishes inside the chamber and relative humidity monitored using a HD500 sensor and datalogger (Extech Instruments). Temperature was adjusted and maintained with a propagation heat mat (PVC, 18W, 220V) and monitored with a thermostat (Vivosun, Shanghai, China).

4.2.2.1.2. Preparation of solutions and microbial suspensions

Deionised water was sterilised by autoclaving at 121 °C for 15 minutes. Saline solutions were prepared as 0.85 wt% NaCl (ThermoFisher Scientific) in deionised water and sterilised by autoclaving. SM buffer was prepared by adding 5.8 g of NaCl, 2 g of $MgSO_4.6H_2O$ and 50 mL 1M Tris-Cl pH 7.5 to 800 mL distilled water and mixed until dissolved, adjusted to 1 L with distilled water and sterilised by autoclaving at 121 °C for 15 minutes. Tris-Cl was prepared by adding 12.11 g of 1 M tris base to 80 mL distilled water and mixed until dissolved with the pH adjusted to 7.5 by adding 30 wt% HCl.

Bacteria were maintained as streak (purity) plates on tryptone soya agar (TSA) at 4 °C until required. *Escherichia coli* (ATCC 13706) and *Pseudomonas syringae* (ATCC 21781) cultures were prepared for the experiments by inoculating one colony of bacteria from the respective streak plates, transferring to 10 mL TSB, and incubating at 37 ^{o}C and 28 ^{o}C, respectively, for 24 hours. Bacterial cultures were then centrifuged at 3500 rpm for 10 minutes. The supernatant was removed, and 10 mL sterile saline added, with the resultant suspension mixed by vortex (this process was repeated once). Suspensions were then adjusted to 0.5 OD at 600 nm (determined by spectrophotometer (Jenway)) using sterile saline (~$2x10^8$ CFU/ml).

Bacteriophage Phi6 (ATCC 21781-B1) and Phi X174 (ATCC 13706-B1) suspensions were prepared following a standard phage assay protocol (Adams, 1959). In brief, a 10-fold serial dilution of stock phage was performed up to 10^{-8} in SM buffer. Subsequently, for each dilution, 100 µL of bacteriophage was mixed with 100 µL of corresponding bacterial overnight culture (*Pseudomonas syringae* (ATCC 21781) for Phi6 and *Escherichia coli* (ATCC 13706) for Phi X174) and 3 mL of soft (0.7 % w/v) molten (45-55°C) TSA and poured onto a

regular strength TSA agar plate. Following an 18-hour incubation (30°C), any plaques present on each dilution were counted and used to calculate the number of plaque forming units (PFU), which allowed the original phage stock to be adjusted a concentration of 5×10^7 PFU/mL.

4.2.2.1.3. Evaluation of solutions and suspensions

To assess the impact of the presence of microorganisms on the time it takes droplets to evaporate, droplets of saline containing either *E. coli* (ATCC 13706) or *P. syringae* (ATCC 21781) were compared with droplets of saline without bacteria. Additionally, droplets of SM buffer containing either Phi6 (ATCC 21781-B1) or Phi X174 (ATCC 13706-B1) bacteriophage were compared with droplets of SM buffer without bacteriophage. Droplets of either 1 ± 0.1 µL or 5 ± 0.2 µL volume were deposited on a test coupon by pipette. The time taken for each droplet to evaporate as observed visually was recorded. To ensure measurement of the evaporation time was consistent, data were collected by one researcher who used a digital stopwatch to record the time each droplet took to evaporate. Droplets were observed by eye continuously and the time by which the droplet had evaporated was taken as when no moisture was apparent.

4.2.2.1.4. Measurement of contact angles

Images of droplets on each material were captured by pipetting droplets of 1 µl or 5 µl on to the surface, followed by measuring the contact angle (average of left and right tangent contact angles) using a goniometer (Krüss mobile drop GH11). Droplets were assessed in triplicate and each measurement was performed on a different coupon of material. To ascertain if contact angles for each liquid type on each material can be considered the same or statistically significantly different ($p < 0.05$), a *t* test was performed comparing contact angles at 1 µl and 5 µl.

4.2.2.1.5. Preparation of scanning electron microscope images

To assess deposition of bacteria on surfaces, 5 µL droplets of either *E. coli* (ATCC 13706) or *P. syringae* (ATCC 21781) were placed on a test coupon and left to evaporate in an environment with RH = 60 % and 22°C. Once dried, the surfaces were immersed in a Petri dish containing 2.5 % glutaraldehyde for 18 hours, then washed with sterile phosphate buffered saline (PBS, 0.85 wt% NaCl), placed in increasing concentrations (20 %, 40 %, 60 %, 80 %) of ethanol for 30 minutes each, and then submerged in 100 % ethanol for 30

minutes, twice. The surfaces were then left to evaporate in a vacuum sealed desiccator for a minimum of 18 hours. Samples were then mounted onto aluminium pin stubs using adhesive carbon tabs and coated with a thin layer (25nm) of Au metal using a sputter coater (Polaron, 30 s, 800V, 5 mA). The stubs were then loaded into the FE-SEM (Carl Zeiss Ltd, Supra 40VP, SmartSEM) for imaging and analysis. The secondary electron detector was used to obtain images of the samples, using an acceleration voltage of 2 kV and a working distance of approximately 5 mm.

4.3. Results

4.3.1. Recovery methods

4.3.1.1. Relative humidity

The CFU recovered from the coupons at the different relative humidity values shows an increase in survival as the relative humidity increases. Although there was a maximum difference of 0.71-log between the 15 % and 75 % coupons, no statistical significance was observed between any relative humidity values. Additionally, all coupon recovery was significantly lower than that of the inoculum at between 1.26-1.97 log ($p < 0.0001$). All significance values were generated with a one-way ANOVA and the p-values are shown in Figure 46. No CFU counts were recovered from the coupons inoculated with sterile saline and have thus not been included.

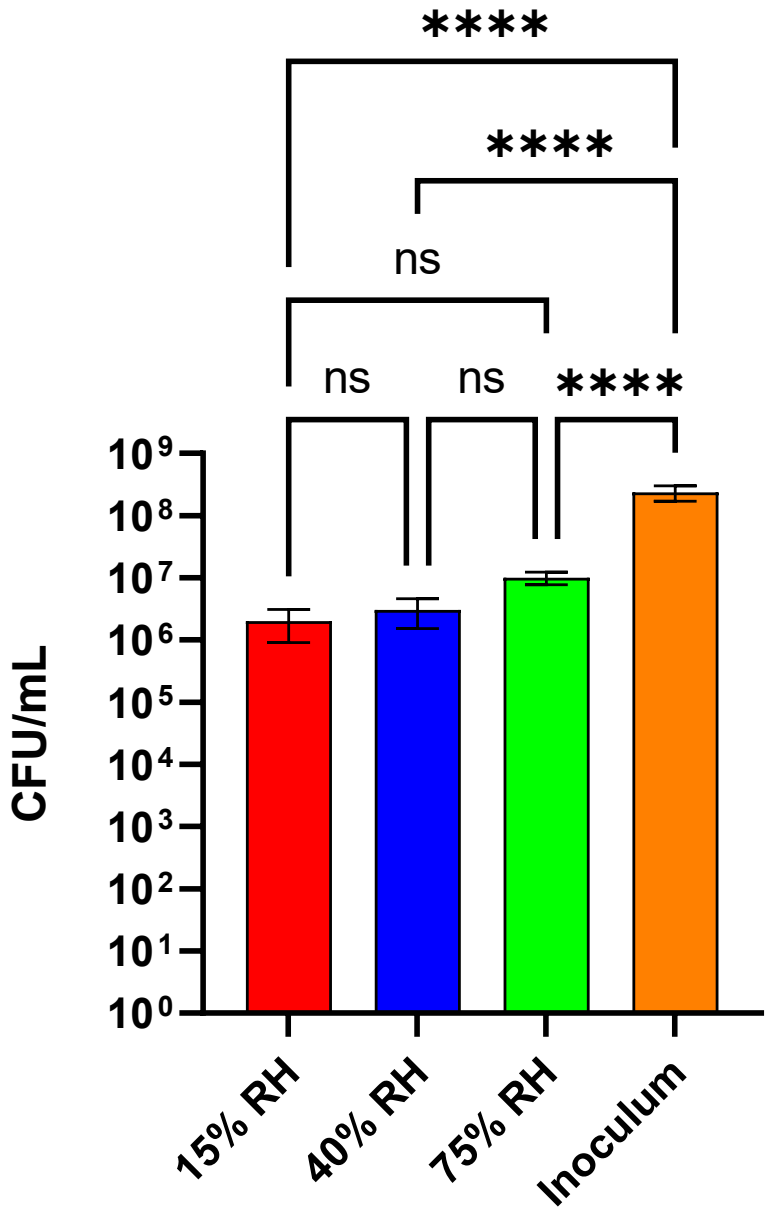

*Figure 46 The colony forming units of E. coli recovered from stainless steel 316L coupons after exposure for one hour to different relative humidity (RH) settings. Each relative humidity was assessed in triplicate and three technical repeats of the experiment were performed. Statistical significance values are represented as follows: ns – not significant, * - $p \leq 0.05$, ** - $p \leq 0.01$, *** - $p \leq 0.001$ and **** - $p \leq 0.0001$.*

4.3.1.2. *Inoculum volume and concentration*

The CFU/mL recovered from the coupons shows an increase in recovery as the droplet size of the inoculum increases, except for 10 microlitres at 1.0 OD (Figure 47). Although differences are a maximum of one-log, some statistical significance was observed in the 1.0 OD data with recovery from coupons inoculated with 20µl droplets recovering significantly higher CFU than the other droplet sizes ($p < 0.0001$) and being higher than the inoculum (although not significantly). No statistical significance was observed between the droplet sizes at 0.5 OD. However, the recovery from 5µl droplets was significantly lower than the inoculum. There was also no significant difference between the OD values across all droplet sizes and the inoculum (p-value = 0.7395).

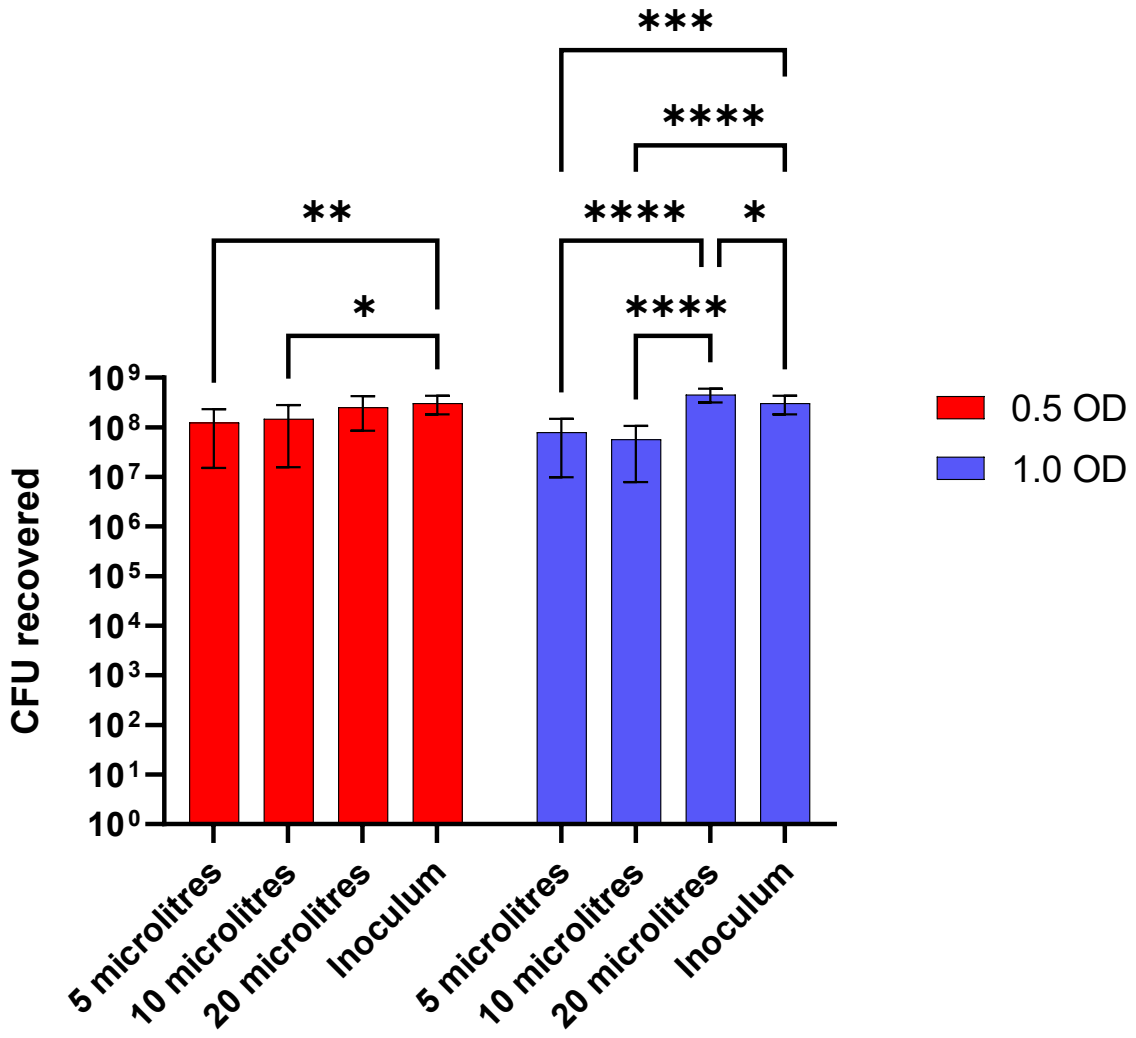

*Figure 47 The CFU recovered from stainless steel coupons when inoculated with droplets at various sizes and varying initial inoculum concentrations. Statistical significance values are represented as follows: ns – not significant, * - p ≤ 0.05, ** - p ≤ 0.01, *** - p ≤ 0.001 and **** - p ≤ 0.0001.*

4.3.2. Droplet evaporation

4.3.2.1. The impact of environmental conditions on droplet evaporation, contact angles and deposition of microorganisms

4.3.2.1.1. Evaporation of solutions and suspensions

The effects of droplet size, relative humidity, material, and droplet composition on the evaporation time is observed in Figure 48. At low relative humidity (Figure 48(a) - faster evaporation rates), the use of saline tends to increase the evaporation times compared to water, whereas the SM buffer evaporation times are like those for water. This effect is more noticeable with the mid-relative humidity data (Figure 48(b)), in which case both saline and SM buffer exhibit longer evaporation times than water. This trend is noted in Figure 48, alongside Appendix D, where the evaporation times were compared to that of a predicted evaporation time from a mathematical model produced by the University of Cambridge for each case (relative humidity, droplet size, material, and inoculum composition) assuming either CWA or CCA mode of evaporation. Agreement between the measured evaporation time and the model indicates the droplet is more closely aligning with that specific mode of evaporation.

The presence of organisms tends to reduce the evaporation time for both saline and SM buffer droplets. This suggests that the species are promoting CWA behaviour, which would be consistent with organisms collecting at the evaporation front, promoting pinning behaviour (but not necessarily fixing the contact line). The trends are recorded in Table 6 and are compared with the observed deposition patterns below. Evaporation times were faster in the low relative humidity scenarios for both 1 μl and 5 μl droplet sizes.

Further analysis comparing evaporation times of droplets containing microorganisms with either saline or SM buffer alone revealed that in all cases of statistically significant differences (p <0.05, n = 11 / 32 for bacteria and n = 6 / 32 for bacteriophages), the addition of microorganisms resulted in more rapid evaporation. When comparing the total number of significantly different evaporation times with respect to relative humidity, medium relative humidity (~40 %) conditions provided a larger number of droplets that evaporated more quickly due to the presence of a microorganism, in both 1 μL and 5 μL scenarios. When comparing evaporation times with respect to droplet size, 1 μL droplets containing microorganisms evaporated significantly more rapidly than ones without more often (than 5 μL droplets) in both low (15 %) and medium (40 %) RH scenarios.

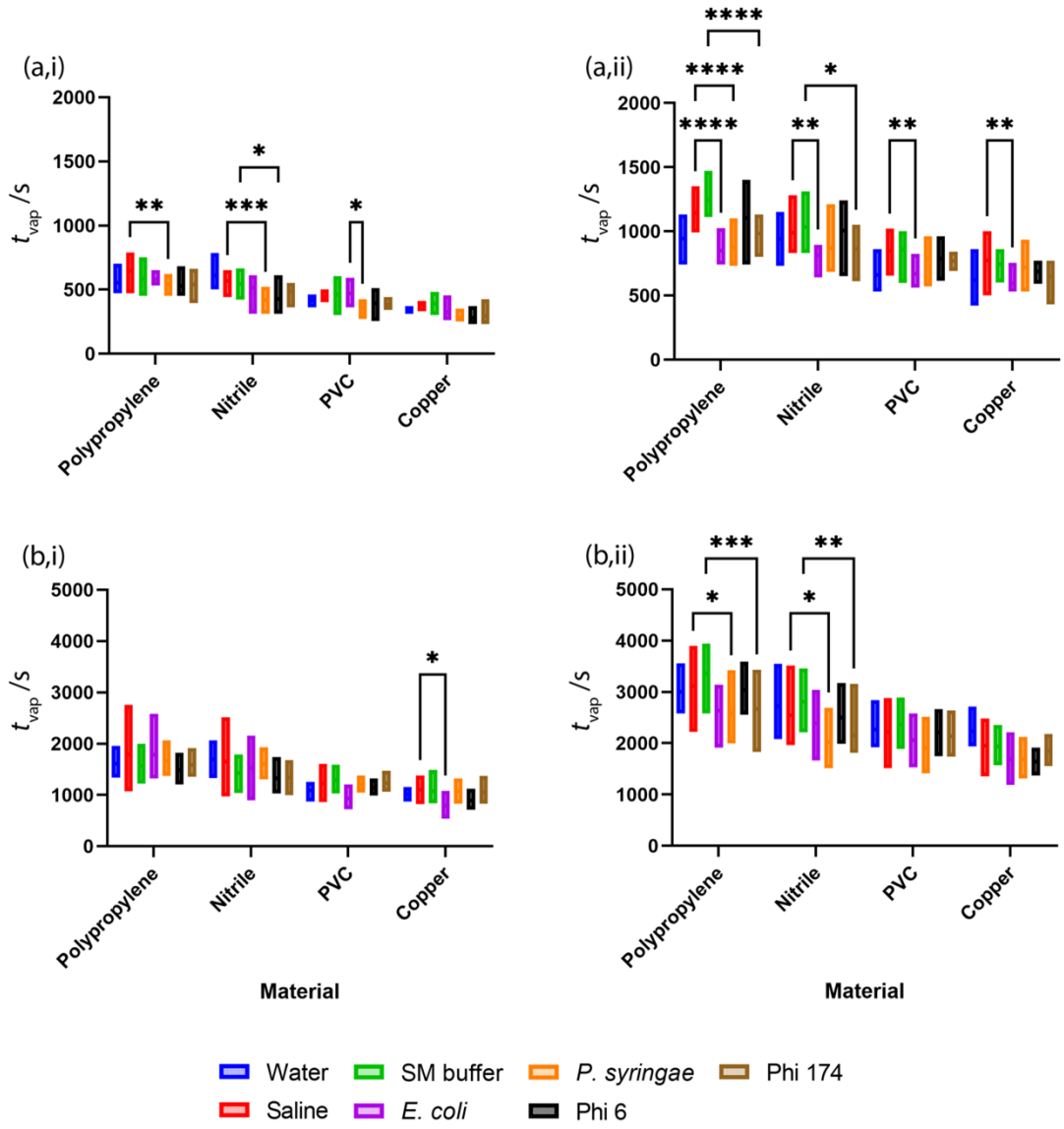

*Figure 48 Effect of material on droplet evaporation times. (a,i) 1 µL droplets in low RH, (a,ii) 1 µL droplets in medium RH, (b,i) 5 µL droplets in low relative humidity and (b,ii) 5 µL droplets in medium relative humidity. All measurements were at room temperature (18 °C). Statistical significance is shown for comparisons of bacteria vs. saline and bacteriophage vs. SM buffer and are represented as follows: * - p ≤ 0.05, ** - p ≤ 0.01, *** - p ≤ 0.001 and **** - p ≤ 0.0001.*

Table 6 Effect of droplet composition on evaporation times, with reference to CCA model (Appendix D). Anova and Tukey HSD tests determined pairwise statistical significance ($p < 0.05$), with ~ denoting no significant difference but observed increase in evaporation time, and > denoting a statistically significant difference supporting the observed increase in evaporation time. SMB – SM buffer.

Surface	Relative humidity range	Droplet volume	Trend in evaporation times	
			Liquids	Suspensions
Polypropene	Low	1 µL	SMB ~ saline > water	Saline > *E. coli* ~ *P. syringae* SMB ~ *Phi X174* ~ *Phi6*
		5 µL	SMB ~ saline > water	Saline ~ *E. coli* ~ *P. syringae* SMB ~ *Phi X174* ~ *Phi6*
	Mid	1 µL	SMB > Saline > water	Saline > *P. syringae* ~ *E. coli* SMB > *Phi6* ~ *Phi X174*
		5 µL	SMB ~ Saline ~ water	Saline ~ *E. coli* ~ *P. syringae* SMB >*Phi6* > *PhiX174*
Nitrile	Low	1 µL	Water ~ saline ~ SMB	Saline > *E. coli* > *P. syringae* SMB > *Phi X174* > *Phi6*
		5 µL	Water ~ Saline ~ SMB	Saline ~ *P. syringae* ~ *E. coli* SMB ~ *Phi X174* ~ *Phi6*
	Mid	1 µL	SMB ~ saline ~ water	Saline ~ *P. syringae* ~ *E. coli* SMB ~ *Phi6* ~ *Phi X174*
		5 µL	SMB ~ water ~ saline	Saline > *E. coli* > *P. syringae* SMB > *Phi6* > *Phi X174*
Copper	Low	1 µL	SMB ~ Saline ~ water	Saline > *E. coli* ~ *P. syringae* SMB > Phi *X174* > *Phi6*

		5 µL	Saline ~ SMB ~ water	Saline ~ *P. syringae* > *E. coli* SMB ~ *Phi X174* ~ *Phi6*
	Mid	1 µL	Saline ~ SMB > water	Saline ~ *E. coli* > *P. syringae* SMB > *Phi6* ~ *Phi X174*
		5 µL	Water ~ Saline ~ SMB	Saline > *P. syringae* ~ *E. coli* SMB > Phi *X174* > *Phi6*
PVC	Low	1 µL	Saline ~ SMB ~ water	Saline ~ *E. coli* > *P. syringae* SMB > *Phi6* ~ *Phi X174*
		5 µL	SMB ~ saline > water	Saline ~ *P. syringae* > *E. coli* SMB ~ *Phi X174* ~ *Phi6*
	Mid	1 µL	Saline ~ SMB > water	Saline ~ *P. syringae* > *E. coli* SMB > Phi *X174* > *Phi6*
		5 µL	SMB ~ saline ~ water	Saline > *P. syringae* ~ *E. coli* SMB ~ *Phi X174* ~ *Phi6*

4.3.2.1.2. Contact angles

The rate of evaporation of droplets containing microorganisms was studied using 1µL and 5 µL droplets on four surfaces under conditions of mid (40 – 47 % RH) and low relative humidity (14 – 16 % RH). Macroscopic advancing contact angles on each surface were determined for 1µL and 5 µL droplets of water, saline and SM buffer as well as the suspensions. The goniometer system used was not a precision device and the results, summarised in Table 6 and Figure 48, are used to identify trends. Most of the contact angle values lie in the range 45-90°. With 1µL droplets (Table 7), the presence of *E. coli* gave different contact angles to the neat saline on nitrile and copper; by comparison, *P. syringae* gave values closer to the saline. The Phi6 and PhiX174 suspensions gave similar (within ~10°) values on nitrile, PVC, and copper: on nitrile, these were different to the neat SM buffer. With the 5 µL drops (Table 8), the contact angles for neat saline, SM buffer and water were similar for all materials except copper, where SM buffer was lower. The contact angles for *E. coli* and *P. syringae* on polypropylene and copper were like those with saline, while those on nitrile were noticeably lower. The contact angles for SM buffer and Phi6 and

PhiX174 suspensions were similar except for copper and PVC, where PhiX174 was higher and lower respectively.

Table 7 Apparent contact angles ($\pm$ standard deviation) measured for 1 µL droplets. All values are rounded to the nearest whole number. Asterisk denotes where contact angle is significantly different (p <0.05) between 1 µL (below) and 5 µL (Table 8) measurements.

Liquid	Organism	Polypropylene	Nitrile	PVC	Copper
Water	-	82° (±3°)	97° (±4°)	60° (±2°)	74° (±3°)
Saline	-	84° (±1°)*	104° (±2°)	65° (±7°)	68° (±4°)
Saline	*E. coli*	86° (±4°)	93° (±2°)	64° (±6°)	51° (±6°)
Saline	*P. syringae*	79° (±2°)	95° (±4°)	71° (±6°)	65° (±9°)
SM buffer	-	85° (±4°)	100° (±6°)	59° (±8°)	58° (±6°)
SM buffer	*Phi6*	82° (±2°)	88° (±5°)	64° (±3°)*	63° (±3°)
SM buffer	*PhiX174*	83° (±2°)	78° (±2°)	65° (±3°)	71° (±2°)

Table 8 Apparent contact angles ($\pm$ standard deviation) measured for 5 µL droplets. All values are rounded to the nearest whole number. Asterisk denotes where contact angle is significantly different (p <0.05) between 1 µL (Table 7) and 5 µL (below) measurements.

Liquid	Organism	Polypropylene	Nitrile	PVC	Copper
Water	-	79° (±0°)	101° (±7°)	57° (±9°)	68° (±4°)
Saline	-	81° (±1°)*	104° (±2°)	70° (±9°)	64° (±2°)
Saline	*E. coli*	80° (±1°)	96° (±2°)	62° (±2°)	49° (±3°)
Saline	*P. syringae*	78° (±1°)	95° (±2°)	67° (±5°)	66° (±5°)
SM buffer	-	82° (±1°)	100° (±6°)	73° (±4°)	54° (±6°)
SM buffer	*Phi6*	88° (±5°)	96° (±3°)	75° (±1°)*	59° (±6°)
SM buffer	*PhiX174*	84° (±1°)	90° (±5°)	60° (±6°)	68° (±2°)

4.3.2.1.3. Scanning electron microscope images of bacterial deposition

The deposition patterns created by evaporation of 5 µL droplets containing *E. coli* or *P. syringae* differed depending on the substrate material. Whilst a ring marking the initial boundary of the droplet (*i.e.* the initial contact line) was visible on all images (see *E. coli* examples in Figure 49 and *P. syringae* in *Figure* 51), deposition of bacteria within the droplet footprint was more evident on polypropylene and copper (*E. coli* - Figure 50, *P. syringae* - *Figure* 52) unlike on nitrile and PVC where deposition within the footprint was less obvious. On polypropylene, the bacteria were deposited with an obvious outer ring, i.e., bacteria deposited in a circular ring at the outer edge followed by an annulus where no bacteria were deposited (although more evident with *E. coli*), followed by an inner region where most bacteria were deposited. In contrast, no annular region is apparent in the copper case.

Comparing the evaporation plots (Appendix D) on copper, the values consistently lay below the CCA line, suggesting mixed mode evaporation, while on polypropylene the data showed a strong correlation with CCA behaviour. Further work is needed to link deposition behaviour and evaporation kinetics. In both instances in Figure 50, bacteria are highly concentrated in different areas, resulting in deposition of bacterial cells on top of one another.

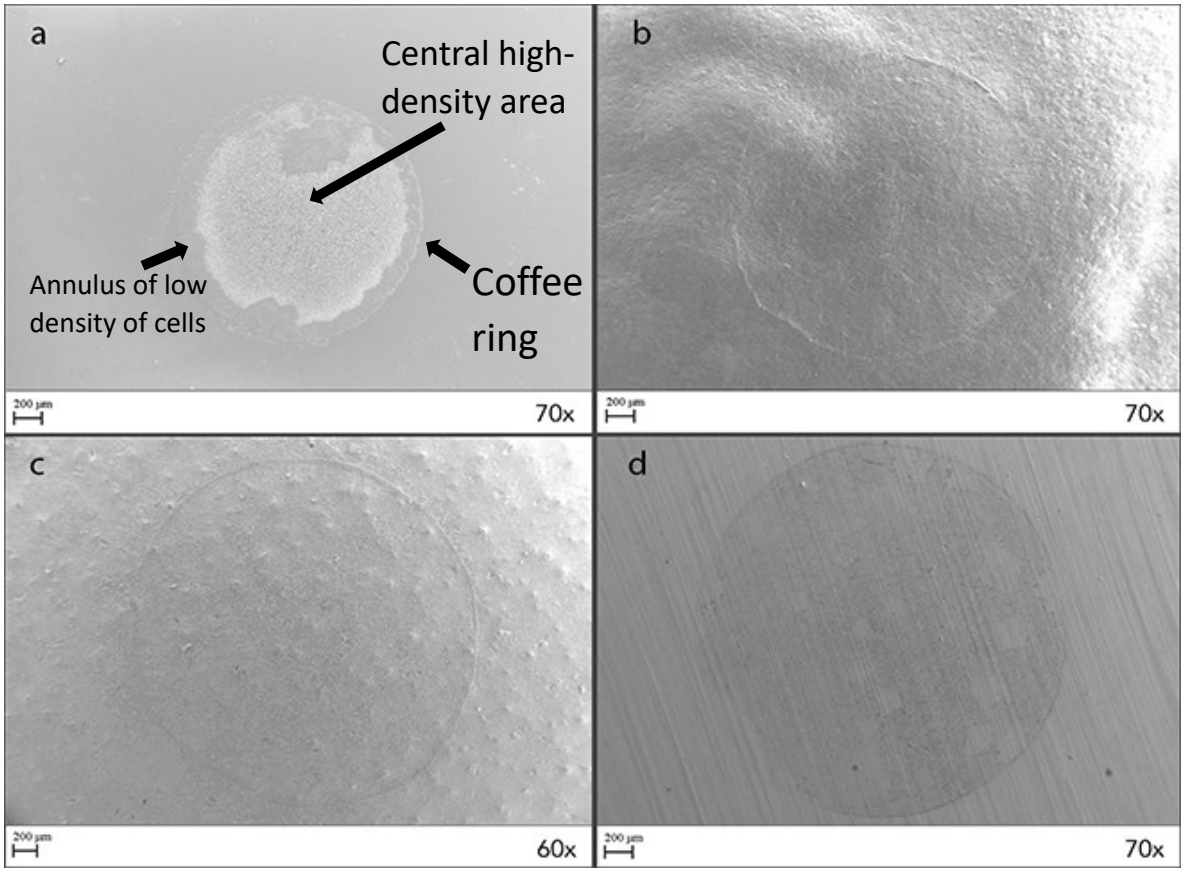

Figure 49 SEM images of (A) polypropylene, (B) nitrile, (C) PVC and (D) copper surfaces following evaporation of a 5 µl droplet containing E. coli at RH = 60 % and 22 ℃.

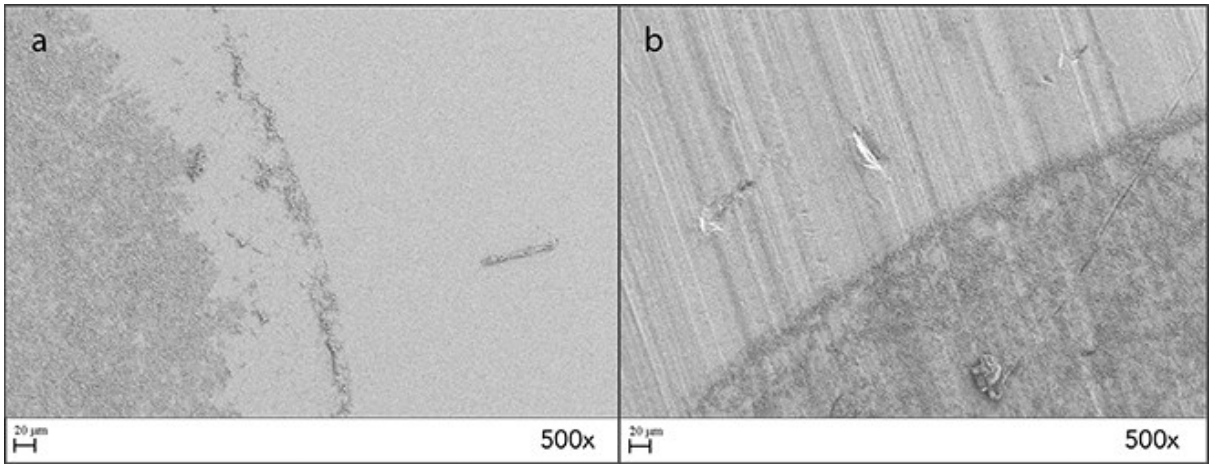

Figure 50 Higher resolution SEM images of (a) polypropylene and (b) copper surfaces (see Figure 49 (a),(d)) following evaporation of a 5 µl droplet containing E. coli at RH = 60 % and 22 ℃.

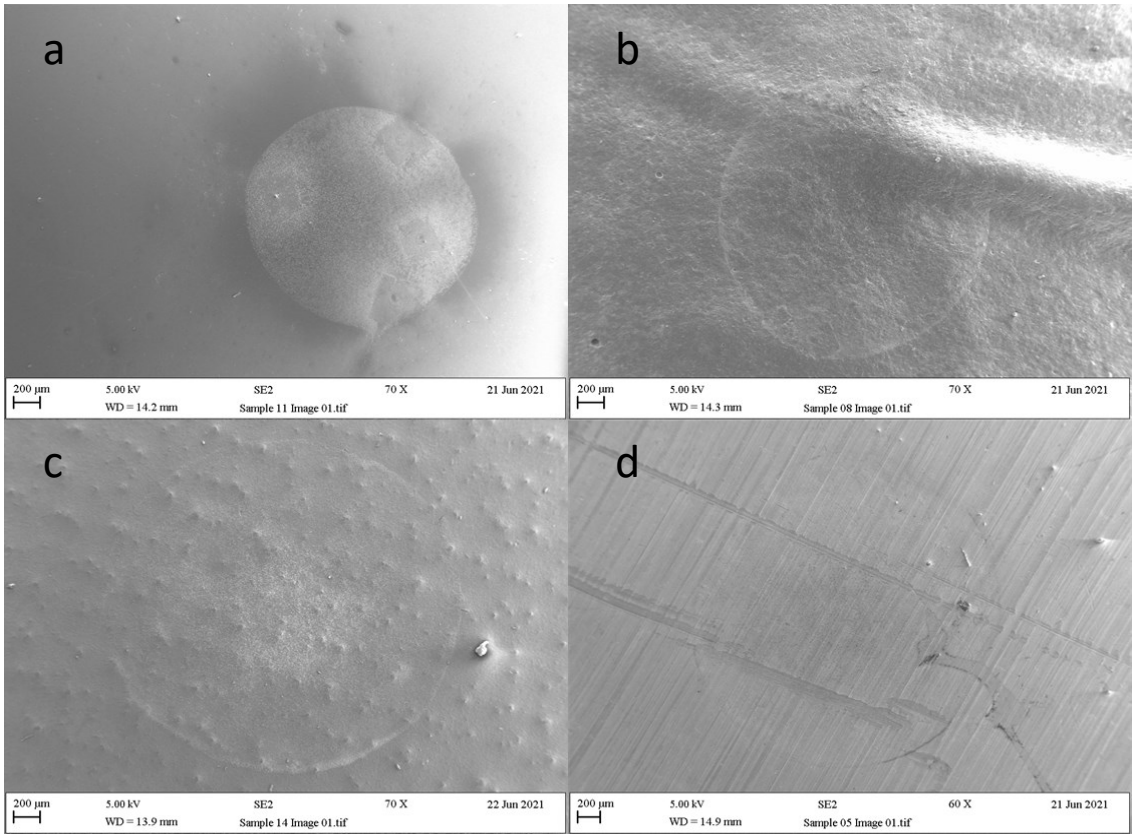

Figure 51 SEM images of (A) polypropylene, (B) nitrile, (C) PVC and (D) copper surfaces following evaporation of a 5 µl droplet containing P. syringae at RH = 60 % and 22 ℃.

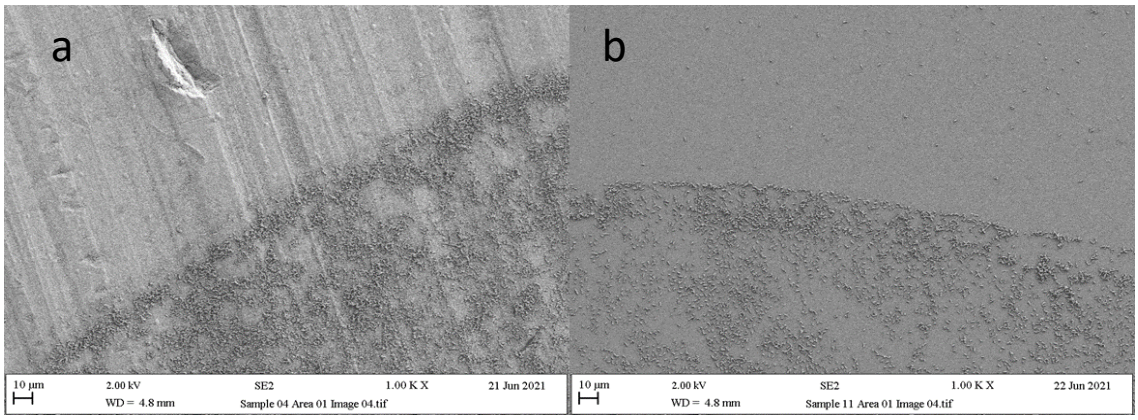

Figure 52 Higher resolution SEM images of (a) copper and (b) polypropylene surfaces (see Figure 51 (a),(d)) following evaporation of a 5 µl droplet containing P. syringae at RH = 60 % and 22 ℃.

4.4. Discussion

4.4.1. Recovery methods

4.4.1.1. Relative humidity

Although it could be expected that a lower relative humidity environment would cause lower organism viability due to desiccation, this trend is not observed here, with no effects of relative humidity observed. As *E. coli* is a desiccation-sensitive bacterial species (depending on the strain (T Møretrø et al., 2010)) it is expected that the evaporation process would cause decreased survival rates on the surface (Bale et al., 1993), although the low incubation time may not allow this to happen completely and could explain why desiccation or other stress factors have not been observed here. Nevertheless, differences were observed between the inoculum and materials, which may be because of methodological issues or biological phenomenon such as bacterial attachment to the surface (Goulter et al., 2009). In this case, *E. coli* was used due to its importance to many STMs, and is prominently used in ISO22196, among many others. While 75 % RH did not produce a statistically significant increase over the other values, it did provide the highest overall mean recovery and thus should be used in future experiments to minimise the effects of relative humidity when it is not being directly tested.

4.4.1.2. Inoculum volume and concentration

From the bacterial viability assessment, it is shown that the variability is generally low when recovering inocula from a surface. It is observed that a higher droplet size does equate to greater recovery overall in higher inoculum concentrations with some statistical significance observed at 1.0 OD, this may be due to the limited but still present evaporation of the inoculum on the surface causing slightly decreased survival at lower droplet sizes or the low inoculum volume deposited from the pipette increasingly becoming less accurate as the inoculum volume is decreased. This limited evaporation can cause cell death in small droplets of salinated droplets due to the increasing concentration of salts causing a higher osmotic pressure as the water in the droplet evaporates (Basu and Mukherjee, 2020). Interestingly, a higher incidence of statistically significant difference is observed at 1.0 OD compared to 0.5 OD, however, the overall effects on recovery and CFU/mL is minimal, with only a 0.183-log and 0.887-log difference between the 5µl and 20µl droplets at 0.5 OD and 1.0 OD respectively. Based on these results subsequent experiments should use a

maximum inoculum concentration of 0.5 OD at 600nm, with any inoculum volume being adequate for future work.

4.4.2. Droplet evaporation

The addition of bacteria reduced the evaporation time significantly for all surface types in at least one of each droplet size / RH scenarios, whereas the addition of bacteriophage did not decrease the evaporation time significantly on PVC or copper in any droplet size / RH scenario. It is possible that the shape and concentration of the particles could have also affected the formation of a coffee ring and the evaporation within the droplet (Yunker et al., 2011; Xin Yang et al., 2014). It should be noted that the *E. coli* strain used in the droplet evaporation work differs from that in other areas of this thesis (ATCC 13706 and NCIMB 8545 respectively) as the strain used here is the host for the PhiX174 phage, whereas the other strain is specified in many current STMs (such as ISO22196). Overall, the 1 μL droplets tend to exhibit less variation in the evaporation time and dried more quickly than the 5 μL droplets, as expected from the model, in some cases the droplet size can affect the evaporation of the droplet (Fukai et al., 2006). A more in-depth analysis of the models and how they relate to evaporation has been performed (Cunliffe et al., 2023) but is not explored here as the primary focus is STMs overall and the implications for AMMs and so is out of the scope of this thesis. The models did not capture the effect of adding bacteria or bacteriophage on the evaporation times, but the experimental values were, nevertheless, consistently closer to the constant contact angle scenario predictions rather than constant wetted area, indicating that the deposition of these microorganisms does not give rise to the contact line pinning effects reported with colloidal suspensions. The bacteria, with sizes greater than 1 μm, are not expected to give rise to colloidal behaviour, whereas the bacteriophage, with lengths 20-30 nm, might if they did not aggregate when suspended, this effect of particle size on the flow inside an evaporating droplet and the impact on the coffee ring effect has been observed (Weon and Je, 2010). Electron microscopy of images of the phages on the surface indicated that agglomerate and network formation did occur, but it was not possible to determine if this happened before they deposited on the surface.

Given that moisture is required for many antimicrobial materials to exhibit antimicrobial activity, understanding that the presence of microorganisms can increase the rate at which

evaporation occurs is important, as a shorter evaporation time will also result in reduced antimicrobial activity. Therefore, for those interested in the development, manufacture, and installation of antimicrobial materials, it is essential to consider what type of microbial contamination the user is trying to control and use this knowledge in the development of their initial antimicrobial efficacy assessment methods.

Other disciplines also benefit from the advances in understanding the evaporation of microorganism-laden droplets. For example, the evaporation of droplets impacts the survival and movement of bacteria in to leaves (Ranjbaran and Datta, 2019). Additionally, the capillary movement toward the contact line can further compound the deposition of bacteria at critical adhesion points of the leaf (such as the trichomes) (Ranjbaran and Datta, 2020). This is a particularly important issue when considering food safety as leafy greens are considered a highly-contaminated product (Olaimat and Holley, 2012).

This cross-disciplinary work revealed that the application of quantitative models for the kinetics of moisture evaporation on surfaces can help to explain and interpret findings when testing for the efficacy of antimicrobial surfaces. The speed of droplet evaporation is affected by a range of factors: temperature, relative humidity, airflow, the nature of the surface and the presence (and nature) of microorganisms (Zang et al., 2019). The kinetics of droplet evaporation affects the presence of moisture on a surface, and hence the survival of microorganisms and, potentially, the mode of action of antimicrobial agents in / on the surface – particularly if the agents require moisture for activity (Maneerung et al., 2008). STMs provide detailed accounts of procedures, but do not always specify with any precision, the ambient conditions where testing takes place. If these factors are not adequately recognised or controlled, results from STMs performed under different (or unspecified) environmental conditions in different laboratories are liable to vary and give rise to confusion, misinterpretation, and potentially misleading claims of effectiveness.

Variability of STMs has been demonstrated widely throughout all aspects of the method, from the recovery method to the environmental conditions that will have a larger impact once STMs transition to more realistic conditions. The development of any novel STMs should consider these variables, and data on each should be included in any report to allow a more thorough assessment on whether the AMM should be accepted for use. When considering this report and the development of future more realistic STMs, factors such as

the environmental conditions should have a greater level of emphasis than material properties as environmental conditions are more variable (depending on location) and have a greater impact on the evaporation of a droplet on the materials. However, all factors that may influence the evaporation should be included in an efficacy report to allow for a greater understanding into how the AMM will perform when in an end-use scenario.

4.5. Conclusion

It is clear from the data that the environmental and physical conditions as well as other experimental decisions influence the evaporation time of a droplet on a surface, which may translate to the antimicrobial efficacy of an AMM if it requires moisture to be active. Therefore, moving forward, these factors should be considered when developing variations of current STMs or novel STMs (such as a simulated splash test (Waltimo et al., 2007)) to properly represent the conditions the material will be subjected to once in use. This will reduce the total number of available products in any given scenario but will provide a greater assurance that the AMMs that are implemented are providing adequate efficacy and reducing the transmission of microorganisms.

5. Droplet evaporation and the reproducibility of the novel chamber

5.1. Introduction

The established impact of evaporation on both the survival of microorganisms on a surface and the efficacy of an AMM is an important consideration in developing a STM that uses realistic conditions. Utilising the novel chamber to perform evaporation rate experiments can demonstrate how evaporation of the droplet may impact on the data generated, particularly those associated with dry deposition or small volume droplets (McDonald et al., 2020), and what considerations might be required when interpreting that with respect to antimicrobial efficacy of a material. For example, if it is known that in a real-world setting it takes <20 minutes for a 4 μL droplet to evaporate (depending on the environmental conditions) (Armstrong et al., 2019), and therefore an antimicrobial coating would only be active for that time, testing microorganisms in suspension over a 24-hour period, which remains active the whole time, is not useful. As such, developing a chamber that can deliver a method where a specified evaporation time can be facilitated should be a consideration.

Additionally, it is also important to verify the reproducibility of such a chamber when performing such experiments. By comparing data generated by the novel chamber described in this thesis to those established in the literature and generated by previous experiments in this thesis, it can be determined whether the chamber can accurately assess the evaporation time for droplets on a surface.

Whilst these data generated through both sets of evaporation and reproducibility experiments with the novel chamber are useful in their own right, the data can also aid in understanding the impacts of airflow on evaporation time by keeping other environmental conditions (e.g. temperature and relative humidity) the same and only varying airflow.

To facilitate the further modification of the novel chamber and to determine how the airflow (among other environmental conditions) impacts the evaporation rate within the chamber, it is important to understand how these environmental conditions behave across the chamber. This would ensure that the user can understand, and use to their advantage, any variation in environmental conditions that their samples may experience.

5.1.1. Chapter specific aims and objectives

The aim of this chapter is to determine how environmental and physical conditions affect droplet evaporation rate in the novel chamber. The objectives include:

- Measuring the evaporation time of droplets of distilled water placed on steel coupons under the following variables:
    - One fan (A) or both fans operating (A and B),
    - 15 % or 40 % relative humidity,
    - 24 ^{o}C or 30 ^{o}C,
    - 1µl or 5µl droplet size.
- Determine the variance of the environmental conditions within the chamber by providing a map of the:
    - Temperature,
    - Relative humidity,
    - Airflow.

5.2. Methods

5.2.1. Modifying the novel environmental control chamber to perform droplet evaporation tests

A modified version of the novel chamber was printed to facilitate the following experiments, where the only change from the design used in Chapter 4 was a 190x47mm hole in the wall of the MT compartment, as shown in Figure 53. This allowed the droplets, placed on coupons of stainless steel to be visible during the experiments. To ensure the box was sealed, a transparent polymer (polymethyl methacrylate) sheet of the appropriate size was fixed to the chamber with silicone sealant. Additionally, a second Arduino microprocessor was added.

5.2.2. Mapping the environmental conditions in the novel environmental control chamber

Data was gathered relating to the temperature and relative humidity across each location a coupon could be placed in the MT compartment. In this experiment, the first Arduino utilised one DHT11 temperature and humidity sensor placed between positions C6 and D6 (as close to the centre of the tray as possible) and adhered to the tray using double-sided tape and gathered data to switch the heat pads on and off depending on the difference between the current and target temperature. The first Arduino was also connected to the two fans present in the HC compartment. The second Arduino was connected to six DHT11 sensors that were placed in the MT compartment of the chamber at each row for the respective column (i.e. columns 1-11 as shown in Figure 18). The code used to control the

second Arduino is shown in Appendix F. Each DHT11 was adhered to the tray using double sided tape and the wiring was taped together as closely as possible to each other to minimise the effects of the wiring on the airflow within the chamber. Potassium carbonate (120g) and water (80 mL) was added to the HC compartment and the heat pads set to 30 ^{o}C. The potassium chloride was replaced and reset each day before testing (six tests were performed each day, spanning 36 potential coupon placements). Before each experiment began, the chamber was left sealed and undisturbed for a minimum of one hour to allow an equilibrium to develop before testing. Temperature and humidity testing for each coupon placement (one column at a time) was performed in duplicate up to 90 minutes. The data generated by the sensors was saved to a microSD card reader connected to the second Arduino. The data was transferred to a computer before resetting for the subsequent experiments (i.e. the next column of coupon placements) . During the experiment containing column six, the DHT11 connected to the first Arduino (to control temperature) was moved to column five so as not to block the sensors connected to the second Arduino. The airflow within the chamber (based on the simulations of previous chambers) was determined by measuring the simulated airflow at each point where the coupons would be placed. All statistical analysis and visualisation of data was performed using GraphPad Prism 9.5.1.

5.2.3. Assessing the droplet evaporation rate in the novel environmental control chamber

The modified novel chamber was set up in the same manner as previously described (5.2.2) with only one DHT11 sensor within placed on the tray between positions C6 and D6, the temperature was set to either 24 ^{o}C or 30 ^{o}C and the relative humidity was controlled to either 15 % or 40 % via saturated lithium chloride or potassium carbonate respectively (both 120g salt and 80mL distilled water), allowing a minimum of one hour for relative humidity stabilisation before placing the coupons on the tray. The tray was removed via the sliding entrance to avoid disturbances to the internal environment of the chamber. Stainless steel 316L or Cu coupons of size 20x20 mm were sterilised by autoclaving at 121 ^{o}C for 20 minutes and inoculated with either 1µl or 5µl of distilled water, saline (0.85 % w/v), or *E. coli* ATCC 13706 (adjusted to 0.5 OD at 600nm as described in 3.2.2) before the tray was inserted into the chamber. A timer was started and stopped once the droplets were visibly dry. Each combination of temperature, relative humidity and droplet size was

tested in quadruplicate in the chamber and twice on separate occasions to ensure reproducibility (i.e. eight droplets were observed for droplet evaporation time in each variation, with four droplets placed in the chamber at one time and repeated once). All statistical analysis and visualisation of data was performed using GraphPad Prism 9.5.1.

5.3. Results

5.3.1. Modifying the novel environmental control chamber to perform droplet evaporation tests

The modifications to the chamber are shown in Figure 53 and Figure 54, whereby the plexiglass was fused to the chamber using silicone sealant, allowing the tray to be visible when in the chamber.

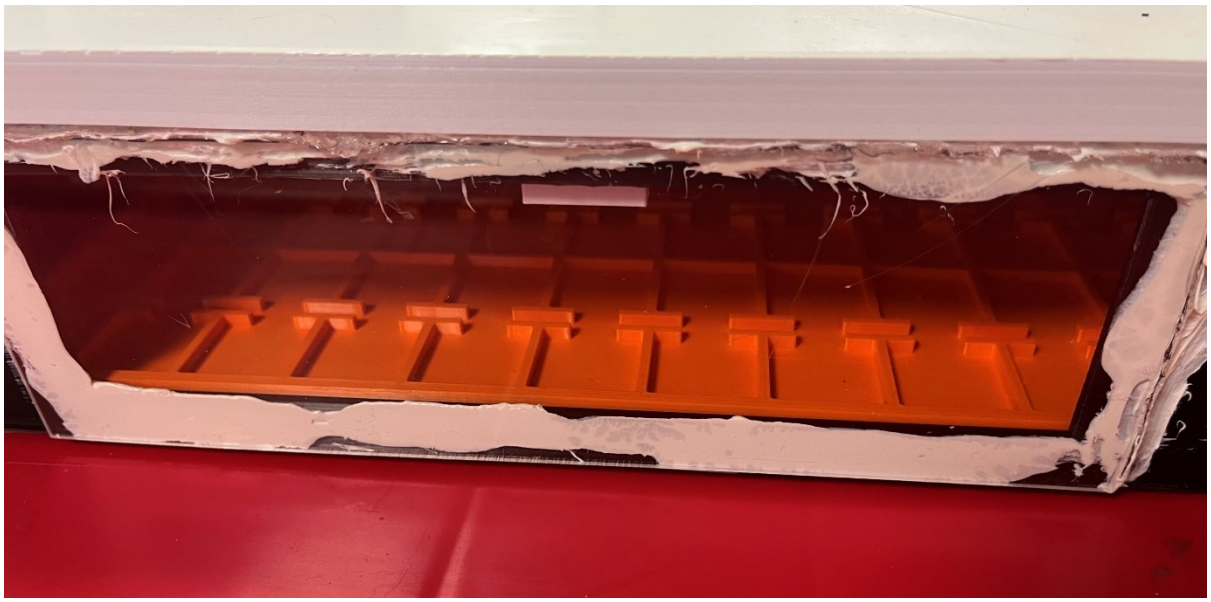

Figure 53 The window added to the novel environmental control chamber to allow for visibility into the MT compartment of the chamber.

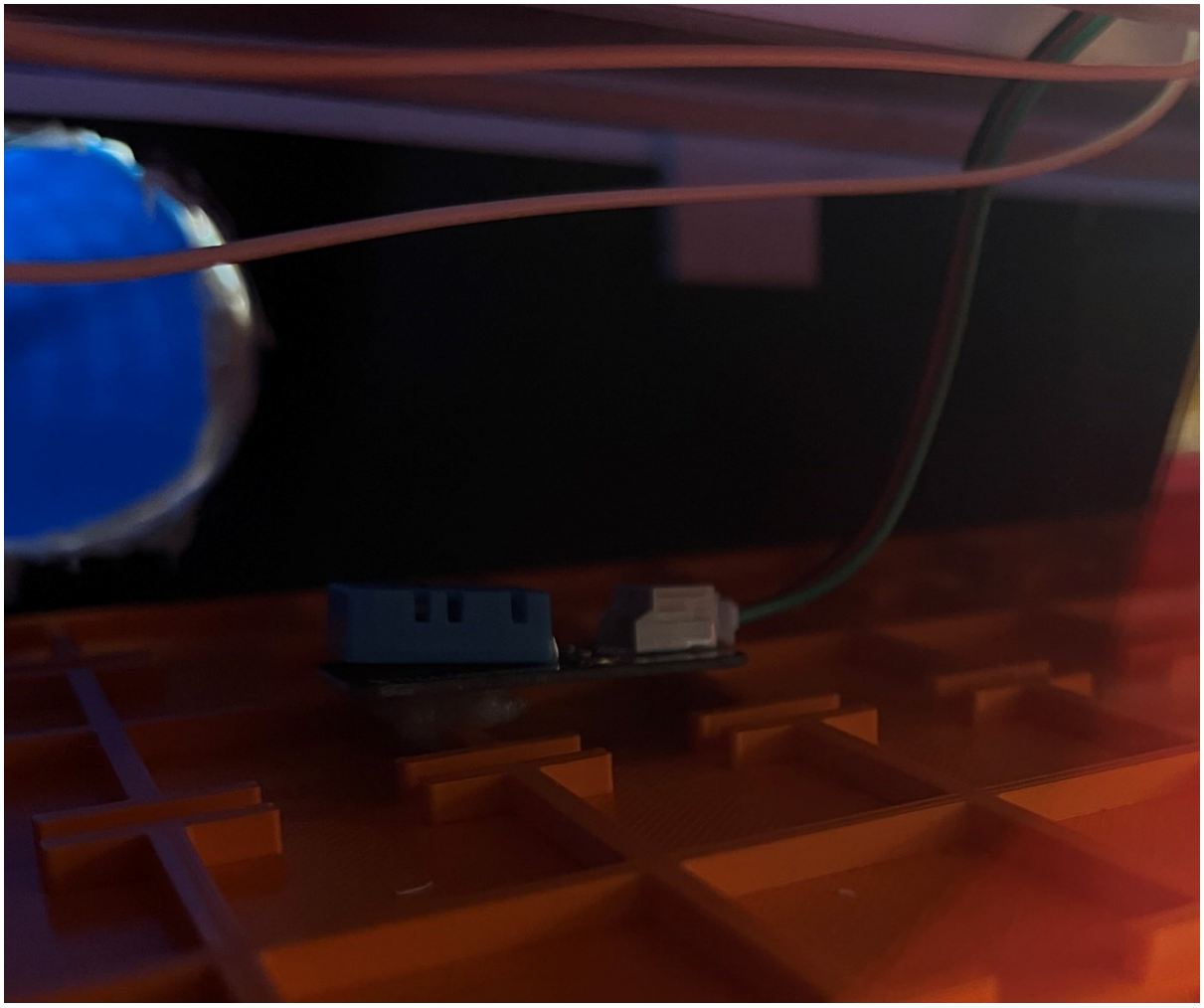

Figure 54 A DHT11 sensor placed in the MT compartment of the environmental control chamber, secured to a coupon location with adhesive tape.

5.3.2. Mapping the environmental conditions in the novel environmental control chamber

The temperature in each of the coupon locations is shown in Table 9, whereby an average maximum temperature of 30.8 ± 0.4 ^{o}C occurred at the location C6 and minimum of 26.6 ± 0.5 ^{o}C at position F1. When considering the overall distribution of temperature within the box, an area of higher temperature at position D6 is evident, which dissipates towards the outer edges of the chamber. Additionally, the relative humidity distribution (Table 10) demonstrates more variable spread of relative humidity values across the MT compartment. A maximum relative humidity of 54.6 ± 0.7 % is observed at position E10 and a minimum relative humidity of 33.3 ± 3.9 % is observed at position C1. Rows A, B, and F are relatively uniform in in relative humidity values, with an individual range (minimum to maximum mean) of less than or equal to ±3 % for each row (when discounting B10, including this position would increase the range of row B to ±3.6 %). However, rows C, D,

and E provided variation, particularly column E, that ranged from 35.42 % at position E1 to 54.42 % at position E8. Table 11 provides the simulated airflow measurements ranging between 0.44m/s and 5.60m/s. A multivariable correlation analysis showed that temperature was not correlated with relative humidity in the chamber ($p = 0.085$). However, airflow had a significant effect on the difference between the target relative humidity and the measured relative humidity within the chamber ($p < 0.05$).

Table 9 The temperature present within the MT compartment of the novel chamber. Each value is measured in ^{o}C and ± represents standard deviation. A-F and 1-11 represents the different coupon locations consistent with that in Figure 18.

	1	2	3	4	5	6	7	8	9	10	11
A	27±0	27.1±0.4	28±0.1	28.1±0.3	28.5±0.5	28.8±0.4	27.9±0.2	27.5±0.5	27.2±0.4	27.7±0.4	29±0
B	27.1±0.4	28±0	28.4±0.5	29.1±0.2	29.9±0.3	29.9±0.3	28.7±0.4	28±0.1	27.5±0.5	27±0	28.9±0.3
C	27.5±0.5	28+0.2	28.9±0.3	29.6±0.5	30.4±0.5	30.8±0.4	29.6±0.5	28.3±0.5	27.7±0.5	27±0	28±0.2
D	27.1±0.3	28.2±0.4	29±0.1	29.7±0.4	30.1±0.3	30.6±0.5	30±0.2	28.5±0.5	27.6±0.6	26.7±0.5	27.5±0.5
E	27±0	28±0	29±0.2	29.7±0.4	29.7±0.4	30.3±0.5	30.5±0.5	29±0.1	27.9±0.5	27.3±0.5	28.1±0.3
F	26.6±0.5	27±0	27.7±0.5	28±0.2	28.9±0.3	29.6±0.5	29.5±0.5	28.8±0.4	28.7±0.7	27±0	27.4±0.5

Table 10 The relative humidity present within the MT compartment of the novel environmental control chamber. Each value is measured in % and ± represents standard deviation. A-F and 1-11 represents the different coupon locations consistent with that in Figure 18.

	1	2	3	4	5	6	7	8	9	10	11
A	35.7±4.3	40±0	38.9±1.4	37.5±0.5	37.8±0.8	40.4±0.9	38±0.2	39±0.1	40.4±0.6	40.7±0.9	38.7±0.8
B	39.2±4	43.1±0.3	42.1±1.4	40.5±0.5	40.3±0.5	42.8±0.8	41.1±0.4	42.9±0.4	44.4±0.6	46.4±0.9	43.5±0.9
C	33.3±3.9	37±0.2	36.2±1.4.	34.3±0.4	33.6±0.5	35.6±0.9	34.2±0.5	36.6±0.5	38.3±0.8	40.8±0.9	38.7±0.8
D	46.8±5.3	51.8±0.9	50.2±4.4	45.9±0.4	45.9±0.8	50.9±0.8	42.8±0.5	46.6±0.5	46.8±1.1	49.6±0.9	46.5±0.6
E	35.4±4.2	39±0	37.4±1.5	35.6±0.5	36.4±0.6	38.1±0.8	48.2±0.7	54.6±0.7	50.6±2.2	51.9±2	36.5±0.8
F	39.9±4.1	43.8±0.4	42.7±1.4	41±0.1	41.1±0.7	42.3±0.8	39±0.5	40.5±0.5	41.2±0.8	44.9±0.9	43.8±0.9

Table 11 The airflow present within the MT compartment of the novel environmental control chamber. Each value is measured in m/s total airflow as measured for each coupon location as part of the airflow simulation in Figure 18.

	1	2	3	4	5	6	7	8	9	10	11
A	0.90	2.01	2.70	3.26	3.39	3.14	2.59	2.01	1.54	0.98	0.44
B	1.81	2.14	2.69	3.24	3.37	3.13	2.52	1.89	1.55	1.13	0.59
C	2.37	2.58	2.66	2.40	2.15	2.36	2.36	2.38	2.06	1.37	1.10
D	2.12	2.80	2.87	1.44	1.09	1.51	2.08	2.40	2.42	2.75	2.46
E	1.48	2.71	3.59	3.87	3.67	3.69	3.71	3.30	3.17	3.84	2.07
F	0.60	1.47	3.35	4.77	5.47	5.60	4.89	3.61	2.57	2.92	1.72

5.3.3. Assessing the droplet evaporation rate in the novel environmental control chamber

The evaporation rate of 1µl and 5µl droplets of distilled water in ~10 % and ~40 % relative humidity at 24 ^{o}C, observed in Figure 55 and Figure 56, was significantly faster ($p < 0.01$) than saline on both materials. In eight of the sixteen combinations of material, droplet size, and relative humidity, significantly faster droplet evaporation ($p < 0.05$) of *E. coli* suspension over sterile saline was observed, whereby 24 ^{o}C (6 / 8) observed statistical significance more often than 30 ^{o}C (2 / 8). There were no overall differences observed between the two materials used. A lower rate of statistical significance was observed at 30 ^{o}C (12 / 24 comparisons were statistically significant) compared to 24 ^{o}C (17 / 24), particularly in the 1µl droplets at ~40 % relative humidity at 30 ^{o}C, where no differences were observed. The same patterns of evaporation time among the droplets occurred at 30 ^{o}C except for 5µl droplets at ~40 % relative humidity, whereby distilled water evaporated at either the same time or slower ($p < 0.01$) than saline. Significantly lower ($p < 0.01$) evaporation times of *E. coli* suspension compared to sterile saline were only observed in two of the eight possible combinations. There were also no differences between the two materials at each droplet size and relative humidity combination.

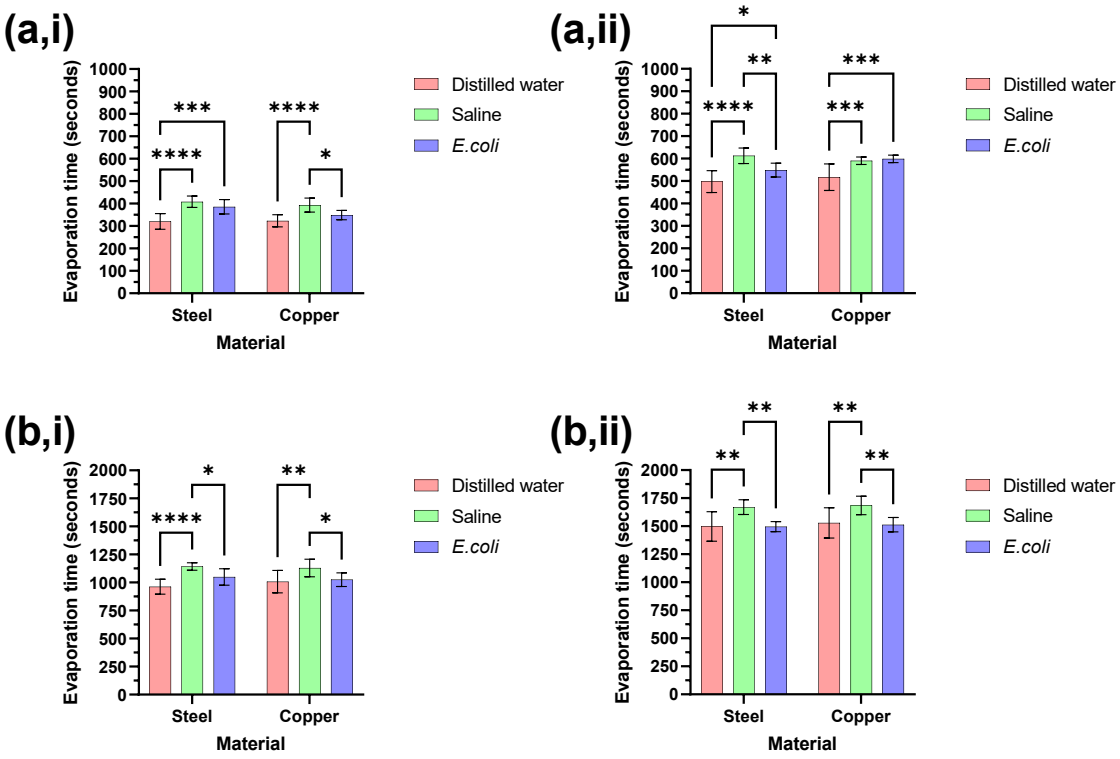

*Figure 55 The evaporation time of (a) 1µl and (b) 5µl droplets in (i) ~10 % and (ii) ~40 % relative humidity at 24 °C. Distilled water, saline (0.85 % w/v) and E. coli NCIMB 8545 (0.5 OD at 600nm) was assessed on stainless steel 316L and copper coupons. Significance values are represented as follows: * - p < 0.05, ** - p < 0.01, *** - p < 0.001, **** - p < 0.0001.*

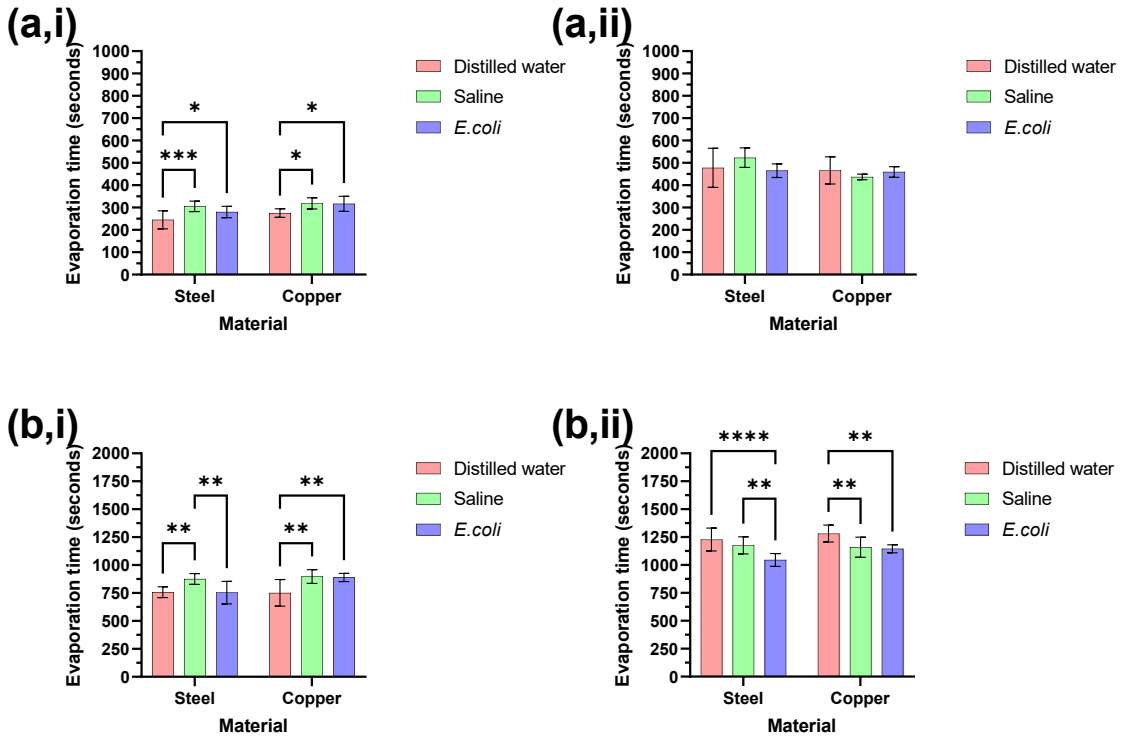

*Figure 56 The evaporation time of (a) 1µl and (b) 5µl droplets in (i) ~10 % and (ii) ~40 % relative humidity at 30 °C. Distilled water, saline (0.85 % w/v) and E. coli NCIMB 8545 (0.5 OD at 600nm) was assessed on stainless steel 316L and copper coupons. Significance values are represented as follows: * - p < 0.05, ** - p < 0.01, *** - p < 0.001, **** - p < 0.0001.*

5.4. Discussion

The modifications made to the chamber demonstrate it is possible to carry out experiments with different rationale (testing antimicrobial activity of surfaces, measuring droplet evaporation time) without the requirement for rigorous retesting of the environmental conditions within (as no fundamental changes have occurred to the temperature, relative humidity, or airflow control). To the understanding of the author, this is the first time such a chamber has been designed for this purpose. The detailed knowledge of temperature and relative humidity and the effects of airflow inside this system, at coupon-to-coupon resolution demonstrate that while the chamber can give users the confidence to test antimicrobial coatings in a variety of realistic environmental conditions, further changes could seek to provide less variation in temperature and relative humidity across the entire platform. However, this current chamber does provide temperature variation within ±2 °C of the target temperature across all coupon placement locations, which is often described as acceptable in numerous STMs for antimicrobial efficacy testing (e.g. ISO 22196). Furthermore, the data demonstrates that the position of the sensor that determines

whether the heat pad is switched on or off is important. In the experiments described in this chapter; the sensor was placed on the tray directly in the centre. However, in future experiments it should be moved so it doesn't block the coupons. This has implications for control of the heat pad as moving the sensor higher will raise the temperature it experiences as it is closer to the heat pad (although the degree of this change is yet untested). It is vital to calibrate the system with the final sensor location to ensure the accuracy of the environmental conditions when performing future tests within the chamber.

The relative humidity data presents a greater variation across the testing platform compared to the variation in temperature, likely because of its relationship with airflow. As lower relative humidity values are rarely required in existing STMs, it is unknown whether this degree of variability is acceptable. One approach may be to suggest testing an antimicrobial surface within a range of relative humidity values (e.g., low – 0-35 %, medium – 35-65 %, high – 65-100 %) to allow for naturally occurring variations that would almost certainly occur in end-use scenarios (Quraishi et al., 2020). Nevertheless, these differences in the environmental conditions across the testing platform should be considered when interpreting results from antimicrobial efficacy testing that has taken place in this chamber, to ensure reproducibility of the data and confidence in antimicrobial efficacy claims. Additionally, further refinement of the chamber to attempt to reduce variation in relative humidity (by the use of less variable airflow) across the testing platform could be achieved by greater numbers (and additional computing power) of airflow simulations (Jasak and Uroić, 2020). It is important to note that the use of saturated salts as a means of controlling relative humidity has been used in this work due to the simplicity and has been extensively used in the past (Gonthier et al., 2019; D'Amato et al., 2021; J. Jung and Schaffner, 2021) but other more accurate and reproducible methods of relative humidity control are available (although they are much more difficult and expensive to implement) (S. X. Q. Lin and Chen, 2005; Toğrul and Arslan, 2006; Xiaogang Liu and Meehan, 2014; Paolucci et al., 2022).

Whilst it is common that a STM prescribes environmental parameters with little room for variation, variations in temperature, relative humidity and airflow may allow for a more analogous testing environment to an end-use scenario. For example, an AMM that will be

implemented into a hospital ward bedside rail will encounter relatively stable environmental conditions as many indoor acclimatised locations have consistent (and in the case of hospitals required (Yuan et al., 2022)) environmental condition control (Wolkoff et al., 2021). However, this will vary with use / occupation due to factors such as proximity to air-conditioning vents, radiators and windows, movement of staff and patients, and the specific orientation of the equipment in the room. These variations, implicit in end-use conditions, are impossible to predict in such a way that they can be modelled within a chamber, and thus being able to ensure an AMMs efficacy across a known range of conditions (within prescribed parameters) can provide confidence in the ability of the AMM to kill microorganisms on its surface. Within this novel chamber, efficacy testing could be performed across all 66 positions (repeating the experiment multiple times) to have the widest degree of confidence of efficacy in an end-use environment, or if a very specific environmental condition is required, targeted placement of the coupons using the data described in this chapter could be used.

A consistent and low variability range of environmental conditions is important when assessing droplet evaporation experiments, and so the natural variability of the chamber is more problematic for this application. However, by separating the chamber into zones of similar environmental conditions it is possible to assess evaporation time of multiple droplets at the same time whilst being confident that the droplets are experiencing similar environmental conditions. Additionally, incorporating airflow in combination with lower relative humidity can result in droplets evaporating quickly. This knowledge that a droplet will dry in a defined time can help elucidate the potential antimicrobial activity of a surface in dry (or at least non-continuously submerged) conditions. The general observations of evaporation time at both temperatures described in the results section of this chapter display a trend of distilled water evaporating faster than that of saline and like that of the *E. coli* suspension, which was also observed in the original evaporation work among almost all materials, droplet sizes, and relative humidity combinations. These trends of salinity are also observed in the literature (Obianyo, 2019) and allows for a better understanding of how the inoculum composition of droplets may affect the antimicrobial efficacy of an AMM, although there is limited work outside of this thesis that observes the direct effects of bacterial contamination on the evaporation rate of droplets.

It is also important to consider the effect of adding airflow into this system. When comparing the results in Figure 55 and Figure 56 to those in Figure 48, it is clear that comparable conditions (with or without airflow present) can lead to differences in evaporation time. This may be because the airflow may be continuously replacing the air at the droplet-air interface, preventing the formation of a more humid microenvironment around the droplet that could slow the evaporation process (L. Liu et al., 2021). Interestingly, the addition of airflow can reduce the evaporation of the droplet by more than half, highlighting once more the complexity of implementing more realistic environmental conditions into STMs. The ability of the chamber to be able to offer more reproducible conditions under these complex end-use case simulations can enable users to test AMMs more rigorously and reduce the variability between laboratories / users, therefore providing a more robust system for testing AMMs. This facilitates the cooperation and unification of international regulation that would allow for one system of testing non-porous AMMs under varying conditions (dependent on the conditions present in the end-use case).

The adaptation of the novel chamber to assess evaporation times is also a proof of concept for further modifications for a variety of purposes. For example, adding a method to provide UV light to the internal chamber structure while preventing this light from escaping the chamber would allow a safe method of evaluating the efficacy of photocatalytic materials (e.g. titanium dioxide) without the requirement for large and specialised equipment, such as a solar chamber (López et al., 2021). Additionally, UV lamps are often currently used to test photocatalytic materials, which require safety equipment for users and can require entire rooms to be sealed off during the experiment. This process can be eliminated provided the chamber is thoroughly tested for safety and allows for a proof of principle that minimal work would be required to modify the chamber to perform a variety of tasks regarding AMMs.

5.5. Conclusion

The modification of the novel environmental control chamber to perform droplet evaporation assessments has been demonstrated, with the variability of the environmental conditions highlighting the complexity of adding realistic conditions in to STMs. Further work to lower this variability could be advantageous by utilising a greater number of

smaller heat pads and by generating more airflow simulations. Nevertheless, the chamber was able to perform droplet evaporation tests with results aligning with that of previous work described in chapter 4. The impact of temperature, relative humidity, airflow, and chemistry / biology of the inoculum on the evaporation rate of a droplet is important in understanding how more realistic conditions can be implemented in to STMs and the implications for the results generated.

6. Project summary and future work

6.1. The factors to consider for novel more realistic standardised test methods

The implementation of realistic environmental conditions and experimental parameters into STMs with the aim to assess efficacy of AMMs is complex and requires extensive research to understand the interactions between environment, microorganism, and surface. More specifically, there are two key considerations for future work:

- how these changes will affect the survival and viability of microorganisms on the surface,
- the impact of different environmental conditions on antimicrobial efficacy of an AMM.

The development of the chamber to overcome these challenges is an important step in improving the standardisation and reproducibility of STMs. However, it is also important to acknowledge the potential areas for improvement regarding the chamber.

This chapter outlines these considerations and recommends future work.

6.1.1. Environmental control chamber advantages and limitations

There are several advantages to the chamber over traditional incubator systems. A complete list is provided below:

- The novel chamber is portable, as opposed to more traditional environmental control chambers that are often very large and difficult to move,
- The novel chamber has precisely controlled airflow to include as a factor in future STMs,
- Laboratories using this chamber will generate reproducible results as they will all be using the same equipment, current chambers are often chosen based on price and availability,
- The novel chamber is relatively inexpensive compared to a traditional chamber,
- Coupons can be removed from the chamber without affecting the internal environmental conditions, which is difficult with other chambers,
- The novel chamber is made mostly from biodegradable materials and requires a low electrical power, and so is less harmful to the environment than other chambers,

- As the novel chamber is 3D printable, it can be created anywhere in the world with access to a 3D printer,
- The design of the novel chamber is modular, and so the chamber can be easily adapted to perform other tests, such as adding a light in to test photocatalytic materials.

On the other hand, the following list includes limitations and improvements that still need to be made to maximise the reproducibility and performance of the chamber:

- Currently, the airflow, temperature, and relative humidity throughout the MT compartment of the novel chamber present heterogeneity, minimising this would allow greater reproducibility between tests.
- The wiring for the novel chamber spans over a large area of the design to reach the different areas, design of a central area for the Arduino to be placed to allow for better cable management to prevent obstructions would be beneficial.
- The novel chamber is optimised for printing with a larger 3D printer than is necessary, smaller / more inexpensive 3D printers may have difficulty printing the larger and more complex components of the novel chamber without acquiring issues such as warping.
- The top of the MT compartment of the novel chamber can be very hot to the touch if working at higher temperatures, a warning for additional care or designing the heat pads to be physically further away from the MT compartment roof may be beneficial.
- Although the objectives of the project have been met, using more accurate sensors would allow for a greater understanding and control of the environmental conditions within the chamber.

Further development of the chamber with these points in consideration would allow for a greater ability to perform STMs and develop methods to assess the efficacy of AMMs.

6.1.2. The effects of standardised test method conditions on the organism

As demonstrated in both section 4.3 and 5.3, the environmental conditions (among other factors) required in an antimicrobial STM will affect the survival of a microorganism on a surface regardless of whether the material is actually antimicrobial or not. Particularly

when considering desiccant-sensitive organisms (e.g., many gram-negative bacteria (Janning and In't Veld, 1994)), and care must be taken to consider how to use these in methods that are focused on dry deposition or fast evaporation time.

For example, if an end-use scenario is likely to be burdened with gram-negative bacteria, is infrequently touched, and in environmental conditions that favour the increased evaporation rate of a droplet (high temperature and airflow, low relative humidity), then it may be that the addition of antimicrobial action into the material will not provide significant benefit to bioburden or transmission of microorganisms. This is because a lower population size of microorganisms is already likely to be present (although some microorganisms may remain). Understanding this limit, and particularly the environments for which the addition of a biocide provides a tangible benefit is important when considering the cost of adding a biocide into a material (although this is reducing over time (Petousis et al., 2022)) as well as the potential environmental impacts it may have (Thakur and Ganguly, 2022).

Other factors also affect the survival of microorganisms on the surface, both in terms of how it affects the droplet evaporation rate as well as biological mechanisms of survival. For example, it was demonstrated that the addition of bacteria into the inoculum provides a larger effect on evaporation rate than viruses (bacteriophage), with bacteria changing the contact angles of the droplets and contact line pinning affecting the mode of evaporation (Rasheed et al., 2023). However, whilst the data in this thesis demonstrates this clearly, it is unclear if this change in droplet evaporation is observed with the inclusion of any bacteria, or if it is species specific. Additionally, it is not clear if the same effect would be observed with a mixed species or mixed microbial kingdom (prokaryotic, eukaryotic (fungi), and viruses) inoculum, and / or with different concentrations of microorganisms. It is also unclear how a mixed-species model would provide beneficial or antagonistic effects to the individual species present. For example, the addition of multiple species of microorganisms may provide protective elements (Yao et al., 2022) such as the secretion of exopolysaccharides that would partially prevent the desiccation of gram-negative organisms on the surface post-evaporation. This complexity becomes more relevant when considering that a consortium of organisms would provide a more realistic approach to STMs, as single species end-use cases are unlikely.

The choice of inoculum media is also important to the survival of microorganisms on a surface, with the inoculation media used in current STMs not of relevance to end-use scenarios. For example, ISO22196 specifies the bacteria is in 1/500 nutrient broth for the duration of the test (ISO, 2011). While this choice provides the advantage of being able to maintain the bacterial population without promoting active growth of the organism, it is likely that this would not occur in many end-use scenarios. However, there are other media choices that are already established in the literature that may be able to provide a more-realistic inoculation to a surface, e.g. blood (Y. Wang et al., 2022) or sputum (Decraene et al., 2008; Biryukov et al., 2020). This can exemplify contamination from hospital patients, offering nutrients and proteins to microorganisms and may facilitate their increased survival or even growth on a surface (da Silva et al., 2022). Whilst there has been some research into the use of artificial saliva for AMM testing, it is of limited use until novel STMs with more realistic conditions can be developed (Taylor, 2022). It is also important to consider that even using very nutrient limiting factors such as saline may not prevent growth in all cases. *Pseudomonas aeruginosa* has been known to have the ability to grow multiple log factors in saline alone and even grow in distilled water (Favero et al., 1971).

Furthermore, the use of more complex inoculum media in STMs, particularly those that contain proteins, could impact the survival or growth of microorganisms on a surface by forming a conditioning film that allows the further attachment of microorganisms, developing the beginning stages of a biofilm (Monteiro et al., 2009). In addition to this, the movement of particles (microorganisms or other inocula contents) that occurs to form the coffee ring effect would exacerbate this conditioning film effect further.

The quantification of multi-species and especially multi-kingdom inocula also presents significant issues. Many species cannot be cultured on the same media and therefore the current method of a dilution plate count that is used in many STMs will not provide accurate results without burdening laboratories with highly increased workloads to plate on multiple culture media. Methods such as live-dead staining would provide a potential answer to this issue but once again raises the difficulty and expense of performing an STM that should fundamentally be able to be performed in a wide range of microbiology laboratories.

6.1.3. The effects of standardised test method conditions on the material

As identified throughout this thesis, the effects of environmental conditions on the ability of an AMM to express its antimicrobial efficacy is profound, mainly relating to the requirement of many AMMs to utilise moisture in the environment to exhibit their antimicrobial effects (e.g., Ag^+ ions (Q. Sun et al., 2014)). This relates closely to the considerations of how adapting the environmental conditions affect microbial survival. For example, when the relative humidity is reduced to ~50 % to simulate a hospital ward, the inoculum will evaporate on the surface, this will negatively influence the microbial viability but also negatively impact the antimicrobial efficacy of the AMM.

The material to be tested will also affect the evaporation rate of the inoculum as different materials often present different surface tension values with the same inoculum, as described in 4.3.2. The movement of particles and microorganisms in a droplet on the surface will also impact the antimicrobial efficacy via the stacking of bacteria caused by the coffee-ring effect that will prevent microorganisms from directly contacting the material, which can be a serious problem if the material requires contact for its mechanism of action. For example, nanoknife type materials such as graphene physically pierce microorganisms to exhibit their antimicrobial effect, which becomes less effective if a conditioning film has already been established (J. Liu et al., 2021). Furthermore, the addition of more realistic inoculum media (e.g., artificial blood) may be problematic to the antimicrobial activity of some materials via their neutralisation. This is highly dependent on the contents of the media and the active ingredient of the AMM but should be considered when assessing the impact of realistic conditions on STMs.

6.1.4. Informing on a more balanced and realistic approach to non-porous antimicrobial material efficacy testing

As discussed above, there are a wide variety of factors that impact on the results generated in an STM. For revisions to occur to these STMs, it is important to consider how each factor should be implemented and the level of specificity required, and how this may be interpreted in different laboratories with varying governmental regulation. The implementation of each of these factors should be considered individually as well as how it may impact on other aspects of a STM and the implications of it. The following factors have been concluded as important to consider altering to improve how realistic an STM is to an end-use scenario:

6.1.4.1. Temperature

Current STMs often state temperature values of 25-35 ^{o}C, while this is closer to the optimal temperature for many microorganisms, this is not commonly found in many end-use cases where fomite transmission or bioburden on surfaces may occur (Juan Wang and Norbäck, 2022). Therefore, adapting the temperature closer to that of end-use scenarios would be beneficial. However, the range of potential temperature values is vast, and can change based on geographical location, weather, time of day etc. There are two possible solutions to this issue, provide a generalised set of temperature values that would likely occur in a wide range of end-use scenarios or allow testing facilities and / or manufacturers to state the likely temperature that would be experienced by the AMM based on either the available literature or prior testing. There are clear advantages and drawbacks to each approach, such as the added difficulty of performing the STM whether it be to initially define a range of end-use scenarios and the accompanying conditions or to require individual laboratories to test or research the conditions present before performing the STM. This also has implications for providing approval to an AMM, as these conditions must also be verified as well as the efficacy of the AMM within those conditions, which presents a higher workload and a greater opportunity for variability to occur between laboratories. The advantages of providing more realistic testing negate some of these concerns, as it could be argued that regardless of the outcome of the current STMs, the efficacy of the AMM has not been verified in realistic conditions, and therefore may be completely ineffective at point of use. Furthermore, the development of equipment to perform STMs at reproducibly lower temperatures (the chamber from this project) will reduce the difficulty and potential for variability to arise.

Temperature is inherently linked to relative humidity and so in the context of performing STMs it is an important consideration. This is both in terms of how for example different seasons and the accompanying temperature changes will affect the relative humidity the material is presented with (which also affects microorganism transmission (Robey and Fierce, 2022)) and thus causing the results of even new more realistic STMs to be misaligned with true end-use scenarios at that time. Also, temperature changes can influence the relative humidity under saturated salts and thus the ability to maintain the desired relative humidity under a variety of temperatures becomes difficult even in a laboratory setting (Hong et al., 2002). However, the changes are relatively minor compared

to the vast differences between current STMs and end-use scenarios and so an improvement can still be made and therefore changes to STMs justified.

6.1.4.2. Relative humidity

Relative humidity is the most critical factor affecting current STMs, as it prevents the inoculum from evaporating on the surface altogether, so modifying this to be more in line with end-use cases is of the utmost importance. The relative humidity in end-use scenarios can range dramatically depending on many factors (Van Wijngaarden and Vincent, 2004) (a number of which overlap with temperature). Therefore, it may be beneficial to allow a wider range of relative humidity values to be used for novel STMs to allow for these changes or perform multiple tests at a range of relative humidity values to accommodate for these differences, although this does once again increase workload. It is also important to note that very high relative humidity regions and scenarios are possible (A. R. Khan et al., 2022), and so current STMs can be assumed to be more accurate in these cases. The approach to relative humidity selection should be in a similar manner to that of temperature, whereby ranges are either predetermined or measured and then the candidate AMM tested under those conditions. The use of the chamber to accommodate these changes can help to alleviate some of the logistical issues with modifying STMs.

6.1.4.3. Airflow

Airflow is a factor that is entirely omitted from most STMs, and is not relevant to others (when testing AMMs that will not experience airflow when in use (ASTM, 2013) e.g. water piping). The choice to omit airflow does provide many advantages, mainly relating to the increased variability of performing an STM with airflow. Even with a dedicated environmental control chamber such as the one described in this thesis; it is difficult to ensure the airflow is consistent across all regions of the chamber to increase reproducibility. Implementing airflow into new STMs however is vital to providing realistic simulated end-use cases and the factor has a large impact on the evaporation rate of an inoculum on a surface (Y. Zhao et al., 2022) and so affects AMM efficacy in the same manner as relative humidity. As the airflow in many indoor end-use scenarios is not likely to differ to a large degree, particularly when considering indoor environments, the presence of airflow alone can be considered adequate to better include realistic conditions in STMs.

6.1.4.4. Choice and concentration of microorganisms

Both the choice and concentration of organism used in STMs may not be realistic to end-use scenarios. In general, the microorganisms are much more diverse, and the concentration is much lower in end-use scenarios compared to those described in STMs. It is unlikely that single species contamination events would be seen in end-use scenarios outside of very specific cases such as coughing during a respiratory infection (N. Zhang et al., 2020) or blood splatter during a systemic infection etc. Therefore, it would be beneficial to include a consortium of microorganisms that simulate the end-use scenario that the AMM would likely be targeted towards. However, the choice of microorganisms for this consortium provides some difficulties relating to the large variety of potential species that could be encountered. It is likely best to form groups of organisms that would likely be co-contaminating surfaces in each area. For example, a hospital will likely encounter many human commensal and pathogenic microorganisms and so the STM should relate to that fact (Sarica et al., 2002). On the other hand, a ship's hull would be more likely to be contaminated with aquatic microorganisms (Qian et al., 2022). It is also recommended to use a consortium of microorganisms that can be cultured in similar (or ideally the same) nutrient media to avoid added workload in the STM. Additionally, reducing the concentration of the microorganisms, while addressing the issue of realistic conditions, may not be possible with many common and simple microbiological techniques, especially those that use agar plates, as the limit of detection is relatively high, and thus there is a requirement to be able to measure a difference in microbial population pre and post treatment.

6.1.4.5. Inoculum media

The inoculum media relates to AMM activity in a very similar manner to the species choice since it will also be determined by the contamination event in the end-use scenario. However, the inoculum media has a much wider range of possible combinations, as spill events from other sources (e.g., bodily fluids) can add a large amount of nutrients into the system (Fulford and Stankiewicz). Cleaning procedures can also impact the nutrients available to the microorganisms on the surface as well as presenting antagonistic effects to microorganisms (Gülsoy and Karagozoglu, 2022). All of which contributes to a complex system that is difficult to simulate meaningfully. One solution is to simulate conditions that would be present during an end-use case, for example using simulated sweat (Argel et al.,

2022). It is possible to mimic a hand-touch contamination event, or sea water could be used for marine end-use cases etc. It is likely that this should be treated in the same way as the inoculum media.

6.1.4.6. Incubation time

The incubation time of the AMMs in current STMs is likely not analogous to end-use scenarios, as it should be informed based on the time between interactions in the case of fomite transmission (very frequent) or over a long period (e.g., 28 days) in cases where preventing bioburden is important. Therefore, like the other factors, it is important to consider the use-case of the AMM in question to determine how long the test should be. This process will also eliminate some candidate AMMs from specific use cases pre-testing, allowing the elimination of some workload to testing laboratories. For example, AMMs that utilise photocatalytic properties generally require a longer period under indoor lighting conditions than the frequency of hand-contact with FTS would allow for (Xiao et al., 2019; Ziling Zhou et al., 2021), making them an inferior option compared to faster acting AMMs such as those that include Cu (Razavipour et al., 2022).

6.1.4.7. Method of applying the microorganisms to the surface

The process of applying the microorganisms to the surface is an important factor in the results generated from an STM. Many common STMs apply an inoculum droplet to the surface and incubate. While this method is simple to perform and increases reproducibility, it does not provide a realistic approach to how many contamination events would occur. For the purposes of this thesis, ISO 22196 has been used to reproducibly validate the environmental control chamber and assess the impact of certain variables (e.g. relative humidity, droplet size, inoculum concentration). However, recently newer methods of antimicrobial assessment of surfaces are being developed that could allow testing of AMMs in conditions more analogous to an end-use scenario. In many cases, if a droplet were to be applied to a surface in an end-use scenario, it would likely either be via microscopic droplets from coughing (could be simulated through a cascade impactor (McDonald et al., 2020)) or through larger spillage-based events, although this would likely invoke a cleaning process to occur in many cases (Aligina et al., 2022). This assumes that a droplet is present on the surface, but when assessing hand-contact contamination events, dry deposition occurs (Aranega-Bou et al., 2023). When translating this to informing on more realistic STMs, it is likely that very limited droplets would be available to the AMM and thus

minimising the droplet size would benefit how realistic the STM would be and offer an improvement over the current system.

6.2. Conclusion

The chamber designed, produced, and tested in this thesis will provide a foundation for the development of novel STMs that can simulate a wide variety of end-use conditions and work towards a system of unification towards the regulation of AMMs as well as provide confidence in their ability to express antimicrobial efficacy in end-use scenarios. This would ultimately allow for the approval of AMMs that can reduce both the bioburden of microorganisms on relevant surfaces and the transmission of microorganisms via fomites.

6.3. Future work

This project has provided extensive background work for the implementation of realistic conditions into STMs and explain some of the complexity involved in this process. Moving forward, it would be advantageous to continue developing an understanding of realistic conditions in STMs and the novel chamber that can facilitate this. There are several areas that would provide a great benefit to this field of work:

6.3.1. Would surfactants affect STMs?

Surfactants are chemicals that can decrease the surface tension of a droplet on a surface and are often used in household cleaning items such as detergent (Farias et al., 2021). The use of surfactants in a range of end-use scenarios has major implications for STMs and AMM efficacy. This is based on the lowering of the surface tension which leads to the droplet not using the constant wetted area mode of drying, preventing the coffee ring from occurring and allowing generally increased efficacy of a material. It would be insightful to quantify this process to determine the impact of a range of surfactant concentrations on the efficacy of various AMMs.

6.3.2. Scaling up the novel chamber

The chamber is currently capable of holding 66 20x20 mm coupons in the MT compartment at a time. Although this number is relatively large for research purposes, industry labs that are verifying AMM efficacy would benefit from as many coupons as possible being able to be tested at once. Scaling up the size of the chamber would be a complex task that would involve retesting the airflow, temperature, and relative humidity capabilities of the

chamber. Particularly when assessing relative humidity, a greater volume of saturated salts would be required to control an increased volume of air. Despite this being possible, it would be prudent to limit modifying the base version of the chamber as much as possible to allow reproducibility across laboratories, focusing on modifying the chamber to perform different types of material testing that would have limited effects on the environmental conditions within (e.g., photocatalytic and biofilm testing).

6.3.3. Testing photocatalytic materials in the novel chamber

Modifying the novel chamber to perform STMs involving photocatalytic materials would be a useful extension of the chamber's capabilities. With the addition of a UV light to the chamber (preferably with variable power output), photocatalytic AMMs could be tested in a range of realistic environments. This would remove the need for large solar chambers while maintaining safety. This process would require minimal testing and modifications to the chamber but ensuring that the environmental conditions have not significantly changed (especially temperature) would be an important step.

6.3.4. Testing biofilm growth in the novel chamber

Like that of photocatalytic materials, it would be interesting to develop the chamber to be able to perform static biofilm tests in realistic environmental conditions. Modifications to the novel chamber for this purpose would likely result from changing the tray to have deeper sections that are locked off from one another so that the appropriate nutrient medium could be added with the intention of the media evaporating over time to determine realistic biofilm growth. This would require very little modification to the chamber, but the extension of the wells could create microenvironments with high relative humidity and so testing for any changes and overall reproducibility would be advised.

Bibliography

AATCC. (2017) AATCC30: Antifungal activity, assessment on textile materials: mildew and rot resistance of textile materials

Abd-Elsalam, K. A. (2021) *Silver Nanomaterials for Agri-Food Applications.* Elsevier.

Adams, M. H. (1959) 'Bacteriophages.' *Bacteriophages.*,

Adlhart, C., Verran, J., Azevedo, N. F., Olmez, H., Keinänen-Toivola, M. M., Gouveia, I., Melo, L. F. and Crijns, F. (2018) 'Surface modifications for antimicrobial effects in the healthcare setting: A critical overview.' *Journal of Hospital Infection*, 99(3) pp. 239-249.

Agency, J. M. *Monthly mean relative humidity (%)*. [Online] [Accessed on 02/03/2023] https://www.data.jma.go.jp/obd/stats/etrn/view/monthly_s3_en.php?block_no=47662&view=7

Agency, U. S. E. P. (2022) *Federal Insecticide, Fungicide, and Rodenticide Act (FIFRA) and Federal Facilities*. [Online] [Accessed on 02/03/2023] https://www.epa.gov/enforcement/federal-insecticide-fungicide-and-rodenticide-act-fifra-and-federal-facilities#Basics%20of%20FIFRA

Ahmad, I., Malak, H. A. and Abulreesh, H. H. (2021) 'Environmental antimicrobial resistance and its drivers: a potential threat to public health.' *Journal of Global Antimicrobial Resistance*, 27 pp. 101-111.

Åhman, J., Matuschek, E. and Kahlmeter, G. (2019) 'The quality of antimicrobial discs from nine manufacturers—EUCAST evaluations in 2014 and 2017.' *Clinical Microbiology and Infection*, 25(3), 2019/03/01/, pp. 346-352.

Ahmed, O. B. and Alamro, T. (2022) 'Evaluation of the antibacterial activities of face masks coated with titanium dioxide nanoparticles.' *Scientific Reports*, 12(1) p. 18739.

Ahmed, S., Sameen, D. E., Lu, R., Li, R., Dai, J., Qin, W. and Liu, Y. (2022) 'Research progress on antimicrobial materials for food packaging.' *Critical Reviews in Food Science and Nutrition*, 62(11) pp. 3088-3102.

Akhavan, O. and Ghaderi, E. (2010) 'Toxicity of Graphene and Graphene Oxide Nanowalls Against Bacteria.' *ACS Nano*, 4(10), 2010/10/26, pp. 5731-5736.

Akhavan, O., Choobtashani, M. and Ghaderi, E. (2012) 'Protein degradation and RNA efflux of viruses photocatalyzed by graphene–tungsten oxide composite under visible light irradiation.' *The Journal of Physical Chemistry C*, 116(17) pp. 9653-9659.

Akyildiz, H. I., Yilmaz, B. A. and Diler, S. (2022) 'Antibacterial Activity of Photodeposited Ag Nanoparticles on Cotton Fibers Enabled by Atomic Layer Deposition.' *Fibers and Polymers*, 23(10), 2022/10/01, pp. 2769-2779.

Al Maghlouth, A., Al Yousef, Y. and Al Bagieh, N. (2004) 'Qualitative and quantitative analysis of bacterial aerosols.' *J Contemp Dent Pract*, 5(4) pp. 91-100.

Albright, V., Zhuk, I., Wang, Y., Selin, V., van de Belt-Gritter, B., Busscher, H. J., van der Mei, H. C. and Sukhishvili, S. A. (2017) 'Self-defensive antibiotic-loaded layer-by-layer coatings: Imaging of localized bacterial acidification and pH-triggering of antibiotic release.' *Acta Biomaterialia*, 61, 2017/10/01/, pp. 66-74.

Aldosari, M. A., Darwish, S. S., Adam, M. A., Elmarzugi, N. A. and Ahmed, S. M. (2019) 'Using ZnO nanoparticles in fungal inhibition and self-protection of exposed marble columns in historic sites.' *Archaeological and Anthropological Sciences*, 11 pp. 3407-3422.

Aligina, K. K., Goru, K. B., Muppidi, V. P. and Korukonda, B. (2022) 'Knowledge in Spill Management among trained and untrained healthcare workers in the Government General Hospital, Kakinada, India.' *Journal of Community Health Research*,

Alotaibi, A. M., Williamson, B. A., Sathasivam, S., Kafizas, A., Alqahtani, M., Sotelo-Vazquez, C., Buckeridge, J., Wu, J., et al. (2020) 'Enhanced photocatalytic and antibacterial ability of Cu-doped anatase TiO2 thin films: theory and experiment.' *ACS applied materials & interfaces*, 12(13) pp. 15348-15361.

Alt, J., Eveland, R., Fiorello, A., Haas, B., Meszaros, J., McEvoy, B., Ridenour, C., Shaffer, D., et al. (2022) 'Development and validation of technologies suitable for the decontamination and re-use of contaminated N95 filtering facepiece respirators in response to the COVID-19 pandemic.' *Journal of Hospital Infection*, 119, 2022/01/01/, pp. 141-148.

Alt, V., Bechert, T., Steinrücke, P., Wagener, M., Seidel, P., Dingeldein, E., Domann, E. and Schnettler, R. (2004) 'In Vitro Testing of Antimicrobial Activity of Bone Cement.' *Antimicrobial Agents and Chemotherapy*, 48(11) pp. 4084-4088.

Aranega-Bou, P., Brown, N., Stigling, A., D'Costa, W., Verlander, N. Q., Pottage, T., Bennett, A. and Moore, G. (2023) 'Laboratory Evaluation of a Quaternary Ammonium Compound-Based Antimicrobial Coating Used in Public Transport during the COVID-19 Pandemic.' *Applied and Environmental Microbiology*, 89(3) pp. e01744-01722.

Arduino. (2023a) *Arduino*. [Online] [Accessed on 28/04/2023] https://www.arduino.cc

Arduino. (2023b) *Arduino*. [Online] [Accessed https://www.arduino.cc/

Arena, F., Coda, A. R. D., Meschini, V., Verzicco, R. and Liso, A. (2021) 'Droplets generated from toilets during urination as a possible vehicle of carbapenem-resistant Klebsiella pneumoniae.' *Antimicrobial Resistance & Infection Control*, 10 pp. 1-8.

Argel, S., Castaño, M., Jimenez, D. E., Rodríguez, S., Vallejo, M. J., Castro, C. I. and Osorio, M. A. (2022) 'Assessment of Bacterial Nanocellulose Loaded with Acetylsalicylic Acid or Povidone-Iodine as Bioactive Dressings for Skin and Soft Tissue Infections.' *Pharmaceutics*, 14(8) p. 1661.

Arif, R. and Uddin, R. (2021) 'A review on recent developments in the biosynthesis of silver nanoparticles and its biomedical applications.' *Medical Devices & Sensors*, 4(1) p. e10158.

Armstrong, S., McHale, G., Ledesma-Aguilar, R. and Wells, G. G. (2019) 'Pinning-free evaporation of sessile droplets of water from solid surfaces.' *Langmuir*, 35(8) pp. 2989-2996.

Articles, S. o. I. t. f. A. *"KOHKIN" Hidden Ingenuity to Global Industry.*

Asif, A., Zeeshan, M. and Jahanzaib, M. (2018) 'Indoor temperature, relative humidity and CO2 levels assessment in academic buildings with different heating, ventilation and air-conditioning systems.' *Building and Environment*, 133 pp. 83-90.

ASTM. (2013) ASTM E2149-13a: Standard test method for determining the antimicrobial activity of antimicrobial agents under dynamic contact conditions

ASTM. (2016) Standard Practice for Evaluation of Effectiveness of Decontamination Procedures for Surfaces When Challenged with Droplets Containing Human Pathogenic Viruses.

ASTM. (2020) ASTM E2647 - Standard Test Method for Quantification of Pseudomonas aeruginosa Biofilm Grown Using Drip Flow Biofilm Reactor with Low Shear and Continuous Flow.

ASTM. (2021a) E3161 - Standard Practice for Preparing a Pseudomonas aeruginosa or Staphylococcus aureus Biofilm using the CDC Biofilm Reactor.

ASTM. (2021b) ASTM E2871-21: Standard test method for determining disinfectant efficacy against biofilm grown in the CDC biofilm reactor using the single tube method

ASTM. (2021c) ASTM G21 - Standard Practice for Determining Resistance of Synthetic Polymeric Materials to Fungi.

ASTM. (2022a) Standard Test Method for Testing Disinfectant Efficacy against Pseudomonas aeruginosa Biofilm using the MBEC Assay.

ASTM. (2022b) ASTM E2562 - Standard Test Method for Quantification of Pseudomonas aeruginosa Biofilm Grown with High Shear and Continuous Flow using CDC Biofilm Reactor.

Atkins, L., Sallis, A., Chadborn, T., Shaw, K., Schneider, A., Hopkins, S., Bunten, A., Michie, S., et al. (2020) 'Reducing catheter-associated urinary tract infections: a systematic review of barriers and facilitators and strategic behavioural analysis of interventions.' *Implementation science*, 15 pp. 1-22.

Azeredo, H. M., Otoni, C. G., Corrêa, D. S., Assis, O. B., de Moura, M. R. and Mattoso, L. H. C. (2019) 'Nanostructured antimicrobials in food packaging—recent advances.' *Biotechnology journal*, 14(12) p. 1900068.

Azizi-Lalabadi, M., Hashemi, H., Feng, J. and Jafari, S. M. (2020) 'Carbon nanomaterials against pathogens; the antimicrobial activity of carbon nanotubes, graphene/graphene oxide, fullerenes, and their nanocomposites.' *Advances in Colloid and Interface Science*, 284, 2020/10/01/, p. 102250.

Bai, A. D., Lo, C. K., Komorowski, A. S., Suresh, M., Guo, K., Garg, A., Tandon, P., Senecal, J., et al. (2022) 'Staphylococcus aureus bacteraemia mortality: a systematic review and meta-analysis.' *Clinical Microbiology and Infection*, 28(8) pp. 1076-1084.

Bale, M. J., Bennett, P. M., Beringer, J. E. and Hinton, M. (1993) 'The survival of bacteria exposed to desiccation on surfaces associated with farm buildings.' *Journal of Applied Bacteriology*, 75(6) pp. 519-528.

Basnett, P., Marcello, E., Lukasiewicz, B., Nigmatullin, R., Paxinou, A., Ahmad, M. H., Gurumayum, B. and Roy, I. (2020) 'Antimicrobial materials with lime oil and a poly (3-hydroxyalkanoate) produced via valorisation of sugar cane molasses.' *Journal of Functional Biomaterials*, 11(2) p. 24.

Basu, N. and Mukherjee, R. (2020) 'Evaporative drying of sodium chloride solution droplet on a thermally controlled substrate.' *The Journal of Physical Chemistry B*, 124(7) pp. 1266-1274.

Basurto-Vázquez, O., Sánchez-Rodríguez, E. P., McShane, G. J. and Medina, D. I. (2021) 'Load distribution on PET-G 3D prints of honeycomb cellular structures under compression load.' *Polymers*, 13(12) p. 1983.

Baudisch, C., Assadian, O. and Kramer, A. (2009) 'Concentration of the genera Aspergillus, Eurotium and Penicillium in 63-µm house dust fraction as a method to predict hidden moisture damage in homes.' *BMC Public Health*, 9 pp. 1-9.

Beveridge, T. and Murray, R. (1980) 'Sites of metal deposition in the cell wall of Bacillus subtilis.' *Journal of bacteriology*, 141(2) pp. 876-887.

Beyth, N., Houri-Haddad, Y., Domb, A., Khan, W. and Hazan, R. (2015) 'Alternative antimicrobial approach: nano-antimicrobial materials.' *Evidence-based complementary and alternative medicine*, 2015

Bezza, F. A., Tichapondwa, S. M. and Chirwa, E. (2020) 'Fabrication of monodispersed copper oxide nanoparticles with potential application as antimicrobial agents.' *Scientific reports*, 10(1) pp. 1-18.

Bhattacharjee, B., Ghosh, S., Patra, D. and Haldar, J. (2022) 'Advancements in release-active antimicrobial biomaterials: A journey from release to relief.' *Wiley Interdisciplinary Reviews: Nanomedicine and Nanobiotechnology*, 14(1) p. e1745.

Bhatti, M. M., Marin, M., Zeeshan, A. and Abdelsalam, S. I. (2020) 'Recent trends in computational fluid dynamics.' *Frontiers in Physics*, 8 p. 593111.

Bieser, A. M., Thomann, Y. and Tiller, J. C. (2011) 'Contact-Active Antimicrobial and Potentially Self-Polishing Coatings Based on Cellulose.' *Macromolecular Bioscience*, 11(1) pp. 111-121.

Bijekar, S., Padariya, H. D., Yadav, V. K., Gacem, A., Hasan, M. A., Awwad, N. S., Yadav, K. K., Islam, S., et al. (2022) 'The state of the art and emerging trends in the wastewater treatment in developing nations.' *Water*, 14(16) p. 2537.

Biryukov, J., Boydston, J. A., Dunning, R. A., Yeager, J. J., Wood, S., Reese, A. L., Ferris, A., Miller, D., et al. (2020) 'Increasing temperature and relative humidity accelerates inactivation of SARS-CoV-2 on surfaces.' *MSphere*, 5(4) pp. e00441-00420.

Bloomfield, S. F. and Looney, E. (1992) 'Evaluation of the repeatability and reproducibility of European suspension test methods for antimicrobial activity of disinfectants and antiseptics.' *Journal of Applied Bacteriology*, 73(1) pp. 87-93.

Bogdanovic, U., Vodnik, V., Mitric, M., Dimitrijevic, S., Skapin, S. D., Zunic, V., Budimir, M. and Stoiljkovic, M. (2015) 'Nanomaterial with High Antimicrobial Efficacy・ Copper/Polyaniline Nanocomposite.' *ACS applied materials & interfaces*, 7(3) pp. 1955-1966.

Bolhuis, A., Hand, L., Marshall, J. E., Richards, A. D., Rodger, A. and Aldrich-Wright, J. (2011) 'Antimicrobial activity of ruthenium-based intercalators.' *European Journal of Pharmaceutical Sciences*, 42(4), 2011/03/18/, pp. 313-317.

Bonten, M., Johnson, J. R., van den Biggelaar, A. H., Georgalis, L., Geurtsen, J., de Palacios, P. I., Gravenstein, S., Verstraeten, T., et al. (2021) 'Epidemiology of Escherichia coli bacteremia: a systematic literature review.' *Clinical Infectious Diseases*, 72(7) pp. 1211-1219.

Buhat, C. A. H., Lutero, D. S. M., Olave, Y. H., Torres, M. C. and Rabajante, J. F. (2020) 'Modeling the Transmission of Respiratory Infectious Diseases in Mass Transportation Systems.' *medRxiv*, p. 2020.2006.2009.20126334.

Bui, R., Labat, M. and Aubert, J.-E. (2017) 'Comparison of the saturated salt solution and the dynamic vapor sorption techniques based on the measured sorption isotherm of barley straw.' *Construction and Building Materials*, 141 pp. 140-151.

Burda, C., Lou, Y., Chen, X., Samia, A. C. S., Stout, J. and Gole, J. L. (2003) 'Enhanced Nitrogen Doping in TiO2 Nanoparticles.' *Nano Letters*, 3(8), 2003/08/01, pp. 1049-1051.

Burghardt, I., Lüthen, F., Prinz, C., Kreikemeyer, B., Zietz, C., Neumann, H.-G. and Rychly, J. (2015) 'A dual function of copper in designing regenerative implants.' *Biomaterials*, 44 pp. 36-44.

Byber, K., Radtke, T., Norbäck, D., Hitzke, C., Imo, D., Schwenkglenks, M., Puhan, M. A., Dressel, H., et al. (2021) 'Humidification of indoor air for preventing or reducing dryness symptoms or upper respiratory infections in educational settings and at the workplace.' *Cochrane Database of Systematic Reviews*, (12)

Callow, M. E. (1986) 'Chapter 1 A World-Wide Survey of Slime Formation on Anti-Fouling Paints.' *In* Evans, L. V. and Hoagland, K. D. (eds.) *Studies in Environmental Science*. Vol. 28. Elsevier, pp. 1-20. https://www.sciencedirect.com/science/article/pii/S0166111608721678

Campoccia, D., Montanaro, L. and Arciola, C. R. (2013) 'A review of the biomaterials technologies for infection-resistant surfaces.' *Biomaterials*, 34(34), 2013/11/01/, pp. 8533-8554.

Campos, R. K., Andrade, K. R., Ferreira, P. C. P., Bonjardim, C. A., La Scola, B., Kroon, E. G. and Abrahão, J. S. (2012) 'Virucidal activity of chemical biocides against mimivirus, a putative pneumonia agent.' *Journal of Clinical Virology*, 55(4), 2012/12/01/, pp. 323-328.

Cao, X., Hao, G., Li, Y.-y., Wang, M. and Wang, J.-X. (2022) 'On male urination and related environmental disease transmission in restrooms: From the perspectives of fluid dynamics.' *Sustainable Cities and Society*, 80 p. 103753.

Carpenter, B. L., Scholle, F., Sadeghifar, H., Francis, A. J., Boltersdorf, J., Weare, W. W., Argyropoulos, D. S., Maggard, P. A., et al. (2015) 'Synthesis, characterization, and antimicrobial efficacy of photomicrobicidal cellulose paper.' *Biomacromolecules*, 16(8) pp. 2482-2492.

Carrier, O., Shahidzadeh-Bonn, N., Zargar, R., Aytouna, M., Habibi, M., Eggers, J. and Bonn, D. (2016) 'Evaporation of water: evaporation rate and collective effects.' *Journal of Fluid Mechanics*, 798 pp. 774-786.

Caschera, A., Mistry, K. B., Bedard, J., Ronan, E., Syed, M. A., Khan, A. U., Lough, A. J., Wolfaardt, G., et al. (2019) 'Surface-attached sulfonamide containing quaternary ammonium antimicrobials for textiles and plastics.' *RSC advances*, 9(6) pp. 3140-3150.

Chaibenjawong, P. and Foster, S. J. (2011) 'Desiccation tolerance in Staphylococcus aureus.' *Archives of microbiology*, 193 pp. 125-135.

Chakrabortee, S., Boschetti, C., Walton, L. J., Sarkar, S., Rubinsztein, D. C. and Tunnacliffe, A. (2007) 'Hydrophilic protein associated with desiccation tolerance exhibits broad protein stabilization function.' *Proceedings of the National Academy of Sciences*, 104(46) pp. 18073-18078.

Chandraleka, S., Ramya, K., Chandramohan, G., Dhanasekaran, D., Priyadharshini, A. and Panneerselvam, A. (2014) 'Antimicrobial mechanism of copper (II) 1,10-phenanthroline and 2,2'-bipyridyl complex on bacterial and fungal pathogens.' *Journal of Saudi Chemical Society*, 18(6), 2014/12/01/, pp. 953-962.

ChemSafetyPro. (2015) *Japan Chemical Substance Control Law (Japan CSCL)*. [Online] [Accessed on 02/03/2023] https://www.chemsafetypro.com/Topics/Japan/Japan_CSCL_Chemical_Substance_Control_Law.html

Chen, F., Yang, X. and Wu, Q. (2009) 'Antifungal capability of TiO2 coated film on moist wood.' *Building and Environment*, 44(5), 2009/05/01/, pp. 1088-1093.

Chen, M. C., Koh, P. W., Ponnusamy, V. K. and Lee, S. L. (2022) 'Titanium dioxide and other nanomaterials based antimicrobial additives in functional paints and coatings.' *Progress in Organic Coatings*, 163 p. 106660.

Chen, S., Li, L., Zhao, C. and Zheng, J. (2010) 'Surface hydration: Principles and applications toward low-fouling/nonfouling biomaterials.' *Polymer*, 51(23) pp. 5283-5293.

Chen, S., De Guzman, M. R., Tsou, C.-H., Li, M., Suen, M.-C., Gao, C. and Tsou, C.-Y. (2023) 'Hydrophilic and absorption properties of reversible nanocomposite polyvinyl alcohol hydrogels reinforced with graphene-doped zinc oxide nanoplates for enhanced antibacterial activity.' *Polymer Journal*, 55(1) pp. 45-61.

Cheng, V. C. C., Chau, P. H., Lee, W. M., Ho, S. K. Y., Lee, D. W. Y., So, S. Y. C., Wong, S. C. Y., Tai, J. W. M., et al. (2015) 'Hand-touch contact assessment of high-touch and mutual-touch surfaces among healthcare workers, patients, and visitors.' *Journal of Hospital Infection*, 90(3), 2015/07/01/, pp. 220-225.

Cheng, Y.-H., Wang, C.-H., You, S.-H., Hsieh, N.-H., Chen, W.-Y., Chio, C.-P. and Liao, C.-M. (2016) 'Assessing coughing-induced influenza droplet transmission and implications for infection risk control.' *Epidemiology & Infection*, 144(2) pp. 333-345.

Church, D., Elsayed, S., Reid, O., Winston, B. and Lindsay, R. (2006) 'Burn wound infections.' *Clinical microbiology reviews*, 19(2) pp. 403-434.

Chyderiotis, S., Legeay, C., Verjat-Trannoy, D., Le Gallou, F., Astagneau, P. and Lepelletier, D. (2018) 'New insights on antimicrobial efficacy of copper surfaces in the healthcare environment: a systematic review.' *Clinical Microbiology and Infection*, 24(11) pp. 1130-1138.

Coman, A. N., Mare, A., Tanase, C., Bud, E. and Rusu, A. (2021) 'Silver-deposited nanoparticles on the titanium nanotubes surface as a promising antibacterial material into implants.' *Metals*, 11(1) p. 92.

Cox, C. (1989) 'Airborne bacteria and viruses.' *Science Progress (1933-)*, pp. 469-499.

Cunliffe, A. J., Wang, R., Redfern, J., Verran, J. and Wilson, D. I. (2023) 'Effect of environmental factors on the kinetics of evaporation of droplets containing bacteria or viruses on different surfaces.' *Journal of Food Engineering*, 336 p. 111195.

Cunliffe, A. J., Askew, P. D., Stephan, I., Iredale, G., Cosemans, P., Simmons, L. M., Verran, J. and Redfern, J. (2021) 'How do we determine the efficacy of an antibacterial surface? A review of standardised antibacterial material testing methods.' *Antibiotics*, 10(9) p. 1069.

D'Amato, R., Polimadei, A., Terranova, G. and Caponero, M. A. (2021) 'Humidity sensing by chitosan-coated fibre bragg gratings (Fbg).' *Sensors*, 21(10) p. 3348.

da Silva, N. D. G., de Paiva, P. R. B., Magalhães, T. V. M., Braga, A. S., Santos, P. S. d. S., Henrique-Silva, F., Magalhães, A. C. and Buzalaf, M. A. R. (2022) 'Effect of experimental and commercial artificial saliva formulations on the activity and viability of microcosm biofilm and on enamel demineralization for irradiated patients with head and neck cancer (HNC).' *Biofouling*, 38(7) pp. 674-686.

Dafforn, K. A., Lewis, J. A. and Johnston, E. L. (2011) 'Antifouling strategies: History and regulation, ecological impacts and mitigation.' *Marine Pollution Bulletin*, 62(3), 2011/03/01/, pp. 453-465.

Damian, L. and Patachia, S. (2016) 'Antimicrobial polypropylene as material for safe water supply.' *Bulletin of the Transilvania University of Brasov. Engineering Sciences. Series I*, 9(1) p. 41.

Danko, D., Bezdan, D., Afshin, E. E., Ahsanuddin, S., Bhattacharya, C., Butler, D. J., Chng, K. R., Donnellan, D., et al. (2021) 'A global metagenomic map of urban microbiomes and antimicrobial resistance.' *Cell*, 184(13) pp. 3376-3393. e3317.

Das, S., Saha, S., Sen, D., Ghorai, U. K., Banerjee, D. and Chattopadhyay, K. K. (2014) 'Highly oriented cupric oxide nanoknife arrays on flexible carbon fabric as high performing cold cathode emitter.' *Journal of Materials Chemistry C*, 2(7) pp. 1321-1330.

Das, S. K., Alam, J.-e., Plumari, S. and Greco, V. (2020) 'Transmission of airborne virus through sneezed and coughed droplets.' *Physics of Fluids*, 32(9) p. 097102.

Dauvergne, E. and Mullié, C. (2021) 'Brass alloys: Copper-bottomed solutions against hospital-acquired infections?' *Antibiotics*, 10(3) p. 286.

Dbouk, T. and Drikakis, D. (2020) 'On coughing and airborne droplet transmission to humans.' *Physics of Fluids*, 32(5) p. 053310.

De Angelis, G., Murthy, A., Beyersmann, J. and Harbarth, S. (2010) 'Estimating the impact of healthcare-associated infections on length of stay and costs.' *Clinical microbiology and infection*, 16(12) pp. 1729-1735.

Decraene, V., Pratten, J. and Wilson, M. (2008) 'Novel light-activated antimicrobial coatings are effective against surface-deposited Staphylococcus aureus.' *Current microbiology*, 57 pp. 269-273.

Deegan, R. D., Bakajin, O., Dupont, T. F., Huber, G., Nagel, S. R. and Witten, T. A. (2000) 'Contact line deposits in an evaporating drop.' *Physical review E*, 62(1) p. 756.

Delauney, L., Compère, C. and Lehaitre, M. (2009) 'Biofouling protection for marine environmental sensors.' *Ocean Science Discussions*, 6(4)

Deleplace, M., Dallagi, H., Dubois, T., Richard, E., Ipatova, A., Bénézech, T. and Faille, C. (2022) 'Structure of deposits formed by drying of droplets contaminated with Bacillus spores determines their resistance to rinsing and cleaning.' *Journal of Food Engineering*, 318, 2022/04/01/, p. 110873.

Dhanapriya, P. and Ratna, U. 'Effect of Antimicrobial Activity of Herbal Treated Cotton, Bamboo, and Tencel Socks.'

Dionísio, M. and Sotomayor, J. (2000) 'A surface chemistry experiment using an inexpensive contact angle goniometer.' *Journal of Chemical Education*, 77(1) p. 59.

Dobretsov, S., Al-Shibli, H., Maharachchikumbura, S. S. and Al-Sadi, A. M. (2021) 'The presence of marine filamentous fungi on a copper-based antifouling paint.' *Applied Sciences*, 11(18) p. 8277.

Dominguez-Wong, C., Loredo-Becerra, G., Quintero-González, C., Noriega-Treviño, M., Compeán-Jasso, M., Niño-Martínez, N., DeAlba-Montero, I. and Ruiz, F. (2014) 'Evaluation of the antibacterial activity of an indoor waterborne architectural coating containing Ag/TiO2 under different relative humidity environments.' *Materials Letters*, 134 pp. 103-106.

Donlan, R. M. (2002) 'Biofilms: microbial life on surfaces.' *Emerging infectious diseases*, 8(9) p. 881.

Dryden, M., Cooke, J., Salib, R., Holding, R., Pender, S. L. and Brooks, J. (2017) 'Hot topics in reactive oxygen therapy: antimicrobial and immunological mechanisms, safety and clinical applications.' *Journal of global antimicrobial resistance*, 8 pp. 194-198.

Dumitrache, A., Eberl, H. J., Allen, D. G. and Wolfaardt, G. M. (2015) 'Mathematical modeling to validate on-line CO2 measurements as a metric for cellulolytic biofilm activity in continuous-flow bioreactors.' *Biochemical Engineering Journal*, 101, 2015/09/15/, pp. 55-67.

Dunne, S. S., Ahonen, M., Modic, M., Crijns, F. R. L., Keinänen-Toivola, M. M., Meinke, R., Keevil, C. W., Gray, J., et al. (2018) 'Specialized cleaning associated with antimicrobial coatings for reduction of hospital-acquired infection: opinion of the COST Action Network AMiCI (CA15114).' *Journal of Hospital Infection*, 99(3), 2018/07/01/, pp. 250-255.

Eales, A. D. and Routh, A. F. (2016) 'Elimination of coffee-ring formation by humidity cycling: a numerical study.' *Langmuir*, 32(2) pp. 505-511.

Eggert, G. (2022) 'Saturated salt solutions in showcases: Humidity control and pollutant absorption.' *Heritage Science*, 10(1) pp. 1-6.

El Jaouhari, A., El Asbahani, A., Bouabdallaoui, M., Aouzal, Z., Filotás, D., Bazzaoui, E., Nagy, L., Nagy, G., et al. (2017) 'Corrosion resistance and antibacterial activity of electrosynthesized polypyrrole.' *Synthetic Metals*, 226 pp. 15-24.

Elsmore, R. (2013) 'The new Biocidal Products Regulation.' *Chimica Oggi-Chemistry Today*, 31 p. 3.

England, N. and Improvement, N. Health Technical Memorandum 03-01 Specialised ventilation for healthcare premises Part A: The concept, design, specification, installation and acceptance testing of healthcare ventilation systems, 2021.

Erbil, H. Y., McHale, G. and Newton, M. (2002) 'Drop evaporation on solid surfaces: constant contact angle mode.' *Langmuir*, 18(7) pp. 2636-2641.

Esbelin, J., Santos, T. and Hébraud, M. (2018) 'Desiccation: an environmental and food industry stress that bacteria commonly face.' *Food microbiology*, 69 pp. 82-88.

Evaluation, N. I. o. T. a. *International Accreditation Japan (IAJapan)*. [Online] [Accessed on 14/04/2023] https://www.nite.go.jp/en/iajapan/jnla/index.html

Executive, H. a. S. (2022) *Technical equivalence of an active substance: biocides*. [Online] [Accessed on 02/03/2023] https://www.hse.gov.uk/biocides/technical-equivalence.htm

Faille, C., Bihi, I., Ronse, A., Ronse, G., Baudoin, M. and Zoueshtiagh, F. (2016) 'Increased resistance to detachment of adherent microspheres and Bacillus spores subjected to a drying step.' *Colloids and Surfaces B: Biointerfaces*, 143, 2016/07/01/, pp. 293-300.

Fakhri, A. and Behrouz, S. (2015) 'Assessment of SnS2 nanoparticles properties for photocatalytic and antibacterial applications.' *Solar Energy*, 117, 2015/07/01/, pp. 187-191.

Farias, C. B. B., Almeida, F. C., Silva, I. A., Souza, T. C., Meira, H. M., Rita de Cássia, F., Luna, J. M., Santos, V. A., et al. (2021) 'Production of green surfactants: Market prospects.' *Electronic Journal of Biotechnology*, 51 pp. 28-39.

Favero, M., Carson, L., Bond, W. and Petersen, N. (1971) 'Pseudomonas aeruginosa: growth in distilled water from hospitals.' *Science*, 173(3999) pp. 836-838.

Feng, Y., Gu, D., Wang, Z., Lu, C., Fan, J., Zhou, J., Wang, R. and Su, X. (2022) 'Comprehensive evaluation and analysis of the salinity stress response mechanisms based on transcriptome and metabolome of Staphylococcus aureus.' *Archives of Microbiology*, 204 pp. 1-14.

Fu, X., Lindgren, T., Guo, M., Cai, G.-H., Lundgren, H. and Norbäck, D. (2013) 'Furry pet allergens, fungal DNA and microbial volatile organic compounds (MVOCs) in the commercial aircraft cabin environment.' *Environmental Science: Processes & Impacts*, 15(6) pp. 1228-1234.

Fukai, J., Ishizuka, H., Sakai, Y., Kaneda, M., Morita, M. and Takahara, A. (2006) 'Effects of droplet size and solute concentration on drying process of polymer solution droplets deposited on homogeneous surfaces.' *International Journal of Heat and Mass Transfer*, 49(19-20) pp. 3561-3567.

Fulford, M. and Stankiewicz, N. '12.1 Fomites.'

Gadgil, A. (1998) 'Drinking water in developing countries.' *Annual review of energy and the environment*, 23(1) pp. 253-286.

Gaeini, M., Shaik, S. and Rindt, C. (2019) 'Characterization of potassium carbonate salt hydrate for thermochemical energy storage in buildings.' *Energy and Buildings*, 196 pp. 178-193.

Gaidau, C., Calin, M., Rebleanu, D. and Constantinescu, C. (2019) 'Added functions of leather surface by Ag/TiO2 nanoparticles use and some considerations on their cytotoxicity.'

Gallagher, J. E., KC, S., Johnson, I. G., Al-Yaseen, W., Jones, R., McGregor, S., Robertson, M., Harris, R., et al. (2020) 'A systematic review of contamination (aerosol, splatter and droplet generation) associated with oral surgery and its relevance to COVID-19.' *BDJ open*, 6(1) p. 25.

Ganguli, P. and Chaudhuri, S. (2021) 'Nanomaterials in antimicrobial paints and coatings to prevent biodegradation of man-made surfaces: A review.' *Materials Today: Proceedings*, 45 pp. 3769-3777.

García de Castro, A., Bredholt, H., Strøm, A. R. and Tunnacliffe, A. (2000) 'Anhydrobiotic engineering of gram-negative bacteria.' *Applied and Environmental Microbiology*, 66(9) pp. 4142-4144.

Giannousi, K., Lafazanis, K., Arvanitidis, J., Pantazaki, A. and Dendrinou-Samara, C. (2014) 'Hydrothermal synthesis of copper based nanoparticles: Antimicrobial screening and interaction with DNA.' *Journal of Inorganic Biochemistry*, 133, 2014/04/01/, pp. 24-32.

Goeres, D. M., Walker, D. K., Buckingham-Meyer, K., Lorenz, L., Summers, J., Fritz, B., Goveia, D., Dickerman, G., et al. (2019) 'Development, standardization, and validation of a biofilm efficacy test: The single tube method.' *Journal of Microbiological Methods*, 165, 2019/10/01/, p. 105694.

Gomes, R. N., Borges, I., Pereira, A. T., Maia, A. F., Pestana, M., Magalhães, F. D., Pinto, A. M. and Gonçalves, I. C. (2018) 'Antimicrobial graphene nanoplatelets coatings for silicone catheters.' *Carbon*, 139 pp. 635-647.

Gonthier, J., Barrett, M. A., Aguettaz, O., Baudoin, S., Bourgeat-Lami, E., Demé, B., Grimm, N., Hauß, T., et al. (2019) 'BerILL: The ultimate humidity chamber for neutron scattering.' *Journal of Neutron Research*, 21(1-2) pp. 65-76.

Goulter, R., Gentle, I. and Dykes, G. (2009) 'Issues in determining factors influencing bacterial attachment: a review using the attachment of Escherichia coli to abiotic surfaces as an example.' *Letters in applied microbiology*, 49(1) pp. 1-7.

Govind, V., Bharadwaj, S., Sai Ganesh, M., Vishnu, J., Shankar, K. V., Shankar, B. and Rajesh, R. (2021) 'Antiviral properties of copper and its alloys to inactivate covid-19 virus: a review.' *Biometals*, 34(6) pp. 1217-1235.

Grass, G., Rensing, C. and Solioz, M. (2011) 'Metallic Copper as an Antimicrobial Surface.' *Applied and Environmental Microbiology*, 77(5), March 1, 2011, pp. 1541-1547.

Grengg, C., Mittermayr, F., Baldermann, A., Böttcher, M. E., Leis, A., Koraimann, G., Grunert, P. and Dietzel, M. (2015) 'Microbiologically induced concrete corrosion: A case study from a combined sewer network.' *Cement and Concrete Research*, 77 pp. 16-25.

Grinberg, M., Orevi, T., Steinberg, S. and Kashtan, N. (2019) 'Bacterial survival in microscopic surface wetness.' *Elife*, 8 p. e48508.

Gross, T. M., Lahiri, J., Golas, A., Luo, J., Verrier, F., Kurzejewski, J. L., Baker, D. E., Wang, J., et al. (2019) 'Copper-containing glass ceramic with high antimicrobial efficacy.' *Nature communications*, 10(1) p. 1979.

Gu, G., Erişen, D. E., Yang, K., Zhang, B., Shen, M., Zou, J., Qi, X., Chen, S., et al. (2022) 'Antibacterial and anti-inflammatory activities of chitosan/copper complex coating on medical catheters: In vitro and in vivo.' *Journal of Biomedical Materials Research Part B: Applied Biomaterials*, 110(8) pp. 1899-1910.

Guevarra, R. B., Hwang, J., Lee, H., Kim, H. J., Lee, Y., Danko, D., Ryon, K. A., Young, B. G., et al. (2022) 'Metagenomic characterization of bacterial community and antibiotic resistance genes found in the mass transit system in Seoul, South Korea.' *Ecotoxicology and Environmental Safety*, 246 p. 114176.

Gülsoy, Z. and Karagozoglu, S. (2022) 'The efficiency of cleaning in intensive care units: A systematic review.' *Enfermeria intensiva*, 33(2) pp. 92-106.

Habibi Mohraz, M., Golbabaei, F. and Je Yu, I. (2021) 'Evaluation of Antibacterial Properties of Electrospun Polyurethane-chitosan Nanofiber Media.' *Journal of Occupational Hygiene Engineering*, 8(3) pp. 67-73.

Hamouda, R. A., Abd El-Mongy, M. and Eid, K. F. (2019) 'Comparative study between two red algae for biosynthesis silver nanoparticles capping by SDS: Insights of characterization and antibacterial activity.' *Microbial pathogenesis*, 129 pp. 224-232.

Han, C., Lalley, J., Namboodiri, D., Cromer, K. and Nadagouda, M. N. (2016) 'Titanium dioxide-based antibacterial surfaces for water treatment.' *Current opinion in chemical engineering*, 11 pp. 46-51.

Han, J. H. (2003) 'Antimicrobial food packaging.' *Novel food packaging techniques*, 8 pp. 50-70.

Han, Y., Zhou, Z.-C., Zhu, L., Wei, Y.-Y., Feng, W.-Q., Xu, L., Liu, Y., Lin, Z.-J., et al. (2019) 'The impact and mechanism of quaternary ammonium compounds on the transmission of antibiotic resistance genes.' *Environmental Science and Pollution Research*, 26(27), 2019/09/01, pp. 28352-28360.

Hans, M., Erbe, A., Mathews, S., Chen, Y., Solioz, M. and Mücklich, F. (2013) 'Role of Copper Oxides in Contact Killing of Bacteria.' *Langmuir*, 29(52), 2013/12/31, pp. 16160-16166.

Hasan, H. A. and Muhammad, M. H. (2020) 'A review of biological drinking water treatment technologies for contaminants removal from polluted water resources.' *Journal of Water Process Engineering*, 33 p. 101035.

Hasan, M. F., Ahmed Himika, T. and Molla, M. M. (2017) 'Lattice Boltzmann simulation of airflow and heat transfer in a model ward of a hospital.' *Journal of Thermal Science and Engineering Applications*, 9(1) p. 011011.

Hassan, I. A., Parkin, I. P., Nair, S. P. and Carmalt, C. J. (2014) 'Antimicrobial activity of copper and copper (I) oxide thin films deposited via aerosol-assisted CVD.' *Journal of Materials Chemistry B*, 2(19) pp. 2855-2860.

Healthcare, N. D. (2018) Bed and mattress cleaning standard operating procedure

Heller, L. C. and Edelblute, C. M. (2018) 'Long-term metabolic persistence of gram-positive bacteria on health care-relevant plastic.' *American Journal of Infection Control*, 46(1), 2018/01/01/, pp. 50-53.

Hellio, C. and Yebra, D. (2009) *Advances in marine antifouling coatings and technologies.* Elsevier.

Héquet, A., Humblot, V., Berjeaud, J.-M. and Pradier, C.-M. (2011) 'Optimized grafting of antimicrobial peptides on stainless steel surface and biofilm resistance tests.' *Colloids and Surfaces B: Biointerfaces*, 84(2), 2011/06/01/, pp. 301-309.

Hincha, D. K. and Thalhammer, A. (2012) 'LEA proteins: IDPs with versatile functions in cellular dehydration tolerance.' *Biochemical Society Transactions*, 40(5) pp. 1000-1003.

Hodek, J., Zajícová, V., Lovětinská-Šlamborová, I., Stibor, I., Müllerová, J. and Weber, J. (2016) 'Protective hybrid coating containing silver, copper and zinc cations effective against human immunodeficiency virus and other enveloped viruses.' *BMC Microbiology*, 16(1), 2016/04/01, p. 56.

Holm, E. R. (2012) Barnacles and biofouling. Oxford University Press.

Holmes, P. F., Currie, E. P. K., Thies, J. C., van der Mei, H. C., Busscher, H. J. and Norde, W. (2009) 'Surface-modified nanoparticles as a new, versatile, and mechanically robust nonadhesive coating: Suppression of protein adsorption and bacterial adhesion.' *Journal of Biomedical Materials Research Part A*, 91A(3) pp. 824-833.

Hong, T., Ellis, R., Gunn, J. and Moore, D. (2002) 'Relative humidity, temperature, and the equilibrium moisture content of conidia of Beauveria bassiana (Balsamo) Vuillemin: a quantitative approach.' *Journal of Stored Products Research*, 38(1) pp. 33-41.

Hosein, I., Madeloso, R., Nagaratnam, W., Villamaria, F., Stock, E. and Jinadatha, C. (2016) 'Evaluation of a pulsed xenon ultraviolet light device for isolation room disinfection in a United Kingdom hospital.' *American Journal of Infection Control*, 44(9), 2016/09/01/, pp. e157-e161.

Hrenovic, J. and Ivankovic, T. (2009) 'Survival of Escherichia coli and Acinetobacter junii at various concentrations of sodium chloride.' *EurAsian Journal of Biosciences*, 3

Huang, H.-L., Lin, C.-C. and Hsu, K. (2015) 'Comparison of resistance improvement to fungal growth on green and conventional building materials by nano-metal impregnation.' *Building and Environment*, 93, 2015/11/01/, pp. 119-127.

Huang, Z., Jiang, X., Guo, D. and Gu, N. (2011) 'Controllable synthesis and biomedical applications of silver nanomaterials.' *Journal of nanoscience and nanotechnology*, 11(11) pp. 9395-9408.

Hübner, N.-O., Hübner, C., Kramer, A. and Assadian, O. (2011) 'Survival of bacterial pathogens on paper and bacterial retrieval from paper to hands: preliminary results.' *AJN The American Journal of Nursing*, 111(12) pp. 30-34.

Huslage, K., Rutala, W. A., Sickbert-Bennett, E. and Weber, D. J. (2010) 'A Quantitative Approach to Defining "High-Touch" Surfaces in Hospitals.' *Infection Control & Hospital Epidemiology*, 31(8) 2015/01/02, pp. 850-853.

Instruments, n. (2023) *Contact angle goniometery - Tensiometry*. [Online] [Accessed https://www.nanoscience.com/techniques/tensiometry/

Ioannidis, J. P. (2005) 'Why most published research findings are false.' *PLoS medicine*, 2(8) p. e124.

ISO. (2004a) ISO 20645 - Textile fabrics — Determination of antibacterial activity — Agar diffusion plate test.

ISO. (2004b) ISO20645: Textile fabrics - determination of antibacterial activity - agar diffusion plate test.

ISO. (2011) ISO22196: Measurement of antibacterial activity on plastics and other non-porous surfaces.

ISO. (2021) ISO20743: Determination of antibacterial activity of textile products.

Iswadi, A., Porter, J. S., Bell, M. C., Garniati, L., Harris, R. E. and Priyotomo, G. (2022) 'Establishing an agenda for biofouling research for the development of the marine renewable energy industry in Indonesia.' *Journal of Marine Science and Engineering*, 10(3) p. 384.

Janning, B. and In't Veld, P. (1994) 'Susceptibility of bacterial strains to desiccation: a simple method to test their stability in microbiological reference materials.' *Analytica chimica acta*, 286(3) pp. 469-476.

Jaradat, Z. W., Ababneh, Q. O., Sha'aban, S. T., Alkofahi, A. A., Assaleh, D. and Al Shara, A. (2020) 'Methicillin Resistant Staphylococcus aureus and public fomites: a review.' *Pathogens and Global Health*, 114(8), 2020/11/16, pp. 426-450.

Jasak, H. and Uroić, T. (2020) 'Practical computational fluid dynamics with the finite volume method.' *Modeling in Engineering Using Innovative Numerical Methods for Solids and Fluids*, pp. 103-161.

Jayaweera, M., Perera, H., Gunawardana, B. and Manatunge, J. (2020) 'Transmission of COVID-19 virus by droplets and aerosols: A critical review on the unresolved dichotomy.' *Environmental research*, 188 p. 109819.

Jędrzejczak, P., Ławniczak, Ł., Ślosarczyk, A. and Klapiszewski, Ł. (2022) 'Physicomechanical and antimicrobial characteristics of cement composites with selected nano-sized oxides and binary oxide systems.' *Materials*, 15(2) p. 661.

Jennings, M. C., Minbiole, K. P. C. and Wuest, W. M. (2015) 'Quaternary Ammonium Compounds: An Antimicrobial Mainstay and Platform for Innovation to Address Bacterial Resistance.' *ACS Infectious Diseases*, 1(7), 2015/07/10, pp. 288-303.

Jiang, H., Liu, G.-L., Chi, Z., Hu, Z. and Chi, Z.-M. (2018) 'Genetics of trehalose biosynthesis in desert-derived Aureobasidium melanogenum and role of trehalose in the adaptation of the yeast to extreme environments.' *Current genetics*, 64 pp. 479-491.

Jung, I. Y., Choi, W., Kim, J., Wang, E., Park, S. W., Lee, W. J., Choi, J. Y., Kim, H. Y., et al. (2019) 'Nosocomial person-to-person transmission of severe fever with thrombocytopenia syndrome.' *Clinical Microbiology and Infection*, 25(5), 2019/05/01/, pp. 633.e631-633.e634.

Jung, J. and Schaffner, D. W. (2021) 'Modeling the survival of Salmonella on whole cucumbers as a function of temperature and relative humidity.' *Food Microbiology*, 100 p. 103840.

Kakakhel, M. A., Wu, F., Sajjad, W., Zhang, Q., Khan, I., Ullah, K. and Wang, W. (2021) 'Long-term exposure to high-concentration silver nanoparticles induced toxicity, fatality, bioaccumulation, and histological alteration in fish (Cyprinus carpio).' *Environmental Sciences Europe*, 33 pp. 1-11.

Kalb, L., Bäßler, P., Schneider-Brachert, W. and Eckl, D. B. (2022) 'Antimicrobial Photodynamic Coatings Reduce the Microbial Burden on Environmental Surfaces in Public Transportation—A Field Study in Buses.' *International journal of environmental research and public health*, 19(4) p. 2325.

Karimzadeh, F., Sajedi, S. M., Taram, S. and Karimzadeh, F. (2021) 'Comparative evaluation of bacterial colonization on removable dental prostheses in patients with COVID-19: A clinical study.' *The Journal of Prosthetic Dentistry*,

Kashiri, M., Cerisuelo, J. P., Domínguez, I., López-Carballo, G., Hernández-Muñoz, P. and Gavara, R. (2016) 'Novel antimicrobial zein film for controlled release of lauroyl arginate (LAE).' *Food Hydrocolloids*, 61, 2016/12/01/, pp. 547-554.

Kaur, R. and Liu, S. (2016) 'Antibacterial surface design – Contact kill.' *Progress in Surface Science*, 91(3), 2016/08/01/, pp. 136-153.

Khadka, P., Haque, M., Krishnamurthi, V. R., Niyonshuti, I., Chen, J. and Wang, Y. (2018) 'Quantitative investigations reveal new antimicrobial mechanism of silver nanoparticles and ions.' *Biophysical Journal*, 114(3) p. 690a.

Khalaj, A. H. and Halgamuge, S. K. (2017) 'A Review on efficient thermal management of air-and liquid-cooled data centers: From chip to the cooling system.' *Applied energy*, 205 pp. 1165-1188.

Khan, A. and Horner, C. (2007) Nanosized metal and metal oxide particles as a biocides in roofing coatings. Google Patents.

Khan, A. R., Abedin, S. and Khan, S. (2022) 'Interaction of temperature and relative humidity for growth of COVID-19 cases and death rates.' *Environmental Research Letters*, 17(3) p. 034048.

Khan, S. A., Jain, M., Pandey, A., Pant, K. K., Ziora, Z. M., Blaskovich, M. A., Shetti, N. P. and Aminabhavi, T. M. (2022) 'Leveraging the potential of silver nanoparticles-based materials towards sustainable water treatment.' *Journal of Environmental Management*, 319 p. 115675.

Kim, H.-S., Lee, J. Y., Ham, S.-Y., Lee, J. H., Park, J.-H. and Park, H.-D. (2019) 'Effect of biofilm inhibitor on biofouling resistance in RO processes.' *Fuel*, 253, 2019/10/01/, pp. 823-832.

Kirthika, S., Goel, G., Matthews, A. and Goel, S. (2022) 'Review of the untapped potentials of antimicrobial materials in the construction sector.' *Progress in Materials Science*, p. 101065.

Kraay, A. N. M., Hayashi, M. A. L., Hernandez-Ceron, N., Spicknall, I. H., Eisenberg, M. C., Meza, R. and Eisenberg, J. N. S. (2018) 'Fomite-mediated transmission as a sufficient pathway: a comparative analysis across three viral pathogens.' *BMC Infectious Diseases*, 18(1), 2018/10/29, p. 540.

Kramer, A. and Assadian, O. (2014) 'Survival of microorganisms on inanimate surfaces.' *Use of biocidal surfaces for reduction of healthcare acquired infections*, pp. 7-26.

Kulinich, S. A. and Farzaneh, M. (2009) 'Effect of contact angle hysteresis on water droplet evaporation from super-hydrophobic surfaces.' *Applied Surface Science*, 255(7), 2009/01/15/, pp. 4056-4060.

Kusiak-Nejman, E. and Morawski, A. W. (2019) 'TiO2/graphene-based nanocomposites for water treatment: A brief overview of charge carrier transfer, antimicrobial and photocatalytic performance.' *Applied Catalysis B: Environmental*, 253 pp. 179-186.

Kwok, D., Gietzelt, T., Grundke, K., Jacobasch, H.-J. and Neumann, A. W. (1997) 'Contact angle measurements and contact angle interpretation. 1. Contact angle measurements by axisymmetric drop shape analysis and a goniometer sessile drop technique.' *Langmuir*, 13(10) pp. 2880-2894.

Laird, K. and Riley, K. (2016) 'Antimicrobial textiles for medical environments.' *In Antimicrobial Textiles*. Elsevier, pp. 249-262.

Lalley, J., Dionysiou, D. D., Varma, R. S., Shankara, S., Yang, D. J. and Nadagouda, M. N. (2014) 'Silver-based antibacterial surfaces for drinking water disinfection—an overview.' *Current Opinion in Chemical Engineering*, 3 pp. 25-29.

Larson, R. G. (2014) 'Transport and deposition patterns in drying sessile droplets.' *AIChE Journal*, 60(5) pp. 1538-1571.

Laxminarayan, R., Sridhar, D., Blaser, M., Wang, M. and Woolhouse, M. (2016) 'Achieving global targets for antimicrobial resistance.' *Science*, 353(6302) pp. 874-875.

Lee, H. U., Lee, S. C., Choi, S., Son, B., Lee, S. M., Kim, H. J. and Lee, J. (2013) 'Efficient visible-light induced photocatalysis on nanoporous nitrogen-doped titanium dioxide catalysts.' *Chemical Engineering Journal*, 228, 2013/07/15/, pp. 756-764.

Lei, H., Li, Y., Xiao, S., Yang, X., Lin, C., Norris, S. L., Wei, D., Hu, Z., et al. (2017) 'Logistic growth of a surface contamination network and its role in disease spread.' *Scientific Reports*, 7(1), 2017/11/01, p. 14826.

Lemire, J. A., Harrison, J. J. and Turner, R. J. (2013) 'Antimicrobial activity of metals: mechanisms, molecular targets and applications.' *Nature Reviews Microbiology*, 11(6), 2013/06/01, pp. 371-384.

Lewis, A. (2009) The hygienic benefits of antimicrobial copper alloy surfaces in healthcare settings. International Copper Association Inc. https://cuverro. com/sites/default ….

Li, B., Luo, Y., Zheng, Y., Liu, X., Tan, L. and Wu, S. (2022) 'Two-dimensional antibacterial materials.' *Progress in Materials Science*, p. 100976.

Li, P. and Wu, J. (2019) 'Drinking water quality and public health.' *Exposure and Health*, 11(2) pp. 73-79.

Li, X.-J., Zhang, J.-z., Tan, X.-m. and Wang, Y. (2022) 'Enhancing forced-convection heat transfer of a channel surface with piezo-fans.' *International Journal of Mechanical Sciences*, 227 p. 107437.

Lima, E., Guerra, R., Lara, V. and Guzmán, A. (2013) 'Gold nanoparticles as efficient antimicrobial agents for Escherichia coli and Salmonella typhi.' *Chemistry Central Journal*, 7(1) pp. 1-7.

Lin, K. and Marr, L. C. (2019) 'Humidity-dependent decay of viruses, but not bacteria, in aerosols and droplets follows disinfection kinetics.' *Environmental Science & Technology*, 54(2) pp. 1024-1032.

Lin, S. X. Q. and Chen, X. D. (2005) 'An effective laboratory air humidity generator for drying research.' *Journal of food engineering*, 68(1) pp. 125-131.

Liu, J., Li, R. S., He, M., Xu, Z., Xu, L. Q., Kang, Y. and Xue, P. (2021) 'Multifunctional SGQDs-CORM@ HA nanosheets for bacterial eradication through cascade-activated “nanoknife” effect and photodynamic/CO gas therapy.' *Biomaterials*, 277 p. 121084.

Liu, L., Liang, X., Wang, X., Kong, S., Zhang, K. and Mi, M. (2021) 'Evaporation of a sessile water droplet during depressurization.' *International Journal of Thermal Sciences*, 159 p. 106587.

Liu, X. and Meehan, P. A. (2014) 'Investigation of the effect of relative humidity on lateral force in rolling contact and curve squeal.' *Wear*, 310(1-2) pp. 12-19.

Liu, X. and Chang, Y.-C. (2020) 'An emergency responding mechanism for cruise epidemic prevention—taking COVID-19 as an example.' *Marine Policy*, 119, 2020/09/01/, p. 104093.

López, J., Chávez, A. M., Rey, A. and Álvarez, P. M. (2021) 'Insights into the stability and activity of MIL-53 (Fe) in solar photocatalytic oxidation processes in water.' *Catalysts*, 11(4) p. 448.

Lu, J., Wang, Y., Jin, M., Yuan, Z., Bond, P. and Guo, J. (2020) 'Both silver ions and silver nanoparticles facilitate the horizontal transfer of plasmid-mediated antibiotic resistance genes.' *Water Research*, 169 p. 115229.

Malhotra, B., Keshwani, A. and Kharkwal, H. (2015) 'Antimicrobial food packaging: Potential and pitfalls.' *Frontiers in microbiology*, 6 p. 611.

Maneerung, T., Tokura, S. and Rujiravanit, R. (2008) 'Impregnation of silver nanoparticles into bacterial cellulose for antimicrobial wound dressing.' *Carbohydrate polymers*, 72(1) pp. 43-51.

Mayr, A., Knobloch, J., Hinterberger, G., Seewald, V., Wille, I., Kaltseis, J., Knobling, B., Klupp, E.-M., et al. (2023) 'Interlaboratory reproducibility of a touch-transfer assay for the assessment of antimicrobial surfaces.' *Journal of Hospital Infection*, 134 pp. 1-6.

McDonald, M., Wesgate, R., Rubiano, M., Holah, J., Denyer, S., Jermann, C. and Maillard, J. (2020) 'Impact of a dry inoculum deposition on the efficacy of copper-based antimicrobial surfaces.' *Journal of Hospital Infection*, 106(3) pp. 465-472.

McKERNAN, L. T., BURGE, H., WALLINGFORD, K. M., HEIN, M. J. and HERRICK, R. (2007) 'Evaluating Fungal Populations by Genera/Species on Wide Body Commercial Passenger Aircraft and in Airport Terminals.' *The Annals of Occupational Hygiene*, 51(3) pp. 281-291.

McKernan, L. T., Wallingford, K. M., Hein, M. J., Burge, H., Rogers, C. A. and Herrick, R. (2008) 'Monitoring microbial populations on wide-body commercial passenger aircraft.' *Annals of Occupational Hygiene*, 52(2) pp. 139-149.

McManus, C. and Kelley, S. (2005) 'Molecular survey of aeroplane bacterial contamination.' *Journal of applied microbiology*, 99(3) pp. 502-508.

Mei, L., Teng, Z., Zhu, G., Liu, Y., Zhang, F., Zhang, J., Li, Y., Guan, Y., et al. (2017) 'Silver nanocluster-embedded zein films as antimicrobial coating materials for food packaging.' *ACS applied materials & interfaces*, 9(40) pp. 35297-35304.

Meinke, R., Meyer, B., Frei, R., Passweg, J. and Widmer, A. F. (2012) 'Equal Efficacy of Glucoprotamin and an Aldehyde Product for Environmental Disinfection in a Hematologic

Transplant Unit: A Prospective Crossover Trial.' *Infection Control & Hospital Epidemiology*, 33(11) 2015/01/02, pp. 1077-1080.

Menderes, K. and Ipekci, A. (2021) 'Optimization of 3D printing process parameters on mechanical behaviors and printing time of ABS, PLA, PET-G products using taguchi method.' *中國機械工程學刊*, 42(4) pp. 393-401.

Meyer, J. C., Geim, A. K., Katsnelson, M. I., Novoselov, K. S., Booth, T. J. and Roth, S. (2007) 'The structure of suspended graphene sheets.' *Nature*, 446(7131) pp. 60-63.

Michael, C. A., Dominey-Howes, D. and Labbate, M. (2014) 'The antimicrobial resistance crisis: causes, consequences, and management.' *Frontiers in public health*, 2 p. 145.

Michels, H., Noyce, J. and Keevil, C. W. (2009) 'Effects of temperature and humidity on the efficacy of methicillin-resistant Staphylococcus aureus challenged antimicrobial materials containing silver and copper.' *Letters in applied microbiology*, 49(2) pp. 191-195.

Mirhoseini, S. H., Nikaeen, M., Khanahmad, H., Hatamzadeh, M. and Hassanzadeh, A. (2015) 'Monitoring of airborne bacteria and aerosols in different wards of hospitals-Particle counting usefulness in investigation of airborne bacteria.' *Annals of Agricultural and Environmental Medicine*, 22(4)

Mitchell, A., Spencer, M. and Edmiston Jr, C. (2015) 'Role of healthcare apparel and other healthcare textiles in the transmission of pathogens: a review of the literature.' *Journal of Hospital Infection*, 90(4) pp. 285-292.

Mitra, D., Kang, E.-T. and Neoh, K. G. (2019) 'Antimicrobial copper-based materials and coatings: potential multifaceted biomedical applications.' *ACS applied materials & interfaces*, 12(19) pp. 21159-21182.

Monteiro, D. R., Gorup, L. F., Takamiya, A. S., Ruvollo-Filho, A. C., de Camargo, E. R. and Barbosa, D. B. (2009) 'The growing importance of materials that prevent microbial adhesion: antimicrobial effect of medical devices containing silver.' *International journal of antimicrobial agents*, 34(2) pp. 103-110.

Morawska, L. (2005) *Droplet fate in indoor environments, or can we prevent the spread of infection?* : Tsinghua University Press.

Møretrø, T., Høiby-Pettersen, G. S., Halvorsen, C. K. and Langsrud, S. (2012) 'Antibacterial activity of cutting boards containing silver.' *Food Control*, 28(1) pp. 118-121.

Møretrø, T., Heir, E., Mo, K., Habimana, O., Abdelgani, A. and Langsrud, S. (2010) 'Factors affecting survival of Shigatoxin-producing Escherichia coli on abiotic surfaces.' *International Journal of Food Microbiology*, 138(1-2) pp. 71-77.

Moruno Algara, M., Kuczyńska-Wiśnik, D., Dębski, J., Stojowska-Swędrzyńska, K., Sominka, H., Bukrejewska, M. and Laskowska, E. (2019) 'Trehalose protects Escherichia coli against carbon stress manifested by protein acetylation and aggregation.' *Molecular Microbiology*, 112(3) pp. 866-880.

Moustafa, H., Youssef, A. M., Darwish, N. A. and Abou-Kandil, A. I. (2019) 'Eco-friendly polymer composites for green packaging: Future vision and challenges.' *Composites Part B: Engineering*, 172 pp. 16-25.

Mozes, N. and Rouxhet, P. (1987) 'Methods for measuring hydrophobicity of microorganisms.' *Journal of Microbiological Methods*, 6(2) pp. 99-112.

Mu, B., Ying, X., Petropoulos, E. and He, S. (2021) 'Preparation of AgCl/ZnO nano-composite for effective antimicrobial protection of stone-made building elements.' *Materials Letters*, 285 p. 129143.

Munekata, T., Suzuki, T., Yamakawa, S. and Asahi, R. (2013) 'Effects of viscosity, surface tension, and evaporation rate of solvent on dry colloidal structures: A lattice Boltzmann study.' *Physical Review E*, 88(5) p. 052314.

Murphy, N., Boland, M., Bambury, N., Fitzgerald, M., Comerford, L., Dever, N., O'Sullivan, M. B., Petty-Saphon, N., et al. (2020) 'A large national outbreak of COVID-19 linked to air travel, Ireland, summer 2020.' *Eurosurveillance*, 25(42) p. 2001624.

Nakajima, A. (2011) 'Design of hydrophobic surfaces for liquid droplet control.' *NPG Asia Materials*, 3(5), 2011/05/01, pp. 49-56.

Neely, A. N. (2000) 'A Survey of Gram-Negative Bacteria Survival on Hospital Fabrics and Plastics.' *The Journal of Burn Care & Rehabilitation*, 21(6) pp. 523-527.

Netuschil, L., Auschill, T. M., Sculean, A. and Arweiler, N. B. (2014) 'Confusion over live/dead stainings for the detection of vital microorganisms in oral biofilms - which stain is suitable?' *BMC Oral Health*, 14(1), 2014/01/11, p. 2.

Nguyen, T. A., Nguyen, A. V., Hampton, M. A., Xu, Z. P., Huang, L. and Rudolph, V. (2012) 'Theoretical and experimental analysis of droplet evaporation on solid surfaces.' *Chemical engineering science*, 69(1) pp. 522-529.

Noyce, J. O., Michels, H. and Keevil, C. W. (2006) 'Potential use of copper surfaces to reduce survival of epidemic meticillin-resistant Staphylococcus aureus in the healthcare environment.' *Journal of Hospital Infection*, 63(3), 2006/07/01/, pp. 289-297.

Noyce, J. O., Michels, H. and Keevil, C. W. (2007) 'Inactivation of Influenza A Virus on Copper versus Stainless Steel Surfaces.' *Applied and Environmental Microbiology*, 73(8) pp. 2748-2750.

Obianyo, J. I. (2019) 'Effect of salinity on evaporation and the water cycle.' *Emerging Science Journal*, 3(4) pp. 255-262.

Oelofse, S. H. and Nahman, A. (2013) 'Estimating the magnitude of food waste generated in South Africa.' *Waste Management & Research*, 31(1) pp. 80-86.

Ojeil, M., Jermann, C., Holah, J., Denyer, S. P. and Maillard, J. Y. (2013) 'Evaluation of new in vitro efficacy test for antimicrobial surface activity reflecting UK hospital conditions.' *Journal of Hospital Infection*, 85(4), 2013/12/01/, pp. 274-281.

Olaimat, A. N. and Holley, R. A. (2012) 'Factors influencing the microbial safety of fresh produce: a review.' *Food microbiology*, 32(1) pp. 1-19.

Oosterhof, J. J. H., Buijssen, K. J. D. A., Busscher, H. J., Laan, B. F. A. M. v. d. and Mei, H. C. v. d. (2006) 'Effects of Quaternary Ammonium Silane Coatings on Mixed Fungal and Bacterial Biofilms on Tracheoesophageal Shunt Prostheses.' *Applied and Environmental Microbiology*, 72(5) pp. 3673-3677.

Organisation, I. S. (2020) ISO 22551: Fine ceramics (advanced ceramics, advanced technical ceramics). Determination of bacterial reduction rate by semiconducting photocatalytic materials under indoor lighting environment. Semi-dry method for estimating antibacterial activity on the actual environmental bacteria contamination surface.

organisation, W. h. (2022) *Cholera*. [Online] [Accessed on 02/03/2023] https://www.who.int/news-room/fact-sheets/detail/cholera

Ormandy, D. and Ezratty, V. (2012) 'Health and thermal comfort: From WHO guidance to housing strategies.' *Energy Policy*, 49 pp. 116-121.

Oswin, H. P., Haddrell, A. E., Otero-Fernandez, M., Mann, J. F., Cogan, T. A., Hilditch, T. G., Tian, J., Hardy, D. A., et al. (2022) 'The dynamics of SARS-CoV-2 infectivity with changes in aerosol microenvironment.' *Proceedings of the National Academy of Sciences*, 119(27) p. e2200109119.

Özkan, İ., Duru Baykal, P. and Gülnaz, O. (2019) 'Investigation of antibacterial and antifungal properties of tufting carpets containing metal composite yarns.' *The Journal of The Textile Institute*, 110(5), 2019/05/04, pp. 756-763.

Page, K., Wilson, M. and Parkin, I. P. (2009) 'Antimicrobial surfaces and their potential in reducing the role of the inanimate environment in the incidence of hospital-acquired infections.' *Journal of materials chemistry*, 19(23) pp. 3819-3831.

Pandit, S., Gaska, K., Kádár, R. and Mijakovic, I. (2021) 'Graphene-based antimicrobial biomedical surfaces.' *ChemPhysChem*, 22(3) pp. 250-263.

Paolucci, V., De Santis, J., Ricci, V., Lozzi, L., Giorgi, G. and Cantalini, C. (2022) 'Bidimensional Engineered Amorphous a-SnO2 Interfaces: Synthesis and Gas Sensing Response to H2S and Humidity.' *ACS sensors*, 7(7) pp. 2058-2068.

Parandhaman, T., Das, A., Ramalingam, B., Samanta, D., Sastry, T., Mandal, A. B. and Das, S. K. (2015) 'Antimicrobial behavior of biosynthesized silica–silver nanocomposite for water disinfection: A mechanistic perspective.' *Journal of Hazardous Materials*, 290 pp. 117-126.

Park, G. W., Cho, M., Cates, E. L., Lee, D., Oh, B.-T., Vinjé, J. and Kim, J.-H. (2014) 'Fluorinated TiO2 as an ambient light-activated virucidal surface coating material for the control of human norovirus.' *Journal of Photochemistry and Photobiology B: Biology*, 140, 2014/11/01/, pp. 315-320.

Patel, M. (2020) 'Antimicrobial paper embedded with nanoparticles as spread-breaker for corona virus.' *J. Environ. Life Sci*, 6 pp. 001-012.

Petousis, M., Vidakis, N., Velidakis, E., Kechagias, J. D., David, C. N., Papadakis, S. and Mountakis, N. (2022) 'Affordable Biocidal Ultraviolet Cured Cuprous Oxide Filled Vat Photopolymerization Resin Nanocomposites with Enhanced Mechanical Properties.' *Biomimetics*, 7(1) p. 12.

Pommepuy, M., Butin, M., Derrien, A., Gourmelon, M., Colwell, R. and Cormier, M. (1996) 'Retention of enteropathogenicity by viable but nonculturable Escherichia coli exposed to seawater and sunlight.' *Applied and Environmental Microbiology*, 62(12) pp. 4621-4626.

Popa, G. L. and Papa, M. I. (2021) 'Salmonella spp. infection-a continuous threat worldwide.' *Germs*, 11(1) p. 88.

Pulingam, T., Thong, K. L., Ali, M. E., Appaturi, J. N., Dinshaw, I. J., Ong, Z. Y. and Leo, B. F. (2019) 'Graphene oxide exhibits differential mechanistic action towards Gram-positive and Gram-negative bacteria.' *Colloids and Surfaces B: Biointerfaces*, 181 pp. 6-15.

Qian, P.-Y., Cheng, A., Wang, R. and Zhang, R. (2022) 'Marine biofilms: diversity, interactions and biofouling.' *Nature Reviews Microbiology*, 20(11) pp. 671-684.

Qiu, H., Feng, K., Gapeeva, A., Meurisch, K., Kaps, S., Li, X., Yu, L., Mishra, Y. K., et al. (2022) 'Functional polymer materials for modern marine biofouling control.' *Progress in Polymer Science*, p. 101516.

Quraishi, S. A., Berra, L. and Nozari, A. (2020) 'Indoor temperature and relative humidity in hospitals: Workplace considerations during the novel coronavirus pandemic.' *Occupational and Environmental Medicine*, 77(7) pp. 508-508.

Rai, M., Yadav, A. and Gade, A. (2009) 'Silver nanoparticles as a new generation of antimicrobials.' *Biotechnology Advances*, 27(1), 2009/01/01/, pp. 76-83.

Ramamurthy, T., Ghosh, A., Pazhani, G. P. and Shinoda, S. (2014) 'Current perspectives on viable but non-culturable (VBNC) pathogenic bacteria.' *Frontiers in public health*, 2 p. 103.

Ramos, T., Dedesko, S., Siegel, J. A., Gilbert, J. A. and Stephens, B. (2015) 'Spatial and temporal variations in indoor environmental conditions, human occupancy, and operational characteristics in a new hospital building.' *PLoS One*, 10(3) p. e0118207.

Ranjbaran, M. and Datta, A. K. (2019) 'Retention and infiltration of bacteria on a plant leaf driven by surface water evaporation.' *Physics of Fluids*, 31(11)

Ranjbaran, M. and Datta, A. K. (2020) 'A mechanistic model for bacterial retention and infiltration on a leaf surface during a sessile droplet evaporation.' *Langmuir*, 36(41) pp. 12130-12142.

Rasheed, A., Hegde, O., Chatterjee, R., Sampathirao, S. R., Chakravortty, D. and Basu, S. (2023) 'Physics of self-assembly and morpho-topological changes of Klebsiella pneumoniae in desiccating sessile droplets.' *Journal of Colloid and Interface Science*, 629 pp. 620-631.

Razavipour, M., Gonzalez, M., Singh, N., Cimenci, C. E., Chu, N., Alarcon, E. I., Villafuerte, J. and Jodoin, B. (2022) 'Biofilm Inhibition and Antiviral Response of Cold Sprayed and Shot Peened Copper Surfaces: Effect of Surface Morphology and Microstructure.' *Journal of Thermal Spray Technology*, 31(1-2) pp. 130-144.

Redfern, J. and Verran, J. (2017) 'Effect of humidity and temperature on the survival of Listeria monocytogenes on surfaces.' *Letters in Applied Microbiology*, 64(4) pp. 276-282.

Redfern, J., Tucker, J., Simmons, L. M., Askew, P., Stephan, I. and Verran, J. (2018) 'Environmental and experimental factors affecting efficacy testing of nonporous plastic antimicrobial surfaces.' *Methods and Protocols*, 1(4) p. 36.

Reid, M., Whatley, V., Spooner, E., Nevill, A. M., Cooper, M., Ramsden, J. J. and Dancer, S. J. (2018) 'How does a photocatalytic antimicrobial coating affect environmental bioburden in hospitals?' *infection control & hospital epidemiology*, 39(4) pp. 398-404.

Ren, S.-Y., Wang, W.-B., Hao, Y.-G., Zhang, H.-R., Wang, Z.-C., Chen, Y.-L. and Gao, R.-D. (2020) 'Stability and infectivity of coronaviruses in inanimate environments.' *World journal of clinical cases*, 8(8) p. 1391.

Richard, E., Dubois, T., Allion-Maurer, A., Jha, P. K. and Faille, C. (2020) 'Hydrophobicity of abiotic surfaces governs droplets deposition and evaporation patterns.' *Food Microbiology*, 91, 2020/10/01/, p. 103538.

Robey, A. J. and Fierce, L. (2022) 'Sensitivity of airborne transmission of enveloped viruses to seasonal variation in indoor relative humidity.' *International Communications in Heat and Mass Transfer*, 130 p. 105747.

Romero-Vargas Castrillón, S., Perreault, F. o., De Faria, A. F. and Elimelech, M. (2015) 'Interaction of graphene oxide with bacterial cell membranes: insights from force spectroscopy.' *Environmental Science & Technology Letters*, 2(4) pp. 112-117.

Ronan, E., Yeung, C. W., Hausner, M. and Wolfaardt, G. M. (2013) 'Interspecies interaction extends bacterial survival at solid–air interfaces.' *Biofouling*, 29(9), 2013/10/01, pp. 1087-1096.

Salazar, H., Martins, P. M., Santos, B., Fernandes, M. M., Reizabal, A., Sebastián, V., Botelho, G., Tavares, C. J., et al. (2020) 'Photocatalytic and antimicrobial multifunctional nanocomposite membranes for emerging pollutants water treatment applications.' *Chemosphere*, 250, 2020/07/01/, p. 126299.

Salwiczek, M., Qu, Y., Gardiner, J., Strugnell, R. A., Lithgow, T., McLean, K. M. and Thissen, H. (2014) 'Emerging rules for effective antimicrobial coatings.' *Trends in Biotechnology*, 32(2), 2014/02/01/, pp. 82-90.

Sarica, S., Asan, A., Otkun, M. T. and Ture, M. (2002) 'Monitoring indoor airborne fungi and bacteria in the different areas of Trakya University Hospital, Edirne, Turkey.' *Indoor and built Environment*, 11(5) pp. 285-292.

Schachter, B. (2003) 'Slimy business—the biotechnology of biofilms.' *Nature Biotechnology*, 21(4), 2003/04/01, pp. 361-365.

Schmidt, M. G., von Dessauer, B., Benavente, C., Benadof, D., Cifuentes, P., Elgueta, A., Duran, C. and Navarrete, M. S. (2016) 'Copper surfaces are associated with significantly lower concentrations of bacteria on selected surfaces within a pediatric intensive care unit.' *American journal of infection control*, 44(2) pp. 203-209.

Schreiber, P. W., Sax, H., Wolfensberger, A., Clack, L. and Kuster, S. P. (2018) 'The preventable proportion of healthcare-associated infections 2005–2016: systematic review and meta-analysis.' *Infection Control & Hospital Epidemiology*, 39(11) pp. 1277-1295.

Schweizer, M., Graham, M., Ohl, M., Heilmann, K., Boyken, L. and Diekema, D. (2012) 'Novel hospital curtains with antimicrobial properties: a randomized, controlled trial.' *Infection Control & Hospital Epidemiology*, 33(11) pp. 1081-1085.

Scott, R. D. (2009) 'The direct medical costs of healthcare-associated infections in US hospitals and the benefits of prevention.'

Seberini, A. (2020) *Economic, social and environmental world impacts of food waste on society and Zero waste as a global approach to their elimination.* Vol. 74: EDP Sciences.

Serra-Burriel, M., Keys, M., Campillo-Artero, C., Agodi, A., Barchitta, M., Gikas, A., Palos, C. and Lopez-Casasnovas, G. (2020) 'Impact of multi-drug resistant bacteria on economic and clinical

outcomes of healthcare-associated infections in adults: Systematic review and meta-analysis.' *PloS one*, 15(1) p. e0227139.

Shahrubudin, N., Lee, T. C. and Ramlan, R. (2019) 'An overview on 3D printing technology: Technological, materials, and applications.' *Procedia Manufacturing*, 35 pp. 1286-1296.

Shaikh, S., Nazam, N., Rizvi, S. M. D., Ahmad, K., Baig, M. H., Lee, E. J. and Choi, I. (2019) 'Mechanistic insights into the antimicrobial actions of metallic nanoparticles and their implications for multidrug resistance.' *International journal of molecular sciences*, 20(10) p. 2468.

Sharma, T. K., Sapra, M., Chopra, A., Sharma, R., Patil, S. D., Malik, R. K., Pathania, R. and Navani, N. K. (2012) 'Interaction of bacteriocin-capped silver nanoparticles with food pathogens and their antibacterial effect.' *International Journal of Green Nanotechnology*, 4(2) pp. 93-110.

Shukla, A., Fleming, K. E., Chuang, H. F., Chau, T. M., Loose, C. R., Stephanopoulos, G. N. and Hammond, P. T. (2010) 'Controlling the release of peptide antimicrobial agents from surfaces.' *Biomaterials*, 31(8), 2010/03/01/, pp. 2348-2357.

Sichel, C., Tello, J., de Cara, M. and Fernández-Ibáñez, P. (2007) 'Effect of UV solar intensity and dose on the photocatalytic disinfection of bacteria and fungi.' *Catalysis Today*, 129(1), 2007/11/15/, pp. 152-160.

SimScale. (2023) *SimScale*. [Online] [Accessed https://www.simscale.com/

Sinclair, R. G. and Gerba, C. P. (2011) 'Microbial contamination in kitchens and bathrooms of rural Cambodian village households.' *Letters in Applied Microbiology*, 52(2) pp. 144-149.

Singh, S., Singh, G., Prakash, C. and Ramakrishna, S. (2020) 'Current status and future directions of fused filament fabrication.' *Journal of Manufacturing Processes*, 55 pp. 288-306.

Sjollema, J., Keul, H., van der Mei, H., Dijkstra, R., Rustema-Abbing, M., de Vries, J., Loontjens, T., Dirks, T., et al. (2017) 'A Trifunctional, Modular Biomaterial Coating: Nonadhesive to Bacteria, Chlorhexidine-Releasing and Tissue-Integrating.' *Macromolecular Bioscience*, 17(4) p. 1600336.

Sjollema, J., Zaat, S. A. J., Fontaine, V., Ramstedt, M., Luginbuehl, R., Thevissen, K., Li, J., van der Mei, H. C., et al. (2018) 'In vitro methods for the evaluation of antimicrobial surface designs.' *Acta Biomaterialia*, 70, 2018/04/01/, pp. 12-24.

Soboleva, O. and Summ, B. (2003) 'The kinetics of dewetting of hydrophobic surfaces during the evaporation of surfactant solution drops.' *Colloid Journal*, 65(1) pp. 89-93.

Sondi, I. and Salopek-Sondi, B. (2004) 'Silver nanoparticles as antimicrobial agent: a case study on E. coli as a model for Gram-negative bacteria.' *Journal of Colloid and Interface Science*, 275(1), 2004/07/01/, pp. 177-182.

Soulié, V., Karpitschka, S., Lequien, F., Prené, P., Zemb, T., Moehwald, H. and Riegler, H. (2015) 'The evaporation behavior of sessile droplets from aqueous saline solutions.' *Physical Chemistry Chemical Physics*, 17(34) pp. 22296-22303.

Standards, J. I. (2012) Measurement of Antibacterial Activity on Plastics Surfaces (Plastics).

Stephens, B., Azimi, P., Thoemmes, M. S., Heidarinejad, M., Allen, J. G. and Gilbert, J. A. (2019) 'Microbial exchange via fomites and implications for human health.' *Current Pollution Reports*, 5(4) pp. 198-213.

Sun, H., Chan, C.-W., Wang, Y., Yao, X., Mu, X., Lu, X., Zhou, J., Cai, Z., et al. (2019) 'Reliable and reusable whole polypropylene plastic microfluidic devices for a rapid, low-cost antimicrobial susceptibility test.' *Lab on a Chip*, 19(17) pp. 2915-2924.

Sun, Q., Cai, X., Li, J., Zheng, M., Chen, Z. and Yu, C.-P. (2014) 'Green synthesis of silver nanoparticles using tea leaf extract and evaluation of their stability and antibacterial activity.' *Colloids and surfaces A: Physicochemical and Engineering aspects*, 444 pp. 226-231.

Suwantarat, N., Supple, L. A., Cadnum, J. L., Sankar, T. and Donskey, C. J. (2017) 'Quantitative assessment of interactions between hospitalized patients and portable medical equipment and other fomites.' *American Journal of Infection Control*, 45(11), 2017/11/01/, pp. 1276-1278.

Szczesny, G., Leszczynski, P., Sokol-Leszczynska, B. and Maldyk, P. (2022) 'Identification of human-dependent routes of pathogen's transmission in a tertiary care hospital.' *Joint Diseases and Related Surgery*, 33(2) p. 330.

Sze-To, G. N., Yang, Y., Kwan, J. K., Yu, S. C. and Chao, C. Y. (2014) 'Effects of surface material, ventilation, and human behavior on indirect contact transmission risk of respiratory infection.' *Risk analysis*, 34(5) pp. 818-830.

Talapko, J., Juzbašić, M., Matijević, T., Pustijanac, E., Bekić, S., Kotris, I. and Škrlec, I. (2021) 'Candida albicans—the virulence factors and clinical manifestations of infection.' *Journal of Fungi*, 7(2) p. 79.

Tang, J. W. (2009) 'The effect of environmental parameters on the survival of airborne infectious agents.' *Journal of the Royal Society Interface*, 6(suppl_6) pp. S737-S746.

Tang, J. W., Li, Y., Eames, I., Chan, P. K. S. and Ridgway, G. L. (2006) 'Factors involved in the aerosol transmission of infection and control of ventilation in healthcare premises.' *Journal of Hospital Infection*, 64(2), 2006/10/01/, pp. 100-114.

Tapia, H. and Koshland, D. E. (2014) 'Trehalose is a versatile and long-lived chaperone for desiccation tolerance.' *Current Biology*, 24(23) pp. 2758-2766.

Taylor, H. (2022) *Application of Silver Nanoparticles in Orthodontic Bonding Agent and Their Long-Term Release into Artificial Saliva.* State University of New York at Stony Brook.

Teixeira-Santos, R., Gomes, M., Gomes, L. C. and Mergulhao, F. J. (2021) 'Antimicrobial and anti-adhesive properties of carbon nanotube-based surfaces for medical applications: A systematic review.' *Iscience*, 24(1) p. 102001.

Terlizzi, A., Conte, E., Zupo, V. and Mazzella, L. (2000) 'Biological succession on silicone fouling-release surfaces: Long-term exposure tests in the harbour of ischia, Italy.' *Biofouling*, 15(4), 2000/09/01, pp. 327-342.

Thakur, D. and Ganguly, R. (2022) 'Biocides.' *In Environmental Micropollutants*. Elsevier, pp. 81-90.

Thomas Wu, W. Y., Qinde Liu, Richard Shin, Tang Teo (2022) *Test liquid preparation and artificial saliva composition analysis for droplet size measurement* Researchgate.

Thornley, C. N., Emslie, N. A., Sprott, T. W., Greening, G. E. and Rapana, J. P. (2011) 'Recurring Norovirus Transmission on an Airplane.' *Clinical Infectious Diseases*, 53(6) pp. 515-520.

Tiller, J. C., Liao, C.-J., Lewis, K. and Klibanov, A. M. (2001) 'Designing surfaces that kill bacteria on contact.' *Proceedings of the National Academy of Sciences*, 98(11) pp. 5981-5985.

Toğrul, H. and Arslan, N. (2006) 'Moisture sorption behaviour and thermodynamic characteristics of rice stored in a chamber under controlled humidity.' *Biosystems Engineering*, 95(2) pp. 181-195.

Tümer, E. H. and Erbil, H. Y. (2021) 'Extrusion-based 3d printing applications of pla composites: A review.' *Coatings*, 11(4) p. 390.

UK, H. a. S. A. (2022a) *The GB Article 95 List*. [Online] [Accessed on 02/03/2023] https://www.hse.gov.uk/biocides/uk-article-95-list.htm

UK, H. a. S. A. (2022b) *Treated articles*. [Online] [Accessed on 02/03/2023] https://www.hse.gov.uk/biocides/treated-articles.htm

Vaglenov, K. (2014) *Survival and transmission of selected pathogens on airplane cabin surfaces and selection of phages specific for Campylobacter jejuni.*

Vaishampayan, A., de Jong, A., Wight, D. J., Kok, J. and Grohmann, E. (2018) 'A Novel Antimicrobial Coating Represses Biofilm and Virulence-Related Genes in Methicillin-Resistant Staphylococcus aureus.' *Frontiers in Microbiology*, 9, 2018-February-15,

van de Lagemaat, M., Grotenhuis, A., van de Belt-Gritter, B., Roest, S., Loontjens, T. J. A., Busscher, H. J., van der Mei, H. C. and Ren, Y. (2017) 'Comparison of methods to evaluate bacterial contact-killing materials.' *Acta Biomaterialia*, 59, 2017/09/01/, pp. 139-147.

Van Doremalen, N., Bushmaker, T., Morris, D. H., Holbrook, M. G., Gamble, A., Williamson, B. N., Tamin, A., Harcourt, J. L., et al. (2020) 'Aerosol and surface stability of SARS-CoV-2 as compared with SARS-CoV-1.' *New England journal of medicine*, 382(16) pp. 1564-1567.

Van Wijngaarden, W. A. and Vincent, L. A. (2004) 'Trends in relative humidity in Canada from 1953–2003.' *Bull. Am. Meteorol. Soc*, pp. 4633-4636.

Venkatasubbu, G. D., Baskar, R., Anusuya, T., Seshan, C. A. and Chelliah, R. (2016) 'Toxicity mechanism of titanium dioxide and zinc oxide nanoparticles against food pathogens.' *Colloids and Surfaces B: Biointerfaces*, 148 pp. 600-606.

Vincent, M., Duval, R. E., Hartemann, P. and Engels-Deutsch, M. (2018) 'Contact killing and antimicrobial properties of copper.' *Journal of Applied Microbiology*, 124(5) pp. 1032-1046.

Wainwright, C. E., France, M. W., O'Rourke, P., Anuj, S., Kidd, T. J., Nissen, M. D., Sloots, T. P., Coulter, C., et al. (2009) 'Cough-generated aerosols of Pseudomonas aeruginosa and other Gram-negative bacteria from patients with cystic fibrosis.' *Thorax*, 64(11) pp. 926-931.

Waltimo, T., Brunner, T., Vollenweider, M., Stark, W. J. and Zehnder, M. (2007) 'Antimicrobial effect of nanometric bioactive glass 45S5.' *Journal of dental research*, 86(8) pp. 754-757.

Wang, J. and Norbäck, D. (2022) 'Subjective indoor air quality and thermal comfort among adults in relation to inspected and measured indoor environment factors in single-family houses in Sweden-the BETSI study.' *Science of The Total Environment*, 802 p. 149804.

Wang, J., Wei, Y., Shi, X. and Gao, H. (2013) 'Cellular entry of graphene nanosheets: the role of thickness, oxidation and surface adsorption.' *Rsc Advances*, 3(36) pp. 15776-15782.

Wang, Y., Li, Z., Wang, J., Wang, J., Li, X. and Kuang, C. (2022) 'Superhydrophobic coating constructed from rosin acid and TiO2 used as blood repellent dressing.' *Materials & Design*, 222 p. 111072.

Warnes, S. L. and Keevil, C. W. (2011) 'Mechanism of Copper Surface Toxicity in Vancomycin-Resistant Enterococci following Wet or Dry Surface Contact.' *Applied and Environmental Microbiology*, 77(17) pp. 6049-6059.

Warnes, S. L., Summersgill, E. N. and Keevil, C. W. (2015) 'Inactivation of Murine Norovirus on a Range of Copper Alloy Surfaces Is Accompanied by Loss of Capsid Integrity.' *Applied and Environmental Microbiology*, 81(3) pp. 1085-1091.

Weber, K. L., LeSassier, D. S., Kappell, A. D., Schulte, K. Q., Westfall, N., Albright, N. C., Godbold, G. D., Palsikar, V., et al. (2020) 'Simulating transmission of ESKAPE pathogens plus C. difficile in relevant clinical scenarios.' *BMC Infectious Diseases*, 20(1), 2020/06/12, p. 411.

Wei, T., Yu, Q. and Chen, H. (2019) 'Responsive and synergistic antibacterial coatings: fighting against bacteria in a smart and effective way.' *Advanced healthcare materials*, 8(3) p. 1801381.

Weon, B. M. and Je, J. H. (2010) 'Capillary force repels coffee-ring effect.' *Physical Review E*, 82(1) p. 015305.

Werapun, U. and Pechwang, J. (2019) *Synthesis and antimicrobial activity of Fe: TiO2 particles.* Vol. 56: Trans Tech Publ.

Wexler, A. and Hasegawa, S. (1954) 'Relative humidity-temperature relationships of some saturated salt solutions in the temperature.' *Journal of research of the National Bureau of standrds*, 53(1) pp. 19-26.

Wiegand, C., Völpel, A., Ewald, A., Remesch, M., Kuever, J., Bauer, J., Griesheim, S., Hauser, C., et al. (2018) 'Critical physiological factors influencing the outcome of antimicrobial testing according to ISO 22196/JIS Z 2801.' *Plos one*, 13(3) p. e0194339.

Winfield, M. D. and Groisman, E. A. (2003) 'Role of nonhost environments in the lifestyles of Salmonella and Escherichia coli.' *Applied and environmental microbiology*, 69(7) pp. 3687-3694.

Wolkoff, P., Azuma, K. and Carrer, P. (2021) 'Health, work performance, and risk of infection in office-like environments: The role of indoor temperature, air humidity, and ventilation.' *International Journal of Hygiene and Environmental Health*, 233 p. 113709.

Wong, K. Y., Haslinda, M. K., Nazri, K. and Alia, S. N. (2019) 'Effects of surgical staff turning motion on airflow distribution inside a hospital operating room.'

Wu, M., Wang, T., Wu, K. and Kan, L. (2020) 'Microbiologically induced corrosion of concrete in sewer structures: A review of the mechanisms and phenomena.' *Construction and Building Materials*, 239 p. 117813.

Wu, P. and Grainger, D. W. (2006) 'Drug/device combinations for local drug therapies and infection prophylaxis.' *Biomaterials*, 27(11), 2006/04/01/, pp. 2450-2467.

Xiao, S., Jones, R. M., Zhao, P. and Li, Y. (2019) 'The dynamic fomite transmission of Methicillin-resistant Staphylococcus aureus in hospitals and the possible improved intervention methods.' *Building and Environment*, 161 p. 106246.

Xiong, R., Liu, P., Zhang, Y., Nan, Y., Chen, J., Chen, X., Ma, S., Lin, G., et al. (2021) 'Analysis of Pollution and Blockage of Titanium Rod Sintered Microporous Filter Element.' *Open Journal of Applied Sciences*, 11(5) pp. 614-622.

Yan, X., He, B., Liu, L., Qu, G., Shi, J., Hu, L. and Jiang, G. (2018) 'Antibacterial mechanism of silver nanoparticles in Pseudomonas aeruginosa: proteomics approach†.' *Metallomics*, 10(4) pp. 557-564.

Yang, W., Elankumaran, S. and Marr, L. C. (2011) 'Concentrations and size distributions of airborne influenza A viruses measured indoors at a health centre, a day-care centre and on aeroplanes.' *Journal of The Royal Society Interface*, 8(61) pp. 1176-1184.

Yang, X., Li, C. Y. and Sun, Y. (2014) 'From multi-ring to spider web and radial spoke: competition between the receding contact line and particle deposition in a drying colloidal drop.' *Soft Matter*, 10(25) pp. 4458-4463.

Yang, X., Ou, C., Yang, H., Liu, L., Song, T., Kang, M., Lin, H. and Hang, J. (2020) 'Transmission of pathogen-laden expiratory droplets in a coach bus.' *Journal of hazardous materials*, 397 p. 122609.

Yao, S., Hao, L., Zhou, R., Jin, Y., Huang, J. and Wu, C. (2022) 'Multispecies biofilms in fermentation: Biofilm formation, microbial interactions, and communication.' *Comprehensive Reviews in Food Science and Food Safety*, 21(4) pp. 3346-3375.

Yaragalla, S., Bhavitha, K. B. and Athanassiou, A. (2021) 'A review on graphene based materials and their antimicrobial properties.' *Coatings*, 11(10) p. 1197.

Yebra, D. M., Kiil, S. and Dam-Johansen, K. (2004) 'Antifouling technology—past, present and future steps towards efficient and environmentally friendly antifouling coatings.' *Progress in Organic Coatings*, 50(2), 2004/07/01/, pp. 75-104.

Yebra, D. M., Kiil, S., Dam-Johansen, K. and Weinell, C. (2005) 'Reaction rate estimation of controlled-release antifouling paint binders: Rosin-based systems.' *Progress in Organic Coatings*, 53(4), 2005/08/01/, pp. 256-275.

Younis, A. B., Haddad, Y., Kosaristanova, L. and Smerkova, K. (2022) 'Titanium dioxide nanoparticles: Recent progress in antimicrobial applications.' *Wiley Interdisciplinary Reviews: Nanomedicine and Nanobiotechnology*, p. e1860.

Yuan, F., Yao, R., Sadrizadeh, S., Li, B., Cao, G., Zhang, S., Zhou, S., Liu, H., et al. (2022) 'Thermal comfort in hospital buildings–A literature review.' *Journal of Building Engineering*, 45 p. 103463.

Yunker, P. J., Still, T., Lohr, M. A. and Yodh, A. (2011) 'Suppression of the coffee-ring effect by shape-dependent capillary interactions.' *nature*, 476(7360) pp. 308-311.

Zang, D., Tarafdar, S., Tarasevich, Y. Y., Choudhury, M. D. and Dutta, T. (2019) 'Evaporation of a Droplet: From physics to applications.' *Physics Reports*, 804 pp. 1-56.

Zhang, N., Chen, W., Chan, P. T., Yen, H. L., Tang, J. W. T. and Li, Y. (2020) 'Close contact behavior in indoor environment and transmission of respiratory infection.' *Indoor air*, 30(4) pp. 645-661.

Zhang, S., Wang, L., Liang, X., Vorstius, J., Keatch, R., Corner, G., Nabi, G., Davidson, F., et al. (2019) 'Enhanced antibacterial and antiadhesive activities of silver-PTFE nanocomposite coating for urinary catheters.' *ACS Biomaterials Science & Engineering*, 5(6) pp. 2804-2814.

Zhang, W., Wahlgren, M. and Sivik, B. (1989) 'Membrane characterization by the contact angle technique: II. Characterization of UF-membranes and comparison between the captive bubble and sessile drop as methods to obtain water contact angles.' *Desalination*, 72(3) pp. 263-273.

Zhao, B., Dewald, C., Hennig, M., Bossert, J., Bauer, M., Pletz, M. W. and Jandt, K. D. (2019) 'Microorganisms@ materials surfaces in aircraft: Potential risks for public health?–A systematic review.' *Travel medicine and infectious disease*, 28 pp. 6-14.

Zhao, T. and Jiang, L. (2018) 'Contact angle measurement of natural materials.' *Colloids and Surfaces B: Biointerfaces*, 161 pp. 324-330.

Zhao, Y., Feng, Y. and Ma, L. (2022) 'Impacts of human movement and ventilation mode on the indoor environment, droplet evaporation, and aerosol transmission risk at airport terminals.' *Building and Environment*, 224 p. 109527.

Zheng, H., Ji, Z., Roy, K. R., Gao, M., Pan, Y., Cai, X., Wang, L., Li, W., et al. (2019) 'Engineered Graphene Oxide Nanocomposite Capable of Preventing the Evolution of Antimicrobial Resistance.' *ACS Nano*, 13(10), 2019/10/22, pp. 11488-11499.

Zhou, Z., Xu, L., Zhu, L., Liu, Y., Shuai, X., Lin, Z. and Chen, H. (2021) 'Metagenomic analysis of microbiota and antibiotic resistome in household activated carbon drinking water purifiers.' *Environment International*, 148 p. 106394.

Zhou, Z., Li, B., Liu, X., Li, Z., Zhu, S., Liang, Y., Cui, Z. and Wu, S. (2021) 'Recent progress in photocatalytic antibacterial.' *ACS Applied Bio Materials*, 4(5) pp. 3909-3936.

Zhu, C., Gao, Y., Li, H., Meng, S., Li, L., Francisco, J. S. and Zeng, X. C. (2016) 'Characterizing hydrophobicity of amino acid side chains in a protein environment via measuring contact angle of a water nanodroplet on planar peptide network.' *Proceedings of the National Academy of Sciences*, 113(46) pp. 12946-12951.

Ziem, B., Azab, W., Gholami, M., Rabe, J. P., Osterrieder, N. and Haag, R. (2017) 'Size-dependent inhibition of herpesvirus cellular entry by polyvalent nanoarchitectures.' *Nanoscale*, 9(11) pp. 3774-3783.

Zimlichman, E., Henderson, D., Tamir, O., Franz, C., Song, P., Yamin, C. K., Keohane, C., Denham, C. R., et al. (2013) 'Health care–associated infections: a meta-analysis of costs and financial impact on the US health care system.' *JAMA internal medicine*, 173(22) pp. 2039-2046.

Zoz, F., Iaconelli, C., Lang, E., Iddir, H., Guyot, S., Grandvalet, C., Gervais, P. and Beney, L. (2016) 'Control of relative air humidity as a potential means to improve hygiene on surfaces: a preliminary approach with Listeria monocytogenes.' *PLoS One*, 11(2) p. e0148418.

Appendix A

antibiotics

MDPI

Review

How Do We Determine the Efficacy of an Antibacterial Surface? A Review of Standardised Antibacterial Material Testing Methods

Alexander J. Cunliffe [1], Peter D. Askew [2], Ina Stephan [3], Gillian Iredale [2], Patrick Cosemans [4], Lisa M. Simmons [5], Joanna Verran [6] and James Redfern [1,*]

[1] Department of Natural Sciences, Faculty of Science and Engineering, Manchester Metropolitan University, Chester Street, Manchester M1 5GD, UK; Alexander.J.Cunliffe@stu.mmu.ac.uk
[2] (Industrial Microbiological Services Ltd.) IMSL, Pale Lane, Hartley Whitney, Hants RG27 8DH, UK; Peter.Askew@imsl-uk.com (P.D.A.); Gillian.Iredale@imsl-uk.com (G.I.)
[3] (Bundesanstalt für Materialforschung und -prüfung) BAM, Unter den Eichen 87, 12205 Berlin, Germany; Ina.stephan@bam.de
[4] Sirris, Wetenschapspark 3, B-3590 Diepenbeek, Belgium; Patrick.Cosemans@sirris.be
[5] Department of Engineering, Faculty of Science and Engineering, Manchester Metropolitan University, Chester Street, Manchester M1 5GD, UK; L.Simmons@mmu.ac.uk
[6] Department of Life Sciences, Faculty of Science and Engineering, Manchester Metropolitan University, Chester Street, Manchester M1 5GD, UK; J.Verran@mmu.ac.uk
* Correspondence: J.Redfern@mmu.ac.uk

Citation: Cunliffe, A.J.; Askew, P.D.; Stephan, I.; Iredale, G.; Cosemans, P.; Simmons, L.M.; Verran, J.; Redfern, J. How Do We Determine the Efficacy of an Antibacterial Surface? A Review of Standardised Antibacterial Material Testing Methods. *Antibiotics* **2021**, *10*, 1069. https://doi.org/10.3390/antibiotics10091069

Academic Editors: Marc Maresca, Catherine Lefay and Vincent Humblot

Received: 16 August 2021
Accepted: 1 September 2021
Published: 3 September 2021

Abstract: Materials that confer antimicrobial activity, be that by innate property, leaching of biocides or design features (e.g., non-adhesive materials) continue to gain popularity to combat the increasing and varied threats from microorganisms, e.g., replacing inert surfaces in hospitals with copper. To understand how efficacious these materials are at controlling microorganisms, data is usually collected via a standardised test method. However, standardised test methods vary, and often the characteristics and methodological choices can make it difficult to infer that any perceived antimicrobial activity demonstrated in the laboratory can be confidently assumed to an end-use setting. This review provides a critical analysis of standardised methodology used in academia and industry, and demonstrates how many key methodological choices (e.g., temperature, humidity/moisture, airflow, surface topography) may impact efficacy assessment, highlighting the need to carefully consider intended antimicrobial end-use of any product.

Keywords: antimicrobial materials; antimicrobial testing; 22196; antimicrobial surfaces; antibacterial coatings

1. Introduction

In order for a microorganism to cause disease, it must first reach the potential host. Microorganisms can move around an environment in various but typically passive ways, including via aerosols (inside droplets of water) [1], direct contact between two animated objects [2], and fomites (a contaminated inanimate object) [3]. Some microorganisms can retain their pathogenic potential whilst outside their host for extended periods of time [4], with studies suggesting survival for days and even weeks on inanimate surfaces such as plastics and metals which are often considered to be 'hygienic surfaces' [5,6]. Many of these materials are used to construct frequently touched surfaces (FTS) such as door handles, lift buttons, light switches and digital locks [7,8]. Viability of microorganisms on FTS has been demonstrated, and more critically, the evidence of transfer of potentially harmful microorganisms from the FTS to a biological surface (e.g., human skin) via touch has also been reported numerous times in the literature, e.g., [9–11]. In the clinical setting, studies highlight bedsteads, supply carts, over-bed tables, lockers, patient bodies, bed-linen, curtains and intravenous pumps as frequently touched when specifically considering

interactions between hospital staff and patients [12,13]. These patient-care items can serve as a potential reservoir for pathogenic microorganisms and may be the cause of infection of, and cross-infection between, hospital patients. Non-clinical environmental reservoirs of pathogens can cause further problems where compounding factors also occur, such as on cruise ships where advanced medical treatments are not available [14].

There are various methods that can be utilised to control microorganisms on surfaces in these settings. In clinical environments, methods to chemically disinfect surfaces are often used, but may be performed inadequately, (through poor adherence to cleaning protocols), allowing pathogens to be spread more rapidly throughout wards, following recontamination of disinfected surfaces via contact with fomites [15]. Additionally, disinfectants may themselves drive the evolution of resistance. For example, quaternary ammonium compounds (QAC) have long been considered an effective class of disinfectants and were once thought to be impervious to bacterial resistance. However, an approximate 30% increase of QAC resistance genes has been observed in methicillin-resistant *Staphylococcus aureus* (MRSA) isolates in the years 1990–2010 [16]. To compound this issue further, QAC resistance can undergo horizontal gene transfer to spread resistance and can also propagate the transfer of other antibiotic resistance genes [17]. Disinfecting rooms through exposure to high intensity UV light can be effective at killing the majority of microorganisms it illuminates, but requires all staff and patients to leave the room during the process as a safety requirement [18].

Therefore, methods that reduce human error and do not impact on the availability of facilities would be beneficial, such as materials that exhibit antimicrobial activity. Such materials may be innately antimicrobial, produced with a biocide embedded within, or there may be some coating or treatment that confers antimicrobial properties onto the surface—many of which have gained popularity over recent years [19]. For example, in some hospitals and other end-use environments, copper has been exploited as an antimicrobial material (AMM) [20], whilst brass has also been used extensively for FTS, demonstrating an oligodynamic effect [21]. Other materials and additives are now gaining focus in the literature, for example, materials with photocatalytic properties such as certain forms of titanium dioxide, various metal salts and oxides as well as certain dyes [22], other metal ions [23] and some organic agents [24] and materials used in their nano form, such as silver, copper and zinc [25]. Due to the variety and scope of these materials, we will use the term AMM to describe such materials.

The mechanism of action of AMMs can be divided into three major subgroups: active substance release, potentiated surfaces and non-adhesive properties. Each of these approaches has their own advantages and limitations in situ [26]. Contact killing-based claims are the most abundant in the literature, being delivered by both active substance release systems and those with potentiated surfaces. Arguably systems that release less active substance may mitigate any increase in prevalence of antimicrobial resistance associated with AMM's [27].

Active substance release systems discharge a biocide or antimicrobial agent and this is often triggered through hydration which is then intended to kill microorganisms on the surface and can be highly effective [28]. They can be applied to and incorporated into a wide range of materials (e.g., synthetic polymers) and deployed in a wide range of environments, from FTS in hospital wards to internal devices in patients such as orthopaedic and cardiovascular implants [29], as well as in non-clinical environments such as call buttons and in coatings on hand rails on public transport [30].

Potentiated surface-based AMM's can be fabricated by the inclusion of a biocide, metal, peptides or amines on the surface of the material in order to add an antimicrobial function to that surface [31–33]. Common materials used include silver nanoparticles (AgNPs) [25,34,35], copper (Cu) [36–39], tin disulphide (SnS_2) [40], ruthenium (Ru) [41,42] and titanium dioxide (TiO_2) [43]. Within this subcategory of AMMs are photocatalytic materials, that present their antimicrobial effect when exposed to light (e.g., TiO_2); however, a longer time period is often required to significantly reduce the microbial bioburden, with

hours upon exposure to typical solar light [44]. However, doping (e.g., nitrogen [45]) does add further potential for increased efficacy [46].

In addition to the mechanisms described above, which focus on a molecule entering or interacting with a cell in some detrimental way, other mechanisms for modifying and potentiating surfaces also exist. For example, carbon nanomaterials (e.g., graphene oxide) have also been shown to be effective at reducing the microbial bioburden on a surface by piercing/damaging cells using jagged, sharp and sturdy surface features [47]. Graphene oxide can also 'generate' reactive oxygen species (ROS) [48], and therefore uses multiple features to achieve the desired antimicrobial effect [49].

Non-adhesive AMMs have been designed to combat the transfer of microorganisms, as they prevent a microorganism from being able to adhere to the surface, which is therefore also easily cleaned (e.g., by presenting hydrophilic properties [50]). However, it is important to note that an AMM only incorporating this method would likely not reduce the rate of infection in patients, as studies have shown that, particularly bacteria, are able to overcome this 'line of defence' when no other antimicrobial properties are being exhibited [51].

As described above, there exists a range of applications for which an antimicrobial surface may be a desired option in some settings, with numerous options for manufacturers including different materials/additives and manufacturing processes. However, the variation in approach means that not all AMMs are equal and are likely to all exhibit individual levels of efficacy specific to their product design and intended end-use. As the market for these materials increases, manufacturers of AMMs are required to demonstrate their materials work as intended—meaning efficacy testing is a critical component in AMM development, sale, purchase and end-use decision-making.

2. Testing the Efficacy of an AMM

Standardised test methods are a necessary and important step in the development of a novel antimicrobial material. To define a material as antimicrobial, efficacy should be assessed under reproducible conditions that mimic later in-use environments. If the predetermined threshold (usually a 2 or 3-log reduction in viable cells although often individually agreed upon by all parties involved) is not met, then the surface cannot be considered as antimicrobial. This process should enable those interested in AMM's to ascertain a level of confidence in their material, providing some preliminary positive data that encourages further exploration for testing the material either under conditions more appropriate to the intended point of use or even in practice. For example, bacterial inocula used in standardized testing (~10^5–10^8 CFU/mL) are significantly higher than those found in most potential end-use settings (e.g., ~10^2–10^4) [52].

Additionally, in order to validate the reproducibility of an antimicrobial material, ideally several different labs should perform the relevant standardised test method and achieve results that are all within the natural error range for such test [53]. Whilst the validity of individual test method data should be acknowledged, a growing need exists for precise and reproducible methods, as many different AMM´s fall short when being tested by independent reviewers [54].

In several cases, the test methods used to determine the efficacy of an AMM are inadequate due to a variety of factors including the incubation time/environmental conditions. In some cases this can artificially favour the increased and/or prolonged efficacy of the material, particularly by raising the humidity to >90%, a condition which is almost never seen in end-use environments [55,56]. Many of the materials used in AMM's require moisture to be antimicrobial, metallic silver for example, which is ionised in the presence of moisture to form silver ions which have numerous antimicrobial properties. Therefore, knowledge of the length of time a surface remains moist for (the drying time of the deposit carrying the contaminating microorganism on the surface) is vital for an accurate judgement on the efficacy of the surface [57]. This reliance on moisture must be considered when testing surfaces for effectiveness at point of use. Indeed, knowing the time it takes for an

inoculum (a suspension of microbial cells of any manner) applied as a liquid to dry in each environment is key to assessing the activity of many AMMs.

3. Standardised Tests for AMMs In Vitro

There are five general categories of test for an antimicrobial material in vitro: (1) high surface area to volume ratio tests, (2) agar zone of inhibition tests, (3) suspension tests, (4) adhesion tests, (5) biofilm tests [26]. These tests differ based on the mechanism of action they are intended to evaluate (among other factors) and are explored below. Many test methods are constructed and defined by several different test method development organisations such as ISO (International Standards Organisation), BS (British Standards), IBRG (International Biodeterioration Research Group), and ASTM (American Society for Testing and Materials). There have been many iterations and modifications of these methods described in the literature that deviate based on the individual preferences of the testing laboratory, which then makes comparison of data generated for similar materials in different laboratories problematic.

3.1. Methods Constituting High Surface Area to Volume Ratio

These methods focus on maximising the contact between the surface and the microorganism, so the cells and the surface are essentially always touching and interacting. This is usually done by placing the bacteria between the test sample and another sterilised non-antimicrobial material such as glass or plastic. The most used test method for antimicrobial materials in this category is ISO 22196:2011 (and similar methods such as JIS Z 2801). Here, a surface is inoculated with a bacterial suspension of known concentration and volume (Figure 1). A polyethylene film is placed on top of the inoculum, and the material is incubated at 35 °C in upwards of 90% humidity for 24 h. Bacteria are removed from the surface by mechanical detachment and re-suspension in a neutralising diluent, before the number of colony forming units (CFUs) is determined by plate count [58]. This method is relatively straight-forward and cheap to run, and so has been widely adopted. However, none of the experimental conditions relate to end-use environments. Indeed, in the majority of cases, the opposite is true, ISO 22196:2011 keeps a microbial inoculum wet for the duration of a 24-h test, allowing the antimicrobial material to provide a sustained antimicrobial action by dissolving into the water and this way ensuring contact between the cell wall of a microorganism and the biocidal active substance—which will not mirror the conditions when an AMM is implemented. To overcome such shortcomings, recent developments include a test method where bacteria are aerosolised, so they are deposited onto a dry surface, in an attempt to reduce artificial antimicrobial action resulting from the deposition of a wet microbial inoculum [59]. However, dry deposition is not without its own challenges, for example ensuring reproducible inoculum quantity and ensuring a safe working environment from the release pathogens into the air.

Other methods using a high surface area to volume ratio have been reported in the literature. One method (a modification of ISO 22196:2011) involves inoculation of the antimicrobial material with a bacterial suspension within a film of agar (commonly made into a slurry) to ensure that contact is maintained between the AMM and the test organism. When recovering the bacteria from the material, a neutraliser is used to resuspend the inoculum (neutralising diluent is a key step in a majority of antimicrobial test methods to prevent superfluous interactions between the material and microorganism) and CFU counts are determined. However, it is possible that the slurry (when required) has a soiling effect on the material preventing it from performing its antimicrobial effect as efficiently as possible as different antimicrobial materials will present largely different diffusion rates and characteristics into an agar slurry [60,61].

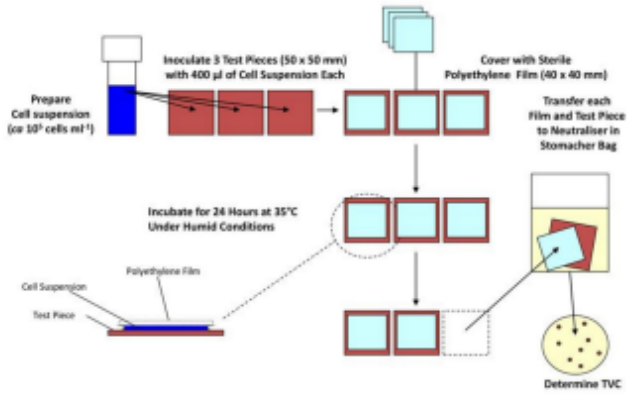

Figure 1. Diagram describing important steps in the ISO 22196 antimicrobial materials efficacy test.

Another modification of ISO 22196:2011 uses a filter, inoculated with bacteria, as the top layer rather than a polyethylene film perhaps to reduce loss of microorganisms through fewer manipulations (omitting drop inoculation) [62]. Alternatively, a liquid bacterial suspension can be sprayed (to simulate the typical deposition of airborne bacteria on to a surface by coughing, etc.) on to the antimicrobial material from a distance of 15 cm, followed by live-dead staining after being air-dried for two minutes. Spraying of microbes rather than deposition has the advantage of being more representative of a patient in a hospital in most cases but is more complicated to run (and standardise) than simply placing a droplet of water on to the surface, as it requires specialist equipment.

In conclusion, several authors have developed methods that are related to ISO 22196, presumably due to their ease of use and relatively low cost. However, there are many limitations in the translation of results obtained to the point of use of the materials, with most relating to the dissimilarity of the conditions standardised in ISO 22196 compared to end-use environments, both clinical and non-clinical, and others arising from difficulties in comparing results from methods that slightly differ from laboratory to laboratory.

3.2. Agar Zone of Inhibition Methods

Methods that utilise zones of inhibition, for which there are two existing standardised methods, are relatively quick and simple but may provide only an indicator of whether any antimicrobial effect might be present under permanently wet conditions. The first, ISO 20645:2004 is based on a disk diffusion method, where the AMM is placed on top of an inoculated nutrient agar plate, incubated at the required temperature for a set time depending on the requirements for the bacteria being tested (such as at 37 °C for 24 h for *E. coli*) [63]. The second, AATCC 30 (which evaluates fungi rather than bacteria), places a spore suspension on to a solid agar medium and covers that with the AMM, inoculation with spores also occurs on top of the AMM after placement, the Petri dish is then sealed to maintain humidity and efficacy evaluation is based on macroscopic or microscopic visibility of fungi [64]. These methods have limitations such as (i) the incubation temperature is not relevant to the end use (often it is the optimal growth temperature for the test organism), (ii) incubation time is not reflective of expected cleaning protocols (FTS's are likely to be touched more than once per day), and (iii) the nutrients present from the agar would likely not be present so abundantly on surfaces, all of which reduce the similarity to end-use environments. In addition, if the active substance is not emitted from the AMM, activity is unlikely to be measured, limiting applicability to a subset of AMMs. Furthermore, the viability of the test microorganisms may be compromised by the material being placed directly on top, even when exhibiting no antimicrobial effect. Nonetheless, the results

provided from these test methods can allow a quick and simple approach to determining whether a material has at least some antimicrobial activity, which may be all that is required at the first stages of product development. Additionally, these methods can be used as a reliable quality control step during the production of an AMM once approved [65].

3.3. Suspension Methods

Suspension methods focus on inoculating and incubating bacteria in a liquid medium containing the antimicrobial surface, and then determining the remaining viable CFUs by taking an aliquot of this liquid and performing a dilution plate count using it. This allows assessment of materials that exhibit antimicrobial-release properties. However, due to the inoculum not being placed directly on the material, only surfaces that release antimicrobials can be tested. There are two current standardised methods. The first, ASTM E2149-13a, requires that the material is immersed in the medium (that is most appropriate for the bacteria used) following bacterial inoculation, then after incubation while shaking to enable increased contact of AMM to the bacteria, the CFU count is determined [66]. This method was developed with the intention of determining the effectiveness of silane QACs by agitating the suspension with sufficient vigour to cause cells to come in to contact with the QAC 'tails' [67], although this method is somewhat disputed. A modification to this method has also been developed whereby the entire suspension container is treated with the antimicrobial to prevent biofilms forming and to avoid complications arising from the extensive agitation that is required for the standard [67]. The second, JIS L 1902 (and also the absorption method within ISO 20743), describes the incubation of a porous material absorbing a specified volume of the appropriate medium, bacteria are then detached from the porous material using a stomacher in 20 mL neutralising diluent, and CFUs are determined in the resultant suspension [68]. For methods where an antimicrobial active substance has likely leached into liquid media (which will then be diluted and plated onto agar), which both of these suspension methods utilise, a neutralising solution is essential—to ensure continued antimicrobial action does not occur during the dilution and CFU determining incubation stages (24 h at the most appropriate temperature for the bacterial strain used). As these methods do not assess contact-killing materials, it is not possible to assess efficacy for using such material in some end-use conditions, for example, as a touch surface.

3.4. Adhesion Methods

These tests focus on quantifying the number of bacteria that can adhere to an antimicrobial material. There are two approaches to this form of testing. The first requires that the test surface is inoculated with the bacteria and incubated for 1 to 4 h. Non-adhering bacteria are removed and either the surface with attached cells is added to a liquid medium or an agar slab is placed on top of the surface and incubated (for counting CFUs), or the microorganisms can be stained (e.g., live-dead staining) to determine cells per unit area [69]. The second method specifies a flow of bacterial suspension through a chamber containing the antimicrobial material, then live-dead staining is performed on the cells attached to the surface to determine survival status of adhered cells. Alternatively, the cells are detached from the surface of the material and re-suspended so that the number of CFUs of the resultant suspension can be calculated [70]. Finally, a proliferation assay can be used, which involves inoculating an AMM for a given time, followed by rinsing and placing in a soy medium. The efficacy of the AMM is determined by the number of clonal counterparts produced by the surviving bacteria that are attached to the AMM, real-time spectrophotometer readings are essential to creating a growth curve to compare a control to the AMM [71]. In both methods, there are issues that arise from how effectively the detachment of bacteria occurs, even by sonication (which can cause the diluent to heat up), as this may also reduce the viability of the organisms and their growth on media.

3.5. Biofilm Methods

A biofilm is an assemblage of microorganisms that are associated with a surface and often become encased in a matrix of polysaccharide material [72–74]. They are one of the most common forms that microorganisms take on Earth and can cause significant problems when they form in certain artificial environments. Due to their impact on health, industry and the environment, the ability to either destroy a biofilm or to stop it from forming in the first instance using AMMs is a focus of increasing importance. However, biofilm development and testing are complex, and whilst recent efforts to advance standardised biofilm growth (e.g., ASTM E2647—20 and ASTM E3161—18) and efficacy testing of disinfectants against biofilm exist [75,76], methods for efficacy testing of anti-biofilm materials are limited and suffer from problems regarding quantification of the bacteria, as staining will offer little insight and sonication may cause a reduction in viability, although some use of bioreactors for biofilm testing is taking place e.g. [77].

4. Incubation/Environmental Factors Affecting the Efficacy of Antimicrobial Test Methods

If a test method should inform on the efficacy of a surface under end-use conditions, the environmental conditions of that test need to be considered carefully. For example, if moisture is essential for activity of an antimicrobial material, a test method that includes a high humidity, no airflow and warm temperature will result in the bacterial inoculum remaining wet for the duration of the test and will provide optimal results for that AMM. However, if that putative AMM would be used in a more realistic setting (such as a hospital ward), humidity is likely to be considerably lower (30% to 65%) as will the temperature (18 °C to 28 °C), and there will be air circulating (e.g., via movement of doors, people and air conditioning) [78]. Contaminating droplets of liquid are likely to dry quickly, reducing the time for which the AMM is active. Most existing standard methods for antimicrobial testing vary in their environmental condition stipulations, but only to a relatively small degree (as seen in Table 1). Environmental conditions such as these can alter the efficacy of an AMM, and therefore careful consideration should be given when designing or interpreting data from an antimicrobial test method.

Table 1. Examples of methodological test conditions used in several standardized efficacy test methods.

Name of Standard	Material Type	Organisms Used	Time	Humidity	Temperature (°C)	Criteria for Being AM	Other Conditions
EN ISO 846:1997	Plastics	*A. niger*; *P. funiculosum*; *P. variotii*; *G. virens*; *C. globosum*; *P. aeruginosa*	4 weeks	97%	29	No visible growth to the naked eye	None
EN ISO 20743:2013	Textiles	*S. aureus*; *K. pneumoniae*	18–24 h	70%	37±2	CFUs < 1 × 10^5 reduction of life of 50%	None
EN ISO 22196:2011	Plastics/non-porous	*S. aureus*; *E. coli*	24+/−1 h	>90%	35±2	Agreed upon by case	None
ISO 27447:2019	Ceramics/photocatalytic	*S. aureus*; *K. pneumoniae*; *E. coli*	18–24 h	No mention	37±1	Log reduction of 0.8	None
EN 16615:2015	Non-porous surfaces	*S. aureus*; *E. hirae*; *P. aeruginosa*; *C. albicans*	60 min	No mention	4–30±2	5 log reduction	None

Table 1. *Cont.*

Name of Standard	Material Type	Organisms Used	Time	Humidity	Temperature (°C)	Criteria for Being AM	Other Conditions
ISO 18184:2019	Textiles	Influenza A; Feline Calcivirus	3–5 days	No mention	34	Antiviral efficiency of >2	5% CO_2
ISO 21702:2019	Plastics/non-porous	Influenza A; Feline Calcivirus	2–3 days	No mention	34	Agreed upon by case	5% CO_2
ISO 18061:2014	Ceramics/photocatalytic	Bacteriophage Q beta; *E. coli*	24 h	No mention	37±1	Log reduction of 0.8	None

Humidity- Humidity is an important determinant for the drying time of liquid droplets [79], and therefore is most likely linked to AMM efficacy. In most cases, a reduction in the humidity of the AMM results in a lower antimicrobial efficacy because of the reduction in moisture at the surface through evaporation. For example, when assessing the activity of a copper alloy surface (with varying copper quantities in the alloy), incubating at 37 °C and 100% relative humidity (RH) provides a 4-log reduction in around 30 min for all alloys higher than 70% copper content. However, when the environmental conditions are more analogous to that of an indoor room, at approximately 20 °C and 40–50% RH, the time taken to achieve the same 4-log reduction of viable bacterial load is doubled to 60 min [80]. In addition, silver ions released from zeolite have demonstrated significant antimicrobial effect at >90% RH, but the same composition showed no significant antimicrobial effects at 24% RH and a temperature of 20 °C. Although neither RH used in this study can be considered typical, it highlights the importance of the role that humidity plays in either increasing or reducing the antimicrobial efficacy of an AMM [55]. Noyce, Michels and Keevil [56] suggests that silver ions exhibit significantly decreased antimicrobial efficacy when the humidity is reduced to around 20%, again emphasizing the requirement for humidity to be considered when performing antimicrobial test methods. Furthermore, Ronan et al. [81] have shown that desiccation resistance is also significantly affected by the relative humidity, and this has downstream effects on the microbial survival on a surface, whereby survival of microorganisms can be greater at lower (25±%) relative humidity's compared to higher (95±%), this work also highlights that interactions between bacterial species also allow for greater survival on materials compared to pure cultures. Finally, this work uses aerosolisation to deposit bacteria on to the surfaces, alleviating the disadvantages that droplets at high humidity possess on the antimicrobial efficacy of a material.

Temperature- Temperature has been shown to affect the survival of microorganisms on a surface, e.g., [82], and has also been shown to significantly affect the release of antimicrobials from a material [83] and probably the method (or at least the speed) with which they interact with the target species. Additionally, temperature does significantly affect the drying time of water on non-porous surfaces [79]—and therefore potentially affects antimicrobial efficacy due to the resulting change in humidity that occurs.

Airflow- There is limited research into the effect of airflow on drying time and/or antimicrobial efficacy of a material. However, drying time of a liquid droplet on a non-porous material has been shown to be slower in the absence of airflow [79]. In addition, the transfer of infectious aerosols in hospitals is well understood and the ventilation system has been associated with much of this concern [84]. Thus, airflow is perhaps an important environmental factor that has been significantly overlooked in the design of testing AMM—even more so than humidity and temperature as it has never been considered in a relevant standardised test method.

Surface topography- In addition to the environmental conditions described above, the surface features such as hydrophobicity and surface roughness can have a significant impact on how long moisture stays on its surface [85]. While a hydrophilic surface allows

water to spread out evenly over the whole surface and to dry evenly, a hydrophobic surface results in the formation of droplets that cover the surface only in parts and that will dry out slower compared to the same volume when place on a hydrophilic material. Hydrophobicity and surface roughness will dictate the contact angle created with a droplet; when the contact angle is larger from an increased hydrophobicity, the droplet will possess a lower surface area to volume ratio, also therefore decreasing drying time [86].

Spreading of the inoculum- Spreading plays an important part of some antimicrobial tests. However, increased care should be taken when considering the spreading of the inoculum, as inconsistencies in the spreading process are almost inevitable between laboratories and even individual persons, leading to differences in the drying time of the droplets/inoculums and the repeatability of the results. Spreading must also be considered alongside hydrophobicity data of the AMM, as hydrophobicity will partially dictate how easily, if at all, the inoculum spreads across the surface, further increasing the possibility of unreliable results [87]. If hydrophobicity/hydrophilicity is part of the function of the coating comparing results from materials on which the inoculum exhibits dissimilar spreading rates may be problematic and will need to be taken into consideration.

Inoculum density- Little work has been done linking the addition of an inoculum to the drying time of a droplet. However, it is likely to cause a difference to drying time either by interaction of the bacteria with the inoculum (to perform metabolic processes) and surface, or simply by taking up a certain volume of the inoculum. The impact of soiling agents in the inoculum may have effects not only on the drying rate, but also by having an impact on the susceptibility of the target species to the effects of desiccation.

Exposure time- A longer exposure time will allow more interactions between the microorganism and the surface, potentially causing an increase in antimicrobial effect (or, under extended conditions its recovery). All current test methods take this factor into account and specify an exact incubation period for the antimicrobial test to occur—however, relating this period of time to the end-use is essential, particularly where an AMM is anticipated to be touched with high frequency.

Threshold to achieve antimicrobial claim- Often a 2–3 log reduction in microbial viability is required although it is at the discretion of all involved parties to agree to a value that is considered to be appropriate to the end-use. The scale and speed of an effect must be appropriate to the benefit that is intended/required.

In addition to those described above, other influences that can have an effect on efficacy in real-life situations and are often not considered. For example, when testing include the use of cleaning agents on the AMM, the cleanliness of a surface over time and the aging of the AMM, especially when using structured surfaces, where topography can change over time.

5. Discussion

As described above, a variety of test methods exist that are capable of determining the antimicrobial activity of a material. With this comes variations and alterations to each method based on the specific conditions of the testing laboratory at the time and date of testing, among other factors, that will likely affect the accuracy and reliability of the resulting antimicrobial efficacy of the material. It is worth noting that some modifications may allow the method to be more appropriate to the question being asked. Whilst the methodological variation from a standard method is with good intention, for example, using a temperature the investigator considers closer to room temperature, the effect on reproducibility can be profound. For example, if two different labs were to consider the antimicrobial efficacy of a given material, following a standardised test method, but one used a test chamber/container that was bigger than the other lab, there would be an impact on the time it takes to reach the intended RH. This would affect the ability of the inoculum to remain wet on the surface, and therefore alter the time the antimicrobial material is likely to be active. The same can be true for other experimental factors such as the method of achieving the desired RH (using concentrations of saturated salts), controlling temperature

(placing a chamber in an incubator compared to using a heat mat), the speed at which samples are removed from a chamber for different time points and so on. Often, these seemingly small changes to methodology alter the reproducibility between laboratories. For example, one study asked different labs to assess the antimicrobial efficacy of the same materials (polyamide 6 and an antibacterial zinc additive at multiple concentrations) using ISO 22196:2011. Following analysis of the data, several factors were found to be inconsistent between labs, such as extraction medium and method of cell enumeration, which led to a large disparity in the final results obtained, where the microbial reduction ranged from 1.73-log to 6.3-log for the same antimicrobial compound [88]. Care should also be taken to ensure the method of cell enumeration is not only consistent across all laboratories using a test method but also that it is appropriate for the specific test method that is being used, live-dead staining for instance is not always effective, particularly when assessing biofilms [89].

Whilst many of the test methods have been designed to be useable and achievable in a range of laboratories, issues remain in terms of the validity of the methods. Most critically, how can efficacy in realistic uses be inferred using the data that the test methods generate—because the current methods are not reflective of realistic in-use conditions. It is abundantly clear that a considerable improvement is required in test methodology of antimicrobial materials if subsequent results are used to support efficacy claims for different environmental conditions while in use. This clash of intention and inference would be best addressed by an interdisciplinary approach to new antimicrobial efficacy test method development. However, the process of making any changes to current test methods should be taken with due diligence, as unexpected consequences are possible. For example, temperature and drying time of a droplet have been found to affect the rate of detachment of *Bacillus* spores from a surface once the droplet has dried, which will be more likely to occur if humidity is lowered to 40–50% to keep in-line with a majority of indoor acclimatised settings [90].

Finally, there have been improvements in recent years that show promise in creating more realistic and higher reliability test methods. One potentially useful addition would be the addition of video protocols to work alongside traditional paper protocols, allowing users to get an exact understanding of the nuances related to the test method. Another answer may lie in the recent advances in both computer simulations of heat/mass transfer and in the decreasing cost of improved microfluidic devices that provide the potential for both cheap and reliable test methods [91], which when integrated in to an environmental control chamber could provide realistic and reliable antimicrobial efficacy assessment.

6. Conclusions

The utilisation and effectiveness of antimicrobial materials in an end-use scenario is likely considerably different from results achieved from the testing methods currently in use and standardised. Using test methods that better reflect end-user environments would enable more realistic efficacy assessment. An approach to efficacy assessment of antimicrobial materials should build on current standard methods but seek to understand and design methods that model the behaviour of the antimicrobial material as if it were placed in its intended end-use setting, such as by adding additional environmental conditions. However, the increased difficulty and cost, and lack of models that explain the impact of drying time of liquids deposited on a surface will require significant work to fully understand and develop into new AMM efficacy test methods.

Funding: This research received no external funding.

Acknowledgments: The authors would like to thank the International Biodeterioration Research Group (IBRG), Manchester Metropolitan University and the COST Action AMiCI (CA15114), (European Cooperation in Science and Technology) for providing funding for this work.

Conflicts of Interest: The authors declare no conflict of interest.

References

1. Mirhoseini, S.H.; Nikaeen, M.; Khanahmad, H.; Hatamzadeh, M.; Hassanzadeh, A. Monitoring of airborne bacteria and aerosols in different wards of hospitals-Particle counting usefulness in investigation of airborne bacteria. *Ann. Agric. Environ. Med.* **2015**, *22*. [CrossRef]
2. Jung, I.; Choi, W.; Kim, J.; Wang, E.; Park, S.-W.; Lee, W.-J.; Choi, J.; Kim, H.; Uh, Y.; Kim, Y. Nosocomial person-to-person transmission of severe fever with thrombocytopenia syndrome. *Clin. Microbiol. Infect.* **2019**, *25*, 633.e1–633.e4. [CrossRef] [PubMed]
3. Stephens, B.; Azimi, P.; Thoemmes, M.S.; Heidarinejad, M.; Allen, J.G.; Gilbert, J.A. Microbial exchange via fomites and implications for human health. *Curr. Pollut. Rep.* **2019**, *5*, 198–213. [CrossRef] [PubMed]
4. Pommepuy, M.; Butin, M.; Derrien, A.; Gourmelon, M.; Colwell, R.; Cormier, M. Retention of enteropathogenicity by viable but nonculturable Escherichia coli exposed to seawater and sunlight. *Appl. Environ. Microbiol.* **1996**, *62*, 4621–4626. [CrossRef] [PubMed]
5. Neely, A.N. A survey of gram-negative bacteria survival on hospital fabrics and plastics. *J. Burn Care Rehabil.* **2000**, *21*, 523–527. [CrossRef]
6. Heller, L.C.; Edelblute, C.M. Long-term metabolic persistence of gram-positive bacteria on health care-relevant plastic. *Am. J. Infect. Control* **2018**, *46*, 50–53. [CrossRef] [PubMed]
7. Jaradat, Z.W.; Ababneh, Q.O.; Sha'aban, S.T.; Alkofahi, A.A.; Assaleh, D.; Al Shara, A. Methicillin Resistant Staphylococcus aureus and public fomites: A review. *Pathog. Glob. Health* **2020**, *114*, 426–450. [CrossRef]
8. Xiao, S.; Jones, R.M.; Zhao, P.; Li, Y. The dynamic fomite transmission of Methicillin-resistant Staphylococcus aureus in hospitals and the possible improved intervention methods. *Build. Environ.* **2019**, *161*, 106246. [CrossRef]
9. Kraay, A.N.; Hayashi, M.A.; Hernandez-Ceron, N.; Spicknall, I.H.; Eisenberg, M.C.; Meza, R.; Eisenberg, J.N. Fomite-mediated transmission as a sufficient pathway: A comparative analysis across three viral pathogens. *BMC Infect. Dis.* **2018**, *18*, 540. [CrossRef]
10. Weber, K.L.; LeSassier, D.S.; Kappell, A.D.; Schulte, K.Q.; Westfall, N.; Albright, N.C.; Godbold, G.D.; Palsikar, V.; Acevedo, C.A.; Ternus, K.L. Simulating transmission of ESKAPE pathogens plus C. difficile in relevant clinical scenarios. *BMC Infect. Dis.* **2020**, *20*, 1–15. [CrossRef]
11. Suwantarat, N.; Supple, L.A.; Cadnum, J.L.; Sankar, T.; Donskey, C.J. Quantitative assessment of interactions between hospitalized patients and portable medical equipment and other fomites. *Am. J. Infect. Control.* **2017**, *45*, 1276–1278. [CrossRef] [PubMed]
12. Huslage, K.; Rutala, W.A.; Sickbert-Bennett, E.; Weber, D.J. A quantitative approach to defining "high-touch" surfaces in hospitals. *Infect. Control. Hosp. Epidemiol.* **2010**, *31*, 850–853. [CrossRef] [PubMed]
13. Cheng, V.; Chau, P.; Lee, W.; Ho, S.; Lee, D.; So, S.; Wong, S.; Tai, J.; Yuen, K. Hand-touch contact assessment of high-touch and mutual-touch surfaces among healthcare workers, patients, and visitors. *J. Hosp. Infect.* **2015**, *90*, 220–225. [CrossRef] [PubMed]
14. Liu, X.; Chang, Y.-C. An emergency responding mechanism for cruise epidemic prevention—taking COVID-19 as an example. *Mar. Policy* **2020**, *119*, 104093. [CrossRef] [PubMed]
15. Meinke, R.; Meyer, B.; Frei, R.; Passweg, J.; Widmer, A.F. Equal efficacy of glucoprotamin and an aldehyde product for environmental disinfection in a hematologic transplant unit: A prospective crossover trial. *Infect. Control. Hosp. Epidemiol.* **2012**, *33*, 1077–1080. [CrossRef] [PubMed]
16. Jennings, M.C.; Minbiole, K.P.; Wuest, W.M. Quaternary ammonium compounds: An antimicrobial mainstay and platform for innovation to address bacterial resistance. *ACS Infect. Dis.* **2015**, *1*, 288–303. [CrossRef] [PubMed]
17. Han, Y.; Zhou, Z.-C.; Zhu, L.; Wei, Y.-Y.; Feng, W.-Q.; Xu, L.; Liu, Y.; Lin, Z.-J.; Shuai, X.-Y.; Zhang, Z.-J. The impact and mechanism of quaternary ammonium compounds on the transmission of antibiotic resistance genes. *Environ. Sci. Pollut. Res.* **2019**, *26*, 28352–28360. [CrossRef]
18. Hosein, I.; Madeloso, R.; Nagaratnam, W.; Villamaria, F.; Stock, E.; Jinadatha, C. Evaluation of a pulsed xenon ultraviolet light device for isolation room disinfection in a United Kingdom hospital. *Am. J. Infect. Control* **2016**, *44*, e157–e161. [CrossRef]
19. Page, K.; Wilson, M.; Parkin, I.P. Antimicrobial surfaces and their potential in reducing the role of the inanimate environment in the incidence of hospital-acquired infections. *J. Mater. Chem.* **2009**, *19*, 3819–3831. [CrossRef]
20. Dunne, S.S.; Ahonen, M.; Modic, M.; Crijns, F.R.; Keinänen-Toivola, M.M.; Meinke, R.; Keevil, C.W.; Gray, J.; O'Connell, N.H.; Dunne, C.P. Specialized cleaning associated with antimicrobial coatings for reduction of hospital-acquired infection: Opinion of the COST Action Network AMiCI (CA15114). *J. Hosp. Infect.* **2018**, *99*, 250–255. [CrossRef]
21. Dauvergne, E.; Mullié, C. Brass Alloys: Copper-Bottomed Solutions against Hospital-Acquired Infections? *Antibiotics* **2021**, *10*, 286. [CrossRef] [PubMed]
22. Salazar, H.; Martins, P.; Santos, B.; Fernandes, M.; Reizabal, A.; Sebastián, V.; Botelho, G.; Tavares, C.J.; Vilas-Vilela, J.L.; Lanceros-Mendez, S. Photocatalytic and antimicrobial multifunctional nanocomposite membranes for emerging pollutants water treatment applications. *Chemosphere* **2020**, *250*, 126299. [CrossRef]
23. Lemire, J.A.; Harrison, J.J.; Turner, R.J. Antimicrobial activity of metals: Mechanisms, molecular targets and applications. *Nat. Rev. Microbiol.* **2013**, *11*, 371–384. [CrossRef]
24. Oosterhof, J.J.; Buijssen, K.J.; Busscher, H.J.; van der Laan, B.F.; van der Mei, H.C. Effects of quaternary ammonium silane coatings on mixed fungal and bacterial biofilms on tracheoesophageal shunt prostheses. *Appl. Environ. Microbiol.* **2006**, *72*, 3673–3677. [CrossRef]

25. Khadka, P.; Haque, M.; Krishnamurthi, V.R.; Niyonshuti, I.; Chen, J.; Wang, Y. Quantitative Investigations Reveal New Antimicrobial Mechanism of Silver Nanoparticles and Ions. *Biophys. J.* **2018**, *114*, 690a. [CrossRef]
26. Sjollema, J.; Zaat, S.A.J.; Fontaine, V.; Ramstedt, M.; Luginbuehl, R.; Thevissen, K.; Li, J.; van der Mei, H.C.; Busscher, H.J. In vitro methods for the evaluation of antimicrobial surface designs. *Acta Biomater* **2018**, *70*, 12–24. [CrossRef] [PubMed]
27. Kaur, R.; Liu, S. Antibacterial surface design–Contact kill. *Prog. Surf. Sci.* **2016**, *91*, 136–153. [CrossRef]
28. Shukla, A.; Fleming, K.E.; Chuang, H.F.; Chau, T.M.; Loose, C.R.; Stephanopoulos, G.N.; Hammond, P.T. Controlling the release of peptide antimicrobial agents from surfaces. *Biomaterials* **2010**, *31*, 2348–2357. [CrossRef] [PubMed]
29. Wu, P.; Grainger, D.W. Drug/device combinations for local drug therapies and infection prophylaxis. *Biomaterials* **2006**, *27*, 2450–2467. [CrossRef]
30. Buhat, C.A.H.; Lutero, D.S.; Olave, Y.H.; Torres, M.C.; Rabajante, J.F. Modeling the Transmission of Respiratory Infectious Diseases in Mass Transportation Systems. *medRxiv* **2020**. [CrossRef]
31. Hans, M.; Erbe, A.; Mathews, S.; Chen, Y.; Solioz, M.; Mücklich, F. Role of copper oxides in contact killing of bacteria. *Langmuir* **2013**, *29*, 16160–16166. [CrossRef]
32. Tiller, J.C.; Liao, C.-J.; Lewis, K.; Klibanov, A.M. Designing surfaces that kill bacteria on contact. *Proc. Natl. Acad. Sci. USA* **2001**, *98*, 5981–5985. [CrossRef] [PubMed]
33. Campoccia, D.; Montanaro, L.; Arciola, C.R. A review of the biomaterials technologies for infection-resistant surfaces. *Biomaterials* **2013**, *34*, 8533–8554. [CrossRef]
34. Yan, X.; He, B.; Liu, L.; Qu, G.; Shi, J.; Hu, L.; Jiang, G. Antibacterial mechanism of silver nanoparticles in Pseudomonas aeruginosa: Proteomics approach. *Metallomics* **2018**, *10*, 557–564. [CrossRef]
35. Sondi, I.; Salopek-Sondi, B. Silver nanoparticles as antimicrobial agent: A case study on E. coli as a model for Gram-negative bacteria. *J. Colloid Interface Sci.* **2004**, *275*, 177–182. [CrossRef] [PubMed]
36. Warnes, S.; Keevil, C. Mechanism of copper surface toxicity in vancomycin-resistant enterococci following wet or dry surface contact. *Appl. Environ. Microbiol.* **2011**, *77*, 6049–6059. [CrossRef] [PubMed]
37. Chandraleka, S.; Ramya, K.; Chandramohan, G.; Dhanasekaran, D.; Priyadharshini, A.; Panneerselvam, A. Antimicrobial mechanism of copper (II) 1, 10-phenanthroline and 2, 2′-bipyridyl complex on bacterial and fungal pathogens. *J. Saudi Chem. Soc.* **2014**, *18*, 953–962. [CrossRef]
38. Vincent, M.; Duval, R.E.; Hartemann, P.; Engels-Deutsch, M. Contact killing and antimicrobial properties of copper. *J. Appl. Microbiol.* **2018**, *124*, 1032–1046. [CrossRef]
39. Giannousi, K.; Lafazanis, K.; Arvanitidis, J.; Pantazaki, A.; Dendrinou-Samara, C. Hydrothermal synthesis of copper based nanoparticles: Antimicrobial screening and interaction with DNA. *J. Inorg. Biochem.* **2014**, *133*, 24–32. [CrossRef]
40. Fakhri, A.; Behrouz, S. Assessment of SnS2 nanoparticles properties for photocatalytic and antibacterial applications. *Sol. Energy* **2015**, *117*, 187–191. [CrossRef]
41. Vaishampayan, A.; de Jong, A.; Wight, D.J.; Kok, J.; Grohmann, E. A novel antimicrobial coating represses biofilm and virulence-related genes in methicillin-resistant Staphylococcus aureus. *Front. Microbiol.* **2018**, *9*, 221. [CrossRef] [PubMed]
42. Bolhuis, A.; Hand, L.; Marshall, J.E.; Richards, A.D.; Rodger, A.; Aldrich-Wright, J. Antimicrobial activity of ruthenium-based intercalators. *Eur. J. Pharm. Sci.* **2011**, *42*, 313–317. [CrossRef] [PubMed]
43. Chen, F.; Yang, X.; Wu, Q. Antifungal capability of TiO2 coated film on moist wood. *Build. Environ.* **2009**, *44*, 1088–1093. [CrossRef]
44. Sichel, C.; Tello, J.; De Cara, M.; Fernández-Ibáñez, P. Effect of UV solar intensity and dose on the photocatalytic disinfection of bacteria and fungi. *Catal. Today* **2007**, *129*, 152–160. [CrossRef]
45. Lee, H.U.; Lee, S.C.; Choi, S.; Son, B.; Lee, S.M.; Kim, H.J.; Lee, J. Efficient visible-light induced photocatalysis on nanoporous nitrogen-doped titanium dioxide catalysts. *Chem. Eng. J.* **2013**, *228*, 756–764. [CrossRef]
46. Burda, C.; Lou, Y.; Chen, X.; Samia, A.C.; Stout, J.; Gole, J.L. Enhanced nitrogen doping in TiO2 nanoparticles. *Nano Lett.* **2003**, *3*, 1049–1051. [CrossRef]
47. Akhavan, O.; Ghaderi, E. Toxicity of graphene and graphene oxide nanowalls against bacteria. *ACS Nano* **2010**, *4*, 5731–5736. [CrossRef]
48. Azizi-Lalabadi, M.; Hashemi, H.; Feng, J.; Jafari, S.M. Carbon nanomaterials against pathogens; the antimicrobial activity of carbon nanotubes, graphene/graphene oxide, fullerenes, and their nanocomposites. *Adv. Colloid Interface Sci.* **2020**, 102250. [CrossRef]
49. Zheng, H.; Ji, Z.; Roy, K.R.; Gao, M.; Pan, Y.; Cai, X.; Wang, L.; Li, W.; Chang, C.H.; Kaweeteerawat, C. Engineered graphene oxide nanocomposite capable of preventing the evolution of antimicrobial resistance. *ACS Nano* **2019**, *13*, 11488–11499. [CrossRef]
50. Holmes, P.; Currie, E.; Thies, J.; Van der Mei, H.; Busscher, H.; Norde, W. Surface-modified nanoparticles as a new, versatile, and mechanically robust nonadhesive coating: Suppression of protein adsorption and bacterial adhesion. *J. Biomed. Mater. Res. Part A: An. Off. J. Soc. Biomater. Jpn. Soc. Biomater. Aust. Soc. Biomater. Korean Soc. Biomater.* **2009**, *91*, 824–833. [CrossRef]
51. Salwiczek, M.; Qu, Y.; Gardiner, J.; Strugnell, R.A.; Lithgow, T.; McLean, K.M.; Thissen, H. Emerging rules for effective antimicrobial coatings. *Trends Biotechnol.* **2014**, *32*, 82–90. [CrossRef] [PubMed]
52. Sinclair, R.G.; Gerba, C.P. Microbial contamination in kitchens and bathrooms of rural cambodian village households. *Lett. Appl. Microbiol.* **2011**, *52*, 144–149. [CrossRef]
53. Bloomfield, S.F.; Looney, E. Evaluation of the repeatability and reproducibility of European suspension test methods for antimicrobial activity of disinfectants and antiseptics. *J. Appl. Bacteriol.* **1992**, *73*, 87–93. [CrossRef] [PubMed]

54. Ioannidis, J.P. Why most published research findings are false. *PLoS Med.* **2005**, *2*, e124. [CrossRef] [PubMed]
55. Michels, H.; Noyce, J.; Keevil, C.W. Effects of temperature and humidity on the efficacy of methicillin-resistant Staphylococcus aureus challenged antimicrobial materials containing silver and copper. *Lett. Appl. Microbiol.* **2009**, *49*, 191–195. [CrossRef]
56. Noyce, J.; Michels, H.; Keevil, C. Potential use of copper surfaces to reduce survival of epidemic meticillin-resistant Staphylococcus aureus in the healthcare environment. *J. Hosp. Infect.* **2006**, *63*, 289–297. [CrossRef]
57. Rai, M.; Yadav, A.; Gade, A. Silver nanoparticles as a new generation of antimicrobials. *Biotechnol. Adv.* **2009**, *27*, 76–83. [CrossRef]
58. International Organization for Standardization, ISO. 22196: Measurement of antibacterial activity on plastics and other non-porous surfaces. International Organization for Standardization: Geneva, Switzerland. 2011. Available online: https://www.iso.org/standard/54431.html (accessed on 20 February 2021).
59. McDonald, M.; Wesgate, R.; Rubiano, M.; Holah, J.; Denyer, S.P.; Jermann, C.; Maillard, J.Y. Impact of a dry inoculum deposition on the efficacy of copper-based antimicrobial surfaces. *J. Hosp. Infect.* **2020**, *106*, 465–472. [CrossRef] [PubMed]
60. Sjollema, J.; Keul, H.; van der Mei, H.; Dijkstra, R.; Rustema-Abbing, M.; de Vries, J.; Loontjens, T.; Dirks, T.; Busscher, H. A Trifunctional, Modular Biomaterial Coating: Nonadhesive to Bacteria, Chlorhexidine-Releasing and Tissue-Integrating. *Macromol. Biosci.* **2017**, *17*. [CrossRef] [PubMed]
61. European Chemicals Agency. *Guidance on the Biocidal Products Regulation*; Volume II European Chemicals Agency: Helskini, Finland, 2016.
62. Van de Lagemaat, M.; Grotenhuis, A.; van de Belt-Gritter, B.; Roest, S.; Loontjens, T.J.; Busscher, H.J.; van der Mei, H.C.; Ren, Y. Comparison of methods to evaluate bacterial contact-killing materials. *Acta Biomater.* **2017**, *59*, 139–147. [CrossRef] [PubMed]
63. International Organization for Standardization, ISO. 20645. Textile fabrics — Determination of antibacterial activity — Agar diffusion plate test, International Organization for Standardization: Geneva, Switzerland. 2004. Available online: https://www.iso.org/standard/35499.html (accessed on 21 February 2021).
64. American Association of Textile Chemists and Colorists. Antifungal Activity, Assessment on Textile Materials: Mildew and Rot Resistance of Textile Materials. American Association of Textile Chemists and Colorists: Research Triangle Park, NC, USA. 2017. Available online: https://members.aatcc.org/store/tm30/491/ (accessed on 30 May 2021).
65. Åhman, J.; Matuschek, E.; Kahlmeter, G. The quality of antimicrobial discs from nine manufacturers—EUCAST evaluations in 2014 and 2017. *Clin. Microbiol. Infect.* **2019**, *25*, 346–352. [CrossRef] [PubMed]
66. ASTM International, ASTM. E2149-13A. Standard Test Method for Determining the Antimicrobial Activity of Antimicrobial Agents Under Dynamic Contact Conditions. ASTM International: West Conshohocken, PA, USA, 2013. [CrossRef]
67. Caschera, A.; Mistry, K.B.; Bedard, J.; Ronan, E.; Syed, M.A.; Khan, A.U.; Lough, A.J.; Wolfaardt, G.; Foucher, D.A. Surface-attached sulfonamide containing quaternary ammonium antimicrobials for textiles and plastics. *RSC Adv.* **2019**, *9*, 3140–3150. [CrossRef]
68. International Organization for Standardization, ISO. 20743-Textiles-Determination of Antibacterial Activity of Textile Products. International Organization for Standardization: Geneva, Switzerland. 2013. Available online: https://www.iso.org/standard/59586.html (accessed on 21 February 2021).
69. Héquet, A.; Humblot, V.; Berjeaud, J.-M.; Pradier, C.-M. Optimized grafting of antimicrobial peptides on stainless steel surface and biofilm resistance tests. *Colloids Surf. B Biointerfaces* **2011**, *84*, 301–309. [CrossRef]
70. Albright, V.; Zhuk, I.; Wang, Y.; Selin, V.; van de Belt-Gritter, B.; Busscher, H.J.; van der Mei, H.C.; Sukhishvili, S.A. Self-defensive antibiotic-loaded layer-by-layer coatings: Imaging of localized bacterial acidification and pH-triggering of antibiotic release. *Acta Biomater.* **2017**, *61*, 66–74. [CrossRef] [PubMed]
71. Alt, V.; Bechert, T.; Steinrücke, P.; Wagener, M.; Seidel, P.; Dingeldein, E.; Domann, E.; Schnettler, R. In vitro testing of antimicrobial activity of bone cement. *Antimicrob. Agents Chemother.* **2004**, *48*, 4084–4088. [CrossRef]
72. Schachter, B. Slimy business—the biotechnology of biofilms. *Nat. Biotechnol.* **2003**, *21*, 361–365. [CrossRef] [PubMed]
73. Kim, H.-S.; Lee, J.Y.; Ham, S.-Y.; Lee, J.H.; Park, J.-H.; Park, H.-D. Effect of biofilm inhibitor on biofouling resistance in RO processes. *Fuel* **2019**, *253*, 823–832. [CrossRef]
74. Donlan, R.M. Biofilms: Microbial life on surfaces. *Emerg. Infect. Dis.* **2002**, *8*, 881–890. [CrossRef]
75. Goeres, D.M.; Walker, D.K.; Buckingham-Meyer, K.; Lorenz, L.; Summers, J.; Fritz, B.; Goveia, D.; Dickerman, G.; Schultz, J.; Parker, A.E. Development, standardization, and validation of a biofilm efficacy test: The single tube method. *J. Microbiol. Methods* **2019**, *165*, 105694. [CrossRef] [PubMed]
76. ASTM. *E2871-19, Standard Test Method for Determining Disinfectant Efficacy Against Biofilm Grown in the CDC Biofilm Reactor Using the Single Tube Method*; ASTM International: West Conshohocken, PA, USA, 2019. [CrossRef]
77. Dumitrache, A.; Eberl, H.J.; Allen, D.G.; Wolfaardt, G.M. Mathematical modeling to validate on-line co2 measurements as a metric for cellulolytic biofilm activity in continuous-flow bioreactors. *Biochem. Eng. J.* **2015**, *101*, 55–67. [CrossRef]
78. Department of Health. *HTM 03-01: Specialised Ventilation for Healthcare Premises: Part A—Design and Validation*; Department of Health: Leeds, UK, 2007.
79. Redfern, J.; Tucker, J.; Simmons, L.M.; Askew, P.; Stephan, I.; Verran, J. Environmental and Experimental Factors Affecting Efficacy Testing of Nonporous Plastic Antimicrobial Surfaces. *Methods Protoc.* **2018**, *1*, 36. [CrossRef] [PubMed]
80. Ojeil, M.; Jermann, C.; Holah, J.; Denyer, S.P.; Maillard, J.-Y. Evaluation of new in vitro efficacy test for antimicrobial surface activity reflecting UK hospital conditions. *J. Hosp. Infect.* **2013**, *85*, 274–281. [CrossRef]

81. Ronan, E.; Yeung, C.W.; Hausner, M.; Wolfaardt, G.M. Interspecies interaction extends bacterial survival at solid–air interfaces. *Biofouling* **2013**, *29*, 1087–1096. [CrossRef]
82. Redfern, J.; Verran, J. Effect of humidity and temperature on the survival of Listeria monocytogenes on surfaces. *Lett. Appl. Microbiol.* **2017**, *64*, 276–282. [CrossRef]
83. Kashiri, M.; Cerisuelo, J.P.; Domínguez, I.; López-Carballo, G.; Hernández-Muñoz, P.; Gavara, R. Novel antimicrobial zein film for controlled release of lauroyl arginate (LAE). *Food Hydrocoll.* **2016**, *61*, 547–554. [CrossRef]
84. Tang, J.; Li, Y.; Eames, I.; Chan, P.; Ridgway, G. Factors involved in the aerosol transmission of infection and control of ventilation in healthcare premises. *J. Hosp. Infect.* **2006**, *64*, 100–114. [CrossRef]
85. Richard, E.; Dubois, T.; Allion-Maurer, A.; Jha, P.-K.; Faille, C. Hydrophobicity of abiotic surfaces governs droplets deposition and evaporation patterns. *Food Microbiol.* **2020**, 103538. [CrossRef] [PubMed]
86. Kulinich, S.; Farzaneh, M. Effect of contact angle hysteresis on water droplet evaporation from super-hydrophobic surfaces. *Appl. Surf. Sci.* **2009**, *255*, 4056–4060. [CrossRef]
87. Nakajima, A. Design of hydrophobic surfaces for liquid droplet control. *NPG Asia Mater.* **2011**, *3*, 49–56. [CrossRef]
88. Wiegand, C.; Völpel, A.; Ewald, A.; Remesch, M.; Kuever, J.; Bauer, J.; Griesheim, S.; Hauser, C.; Thielmann, J.; Tonndorf-Martini, S. Critical physiological factors influencing the outcome of antimicrobial testing according to ISO 22196/JIS Z 2801. *PLoS ONE* **2018**, *13*, e0194339. [CrossRef]
89. Netuschil, L.; Auschill, T.M.; Sculean, A.; Arweiler, N.B. Confusion over live/dead stainings for the detection of vital microorganisms in oral biofilms—Which stain is suitable? *BMC Oral Health* **2014**, *14*, 2. [CrossRef] [PubMed]
90. Faille, C.; Bihi, I.; Ronse, A.; Ronse, G.; Baudoin, M.; Zoueshtiagh, F. Increased resistance to detachment of adherent microspheres and Bacillus spores subjected to a drying step. *Colloids Surf. B Biointerfaces* **2016**, *143*, 293–300. [CrossRef] [PubMed]
91. Sun, H.; Chan, C.-W.; Wang, Y.; Yao, X.; Mu, X.; Lu, X.; Zhou, J.; Cai, Z.; Ren, K. Reliable and reusable whole polypropylene plastic microfluidic devices for a rapid, low-cost antimicrobial susceptibility test. *Lab. A Chip* **2019**, *19*, 2915–2924. [CrossRef] [PubMed]

Appendix B

SOP Number 001

SOP Title 3D printing and construction of an environmental control chamber capable of performing efficacy test methods for antimicrobial hard materials

	NAME	TITLE	SIGNATURE	DATE
Author	Alexander Cunliffe	Mr		
Reviewer				
Authoriser				

Effective Date:	
Review Date:	

READ BY			
NAME	TITLE	SIGNATURE	DATE

Contents

1. PURPOSE

The purpose of this SOP is to guide the user to building and using a novel environmental control chamber to perform a range of antimicrobial material (AMM) related Standardised test methods (STMs) within.

2. INTRODUCTION

Current STMs are not designed to assess how an antimicrobial material would behave in the intended end-use environment. For example, in ISO 22196, the most widely used STM for antimicrobial non-porous materials, relative humidity is required to be above 90% which prevents the bacterial inoculum

from evaporating. As moisture is often essential for antimicrobial activity of an antimicrobial material, results from these STMs may favour an antimicrobial claim when compared to end-use conditions, which are likely less wet/humid. However, methods to control relative humidity, temperature, and airflow simultaneously to perform more realistic methods are lacking. This document outlines the use of a purpose designed chamber capable of performing STMs for antimicrobial hard materials within a range of experimental variables (relative humidity – 15-90%, temperature – room-37^{o}C) to allow users to perform STMs with environmental parameters closer to the intended end-use of the AMM.

The chamber (Figure 1) is printed out of polylactic acid (PLA) and Poly ethyl phthalate (PET-G). It is approximately 560x250x75 mm in size and features two compartments connected by two tubes. The smaller compartment (HC compartment) allows for the control of relative humidity using water and saturated salts and contains three fans to help circulate the air through the remainder of the chamber. The larger compartment (MT compartment) holds test pieces on a custom-printed coupon tray (default print can hold up to 66 20x20 mm coupons at once), with two heat pads inserted in the underside of the roof used to supply heat, regulating temperature/humidity using sensors that are in the testing chamber.

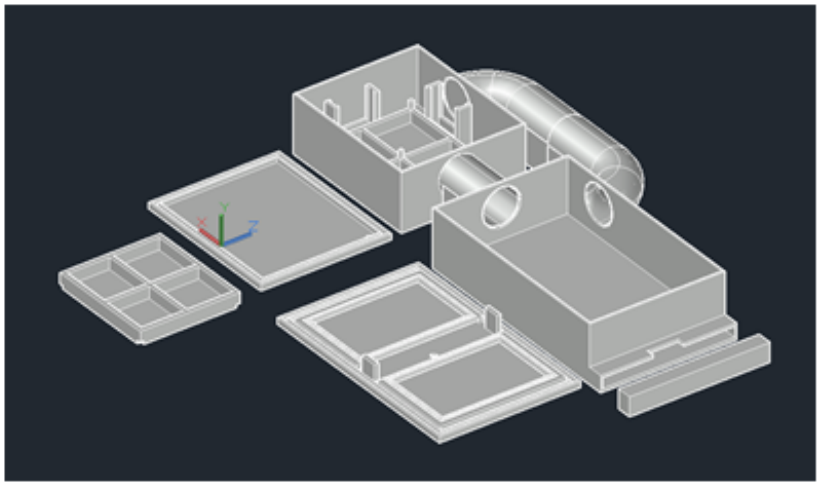

Figure 1. 3D rendering of the environmental control chamber as an AutoCad file.

3. SCOPE

This SOP specifies a method of 3D printing and assembling a chamber capable of controlling temperature, humidity, and airflow. It is not to be used for generalised 3D printing or electronics guidelines.

4. DEFINITIONS

FDM – fused deposition modelling, a technique for 3D printing

.gcode – a file type generated in slicing software that can be read by 3D printers to allow printing

V – voltage

DC – direct current

A – current (measured in Amperes)

IDE – integrated development environment, used to develop software

I/O – on-off switch used in electrical equipment

5. RESPONSIBILITIES

3D printing – roles include cleaning and operation of the 3D printer and replacing filament where necessary

Assembling the chamber – Use of silicone to attach the appropriate parts of the chamber together

Electronics – Wiring the microcontroller to the various components used to control and monitor the chamber

6. SPECIFIC PROCEDURE

6.1 3D printing of the chamber

An FDM 3D printer with minimum usable dimensions (of the print bed) of 300cmx175cm capable of heating the print bed to 60°C is required. All .gcode files should be loaded on to the printer. A filament diameter of 2.85 mm is recommended, (whilst other filament sizes can be used, these have not been tested with this print).

This SOP will illustrate the operation and maintenance of the 3D printer BCN3D Sigma D25 as an example. Please operate under the guidance of the user manual for the specific 3D printer being used for the print.

6.1.1 Loading filament into the 3D printer

Remove the filament from the box and plastic packaging and cut the end of the filament with scissors diagonally thus that the end of the filament is not square. Do not let go of the end of the filament until loading is complete. Place the filament reel on to the spool holders. If the print bed is blocking the spool holders, it is possible to move it using the internal command Utilities > Maintenance > Move platform on the control panel. Once the reel is in place, load the end of the filament into the filament entry (usually next to the reel

once in place) until it cannot be loaded further. Then use the load filament command on the control panel Utilities > Filament > Load filament and follow the on-screen instructions.

Note: if a reel of filament is already present, the unload function will need to be used via the control panel with the command Utilities > Filament > Unload filament and following the on-screen instructions.

6.1.2 Cleaning the glass

The print bed must be thoroughly cleaned before every print takes place. Firstly, carefully remove the glass from the print bed by unlocking the two metal clamps that hold it in place, then wash the print bed thoroughly with water and dry. Finally, replace the glass on to the print bed and clamp back into place.

6.1.3 Levelling the print bed

To ensure an even print, the print bed must be levelled before each print. This is performed under Utilities > Calibration > Build plate levelling, then follow the on-screen instructions. If the print is still uneven despite levelling, it is recommended to perform a mesh map and axis calibration using Utilities > Calibration > Mesh mapping and follow the on-screen instructions. To complete an axis calibration, use Utilities > calibration > Axis calibration, then complete a calibration of the Z axis for the printer head being used for the print, all other calibrations can be skipped.

Note: in some cases, the printer may need to be switched off and on between prints or the levelling will generate faulty results and show the print bed is heavily misaligned when it is not.

6.1.4 Printing each section of the chamber

Before printing, apply 3D print adhesive (e.g., Magigoo) to the entirety of the print bed, then begin the applicable print via Print > 'name'. The files pertaining to this SOP contain ten print sections for the chamber that should be printed in numerical order to avoid waste. Note, if starting with a new 1kg reel of filament, this will require changing after printing piece 7. If using other reel volumes, the requirement to change the reel may vary.

1. A1_trayseal – 28g
2. A2_roof1 – 108g
3. A3_humidity2 – 102g
4. A4_chamber1 – 232g
5. A5_chamber2 – 337g
6. A6_smallpipe – 59g
7. A7_humidity1 – 99g
8. A8_largepipe – 187g
9. A9_roof2 – 244g
10. A10_tray – 210g

Once a print has been completed, remove the print from the print bed using a removal spatula. In some cases, support structures will have been printed within the main print. In this case, it should be removed before use. This can be best done with pliers and filed to create a smooth finish.

6.2 Assembling the chamber

To complete this task, a sealant is required. Silicone is recommended as it is easy to use, widely available and creates an airtight seal. There are four joins

that require sealing. Each joint is marked in red in the following figures. The seal should be completely airtight in each case.

1. A5_chamber2 – A6_smallpipe

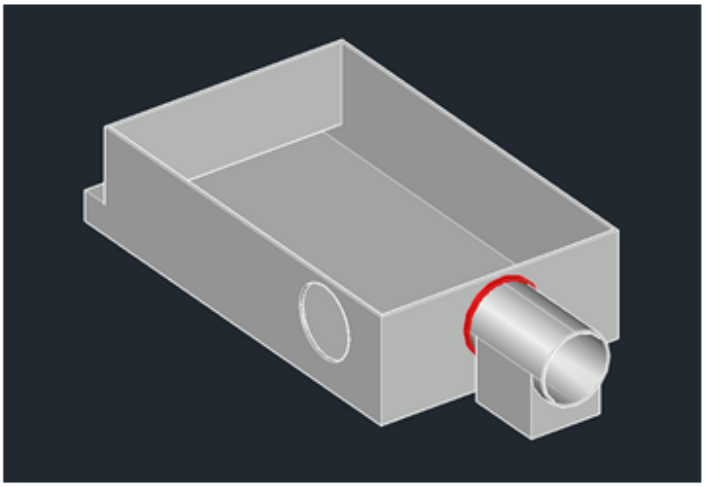

Figure 2. Fuse point 1, silicone placement is marked in red.

2. A5_chamber2 – A8_largepipe

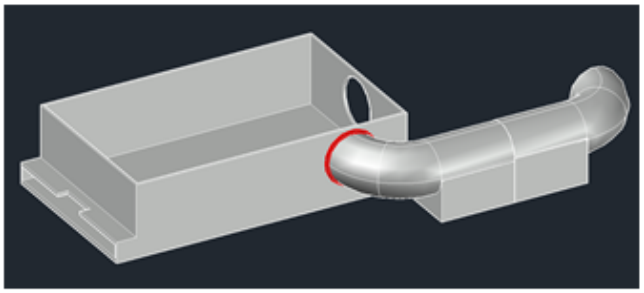

Figure 3. Fuse point 2, silicone placement is marked in red.

3. A4_chamber1 – A8_largepipe

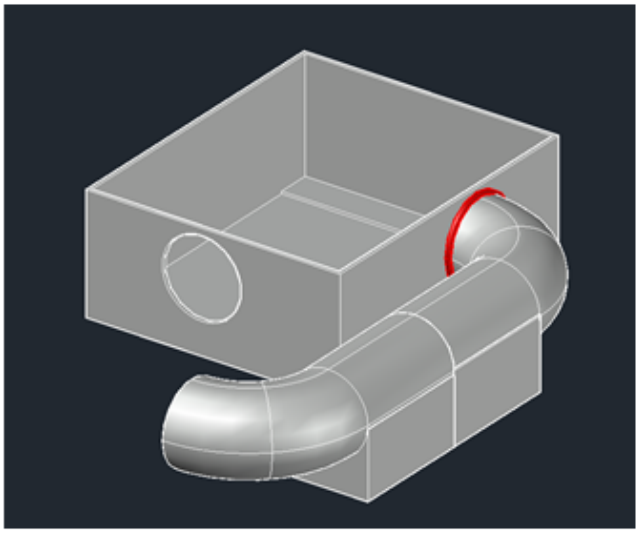

Figure 4. Fuse point 3, silicone placement is marked in red.

4. A4_chamber1 – A8_smallpipe

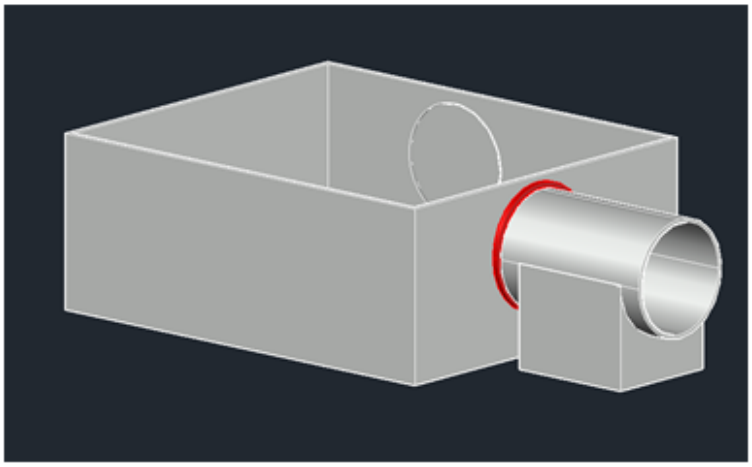

Figure 5. Fuse point 4, silicone placement is marked in red

The silicone should be applied to the outside of the chamber in each case so that it is airtight with no apparent gaps, each application should be done separately and several hours should be given between each to allow to dry (following manufacturer's instructions).

To complete the chamber, the A1_trayseal should be placed on to the end of the main compartment (but not sealed with silicone) thus that no air can escape.

6.3 Electronics

The following equipment will be required to be purchased:

ID	Name	Manufacturer and example link	Indicative price (each)
B1	Arduino Uno R3	RS components - https://my.rs-online.com/web/p/arduino/7154081	£22.09/$24.86/ €25.33
B2	2x Silicone heat pad ~200x50mm	RS components - https://uk.rs-online.com/web/p/heater-pads/1812063	£53.75/$60.50/ €61.63
B3	DHT11 sensor	RS components - https://uk.rs-online.com/web/p/arduino-compatible-boards-kits/2163753	£5.65/$6.36/ €6.48
B4	3x 5V DC axial fan	RS components - https://uk.rs-online.com/web/p/axial-fans/1442027	£23.23/$26.15/ €26.64
B5	Micro-SD card reader Arduino module	Amazon - https://www.amazon.co.uk/kwmobile-Reader-Adapter-Arduino-Microcontrollers/dp/B06XHJTGGC	£5.49/$6.18/ €6.29
B6	Male-Male breadboard wires	RS components - https://uk.rs-online.com/web/p/breadboard-jumper-wires/2048239	£1.20/$1.35/ €1.38
B7	Male-Female breadboard wires	RS components - https://uk.rs-online.com/web/p/breadboard-jumper-wires/2048243	£3.06/$3.44/ €3.51
B8	12v 3A power supply	Farnell - https://cpc.farnell.com/tenma/72-2535/power-supply-1ch-30v-3a-prog/dp/IN07293	£85.73/$96.49/ €98.30
B9	5V 1-channel relay module	Amazon - https://www.amazon.co.uk/Yizhet-Channel-Relay-Control-Optocoupler-Raspberry/dp/B07GXC4FGP?th=1	£5.49/$6.18/ €6.29
B10	9V Arduino power supply	Farnell - https://cpc.farnell.com/pro-elec/pell0028/9v-1a-uk-plug-2-1mm/dp/PW04603	£5.35/$6.02/ €6.13
B11	USB-B to USB-A	RS components - https://uk.rs-online.com/web/p/usb-cables/7587494	£3.06/$3.44/

	cable		€3.51
B12	400-hole breadboard	RS components - https://uk.rs-online.com/web/p/breadboards/1892277	£4.38/$4.93/ €5.02
B13	2x power supply wires with crocodile clips	Amazon - https://www.amazon.co.uk/Akozon-Banana-Output-Adjustable-Regulated/dp/B07K214C6K	£5.74/$6.46/ €6.58
B14	Electrical tape	RS components - https://uk.rs-online.com/web/p/electrical-tapes/4089502	£8.15/$9.17/ €9.34
B15	Micro-SD card	RS components - https://my.rs-online.com/web/p/sd-cards/1805793	£10.64/$11.98/ €12.20
B16	Micro-SD to SD card adaptor	RS components - https://my.rs-online.com/web/p/sd-cards/1805793	£10.64/$11.98/ €12.20
Total	20 items		£343.22/$386.16/ €393.54

Step 1, connect the (B6) male-male wires from the (B1) Arduino to the (B12) breadboard in the following configuration:

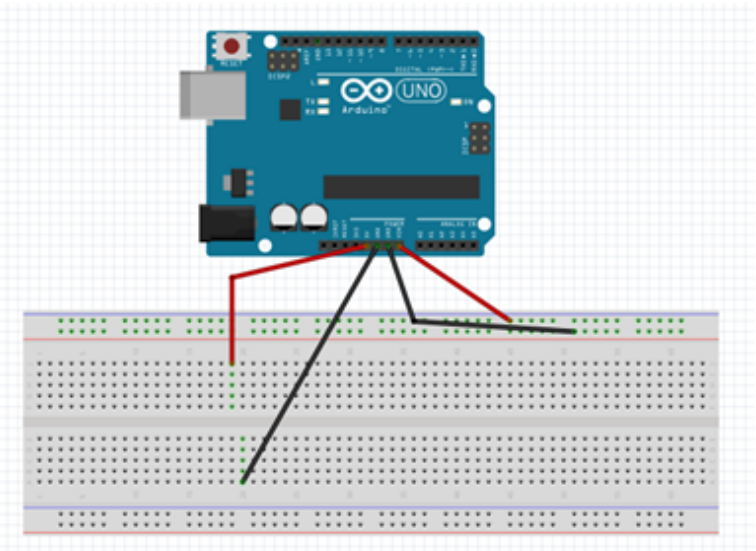

Figure 6. Wiring design connecting wires from the (B1) Arduino to the (B12) breadboard using (B6) male-male wires. Red wires indicate connection to a power source, black wires indicate connection to ground.

Then, connect the wires from the (B4) fans to the (B12) breadboard in the following configuration. Note: the wires from the (B4) fans can be connected directly to the (B12) breadboard, but if more length is required, use (B7) male-female wires with the fan wires being attached to the female end.

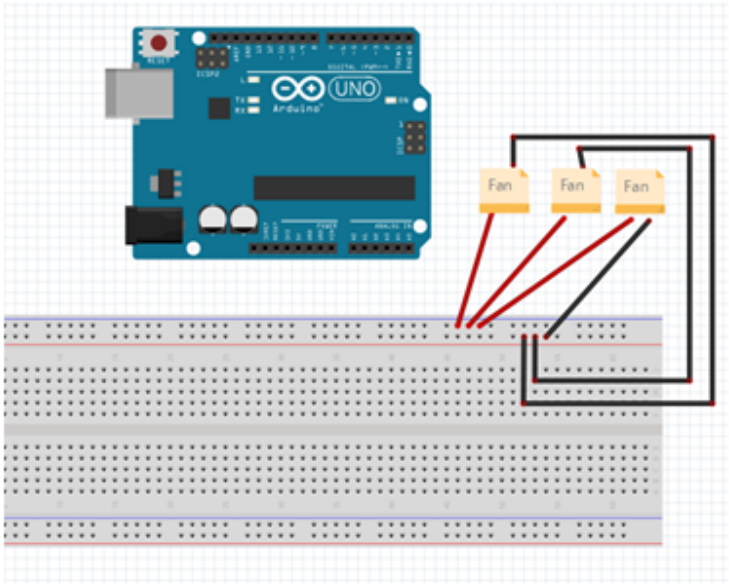

Figure 7. Wiring design connecting (B4) fans to the (B12) breadboard, the (B4) fans will have red and black wires indicating where on the breadboard they should be inserted. Red wires indicate connection to a power source, black wires indicate connection to ground.

With the (B4) fans now connected, connect the (B9) relay module to the (B12) breadboard and (B1) Arduino using (B7) male-female wires in the following configuration:

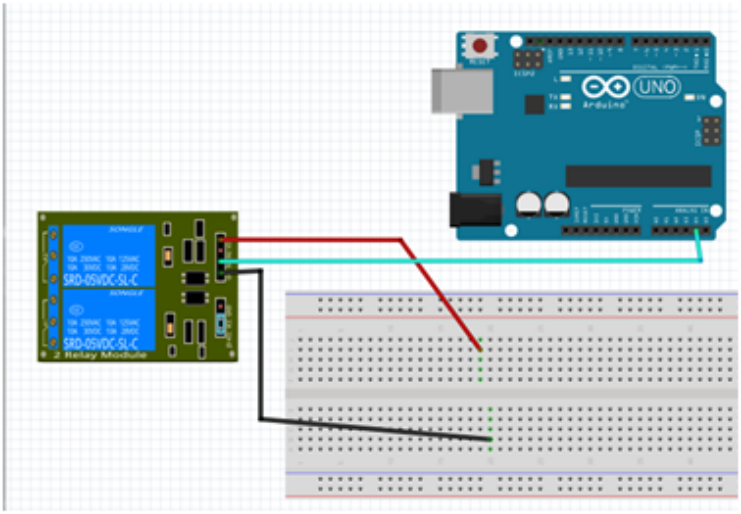

Figrue 8. Wiring design connecting the (B9) relay module to the (B1) Arduino and (B12) breadboard using (B7) male-female wires. Red wires indicate connection to a power source, black wires indicate connection to ground. Blue wires indicate data connection.

Next, connect the (B3) DHT11 sensor to the (B12) breadboard and (B1) arduino via the following configuration:

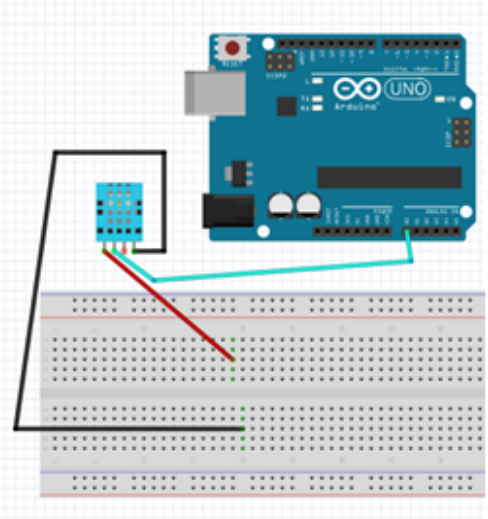

Figrue 9. Wiring design connecting the (B3) DHT11 sensor to the (B1) Arduino and (B12) breadboard using (B7) male-female wires. Red wires indicate connection to a power source, black wires indicate connection to ground. Blue wires indicate data connection.

The final piece of electronics equipment connected to the (B1) Arduino is the (B5) SD card reader, the (B7) female-male wires are connected via the following:

VCC- 5V power supply on breadboard

GND- ground on breadboard

MISO- digital 12 on Arduino

MOSI- digital 11 on Arduino

SCK- digital 13 on Arduino

CS- digital 4 on Arduino

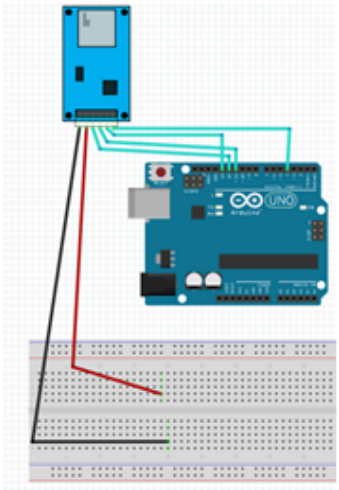

Figrue 10. Wiring design connecting the (B5) SD card module to the (B1) Arduino and (B12) breadboard using (B7) male-female wires. Red wires indicate connection to a power source, black wires indicate connection to ground. Blue wires indicate data connection.

The final step is to connect the (B8) power supply to the (B9) relay module. Firstly, connect the (B13) power supply wires to the (B8) power supply with red-red and black-black. Next, use the crocodile clips to connect the red (B13) power supply wire to a (B6) male-male wire and the other end of the (B6) wire in to the (B9) relay module in the COM1 slot, use a small screwdriver (approximately 3-5mm phillips head) to secure the wire in to place. Then secure the red wire from the first (B2) heat pad in to the 'Normally open' slot (this may be represented as NO1/NO2) next to COM1 and the black wire of the first (B2) heat pad should be taped to the red wire of the second (B2) heat pad with (B14) electrical tape. Finally, the black wire of the second (B2) heat pad should be connected to the crocodile clip for the (B13) black wire of the

power supply. (Note: if the heat pads do not have colours for the wires, any wire choice is acceptable).

With all the electronics connected, the heat pads should be placed in to their respective slots within the (A9_roof2) MT compartment roof section of the build, and the wires led back to the hole located in the centre of the piece and passed through it. Also, the (B3) DHT11 should be placed on the holder for it on the MT compartment roof (A9_roof2) and taped in place. Use silicone to seal the hole, ensuring no air can escape. The same can be repeated for the three (B4) fans in the (A4_chamber1) humidity comprtment using the hole in the roof of the A2_roof1.

6.4 Arduino IDE

The Arduino IDE should be downloaded from the official page at Software | Arduino in order to connect to the (B1) Arduino. Once downloaded and opened, the Arduino file attached to this SOP should be either manually copied or opened in to the Arduino IDE. Load the code from the IDE on to the (B1) Arduino by first plugging the (B1) Arduino in to the (B10) 9V power supply via the black plug on the Arduino and the 5V supply using the (B11) USB cable and plugging it in to the computer running the Arduino IDE, then using the arrow button in the top left corner of the program and wait for the upload to complete.

Once complete, turn on the (B8) power supply using the I/O switch then set the voltage to 12V and the current to 3A, then switch the (B8) power supply to be constant voltage (CV) using the Voltage/Current button. Press the On/Off switch to turn the power supply on. If working, it should display 12V and between 2.5-3A.

In order to switch the temperature that the chamber is attempting to achieve, the code reading:

if (DHT.temperature >= 37) {

AND

else if (DHT.temperature <= 37) {

should be altered thus that the number represents the target temperature. After a test has been completed, the (B15) micro SD card should be inserted in to the (B16) SD card adapter and plugged in to the computer, the text file contains a list of the temperature and humidity values over time (shown as temperature "xx.xx", relative humidity "yy.yy") , and should be saved to the computer then the values deleted and the file resaved within the SD card for the next test. Ensuring the (B15) micro SD card is plugged back in to the (B5) SD module. The SD card currently saves 12 hours of data at 30 second intervals, however this can be changed at the code

if (time > 21600) {

by changing the number to the desired time in seconds.

To begin a test, reclick the arrow button in the Arduino IDE to ensure a fresh start, and open the serial window with the button in the top right of the window.

Note: When performing a test, the order required after the test has started is to close down the serial window first, then plug out the (B11) USB to ensure the data is continuing to save to the SD card properly.

7. FORMS/TEMPLATES TO BE USED

8. INTERNAL AND EXTERNAL REFERENCES

8.1 Internal References

8.2 External References

9. CHANGE HISTORY

SOP no.	Effective Date	Significant Changes	Previous SOP no.

Appendix C

Journal of Food Engineering 336 (2023) 111195

Contents lists available at ScienceDirect

Journal of Food Engineering

journal homepage: www.elsevier.com/locate/jfoodeng

Effect of environmental factors on the kinetics of evaporation of droplets containing bacteria or viruses on different surfaces

Alexander J. Cunliffe [a], Ru Wang [b], James Redfern [a,*], Joanna Verran [c], D. Ian Wilson [b]

[a] Department of Natural Science, Faculty of Science and Engineering, Manchester Metropolitan University, Manchester, M1 5GD, UK
[b] Department of Chemical Engineering and Biotechnology, University of Cambridge, Philippa Fawcett Drive, Cambridge, CB3 0AS, UK
[c] Department of Life Science, Faculty of Science and Engineering, Manchester Metropolitan University, Manchester, M1 5GD, UK

ARTICLE INFO

Keywords:
Bacterial contamination
Viral contamination
Moisture evaporation
Antimicrobial efficacy
Bacterial evaporation

ABSTRACT

The efficacy of antimicrobial surfaces at solid-air interfaces can be assessed using standardised testing methods, typically by placing a droplet inoculated with microorganisms onto the surface and monitoring changes in microbial counts over time (hours). However, the mode of action of the putative antimicrobial may rely on the presence of moisture on the surface, thus it is important to know the time taken for the inoculum to dry, since this will affect resultant counts and thereby deduction as to the efficacy of the antimicrobial.

Droplet (+/− microorganisms) evaporation time was measured on four different surfaces (copper, PVC, polypropylene and nitrile rubber) where temperature, relative humidity and airflow in the test chamber were controlled. The data were compared with simple models based on external mass transfer for predicting the evaporation time: (i) one assuming constant wetted area (CWA), where the diameter of the drop is unchanged but the volume/height decreases; (ii) constant contact angle (CCA), where the diameter of the droplet decreases but the droplet profile/contact angle remains unchanged; and (iii) a mixed mode model.

The mixed mode model gave the best fit to the data, in which evaporation initially followed CWA kinetics, then shifted to CCA when a critical contact angle was reached. The presence of microorganisms consistently and often significantly reduced the evaporation time. Deposited bacteria were visible over the whole wetted area, with a noticeable ring at the original edge of the droplet (the location of the initial solid-liquid-air contact line), consistent with the mixed mode model.

Accumulation of microorganisms and the decrease in evaporation time may affect the effectiveness of antimicrobial materials. The speed of droplet evaporation is affected by a wide range of factors: temperature, humidity, airflow, the nature of the surface and the presence (and nature) of microorganisms. If these factors are not adequately recognised or controlled, then results from testing methods carried out under different (unspecified) environmental conditions in different laboratories, are liable to vary and give rise to confusion and misinterpretation.

1. Introduction

There is widespread interest in the development of active, non-porous surfaces as part of a microbial control strategy. Much of the work in this area has focused on combatting bacterial (and spore) infection but recent events have seen a concerted effort on developing surfaces which are effective at deactivating viruses (Kumari and Chatterjee, 2021). Due to the increasing threat of antimicrobial resistance and increasing awareness and ongoing impact of viral pandemics and understanding that pathogens such as SARS-CoV-2 can remain viable on surfaces for extended periods of time (Chatterjee et al., 2021), novel approaches to controlling microorganisms in indoor settings is likely to remain a priority. As such, many novel methods for generating antimicrobial surfaces are being reported in the literature, e.g. metallic metals such as copper and topographical changes, coatings, and inclusion of nano- and/or photocatalytic materials, (Grass et al., 2011; Hassan et al., 2020; Imani et al., 2020; Ratova et al., 2018). Testing of such surfaces is often based on standardised methods (Cunliffe et al., 2021), designed to enhance lab-to-lab reproducibility (although this is not always achieved). However, the conditions that the methods stipulate are not always applicable to the conditions likely found in the intended end-use environment, such as hospitals. An example of this is relative humidity

* Corresponding author.
E-mail address: J.Redfern@mmu.ac.uk (J. Redfern).

https://doi.org/10.1016/j.jfoodeng.2022.111195
Received 25 February 2022; Received in revised form 19 June 2022; Accepted 21 June 2022
Available online 27 June 2022

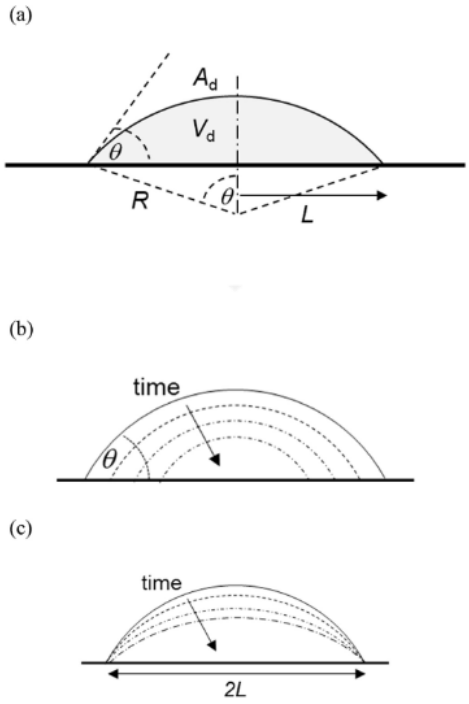

Fig. 1. Schematics of small sessile drops undergoing evaporation. The Bond number is small so surface tension dominates gravity and the drop shape is a truncated sphere. (a) Geometry, showing drop volume V_d, liquid-air interface area A_d, drop radius R, wetted radius L and contact angle θ. Droplet evaporating under (b) constant contact angle (CCA) mode, L decreases over time, and (c) constant wetted area mode (CWA: L constant, θ decreases over time).

(RH), which determines whether a water film will be present on a surface and how long it would take to dry. A second is the presence of convective air currents generated by ventilation, draughts and motion of personnel, which enhance the transport of heat and mass involved in evaporation. In many standardised antimicrobial test methods, such as the commonly used BS ISO 22196 (BS ISO 22196, 2011), relative humidity is kept artificially high (>90%) and airflow is absent. Since the efficacy of many antimicrobial coatings and surfaces may rely on the presence of moisture, e.g. metallic silver (Rai et al., 2009), the ability to predict moisture evaporation times is needed in order to be able to relate laboratory tests to application. This study focuses on humidity and temperature: the effect of convection is demonstrated in benchmarking studies with water and is not considered further here.

Redfern et al. (2018) developed a surface testing chamber which allowed the temperature and relative humidity of the atmosphere, as well as local air flow velocity, to be controlled independently of one another. They showed that the size of water droplets as well as these environmental parameters determined the time taken for a drop of water to evaporate. They fitted their data to a generalised quadratic model which fitted the data reasonably well ($R^2 = 0.872$) and demonstrated the importance of the four factors. One of the challenges with such empirical models is that they are not suited for extrapolation, that is, to predict the result when another parameter is altered: further testing (for training the model) is required.

In this paper we demonstrate that Redfern et al.'s results are consistent with the predictions of a first order quantitative model based on external mass transfer control. Several workers have presented models for droplet evaporation under well-controlled quasi-stagnant air conditions (e.g. Hu and Larson, 2002), and used these to demonstrate the effect of tailored surfaces (e.g. Sobac et al., 2011) on evaporation. The interest in the 'coffee ring effect' observed when droplets of colloidal suspensions evaporate (e.g. Deegan et al., 1997, 2000) has prompted extensive work in this area, including phenomena such as Marangoni flows arising from variation in surface tension generated by non-uniform temperature and concentration profiles. These effects are not considered here.

The nature of the surface influences the rate of evaporation through the behaviour of the three-phase contact line (where the air, solid and liquid interfaces coexist): on a homogeneous solid with no preferential concentration of suspended or dissolved species at the contact line, one would expect the droplet to exhibit a constant contact angle (CCA), θ (Fig. 1(a)) and retain its shape (but not diameter) as it dried, labelled CCA behaviour (Fig. 1(b). With heterogeneous surfaces, effects such as contact line pinning can give rise to a constant wetted solid surface area ($\pi L^2 = \pi(R\sin\theta)^2$, Fig. 1(c)), altering the surface area to volume ratio for the droplet. This is labelled constant wetted area (CWA) behaviour. Other factors determine the transition between CCA and CWA behaviour: for instance, Soulié et al. (2015) observed CCA behaviour in water and saline solutions with NaCl concentrations $<10^{-6}$ M, and CWA behaviour at higher concentrations. This study employs droplets with saline or buffer concentrations above this threshold.

We show that the variation in Redfern et al.'s data for evaporation of water drops can be related to mixed contact line behaviour, involving CWA behaviour initially while the shape of the drop changes from advancing contact angle, θ_a, to receding contact angle, θ_r, mode (appropriate for a shrinking droplet) followed by shrinkage subject to CCA behaviour (i.e. pinned but then shrinks). This demonstrates that the mode of evaporation cannot be assumed to be simply CWA or CCA, and should be taken into account by those interested in the rate at which evaporation occurs from an antimicrobial material, due to the length of time evaporation takes to occur being likely to determine the length of time an antimicrobial material remains active.

The phenomenology underpinning advancing and retreating contact angles is described by Bormashenko (2017): note that $\theta_a - \theta_r > 0$ even for uniform homogeneous surfaces. Contact line pinning is known to arise with the evaporation of suspensions (e.g. Deegan et al., 2000). The evaporation of concentrated colloidal suspensions and polymer solutions has been studied at length (e.g. Larson, 2014; Soulié et al., 2015; Eales et al., 2016) owing to interest in inkjet applications and to the 'coffee ring effect' where a layer or layers of particles is deposited at the initial contact line. Aerosols contaminated by bacteria and other microorganisms represent examples of dilute suspensions, and thus the effect of the presence of microorganisms in the droplets on the rate of droplet evaporation and the pattern of deposition on non-porous surfaces are also investigated in this study. Deleplace et al. (2022) recently presented studies of 'coffee rings' and other deposition patterns generated by evaporation of droplets containing hydrophobic and hydrophilic *Bacillus* spores on stainless steels, polypropylene and glass. They outlined the importance of these factors to process and product hygiene, and the consequences of the deposit patterns on the ease of removal of the organisms using a rinsing or cleaning procedure. They observed noticeable differences arising from surface and organism properties. Deposits that had not dried completely were significantly more resistant to cleaning. Their analysis did not, however, link the observations to evaporation rates.

Few workers have considered the effect of forced convection on droplet evaporation. Investigations of mass transfer from droplets in duct flows (e.g. Coutant and Peuski, 1982) tend to feature well-defined

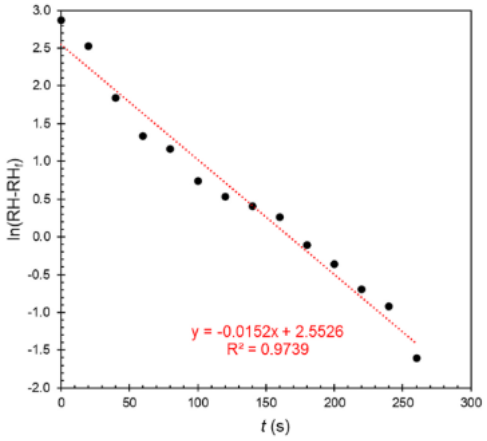

Fig. 2. Approach of chamber relative humidity, RH, to equilibrium value, RH_f, following closure of the chamber lid. The initial value (relative humidity in the room) was 23% and RH_f (saturated K_2CO_3 solution) 43%. Data are plotted in the form of Equation [A3].

duct geometries, where the enhancement of drying by convection can be discussed in terms of a Reynolds number for the bulk flow based on the hydraulic diameter as well as a Reynolds number based on the initial droplet dimensions. Well defined flow conditions are rarely observed in practice and we briefly establish the significance of the convective contribution in Redfern et al.'s tests for aqueous solutions: the impact of an external shear force on the droplet shape and Marangoni effects is beyond the scope of the simple mass transfer models presented here and a study of convective effects on evaporation of droplets containing organisms represents a subject for further work.

The findings of this work can be strengthened by more in-depth and detailed experimentation and analysis, including direct monitoring of the shape of the droplets to confirm the behaviour postulated here. The current study employs a first order model describing evaporation, and there is considerable scope for including the contributions included in more detailed modelling approaches.

2. Modelling

2.1. Transient chamber conditions

A detailed description of the chamber is given by Redfern et al. (2018) and a summary is provided in the Supplementary Information. The temperature was controlled by a heating pad and the relative humidity inside the chamber was set by Petri dishes containing saturated salt solutions. The chamber's use of side compartments to introduce test surfaces on which droplets had been deposited minimised the impact of this operation on the humidity (and relative humidity, RH) within the chamber. Fig. 2 shows that it took around 4 min to re-establish equilibrium in the chamber when the lid had been opened, which would

Table 1
Summary of water droplet evaporation tests by Redfern et al. (2018) on polypropylene.

Volume (μL)	R_0 (mm)	Bo (−)	Temperature (°C)	Relative humidity (%)	t_c (s)
2	1.05	0.15	21.5–31.2	27.3–63.7	32–99
5	1.42	0.27	22.6–29.2	35.4–68.6	69–169
10	1.79	0.43	21.5–31.3	25.8–62.7	92–257
20	2.26	0.69	21.7–31.2	25.5–61.8	146–455

Table 2
Advancing contact angles (± standard deviation) measured for 1 μL droplets. All values are rounded to the nearest whole number. Asterisk denotes where contact angle is significantly different ($p < 0.05$) between 1 μL (below) and 5 μL (Table 3) measurements.

Liquid	Organism	Polypropylene	Nitrile	PVC	Copper
Water	–	82° (±3°)	97° (±4°)	60° (±2°)	74° (±3°)
Saline	–	84° (±1°)*	104° (±2°)	65° (±7°)	68° (±4°)
Saline	*E. coli*	86° (±4°)	93° (±2°)	64° (±6°)	51° (±6°)
Saline	*P. syringae*	79° (±2°)	95° (±4°)	71° (±6°)	65° (±9°)
SM buffer	–	85° (±4°)	100° (±6°)	59° (±6°)	58° (±6°)
SM buffer	*Phi6*	82° (±2°)	88° (±5°)	64° (±3°)	63° (±3°)
SM buffer	*PhiX174*	83° (±2°)	78° (±2°)	65° (±3°)	71° (±2°)

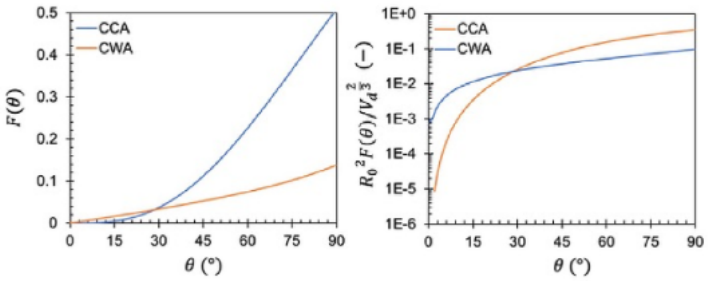

Fig. 3. Effect of contact angle on geometric functions (a) F_θ (CCA mode) and F_1 (CWA mode), Equations [5] and [8], respectively. (b) Scaled products, $R_0^2 F_\theta / V_d^{2/3}$ and $R_0^2 F_1 / V_d^{2/3}$, for initial droplet volume $V_d = 2\,\mu L$. For CWA, θ is the initial contact angle as $\theta \to 0$ as the drop evaporates. Note the log scale on the ordinate axis in (b).

Table 3
Advancing contact angles (± standard deviation) measured for 5 μL droplets. All values are rounded to the nearest whole number. Asterisk denotes where contact angle is significantly different ($p < 0.05$) between 1 μL (Table 2) and 5 μL (below) measurements.

Liquid	Organism	Polypropylene	Nitrile	PVC	Copper
Water	–	79° (±0°)	101° (±7°)	57° (±9°)	68° (±4°)
Saline	–	81° (±1°)*	104° (±2°)	70° (±9°)	64° (±2°)
Saline	*E. coli*	80° (±1°)	96° (±2°)	62° (±2°)	49° (±3°)
Saline	*P. syringae*	78° (±1°)	95° (±2°)	67° (±5°)	66° (±5°)
SM buffer	–	82° (±1°)	100° (±6°)	73° (±4°)	54° (±6°)
SM buffer	*Phi6*	88° (±5°)	96° (±3°)	75° (±1°)*	59° (±6°)
SM buffer	*PhiX174*	84° (±1°)	90° (±5°)	60° (±6°)	68° (±2°)

introduce undesirable transients into any droplet evaporation study, where the evaporation times ranged from 30 to 450 s. The data are plotted in the form $ln(RH\text{-}RH_{final})$ vs. time *t* as this is the trend predicted by mass transfer control models (see Appendix). When the side compartments were used the RH did not change by more than a few percent.

2.2. Drop evaporation

This work considers droplets with Bond numbers <1,[1] so the droplet shape can be approximated as a spherical cap (a truncated sphere, see Fig. 1) and the surface area and volume estimated using geometric relationships. The droplet is assumed to be at constant temperature, *i.e.* heat transfer limitations do not arise nor Marangoni effects arising from temperature differences over the drop. The rate of droplet evaporation will be proportional to the area of the liquid/air interface, $A_d = 2\pi R^2(1 - \cos\theta)$, while its volume is given by $V_d = \frac{1}{3}\pi R^3(2 + \cos\theta)(1 - \cos\theta)^2$. For a drop of liquid with molar density ρ_m, the rate of mass transfer in the absence of thermal effects can be written as

$$\frac{d}{dt}(V_d\rho_m) = -A_c\bar{k}_m C_T(y^* - y_b) \quad [1]$$

where y_b is the mol fraction of the evaporating species in the chamber vapour space (related to the humidity, *H*), y^* is that in equilibrium with the drop, C_T the molar concentration in the vapour phase and $\bar{k}_m$ is an average mass transfer coefficient. Redfern et al. studied water droplets so changes in concentration and vapour pressure over time did not arise. Experiments conducted in the current work also considered aqueous salt and buffer solutions, where the concentration is expected to change over time: the impact of the presence of salts is discussed.

In estimating an evaporation time, we assume quasi-steady state, which is expected to apply as the contact angles considered are not small. Writing $\bar{k}_m$ in terms of the dimensionless mass transfer coefficient for a sphere, the Sherwood number, $\overline{Sh} \equiv 2R\bar{k}_m/D$ (where *D* is the diffusivity of evaporating species in air), gives

$$\frac{d}{dt}(V_d) = -\frac{A_d}{2R}\frac{DC_T\overline{Sh}}{\rho_m}(y^* - y_b) \quad [2]$$

We consider three scenarios: (i) constant contact angle, where the droplet radius *R* decreases from its initial value, R_0, to zero (Fig. 1(b)); (ii) constant wetted area, where dimension $L = R_0\sin\theta_0$ is constant due to contact line pinning or other effects and θ decreases over time (Fig. 1(c)); and (iii) mixed mode, where CWA behaviour is observed initially as the droplet, with shape initially set by the advancing contact angle θ_a, changes to that given by the receding contact angle as liquid evaporates,

[1] The Bond number $Bo = g\Delta\rho R^2/\gamma$ compares gravitational forces to capillary ones. Here γ is the liquid-air surface tension, *g* is the gravitational constant, *R* is the droplet radius and $\Delta\rho$ is the difference in density between the liquid and air.

Table 4
Effect of droplet composition on evaporation times, with reference to CCA model (Figs. 6–9). Anova and Tukey HSD tests determined pairwise statistical significance ($p < 0.05$), with ~ denoting no significant difference but observed increase in evaporation time, and > denoting a statistically significant difference supporting the observed increase in evaporation time. *SMB – SM buffer.*

Surface	Humidity range	Droplet volume	Trend in evaporation times	
			Liquids	Suspensions
Polypropene	Low	1 μL	SMB ~ saline > water	Saline > *E. coli* ~ *P. syringae* SMB ~ *Phi X174* ~ *Phi6*
		5 μL	SMB ~ saline > water	Saline ~ *E. coli* ~ *P. syringae* SMB ~ *Phi X174* ~ *Phi6*
	Mid	1 μL	SMB > Saline > water	Saline > *P. syringae* ~ *E. coli* SMB > *Phi6* ~ *Phi X174*
		5 μL	SMB ~ Saline ~ water	Saline ~ *E. coli* ~ *P. syringae* SMB > *Phi6* > *PhiX174*
Nitrile	Low	1 μL	Water ~ saline ~ SMB	Saline > *E. coli* > *P. syringae* SMB > *Phi X174* > *Phi6*
		5 μL	Water ~ Saline ~ SMB	Saline ~ *P. syringae* ~ *E. coli* SMB ~ *Phi X174* ~ *Phi6*
	Mid	1 μL	SMB ~ saline ~ water	Saline ~ *P. syringae* ~ *E. coli* SMB ~ *Phi6* ~ *Phi X174*
		5 μL	SMB ~ water ~ saline	Saline > *E. coli* > *P. syringae* SMB > *Phi6* > *Phi X174*
Copper	Low	1 μL	SMB ~ Saline ~ water	Saline > *E. coli* ~ *P. syringae* SMB > *Phi X174* > *Phi6*
		5 μL	Saline ~ SMB ~ water	Saline ~ *P. syringae* > *E. coli* SMB ~ *Phi X174* ~ *Phi6*
	Mid	1 μL	Saline ~ SMB > water	Saline ~ *E. coli* > *P. syringae* SMB > *Phi6* ~ *Phi X174*
		5 μL	Water ~ Saline ~ SMB	Saline > *P. syringae* ~ *E. coli* SMB > *Phi X174* > *Phi6*
PVC	Low	1 μL	Saline ~ SMB ~ water	Saline ~ *E. coli* > *P. syringae* SMB > *Phi6* ~ *Phi X174*
		5 μL	SMB ~ saline > water	Saline ~ *P. syringae* > *E. coli* SMB ~ *Phi X174* ~ *Phi6*
	Mid	1 μL	Saline ~ SMB > water	Saline ~ *P. syringae* > *E. coli* SMB > *Phi X174* > *Phi6*
		5 μL	SMB ~ saline ~ water	Saline > *P. syringae* ~ *E. coli* SMB ~ *Phi X174* ~ *Phi6*

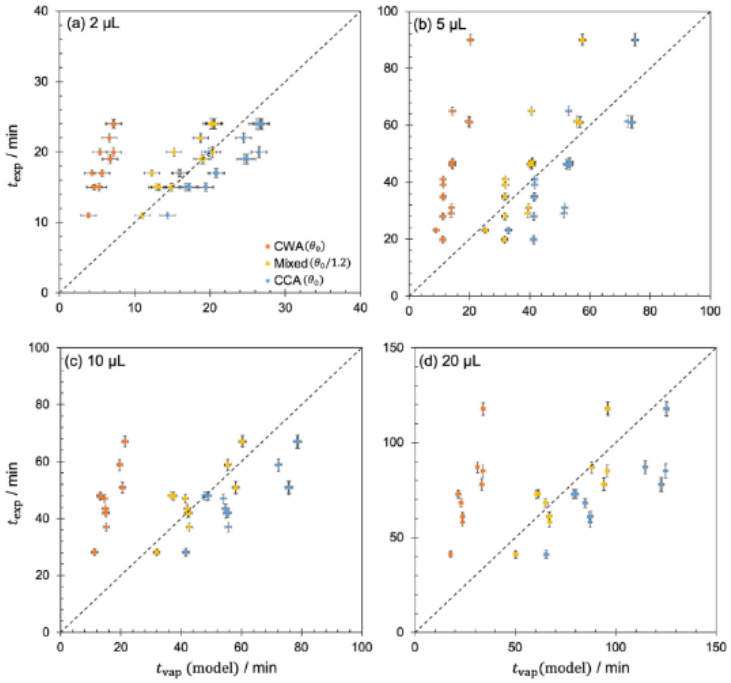

Fig. 4. Comparison of evaporation times of water droplets (Redfern et al., 2018) in stagnant air with model prediction for CCA mode (blue symbols), CWA (orange symbols), and mixed, for $\theta_r = \theta_0/1.2$ (yellow symbols) for drops with initial volume of (a) 2 µL, (b) 5 µL, (c) 10 µL and (d) 20 µL. Dashed locus shows the line of equality, i.e. $y = x$. Vertical error bars indicate the range in experimental values: horizontal error bars indicate the uncertainty in the model predictions.

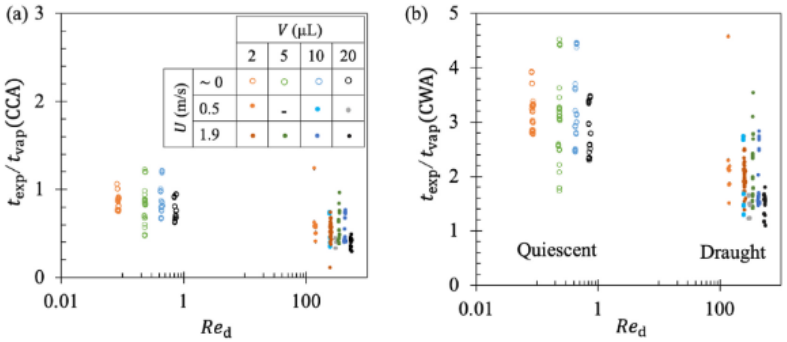

Fig. 5. Effect of convection, expressed as droplet Reynolds number, on evaporation time for water droplets. For the purposes of illustration, a mean velocity of 1 mm s^{-1} is used in the calculation of the Reynolds number for the quasi-static cases ($Re_d \sim 0$ for these cases). The evaporation time is scaled by the predicted evaporation time in stagnant air for (a) CCA mode, and (b) CWA mode. Symbols: hollow, quiescent; solid, fan on.

followed by CCA behaviour with $\theta = \theta_r$.

(i) Constant contact angle, CCA

Writing $\Delta y = (y^* - y_b)$ and introducing the above expressions for V_d and A_d for fixed θ gives:

$$R\frac{dR}{dt} = \frac{1}{2}\frac{dR^2}{dt} = -\frac{1}{(2+\cos\theta)(1-\cos\theta)}\frac{DC_T\Delta y}{\rho_m}\overline{Sh} \quad [3]$$

Integrating from initial radius R_0 at time zero gives

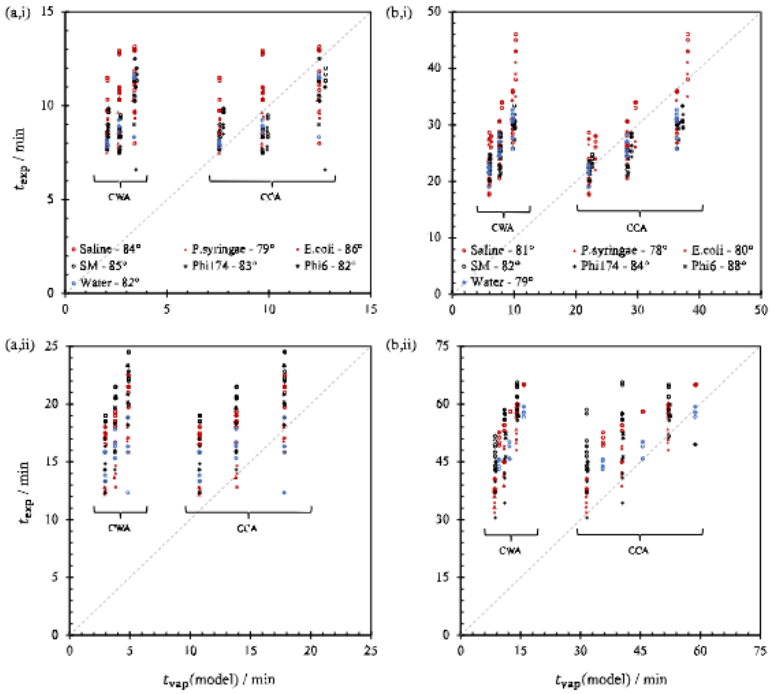

Fig. 6. Comparison of liquid drop evaporation times in stagnant air on polypropylene with CCA and CWA model predictions. Liquid drops with initial volume of (i) 1 μL or (ii) 5 μL, and at (a) low humidity and (b) mid humidity. The three groups in each plot correspond to temperatures of 22, 26 and 30 °C (with higher temperature giving shorter evaporation time). Dashed locus shows the line of equality, i.e. $y = x$. *P. syringae* and *E. coli* prepared in saline, *Phi X174* and *Phi6* in SM buffer. The contact angle indicated in the legend is the measured static contact angle of the liquid drop on the polypropylene surface (see Tables 2 and 3).

$$R_0^2 - R^2 = -\frac{2}{(2+\cos\theta)(1-\cos\theta)}\frac{\overline{Sh}DC_T\Delta y}{\rho_m}t \quad [4]$$

and a time for droplet evaporation, t_{vap}, of

$$t_{vap} = \left[\frac{(2+\cos\theta)(1-\cos\theta)}{2\overline{Sh}}\right]\left[\frac{\rho_m R_0^2}{DC_T\Delta y}\right] = F_\theta t_c \quad [5]$$

where F_θ is a geometric function and t_c is a characteristic timescale for droplet evaporation. For the case of a hemispherical drop ($\theta = \pi/2$, symmetrical), $\overline{Sh} = 2$ and $F_\theta = 1/2$. For other values of θ the local flux varies over the interface: Hu and Larson (2002) reported the following result for $0 \leq \theta \leq \pi/2$ for evaporation controlled by external mass transfer:

$$\frac{d}{dt}(\rho_m V_d) = -\pi R D C_T \Delta y\left(0.27\theta^2 + 1.30\right) \quad [6]$$

which, when substituted into [2], gives the dependency of F_θ on θ shown in Fig. 3. Contributions from natural convection are neglected. Smaller contact angles increase the interfacial area per unit droplet volume and, for the constant θ case, shorten the evaporation time for a given value of R_0.

For a given droplet volume, as used in these experiments, R_0 depends on θ. Equation [5] indicates that the value of θ affects the drying time for a droplet of initial volume V_d via the product $R_0^2 F_i$, where $R_0 \propto \{V_d/(2+\cos\theta)(1-\cos\theta)^2\}^{1/3}$ and subscript i denotes the drying mode.

The other parameters in the characteristic drying time do not depend on the drop size in this model. Fig. 3(b) shows how the product $R_0^2 F_\theta / V_d^{2/3}$ varies with θ for $1 \leq \theta \leq 90°$ (the product is scaled by the characteristic area associated with the droplet volume, $V_d^{2/3}$, to make it dimensionless). The plot shows that $R_0^2 F_\theta$ (and thus the drying time) is very sensitive to θ for $\theta \leq 45°$: over the range of θ values of interest in this work (Tables 2 and 3, 45–90°) the CCA result increases modestly with θ.

The above result indicates that selecting a surface so that a liquid will spread on it (small θ) therefore has the counter-productive property for antimicrobial materials which rely on the surface being wet, as this can enhance the rate at which the liquid evaporates, limiting the amount of time the surface will remain antimicrobial. It should be noted that the CCA model is not valid for $\theta \sim 0$ (when the drop is effectively a puddle).

(ii) Constant wetted area, CWA

When the contact line is pinned, the radius of the wetted area, L, remains constant, and the contact angle changes over time as the volume of the drop decreases. Using the Hu and Larson result, Equation [2] becomes:

$$\frac{1}{3}\frac{(1-\cos\theta)^2}{\sin^4\theta\left(0.27\theta^2+1.30\right)}d\theta = -\frac{DC_T\Delta y}{\rho_m R_0^3 \sin^2\theta_0}dt \quad [7]$$

Integrating from θ_0 to zero gives

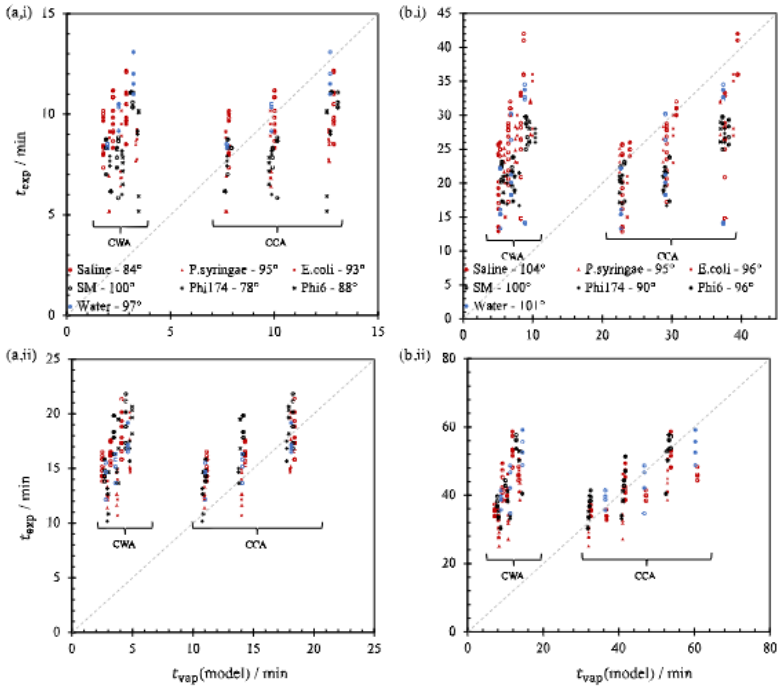

Fig. 7. Comparison of liquid drop evaporation times in stagnant air on nitrile with CCA and CWA model predictions. Liquid drops with initial volume of (i) 1 μL or (ii) 5 μL, and at (a) low humidity and (b) mid humidity at temperatures of 22, 26 and 30 °C. Dashed locus shows the line of equality, i.e. $y = x$. *P. syringae* and *E. coli* prepared in saline, *Phi X174* and *Phi6* in *SM* buffer. The contact angle indicated in the legend is the measured static contact angle of the liquid drop on the nitrile surface (see Tables 2 and 3).

$$t_{vap} = \left\{ \frac{\sin^2\theta_0}{3} \int_0^{\theta_0} \frac{(1-\cos\theta)^2}{\sin^4\theta\left(0.27\theta^2+1.30\right)} d\theta \right\} \left[\frac{\rho_L R_0^2}{DC_T\Delta y} \right] = F_L t_c \qquad [8]$$

with the *same* characteristic timescale. Fig. 3 shows that a smaller contact angle again results in a shorter evaporation time. Comparing F_θ and F_L, there is a transition at 28° indicating that for strongly wetting liquids (small θ) a droplet following CCA behaviour for a given θ will evaporate completely in a shorter time.

Fig. 3 (b) shows the effect of initial contact angle on evaporation of droplets of equal initial volume. The drying time increases with θ, as in the CCA case, but the range is noticeably smaller, varying by 1½ decades compared to 4½ decades for CCA. The two values are similar for $\theta \sim 28°$, with CWA times significantly larger for the CWA mode on surfaces that encourage wetting (low θ).

(iii) Mixed model

In the mixed model, the droplet evaporates initially with constant wetted area as the contact angle decreases from $\theta_0 = \theta_0$ until it reaches θ_r. Thereafter, the decrease in volume of the drop is modelled as the wetted area decreasing following CCA behaviour, with $\theta = \theta_r$. Combining the CWA and CCA models, the evaporation time is given by:

$$\frac{t_{vap}}{t_c} = \left\{ \frac{\sin^2\theta_0}{3} \int_{\theta_r}^{\theta_0} \frac{(1-\cos\theta)^2}{\sin^4\theta\left(0.27\theta^2+1.30\right)} d\theta + \left[\frac{(2+\cos\theta)(1-\cos\theta)}{2\overline{Sh}} \right] \right\} \qquad [9]$$

For a given liquid, t_c is set by the size of the droplet and the atmospheric conditions. The contact angles and the kinetic factors, *e.g.* F_L and F_θ, are determined by the surface and its interaction with the droplet. Comparison of the evaporation times with the model predictions will indicate how long the surface remains wetted and thus the likelihood of antimicrobial activity.

3. Materials and methods

3.1. Preparation of materials and chamber

Non-porous test sections measuring 10 mm × 10 mm were cut from copper (CuSn5), polyvinyl chloride (PVC), polypropylene and nitrile sheet. Prior to use, all sections were wiped thoroughly with cloth soaked in 70% ethanol and left to dry in aseptic conditions for 60 min. Sections were secured to a polystyrene base plate (127.7 × 85.4 mm) using double-sided tape and placed inside the environmental control chamber. The environmental control chamber (internal dimensions 296 mm × 171 mm × 51 mm) allowed temperature and relative humidity (RH) to be controlled independently. To maintain the desired RH, saturated solutions of lithium chloride (180 g and 60 mL of water, producing a RH of 15%) or potassium carbonate (200 g and 60 mL of water, producing a

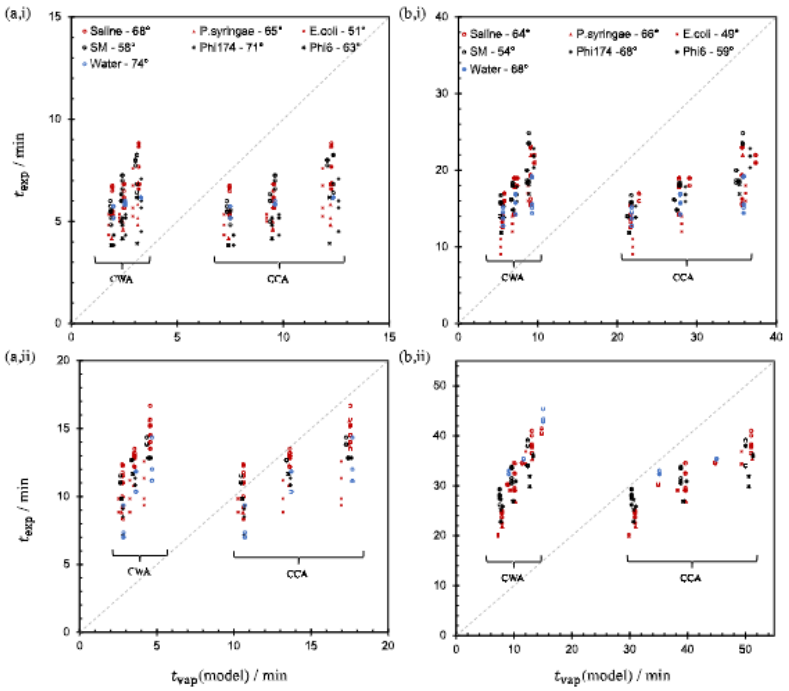

Fig. 8. Comparison of liquid drop evaporation times in stagnant air on copper with CCA and CWA model predictions. Liquid drops with initial volume of (i) 1 μL or (ii) 5 μL, and at (*a*) low humidity and (*b*) mid humidity at temperatures of 22, 26 and 30 °C. Dashed locus shows the line of equality, i.e. $y = x$. *P. syringae* and *E. coli* prepared in saline, *Phi X174* and *Phi6* in SM buffer. The contact angle indicated in the legend is the measured static contact angle of the liquid drop on the copper surface (see Tables 2 and 3).

RH of 40%) were distributed evenly across four Petri dishes inside the chamber and RH monitored using a HD500 sensor and datalogger (Extech Instruments). Temperature was adjusted and maintained with a propagation heat mat (PVC, 18 W, 220 V) and monitored with a thermostat (Vivosun, Shanghai, China).

3.2. Preparation of solutions and microbial suspensions

Deionised water was sterilised by autoclaving at 121 °C for 15 min. Saline solutions were prepared as 0.85 wt% NaCl (ThermoFisher Scientific) in deionised water and sterilised by autoclaving. SM buffer was prepared by adding 5.8 g of NaCl, 2 g of $MgSO_4{\cdot}6H_2O$ and 50 mL 1 M Tris-Cl pH 7.5–800 mL distilled water and mixed until dissolved, adjusted to 1 L with distilled water and sterilised by autoclaving at 121 °C for 15 min. Tris-Cl was prepared by adding 12.11 g of 1 M tris base to 80 mL distilled water and mixed until dissolved with the pH adjusted to 7.5 by adding 30 wt% HCl. Both the saline and buffer solution concentrations are large compared to the concentration at which Soulié et al. (2015) reported the onset of CWA behaviour.

Bacteria were maintained as streak (purity) plates on tryptone soya agar (TSA) at 4 °C until required. *Escherichia coli* (ATCC 13706) and *Pseudomonas syringae* (ATCC 21781) cultures were prepared for the experiments by inoculating one colony of bacteria from the respective streak plates, transferring to 10 mL TSB and incubating at 37 °C and 28 °C, respectively, for 24 h. Bacterial cultures were then centrifuged at 3500 rpm for 10 min. The supernatant was removed, and 10 mL sterile saline added, with the resultant suspension mixed by vortex (this process was repeated once). Suspensions were then adjusted to 0.5OD at 600 nm (determined by spectrophotometer (Jenway)) using sterile saline.

Bacteriophage Phi6 (ATCC 21781-B1) and PhiX174 (ATCC 13706-B1) suspensions were prepared following a standard phage assay protocol (Adams, 1959). In brief, a 10-fold serial dilution of stock phage was performed up to 10^{-8} in SM buffer. Subsequently, for each dilution, 100 μL of bacteriophage was mixed with 100 μL of corresponding bacterial overnight culture (*Pseudomonas syringae* (ATCC 21781) for Phi6 and *Escherichia coli* (ATCC 13706) for Phi ×174) and 3 mL of soft (0.7% w/v) molten (45–55 °C) TSA and poured onto a regular strength TSA agar plate. Following an 18-h incubation (30 °C), any plaques present on each dilution were counted and used to calculate the number of plaque forming units (PFU), which allowed the original phage stock to be adjusted to the desired concentration of 5×10^7 PFU/mL.

3.3. Preparation of scanning electron microscope (SEM) images

To assess deposition of bacteria on surfaces, 5 μL droplets of either *E. coli* (ATCC 13706) or *P. syringae* (ATCC 21781) were placed on a test section and left to dry in an environment with RH = 60% and 22 °C. Once dried, the surfaces were immersed in a Petri dish containing 2.5% glutaraldehyde for 18 h, then washed with sterile phosphate buffered saline (PBS, 0.85 wt% NaCl), placed in increasing concentrations (20%, 40%, 60%, 80%) of ethanol for 30 min each, and then submerged in 100% ethanol for 30 min, twice. The surfaces were then left to dry in a

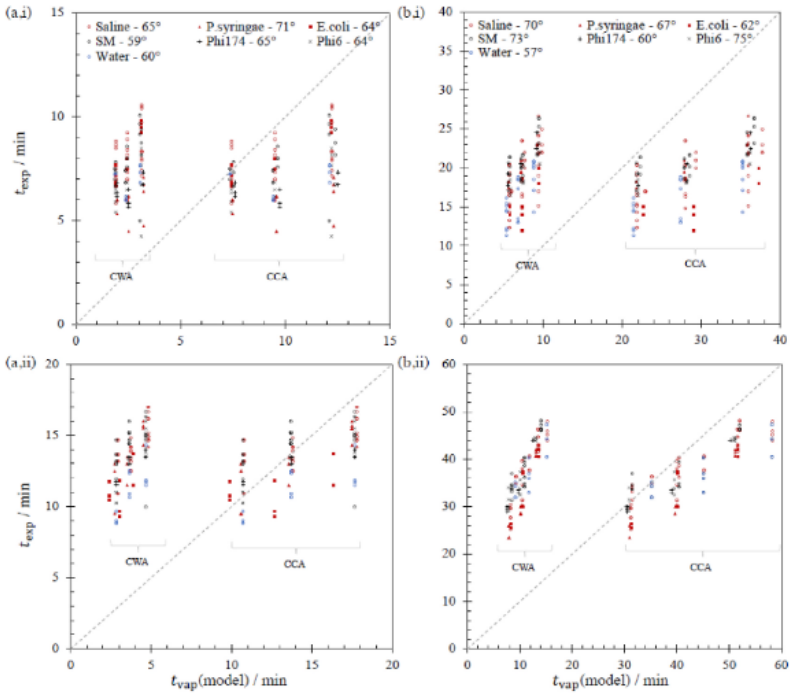

Fig. 9. Comparison of liquid drop evaporation times in stagnant air on PVC with CCA and CWA model predictions. Liquid drops with initial volume of (i) 1 μL or (ii) 5 μL, and at (a) low humidity and (b) mid humidity at temperatures of 22, 26 and 30 °C. Dashed locus shows the line of equality, i.e. $y = x$. *P. syringae* and *E. coli* prepared in saline, *Phi X174* and *Phi6* in SM buffer. The contact angle indicated in the legend is the measured static contact angle of the liquid drop on the PVC surface (see Tables 2 and 3).

vacuum sealed desiccator for a minimum of 18 h. Samples were then mounted onto aluminium pin stubs using adhesive carbon tabs and coated with a thin layer (25 nm) of Au metal using a sputter coater (Polaron, 30 s, 800 V, 5 mA). The stubs were then loaded into the FE-SEM (Carl Zeiss Ltd, Supra 40VP, SmartSEM) for imaging and analysis. The secondary electron detector was used to obtain images of the samples, using an acceleration voltage of 2 kV and a working distance of approximately 5 mm.

3.4. Measurement of contact angles

Images of droplets on each material were captured by pipetting droplets of 1 μl or 5 μl on to the surface, followed by measuring the contact angle (average of left and right tangent contact angles) using a goniometer (Krüss mobile drop GH11). Droplets were assessed in triplicate and each measurement was performed on a different coupon of material. To ascertain if contact angles for each liquid type on each material can be considered the same or statistically significantly different ($p < 0.05$), a *t*-test was performed comparing contact angles at 1 μl and 5 μl.

3.5. Evaporation of solutions and suspensions

To assess the impact of the presence of microorganisms on the time it takes droplets to dry, droplets of saline containing either *E. coli* (ATCC 13706) or *P. syringae* (ATCC 21781) were compared with droplets of saline without bacteria. Additionally, droplets of SM buffer containing either Phi6 (ATCC 21781-B1) or PhiX174 (ATCC 13706-B1) bacteriophage were compared with droplets of SM buffer without bacteriophage. Droplets of either 1 ± 0.1 μL or 5 ± 0.2 μL volume were deposited on a test section by pipette. The time taken for each droplet to dry as observed visually was recorded. To ensure measurement of drying time was consistent, data were collected by one researcher who used a digital stopwatch to record the time each droplet took to evaporate. Droplets were observed by eye continuously and the time by which the droplet had evaporated was taken as when no moisture was apparent.

4. Results and discussion

4.1. Evaporation of water droplets

Redfern et al. studied the effect of temperature and humidity on the evaporation of water droplets from a polypropylene surface. The range of conditions investigated is summarised in Table 1, along with the range of associated characteristic evaporation times t_c (see Equation [5]). The humid air (an air-water mixture) was treated as an ideal gas with thermophysical properties taken from standard texts. The mol fraction of water vapour in equilibrium with the liquid over the temperature range of interest followed $y^* = 0.000054T^2 - 0.031T + 4.31$, where T is in Kelvin. The contact angle for static droplets was reported as 83.4°, which is smaller than those reported in the literature (96.7° - Rios et al., 2007; 104.9° - Choi et al., 2019). The (advancing) contact angle

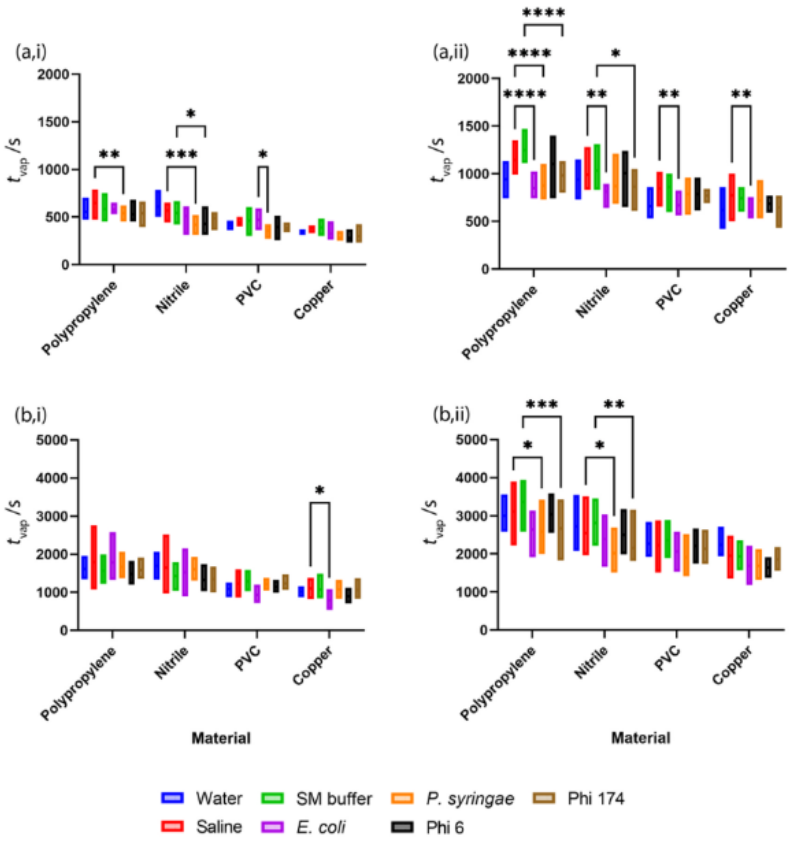

Fig. 10. Effect of material on droplet drying times. (a,i) 1 μL droplets in low RH, (a,ii) 1 μL droplets in medium RH, (b,i) 5 μL droplets in low humidity and (b,ii) 5 μL droplets in medium humidity. All measurements were at room temperature (18 °C). Statistical significance is shown for comparisons of bacteria vs. saline and bacteriophage vs. SM buffer and are represented as follows: * - $p \leq 0.05$, ** - $p \leq 0.01$, *** - $p \leq 0.001$ and **** - $p \leq 0.0001$.

for water measured on polypropylene for the experiments conducted in this work, 103° (Table 4), is consistent with the literature values.

Three convection conditions were considered:

(a) Quasi-stagnant conditions, where there was no forced convection so mass transfer was determined by diffusion: estimates of natural convection indicated that this had little effect in this case;
(b) Fan, half power.
(c) Fan, full power.

The local bulk air velocity in the vicinity of the droplet in (*b*) and (*c*) was estimated using a computational fluid dynamics package (see Redfern et al.): these varied from 0.5 m s^{-1} to 1.9 m s^{-1}, corresponding to droplet Reynolds number, $Re_d = \frac{UR_d}{\nu}$, values of 140–550.

4.1.1. Stagnant air

Fig. 4 compares the observed evaporation times for each droplet volume with the values predicted for water by the two contact modes (CCA, CWA). The evaporation time increases with droplet volume, as expected (since $t_e \propto R_0^2 \sim V_d^{2/3}$). The data points lie close to the CCA prediction, shown by the line of equality, whereas the CWA mode predicts consistently shorter evaporation times. Given the variation in temperatures, humidity and droplet volume, this level of agreement is considered good.

Also shown on the figure are the predictions of the mixed model, where the initial stage of evaporation follows CWA behaviour until the receding contact angle, θ_r, is reached. The latter parameter was set at $\theta_r = \theta_a/1.2$ as this gave reasonably good agreement. This is an interesting result which does not appear to be considered in studies on droplet evaporation, even though it could be expected: a droplet striking a surface would be expected to spread on contact, when it is subject to the advancing contact angle, but on evaporation it will switch to receding angle behaviour.

4.1.2. Forced convection

Activating the fan increased the rate of evaporation, but not in a systematic manner, unlike studies of droplet mass transfer in well-defined duct flows (e.g. Coutant and Penski, 1982; Ganzevles and van der Geld, 1998). Fig. 5 shows the effect of convection, expressed as Re_d, on observed evaporation times. The fan speeds were not sufficiently

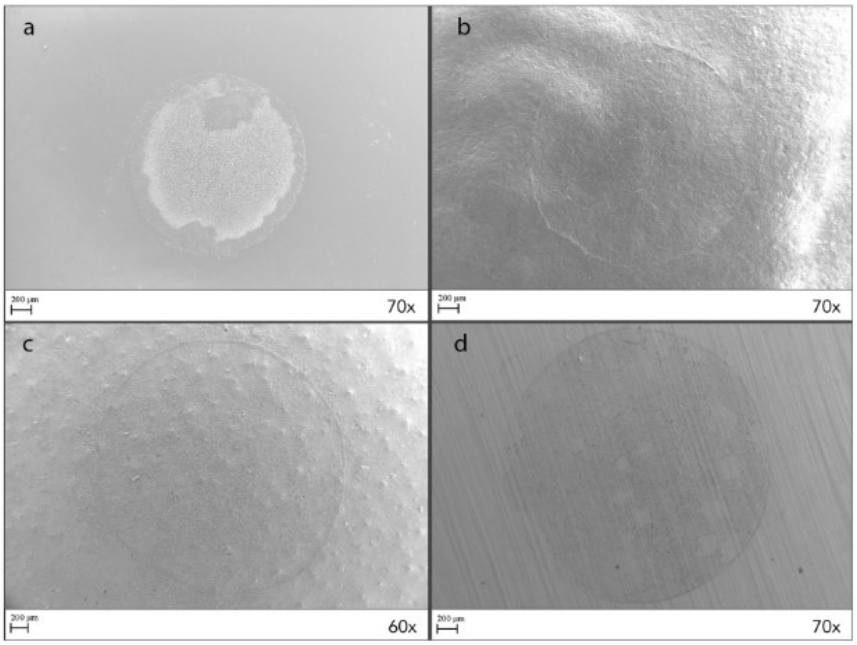

Fig. 11. SEM images of (A) polypropylene, (B) nitrile, (C) PVC and (D) copper surfaces following evaporation of a 5 μl droplet containing *E. coli* at RH = 60% and 22 °C.

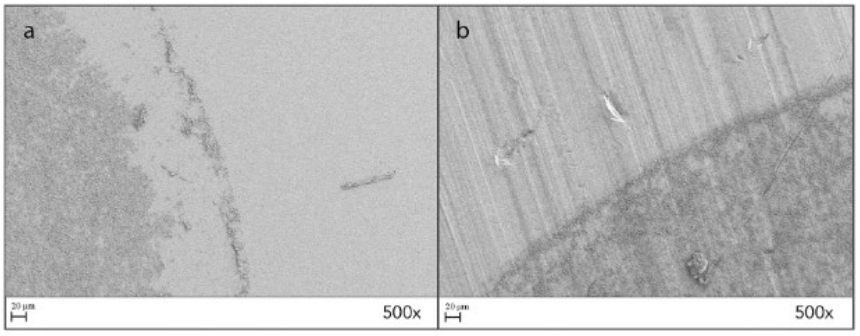

Fig. 12. Higher resolution SEM images of (a) polypropylene and (b) copper surfaces (see Fig. 11(a),(d)) following evaporation of a 5 μl droplet containing *E. coli* at RH = 60% and 22 °C.

large to cause the droplets to move across the surface. The times are divided by the value predicted for CCA (Fig. 5(a)) and CWA (Fig. 5(b)) behaviour. Effects such as shear-induced change in droplet shape were not considered. The values for quasi-stagnant air are plotted for comparison: for these Re_d was calculated with a velocity of 1 mm s^{-1}. There is a general decrease in evaporation time with Re_d, with noticeable scatter as other test conditions are manipulated. The effect of convection is also expected to depend on the Schmidt number, $Sc \equiv \frac{\mu}{\rho D}$ (where ρ is the mass density, see Coutant and Penski, and Ganzelves and van der Geld): this parameter did not vary strongly over the conditions considered here. Fig. 5(a) shows that the experimental values obtained under quiescent conditions lie consistently closer to the CCA predictions.

The effect of draughty conditions can be estimated for these droplets by exploiting the fact that the contact angle is close to 90°, so that they can be approximated as hemispheres. The Sherwood number can then be estimated from the Ranz and Marshall correlation (1952) for mass transport from spheres, *viz.*

$$\overline{Sh} = 2 + 0.6Re^{1/2}Sc^{1/3} \quad [10]$$

which, for the Reynolds and Schmidt numbers considered here, would give values of $\overline{Sh}$ ranging from (initially) 6.1 to 14.2, decreasing to 2 as

the droplet evaporated. Taking a geometric mean of these values as a rough estimate of the Sherwood number over a droplet's evaporation time would give t_{exp}/t_{sap}(CWA) ~ 0.37–0.56 for the cases with forced convection, which is consistent with the observed range of values. The need to consider convection when conducting tests and applying the results to practice is evident.

4.2 Evaporation of solutions and suspensions

The rate of evaporation of droplets containing organisms was studied using 1 μL and 5 μL droplets on four surfaces under conditions of mild (40–47% RH) and low humidity (14–16% RH). Macroscopic advancing contact angles on each surface were determined for 1 μL and 5 μL droplets of water, saline and SM buffer as well as the suspensions. The goniometer system used was not a precision device and the results, summarised in Tables 2 and 3, are used to identify trends. Most of the θ_a values lie in the range 45–90°. With 1 μL droplets (Table 2), the presence of *E. coli* gave different contact angles to the neat saline on nitrile and copper; by comparison, *P. syringae* gave values closer to the saline. The Phi6 and PhiX174 suspensions gave similar (within ~10°) values on nitrile, PVC and copper: on nitrile, these were different to the neat SM buffer. With the 5 μL drops (Table 3), the contact angles for neat saline, SM buffer and water were similar for all materials except copper, where SM buffer was lower. The contact angles for *E. coli* and *P. syringae* on polypropylene and copper were similar to those with saline, while those on nitrile were noticeably lower. The contact angles for SM buffer and Phi6 and PhiX174 suspensions were similar with the exception of copper and PVC, where PhiX174 was higher and lower respectively.

4.2.1. Evaporation times

The salts present in the saline solution (0.85 wt% NaCl) and SM buffer (see method section for composition) reduce the vapour pressure exerted by the water and the initial driving force for mass transfer, Δy, but this proved to be a small effect for the low and mid-humidity cases considered here. For the saline solution, the initial reduction in Δy is of the order of 0.26% at room temperature. If the solutes remain in solution and are not adsorbed on to the surface, one could then expect either (i) evaporation to stop as Δy approached zero, or (ii) the salts to undergo crystallisation, producing precipitates which would be visible under the microscope. Crystals were not evident in SEM images of the dried surfaces (with the exception of *P. syringae* on nitrile, see Supplementary Figure S1) and experiments with neat saline and buffer solutions all evaporated completely, indicating that salts were adsorbed on to the wetted surface.

Fig. 6 shows the effect of droplet composition on drying times, presented in the same format as the Redfern et al. results for water droplets in Fig. 4. A different polypropylene surface was used in these experiments. The observed evaporation times are in broad agreement with the CCA model predictions, as seen in Fig. 4. At low humidity (Fig. 6(a) - faster evaporation rates), the use of saline tends to increase the evaporation times compared to water, whereas the SM buffer times are similar to those for water. This effect is more noticeable with the mid-humidity data (Fig. 6(b)), in which case both saline and SM buffer exhibit longer evaporation times than water. This trend is noted in Table 4, alongside the trends observed for the other surfaces (Figs. 7–9).

The presence of organisms tends to reduce the evaporation time for both saline and SM buffer droplets. This suggests that the species are promoting CWA behaviour, which would be consistent with organisms collecting at the evaporation front, promoting pinning behaviour (but not necessarily fixing the contact line). The trends are recorded in Table 4 and are compared with the observed deposition patterns in the next section. Evaporation times were faster in the low humidity scenarios for both 1 μl and 5 μl droplet sizes, which is consistent with Equations [5] and [8], where $t_e \propto \Delta y^{-1}$.

Further analysis comparing evaporation times of droplets containing microorganisms with either saline or SM buffer alone revealed that in all cases of statistically significant differences ($p < 0.05$, $n = 11/32$ for bacteria and $n = 6/32$ for bacteriophages), the addition of microorganisms resulted in more rapid evaporation (Fig. 10). When comparing the total number of significantly different evaporation times with respect to RH, medium RH (40%) conditions provided a larger number of droplets that evaporated more quickly due to the presence of a microorganism, in both 1 μL and 5 μL scenarios. When comparing evaporation times with respect to droplet size, 1 μL droplets containing microorganisms evaporated significantly more rapidly than ones without more often (than 5 μL droplets) in both low (15%) and medium (40%) RH scenarios.

4.2.2. SEM images of bacterial deposition

The deposition patterns created by evaporation of 5 μL droplets containing *E. coli* or *P. syringae* differed depending on the substrate material. Whilst a ring marking the initial boundary of the droplet (i.e. the initial contact line) was visible on all images (see *E. coli* examples in Fig. 11), deposition of bacteria within the droplet footprint was more evident on polypropylene and copper (Fig. 12) unlike on nitrile and PVC where deposition within the footprint was less obvious (Figure S2). On polypropylene the bacteria were deposited with an obvious outer ring, i.e. bacteria deposited in a circular ring at the outer edge followed by an annulus where no bacteria were deposited, followed by an inner region where the majority of bacteria were deposited. In contrast, no annular region is apparent in the copper case. Deegan et al. (2000) discussed how differences in evaporation flux and change of height profile can promote coffee ring or uniform deposition behaviour: further work would be required to see if this is the reason for these observations.

Comparing the evaporation time plots (Fig. 6(b,ii) – polypropylene and Fig. 8(b,ii) – Cu), on copper the values consistently lay below the CCA line, suggesting mixed mode drying, while on polypropylene the data showed a strong correlation with CCA behaviour. Further work is needed to link deposition behaviour and drying kinetics: Deleplace et al. (2022) reported very pronounced deposition of *Bacillus* spores at the initial contact line on the four surfaces they studied, followed by different patterns in the footprint depending on the surface nature-species combination. In both instances in Fig. 12, bacteria are highly concentrated in different areas, resulting in deposition of bacterial cells on top of one another.

5. Discussion

A combination of modelling and experimental methods have been used to investigate the impact of microorganisms on the evaporation of liquid droplets on solid surfaces. The four surfaces studied are representative of many materials that are found in hospitality, healthcare and food processing facilities. They were not strongly wetting towards water (contact angles ranging from approximately 40°–100°), so that droplets formed or landing on the surface would tend to remain spherical rather than spread out to form a thin film.

The first order (external mass transfer control) model for the time taken for a droplet to evaporate provides useful insights into how the drying dynamics are determined by the contact angle and whether the droplet exhibits contact line pinning, which would be expected to promote constant wetted area behaviour. The evaporation times observed with water alone (Fig. 4) show good agreement with the values predicted for constant contact angle behaviour, and better agreement with the mixed model which incorporates a reasonable switch between the advancing contact angle, associated with the initial contact of the droplet on the surface, and the receding value. The predictions for constant wetted area behaviour, which might be associated with contact line pinning, give consistently poor agreement with the experimental measurements.

The addition of bacteria reduced the evaporation time significantly for all surface types in at least one of each droplet size/RH scenarios, whereas the addition of bacteriophage did not decrease the evaporation

time significantly on PVC or copper in any droplet size/RH scenario. Overall, the 1 μL droplets tend to exhibit less variation in drying time and dried more quickly than the 5 μL droplets, as expected from the model. The models did not capture the effect of adding bacteria or bacteriophage on the drying times, but the experimental values were, nevertheless, consistently closer to the constant contact angle scenario predictions rather than the constant wetted area ones, indicating that the deposition of these microorganisms does not give rise to the contact line pinning effects reported with colloidal suspensions. The bacteria, with sizes greater than 1 μm, are not expected to give rise to colloidal behaviour, whereas the bacteriophage, with lengths 20–30 nm, might if they did not agglomerate when suspended. Electron microscopy of images of the phages on the surface indicated that agglomerate and network formation did occur, but it was not possible to determine if this happened before they deposited on the surface.

Figs. 6–9 indicate that further work is required to capture the impact of these species on the drying kinetics, given that the constant contact angle model gives a reasonable working estimate of the evaporation time. Considering the input parameters to the model, the factor subject to most uncertainty is the effective contact angle. The values used in the calculations were taken from static observations of the solutions or suspensions on dry solid surfaces, whereas the images of the droplet footprints after drying indicated that these were no longer even and uniform, but rough and heterogeneous as a result of organism deposition. For wetting liquids, the Wenzel model predicts that a rougher surface will result in a smaller effective contact angle (the surface becomes more wetting) and Fig. 3 shows that reducing θ will reduce F_θ and the evaporation time. This enhanced roughness hypothesis could explain the observed reduction in evaporation times for the suspensions: predicting the magnitude of the effect would require knowledge of the deposition pattern and structure and is beyond the scope of the current work.

Given that moisture is required for many antimicrobial materials to exhibit antimicrobial activity, understanding that the presence of microorganisms can increase the rate at with evaporation occurs is important, as a shorter evaporation time will also result in reduced antimicrobial activity. Therefore, for those interested in the development, manufacture and installation of antimicrobial materials, it is essential to consider what type of microbial contamination the user is trying to control and use this knowledge in the development of their initial antimicrobial efficacy assessment methods.

6. Conclusions

This cross-disciplinary study revealed that the application of quantitative models for the kinetics of moisture evaporation on surfaces can help to explain and interpret findings when testing for the efficacy of antimicrobial surfaces. The speed of droplet evaporation is affected by a range of factors: temperature, humidity, airflow, the nature of the surface and the presence (and nature) of microorganisms. The kinetics of droplet evaporation affects the presence of moisture on a surface, and thence the survival of microorganisms and, potentially, the mode of action of putative antimicrobial agents in/on the surface – particularly if the agents require moisture for activity. Standardised testing methods provide detailed accounts of procedures, but do not always specify with any precision, the ambient conditions where testing takes place. If these factors are not adequately recognised or controlled, results from testing methods performed under different (or unspecified) environmental conditions in different laboratories are liable to vary and give rise to confusion, misinterpretation, and potentially misleading claims of effectiveness.

Credit author statement

Alexander J. Cunliffe: Investigation, Methodology, Validation, Visualization, Conceptualization, Data curation, Formal analysis, Writing – original draft, Writing – review & editing, Ru Wang: Investigation, Methodology, Validation, Visualization, Conceptualization, Data curation, Formal analysis, Writing – original draft, Writing – review & editing, James Redfern: Methodology, Visualization, Project administration, Resources, Supervision, Conceptualization, Formal analysis, Writing – original draft, Writing – review & editing, Joanna Verran: Methodology, Supervision, Resources, Conceptualization, Writing – review & editing, Ian Wilson: Methodology, Visualization, Supervision, Conceptualization, Formal analysis, Writing – original draft, Writing – review & editing.

Data – open access

All data created during this research is openly available from Manchester Metropolitan University's research repository: https://doi.org/10.23634/MMU.00629876.

Declaration of competing interest

The authors declare that they have no known competing financial interests or personal relationships that could have appeared to influence the work reported in this paper.

Acknowledgements

A PhD studentship for RW from the WD Armstrong Fund is gratefully acknowledged. Match-funding for a PhD studentship for AJC from the International Biodeterioration Research Group is gratefully acknowledged.

Appendix A. Supplementary data

Supplementary data to this article can be found online at https://doi.org/10.1016/j.jfoodeng.2022.111195.

Appendix

Fig. 2 shows that it takes approximately 4 min for the salt solutions to re-establish the desired relative humidity within the chamber after the lid was replaced. The dynamics are consistent with mass transfer control: let the rate of evaporation from the surface of the salt solution can be expressed as a molar flux, N, where

$$N = \overline{k_m} C_T (y^* - y_b) \quad [A1]$$

where $\overline{k_m}$ is a mass transfer coefficient, y_b is the mol fraction of water in the air, and C_T the molar density of the air (given by $P/R_G T$, where P is the total pressure, R_G the gas constant and T the absolute temperature). At the surface of the salt solution the water in the vapour will be in equilibrium with that in the salt solution, with mol fraction y^*. For the closed system when the lid is closed, a mass balance gives

$$\frac{d}{dt}(VC_T y_b) = A_s \overline{k_m} C_T (y^* - y_b) \quad [A2]$$

where V is the volume of the vapour in the chamber, t is time, and A_s is the area of solution surface available for mass transfer. This assumes perfect mixing in the vapour phase. Assuming isothermal operation so that the parameters are constant gives

$$ln\left\{\frac{(y^* - y_{b,o})}{(y^* - y_b)}\right\} = ln\left\{\frac{(RH^* - RH(0))}{(RH^* - RH(t))}\right\} = \frac{A_s \overline{k_m}}{V} t \quad [A3]$$

with $y_{b,o}$ the mol fraction of water in the air at the start of the experiment. For dilute concentrations, $RH \propto y$ (McCabe et al., 1993) and Equation [A3] indicates that a plot of $-ln(RH^* - RH(t))$ against t should be linear with gradient proportional to the ratio of the surface area of the salt reservoirs to the volume of the chamber.

References

Adams, M.H., 1959. *Bacteriophages*, Publ. Interscience Publishers.

BS ISO 22196, 2011. 2011 Measurement of Antibacterial Activity on Plastics and Other Non-porous Surfaces. BSI, London.

Bormashenko, E.Y., 2017. Physics of Wetting. publ. De Gruyter.

Chatterjee, S., Murallidharan, J.S., Agrawal, A., Bhardwaj, R., 2021. Why coronavirus survives longer on impermeable than porous surfaces. Phys. Fluids 33, 021701.

Choi, H.-J., Kim, M.S., Anh, D., Yeo, S.Y., Lee, S., 2019. Electrical percolation threshold of carbon black in a polymer matrix and its application to antistatic fibre. Sci. Rep. 9 (1), 6338.

Coutant, R.W., Penaki, E.C., 1982. Experimental evaluation of mass transfer from sessile drops. Ind. Eng. Chem. Fund. 21, 250–254.

Cunliffe, A.J., Askew, P.D., Stephan, I., Iredale, G., Cosemans, P., Simmons, L.M., Verran, J., Redfern, J., 2021. How do we determine the efficacy of an antibacterial surface? A review of standardised antibacterial material testing methods. *Antibiotics* 10, 1069. https://doi.org/10.3390/antibiotics10091069.

Deegan, R.D., Bakajin, O., Dupont, T.F., Huber, G., Nagel, S.R., Witten, T.A., 1997. Capillary flow as the cause of ring stains from dried liquid drops. Nature 389, 827–829.

Deegan, R.D., Bakajin, O., Dupont, T.F., Huber, G., Nagel, S.R., Witten, T.A., 2000. Contact line deposits in an evaporating drop. Phys. Rev. 62, 756–765.

Deleplace, M., Dallagi, H., Dubois, H., Richard, E., Ipatova, A., Benezech, T., Faille, C., 2022. Structure of deposits formed by drying of droplets contaminated with *Bacillus* spores determines their resistance to rinsing and cleaning. J. Food Eng. 318, 110873.

Eales, A.D., Dartnell, N., Goddard, S., Routh, A.F., 2016. Thin, binary liquid droplets, containing polymer: an investigation of the parameters controlling film shape. J. Fluid Mech. 794, 200–232.

Ganzevles, F.L.A., van der Geld, C.W.M., 1998. Heat and mass transfer from internal flows to hemispheres and flat parts in between. Int. J. Heat Mass Tran. 41, 3705–3718.

Grass, G., Rensing, C., Solioz, M., 2011. Metallic copper as an antimicrobial surface. Appl. Environ. Microbiol. 77 (5), 1541–1547.

Hansan, Abshar, Lee, Kyueui, Tewari, Kunal, Pandey, Lalit M, Messersmith, Phillip B, Faulds, Karen, Maclean, Michelle, Lau, King Hang Aaron, 2020. Surface Design for Immobilization of an Antimicrobial Peptide Mimic for Efficient Anti-Biofouling. Chemistry 7 (26), 5789–5793. https://doi.org/10.1002/chem.202000746.

Hu, H., Larson, R.G., 2002. Evaporation of a sessile droplet on a substrate. J. Phys. Chem. B 106, 1334–1344.

Imani, S.M., Ladouceur, L., Marshall, T., Maclachlan, R., Soleymani, L., Didar, T.F., 2020. Biomaterials-based formulations and surfaces to combat viral infectious diseases. APL Bioeng. 14, 12341–12369.

Kumari, S., Chatterjee, K., 2021. Biomaterials-based formulations and surfaces to combat viral infectious diseases. APL Bioeng. 5, 011503.

Larson, R.G., 2014. Transport and deposition patterns in drying sessile droplets. AIChE J. 60 (5), 1538–1571.

McCabe, W.L., Smith, J.C., Harriott, P., 1993. Unit Operations of Chemical Engineering. McGraw-Hill, NY. Ch. 23, publ.

Rai, M., Yadav, A., Gade, A., 2009. Silver nanoparticles as a new generation of antimicrobials. Biotechnol. Adv. 27 (1), 76–83.

Ranz, W., Marshall, W., 1952. Evaporation from drops. Chem. Eng. Prog. 48, 141–146.

Ratova, M., Redfern, J., Verran, J., Kelly, P.J., 2018. Highly efficient photocatalytic bismuth oxide coatings and their antimicrobial properties under visible light irradiation. Appl. Catal. B Environ. 239, 223–232.

Rios, P.F., Dodiuk, H., Kenig, S., McCarthy, S., Dotan, A., 2007. The effect of polymer surface on the wetting and adhesion of liquid systems. J. Adhes. Sci. Technol. 21 (3–4), 227–241.

Redfern, J., Tucker, J., Simmons, L.M., Askew, P., Stephan, I., Verran, J., 2018. Environmental and experimental factors affecting efficacy testing of non-porous plastic antimicrobial surfaces. Methods Protocols 1, 36. https://doi.org/10.3390/mps1040036.

Sobac, B., Brutin D, D., 2011. Triple-line behavior and wettability controlled by nanocoated substrates: influence on sessile drop evaporation. Langmuir 27, 14999–15007.

Soulié, V., Karpitschka, S., Lequien, F., Prené, P., Zemb, T., Moehwald, H., Riegler, H., 2015. The evaporation behavior of sessile droplets from aqueous saline solutions. Phys. Chem. Chem. Phys. 17, 22296–22303.

Nomenclature

Roman symbols

A_d: Area of liquid-air interface m^2
A_s: Area of solution-air interface m^2
Bo: Bond number
C_T: Total molar concentration, vapour phase mol m^{-3}
D: Diffusivity $m^2\,s^{-1}$
F_A: Factor, constant wetted area
F_θ: Factor, constant contact angle
g: Gravitational acceleration m s^{-2}
H: Humidity ?
$\overline{k_m}$: Average mass transfer coefficient m s^{-1}
L: Radius of wetted area m
n: Number of samples
N: Molar flux mol $m^{-2}s^{-1}$
p: p-value from a statistical test Pa
P: Total pressure Pa
Re_d: Droplet Reynolds number
R: sphere radius m
R_G: Gas constant J $mol^{-1}K^{-1}$
R_0: Initial droplet radius m
R^2: Correlation coefficient
Sc: Schmidt number
Sh: Mean Sherwood number
t: Time s
t_c: Characteristic time s
t_{exp}: Droplet evaporation time (experimental values) s
t_{eqn}: Droplet evaporation time (calculated from models) s
T: Temperature K
V: Volume of vapour m^3
V_d: Volume of drop m^3
y, y_b, y^*: Mol fraction in vapour phase, bulk phase value, saturated value

Greek symbols

γ: Vapour-liquid surface tension N m^{-1}
μ: Liquid dynamic viscosity Pa s
ν: Kinematic viscosity $m^2\,s^{-1}$
$\Delta\rho$: Difference in mass densities kg m^{-3}
ρ_m: Liquid molar density mol m^{-3}
θ: Contact angle °
θ_a θ_r: Advancing, receding contact angle °

Acronyms

CCA: Constant contact angle
CWA: Constant wetted area
PFU: Plaque forming units
PVC: Polyvinylchloride
RH: Relative humidity
SMB: SM Buffer
SEM: Scanning electron microscopy
TSA: Tryptone soya agar

Appendix D

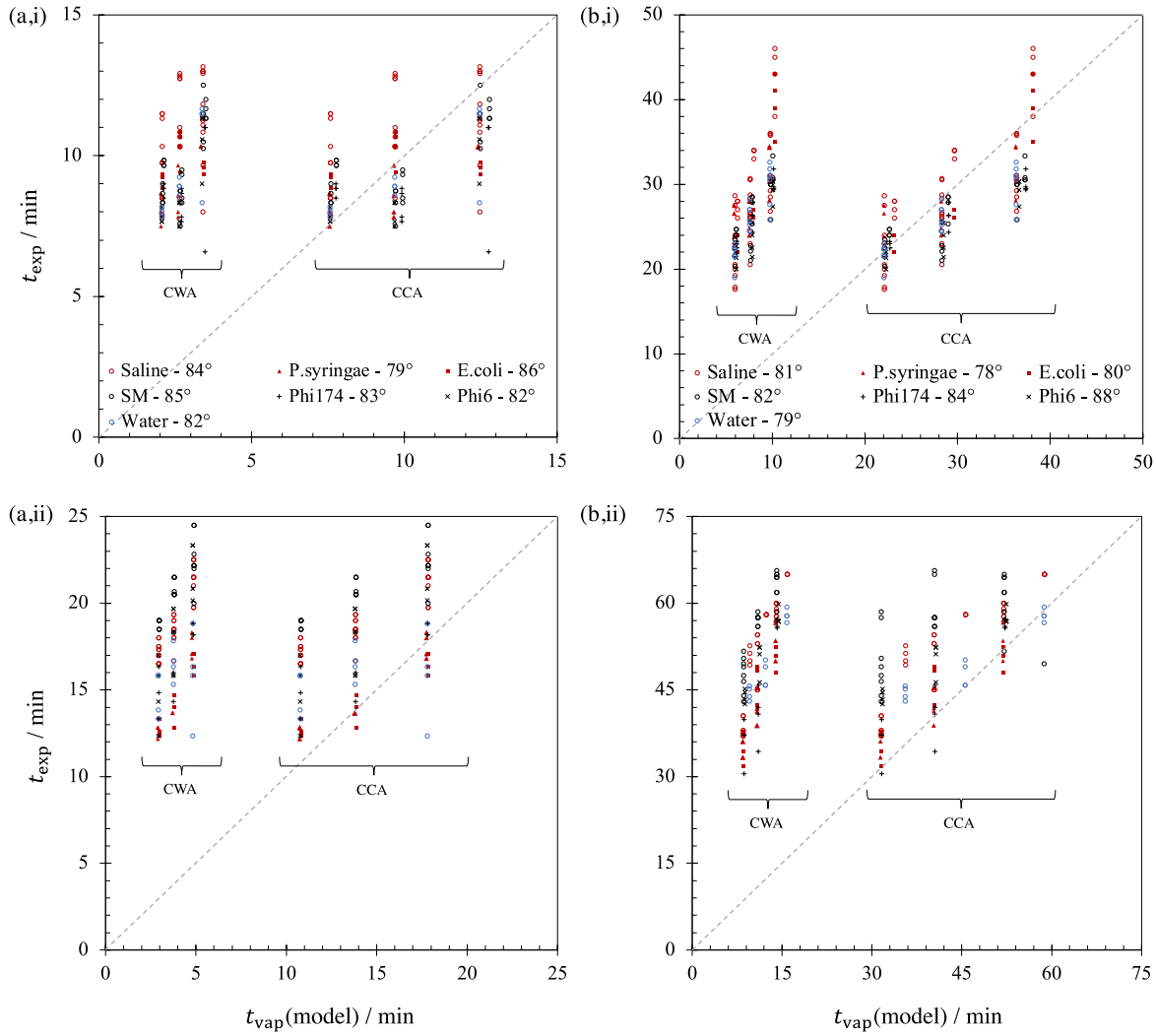

Figure 57 Comparison of liquid drop evaporation times in stagnant air on polypropylene with CCA and CWA model predictions. Liquid drops with initial volume of (i) 1 µL or (ii) 5 µL, and at (a) low relative humidity and (b) mid relative humidity. The three groups in each plot correspond to temperatures of 22, 26 and 30 ℃ (with higher temperature giving shorter evaporation time). Dashed locus shows the line of equality, i.e. y = x. P. syringae and E. coli prepared in saline, Phi X174 and Phi6 in SM buffer. The contact angle indicated in the legend is the measured static contact angle of the liquid drop on the polypropylene surface.

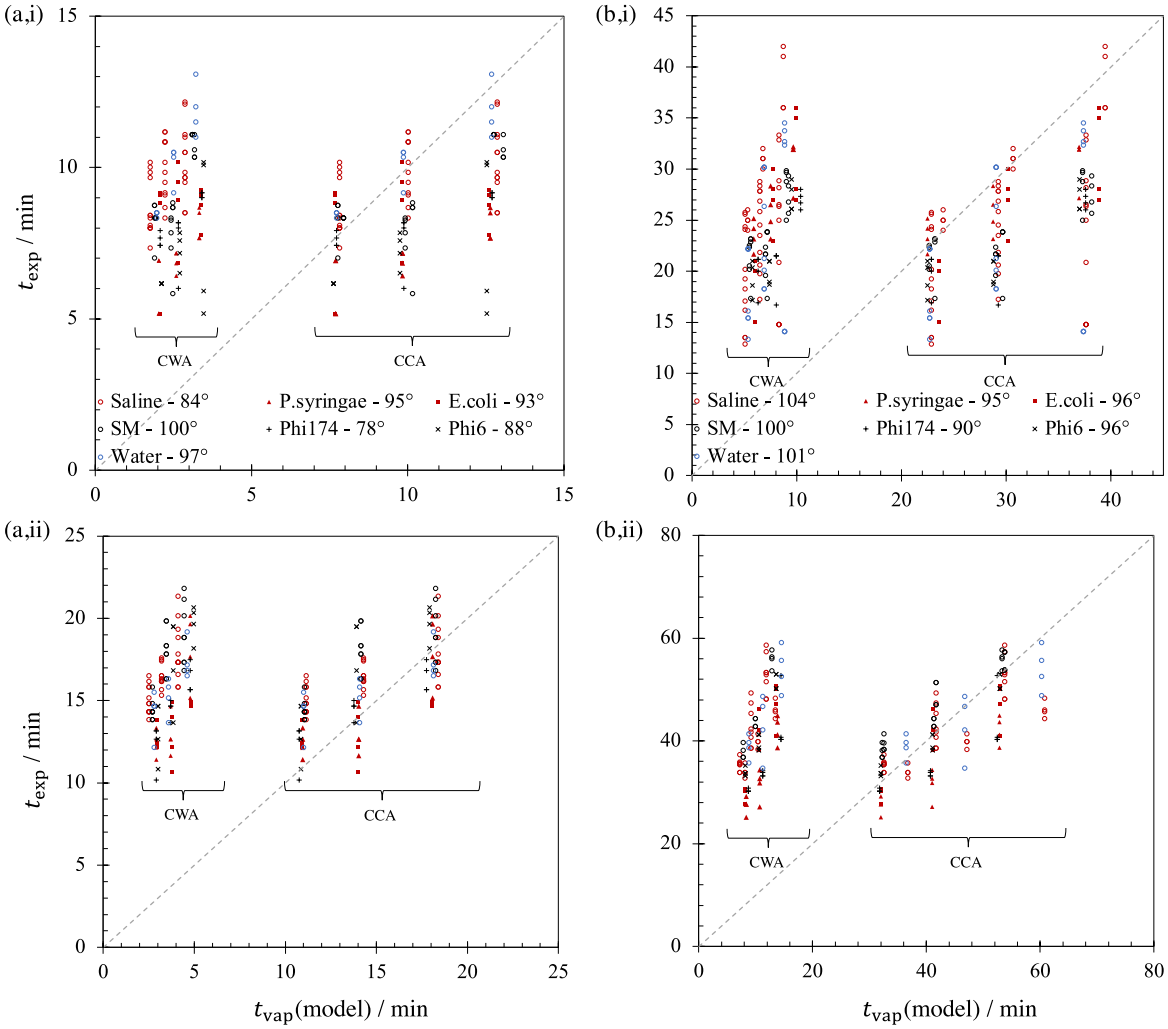

Figure 58 Comparison of liquid drop evaporation times in stagnant air on nitrile with CCA and CWA model predictions. Liquid drops with initial volume of (i) 1 µL or (ii) 5 µL, and at (a) low relative humidity and (b) mid relative humidity at temperatures of 22, 26 and 30 ℃. Dashed locus shows the line of equality, i.e., y = x. P. syringae and E. coli prepared in saline, Phi X174 and Phi6 in SM buffer.

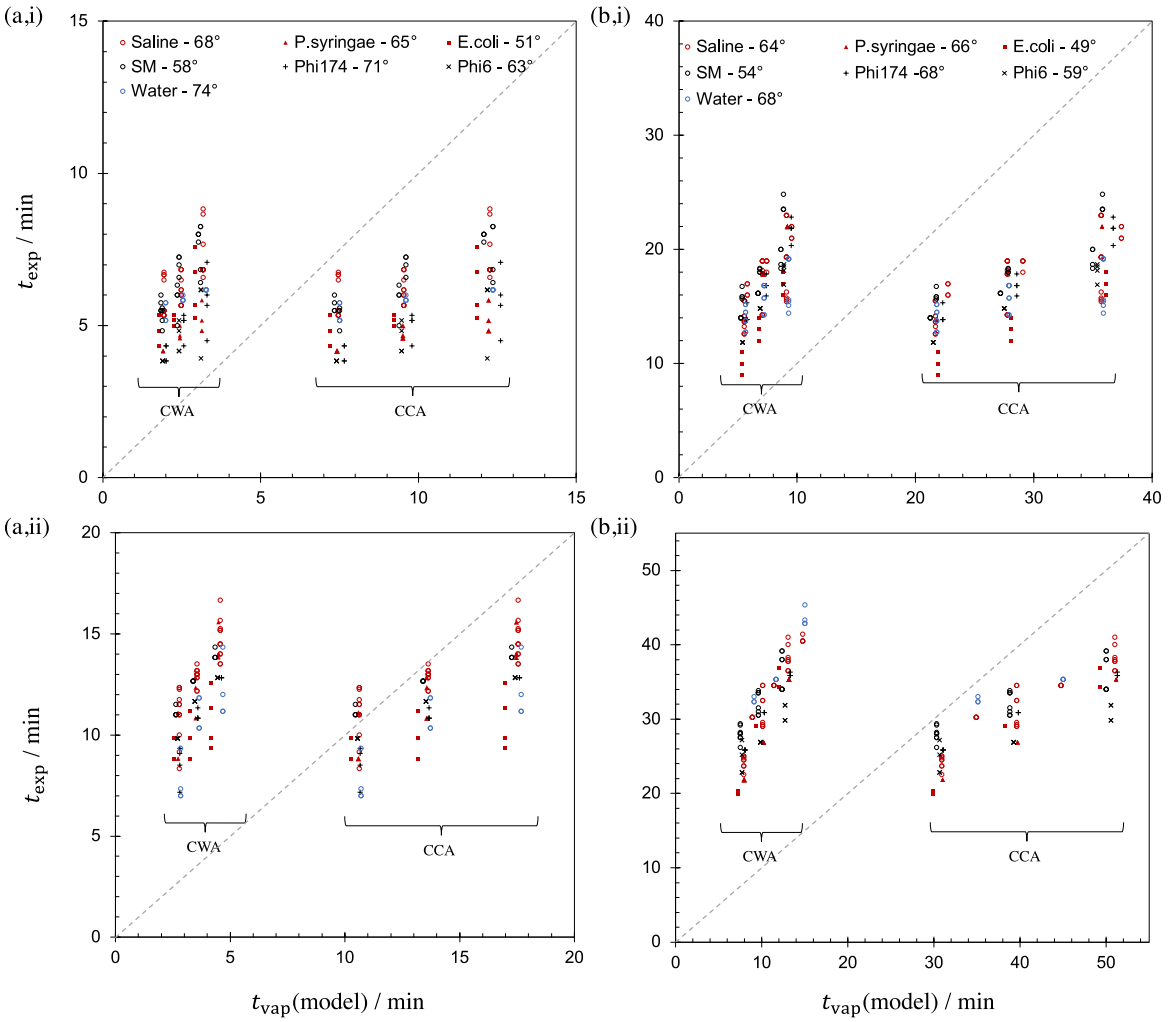

Figure 59 Comparison of liquid drop evaporation times in stagnant air on copper with CCA and CWA model predictions. Liquid drops with initial volume of (i) 1 µL or (ii) 5 µL, and at (a) low relative humidity and (b) mid relative humidity at temperatures of 22, 26 and 30 ℃. Dashed locus shows the line of equality, i.e. y = x. P. syringae and E. coli prepared in saline, Phi X174 and Phi6 in SM buffer.

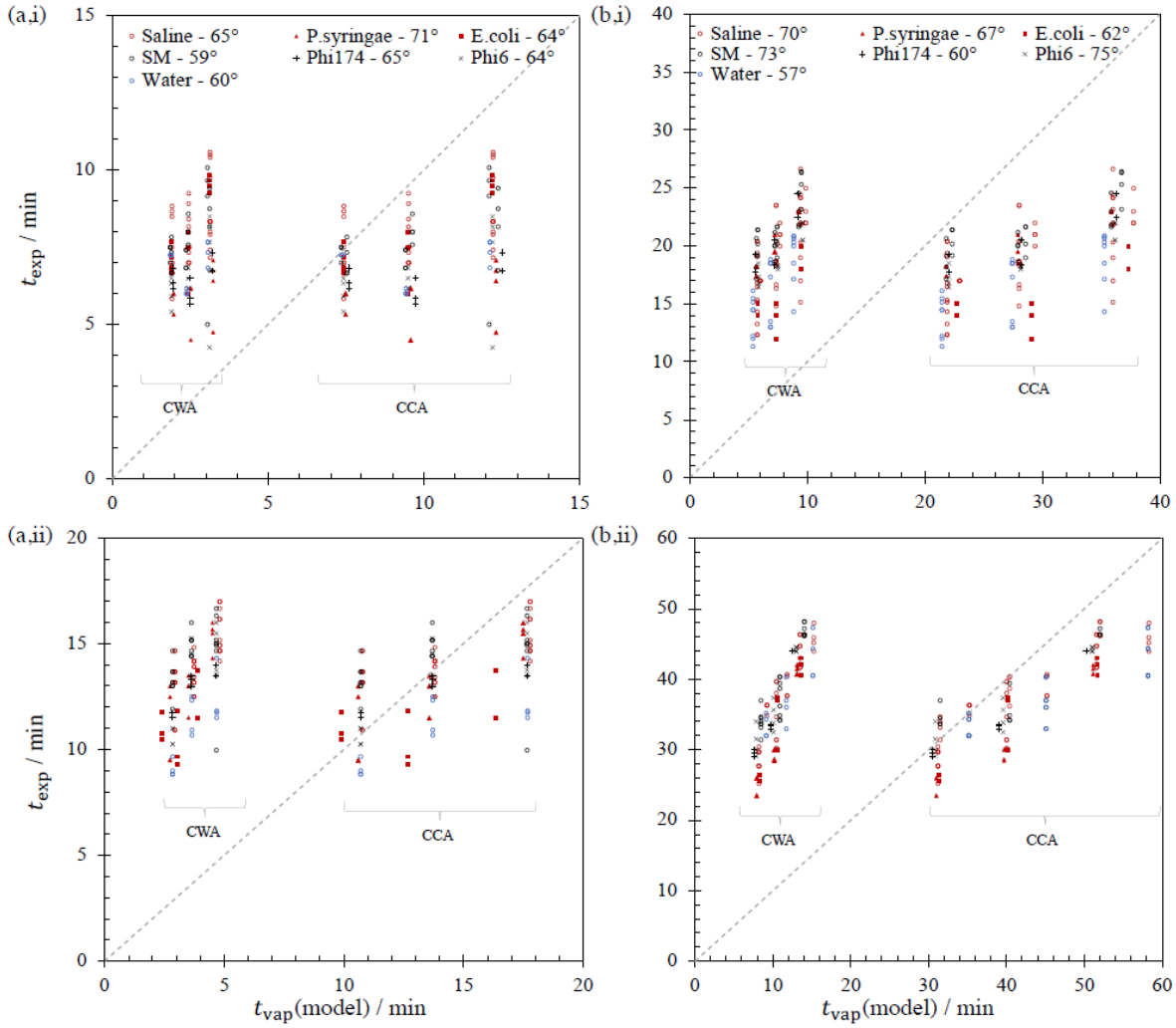

Figure 60 Comparison of liquid drop evaporation times in stagnant air on PVC with CCA and CWA model predictions. Liquid drops with initial volume of (i) 1 µL or (ii) 5 µL, and at (a) low relative humidity and (b) mid relative humidity at temperatures of 22, 26 and 30 ℃. Dashed locus shows the line of equality, i.e. y = x. P. syringae and E. coli prepared in saline, Phi X174 and Phi6 in SM buffer.

Appendix E

```
#include <dht.h>
#include <SPI.h>
#include <SD.h>

#define dht_pin A0
#define RELAY_PIN A4
#define RELAY_PIN2 A5
const int heaterone = 8;
const int heatertwo = 7;

dht DHT;
File myFile;
int time = 0;
int temp = 24;
// close down program, then pull out cord
void setup() {
  // put your setup code here, to run once:
Serial.begin(9600);
Serial.print("Initializing SD card...");
if (!SD.begin(10)) {
Serial.println("initialization failed!");
while (1);
}
Serial.println("initialization done.");
## microSD card needs a file called "text.txt" to function
myFile = SD.open("test.txt", FILE_WRITE);
if (myFile) {
Serial.print("Writing to test.txt...");


// close the file:

} else {
// if the file didn't open, print an error:
Serial.println("error opening test.txt");
}
pinMode(heaterone, OUTPUT);
digitalWrite(heaterone, LOW);
pinMode(RELAY_PIN, OUTPUT);
pinMode(heatertwo, OUTPUT);
digitalWrite(heatertwo, LOW);
}

void loop() {
  DHT.read11(dht_pin);
```

```
    Serial.print("Humidity = ");
    Serial.print(DHT.humidity);
    Serial.print("%    ");
    Serial.print("Temperature = ");
    Serial.print(DHT.temperature);
    Serial.println(" C");
    myFile.print(DHT.humidity);
    myFile.print(", ");
    myFile.println(DHT.temperature);
    ## if you change the delay number at the end, match this add number to
it, note this number is in seconds, delay number is milliseconds
    time = time + 30;
    ## Change the time number below for test duration in seconds
    if (time > 21600) {
      myFile.close();
      Serial.print("Closed");
    }

## change both if/else if statement numbers for temperature required, actual
temperature will be around 0.5 degrees lower than set to, only use whole
numbers
    if (DHT.temperature <= 24) {
      digitalWrite(RELAY_PIN, HIGH);
      digitalWrite(RELAY_PIN2, HIGH);
      digitalWrite(heaterone, HIGH);
      digitalWrite(heatertwo, HIGH);
    }
    else if (DHT.temperature > 24) {
      digitalWrite(RELAY_PIN, LOW);
      digitalWrite(RELAY_PIN2, LOW);
      digitalWrite(heaterone, LOW);
      digitalWrite(heatertwo, LOW);
    }
    ## below delay number specifies time between reads
    delay(30000);
    Serial.flush();

}
```

Appendix F

```
#include <dht.h>
#include <SPI.h>
#include <SD.h>

#define dht_pin1 A0
#define dht_pin2 A1
#define dht_pin3 A2
#define dht_pin4 A3
#define dht_pin5 A4
#define dht_pin6 A5

dht DHT;
File myFile;
int time = 0;

void setup() {

  // put your setup code here, to run once:
Serial.begin(9600);
Serial.print("Initializing SD card...");
if (!SD.begin(10)) {
Serial.println("initialization failed!");
while (1);
}
Serial.println("initialization done.");
## microSD card needs a file called "text.txt" to function
myFile = SD.open("test.txt", FILE_WRITE);
if (myFile) {
Serial.print("Writing to test.txt...");


// close the file:

} else {
// if the file didn't open, print an error:
Serial.println("error opening test.txt");
}
}

void loop() {
DHT.read11(dht_pin1);
myFile.print(time);
myFile.print(", ");
    myFile.print(DHT.humidity);
    myFile.print(", ");
    myFile.print(DHT.temperature);
```

```
    DHT.read11(dht_pin2);
    myFile.print(DHT.humidity);
    myFile.print(", ");
    myFile.print(DHT.temperature);

    DHT.read11(dht_pin3);
    myFile.print(DHT.humidity);
    myFile.print(", ");
    myFile.print(DHT.temperature);

    DHT.read11(dht_pin4);
    myFile.print(DHT.humidity);
    myFile.print(", ");
    myFile.print(DHT.temperature);

    DHT.read11(dht_pin5);
    myFile.print(DHT.humidity);
    myFile.print(", ");
    myFile.print(DHT.temperature);

    DHT.read11(dht_pin6);
    myFile.print(DHT.humidity);
    myFile.print(", ");
    myFile.println(DHT.temperature);

    delay(30000);
    Serial.flush();
}
```